CONTENTS FOR OCTOBER, 1949

PAPERS

PAGE

Frequency Analysis of Beam and Girder Floors.
By Hans H. Bleich 1093

Roads and Pavements, Sampson Naval Training Station.
By Jacob Feld 1133

Aerodynamic Theory of Bridge Oscillations.
By D. B. Steinman 1147

DISCUSSIONS

The Relation of Urban Expressways to Mass Transportation Facilities.
By Curtis G. Bradfield 1185

Effect of Driving Piles Into Soft Clay.
By Stuart B. Avery, Jr., and Stanley D. Wilson, and George L. Freeman and James D. Parsons 1190

Modern Concepts Applied to Concrete Aggregate.
By Herbert K. Cook, Thomas B. Kennedy, and Bryant Mather 1205

An Engineering Concept of Flow in Pipes.
By Ralph W. Powell, J. C. Stevens, George A. Whetstone, G. H. Hickox, and James F. Halsey and William M. Owen 1209

Continuous Arches and Bents Analyzed by Column Analogy.
By Leslie J. Meszaros, A. A. Eremin, and J. J. Polivka 1219

Applied Column Theory.
By Jacob Karol 1224

Photogrammetry, Postwar.
By Courtlandt Eaton 1229

Control of the Hydraulic Jump by Sills.
By Charles Jaeger, and Louis M. Laushey 1231

Mississippi River Bridge at Dubuque, Iowa.
By R. N. Bergendoff and Josef Sorkin 1242

GUIDEPOST FOR TECHNICAL READERS
OCTOBER, 1949, *PROCEEDINGS*

Items of value or significance to readers in various fields are here listed. For convenience the distribution is given in terms of the Society's Technical Divisions

Technical Division	*Pages*
Air Transport	1133, 1147, 1190
City Planning	1185, 1229
Construction	1133, 1190, 1205, 1242
Highway	1133, 1185, 1205, 1242
Hydraulics	1209, 1231
Irrigation	1209, 1231
Power	1209, 1231
Sanitary Engineering	1209
Soil Mechanics and Foundations	1133, 1190
Structural	1093, 1147, 1205, 1219, 1224, 1242
Surveying and Mapping	1229

(A constant effort is made to supply technical material to Society members, over the entire range of possible interest. In so far as your specialty may be covered inadequately in the foregoing list, this fact is a gage of the need for your help toward improvement.—Ed.)

HINTS TO AUTHORS

Those who are planning papers for submission to PROCEEDINGS *will expedite Committee action measurably by first studying the standard instructions as to style, content, and format. For reprints, address the Manager, Technical Publications, 33 W. 39th St., New York 18, N. Y.*

AMERICAN SOCIETY OF CIVIL ENGINEERS

Founded November 5, 1852

PAPERS

FREQUENCY ANALYSIS OF BEAM AND GIRDER FLOORS

By Hans H. Bleich,[1] M. ASCE

Synopsis

A procedure for finding the frequencies and modes of such three-dimensional structures as the floors in boilerhouses by utilizing the solutions of the two-dimensional vibration problems of all the beams of which the system is built up is developed in this paper. The method is explained for the case of floor systems; but the formulas apply also to any other type of structure as, for example, to multiple-story building frames or to airplanes. The method can be used with advantage for the frequency analysis of any complicated structure, and consists in resolving the system into two simpler systems, the frequencies and modes of which are easier to determine. If necessary, this simplifying process can be used repeatedly. The principle is theoretically exact but leads to the use of infinite series; for practical purposes excellent approximations are obtained by using only the first few terms of these series. A reader who wishes to apply the method should have some knowledge of the theory of oscillations and, in particular, of the fundamental notion of "normal modes" and of their properties.

The paper is presented in four sections including a numerical example (Section 4). Section 1 deals with the theory and its application to statically determinate systems. Section 2 contains an extension of the theory to include statically indeterminate systems. Section 3 is a collection of methods and formulas for reference in determining frequencies and modes of simple systems. Although some of these formulas are known, many of them are new. The purpose of Section 4 is to serve as a guide for the arrangement of practical computations. For this reason the simplest system on which all the steps of the method can be demonstrated was chosen, thus enabling the writer to discuss every detail fully. The method was devised (and has been applied successfully)

Note.—Written comments are invited for immediate publication; to insure publication the last discussion should be submitted by March 1, 1950.

[1] Associate Engr., Hardesty and Hanover, Cons. Engrs., New York, N. Y.; Lecturer in Civ. Eng., Columbia Univ., New York, N. Y.

to find the frequencies of much more complicated systems than the one shown in Section 4.

Notation.—The letter symbols, adopted for use in this paper and in its discussions, conform essentially with the American Standard Letter Symbols for Structural Analysis, prepared by a Committee of the American Standards Association with ASCE participation. An important exception is that the symbols m and M in this paper are used for masses and not for bending moments. The latter are designated by $\bar{m}$ and $\bar{M}$. Symbols are defined where they first appear, in the text or by illustration. The most significant symbols are:

c = an arbitrary factor; a coefficient; c_i = a specific value corresponding with ω_i;
i = a number;
j = a number;
k = a number; a panel, or section point number on a beam;
$\bar{M}$ = moment corresponding to an externally applied load;
$\bar{m}$ = value of $\bar{M}$ for a unit load;
M = concentrated masses; dynamic reactions;
m = distributed masses;
u = deflection:
  u_d = deflection in a determinate system;
  u_X = value of u due to redundant moments X;
w = unit weight, in pounds per foot; also elastic weights;
X = redundant moments;
y = amplitude of a mode:
  $\bar{y}$ = an arbitrary function;
  $y^{(1)}, y^{(2)}, \ldots$ = successive approximations of y;
$y(t)$ = displacement, a function of t;
β = a substitution constant in Eqs. 26 and 41;
Δ = a determinant;
ϕ = amplitude of the normal mode, ϕ_i corresponding to ω_i; ϕ_A and ϕ_B = amplitudes for systems A and B, respectively;
ψ = deflection due to redundant moment $X = 1$; and
ω = circular frequency:
  ω_A and ω_B = frequencies for systems A and B, respectively;
  ω_i and ω_k = specific values of ω.

1. Theory Applied to Statically Determinate Structures

Fundamental Facts Concerning Oscillations.—If any mechanical system is in a state of free oscillation the only forces acting on the system are the internal elastic forces and the inertia forces. If such a system consists of the masses m and the displacements are $y(t)$, the inertia forces are

$$-m\frac{d^2y(t)}{dt^2} = m\omega^2 y(t) \ldots\ldots\ldots\ldots\ldots\ldots\ldots\ldots (1)$$

in which ω is the circular frequency and t is the time, in seconds. The frequency, in cycles per minute, is

$$F = \frac{30}{\pi}\omega \quad \ldots\ldots (2)$$

The displacements $y(t)$ are functions of the time and can be expressed as

$$y(t) = y \sin \omega t \quad \ldots\ldots (3)$$

in which the amplitudes y are independent of the time.

A mechanical system can oscillate freely only with certain distinct frequencies ω_i. The amplitudes y_i corresponding to each of these frequencies are called the principal oscillations. It can be shown that the amplitudes y_i and y_k corresponding to two different frequencies ω_i and ω_k are "orthogonal"; that is,

$$\int y_i\, y_k\, dm = 0 \quad \ldots\ldots (4a)$$

Eq. 4 is integrated over all the masses of the system. The amplitudes y_i can be multiplied by an arbitrary factor c, because the product $c\, y_i$ still represents amplitudes of a possible state of principal oscillation. If this factor is so chosen that

$$\int (c\, y_i)^2\, dm = \int \phi^2_i\, dm = 1 \quad \ldots\ldots (4b)$$

the symbol $\phi_i = c\, y_i$ is called the "normal mode" corresponding to ω_i and Eq. 4*b* is an expression for the "normalizing condition." Different normal modes[2] ϕ_i and ϕ_k are orthogonal; that is,

$$\int \phi_i\, \phi_k\, dm = 0 \quad \ldots\ldots (4c)$$

Systems with an axis of symmetry have two types of normal modes—(1) symmetrical modes for which ϕ_i has the same value in symmetrically situated points and (2) asymmetrical modes for which the value of ϕ_i in symmetrical points is equal but of opposite sign. It is usually found advantageous to consider and determine symmetrical and asymmetrical modes separately.

Two important properties of the normal modes ϕ_i are:

(*a*) If any mechanical system is subjected to the inertia forces $\omega^2_i\, m\, \phi_i$ as a static load, the resulting deflections are just the normal mode ϕ_i; and

(*b*) The deflections u of any mechanical system loaded with several arbitrary external forces P can be expressed as an expansion by all the normal modes of the system—

$$u = \sum_i c_i\, \phi_i \quad \ldots\ldots (5)$$

[2] "Mechanical Vibrations," by J. P. Den Hartog, McGraw-Hill Book Co., Inc., New York, N. Y., 2d Ed., 1940, pp. 192–196.

—provided that the forces P act only at points where masses m of the mechanical system occur. The values of the coefficients c_i are

$$c_i = \frac{1}{\omega^2_i} \int \phi_i \, dP \ldots\ldots\ldots\ldots\ldots\ldots\ldots\ldots (6)$$

For approximate computations it is possible to consider only a few terms of Eq. 5 corresponding to the lowest frequencies of the system.

All the integrals $\int \phi_i \, \phi_k \, dm$, etc., have been written in this form to include distributed masses m and concentrated masses M. For numerical computations such integrals must be converted into an integral over the distributed masses plus a sum over all the concentrated masses; that is,

$$\int \phi_i \, \phi_k \, dm = \int m \, \phi_i \, \phi_k \, dx + \sum M \, \phi_i \, \phi_k \ldots\ldots\ldots\ldots\ldots (7)$$

Complementary Systems.—The following theoretical treatment involves two new concepts: The first is the concept of "complementary systems," which is explained in this subsection; and the other is the concept of "dynamic reactions" which will be discussed in the next subsection.

Floor systems usually consist of a number of secondary beams supported by main floor girders which rest either on external supports like columns and walls or, in complicated cases, on other beams. Restricting the subject to statically determinate arrangements, it is required to show how the complicated problem of finding the oscillations of a floor system can be solved if the frequencies and the normal modes of a simpler system, having one main girder less, are known. If the simpler system is still too complex for a direct solution, it can be reduced further until, in the end, a system is derived which consists only of ordinary beams, the frequencies and normal modes of which can be found by a number of well known methods.

One main girder is selected which, while carrying other girders of the system, rests in turn on external supports. In Fig. 1, for example, girder A should be selected. The girders normal to it would not be suitable because one end of each of these girders rests on girder A.

A simpler system is obtained by assuming the rectangular moment of inertia of girder A to be $I_A = \infty$. Thus, this girder does not deflect and all girders supported by it can be considered resting on fixed supports. This new system (simplified system B), therefore, has one girder less than the original system. It has normal modes ϕ_{iB} and frequencies ω_{iB} which, temporarily, are assumed to be known.

Apart from system B, a system A is formed which is identical with the original system as far as dimensions and mass distribution are concerned. The moment of inertia of girder A, Fig. 1, is I_A as in the original system. In all other girders, however, the moment of inertia is $I = \infty$. System A has certain natural frequencies ω_{iA} and normal modes ϕ_{iA}.

An important property of the two artificial systems A and B can now be proved:

Theorem I.—The deflection u of any point in the original system, resulting from an arbitrary external load, is equal to the sum $u_A + u_B$ of the deflections of the two systems caused by the same load.

If the moments corresponding to the external load are called $\bar{M}$, and the moments due to a unit load, acting at the point where the deflection is contemplated, are called $\bar{m}$, then the deflection of the original system consisting of the girders a, b, c, $\cdots$, can be expressed as

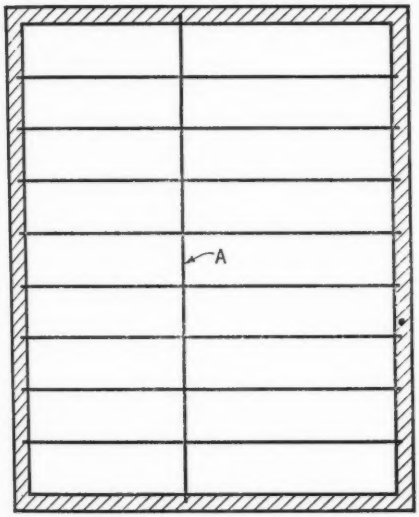

FIG. 1

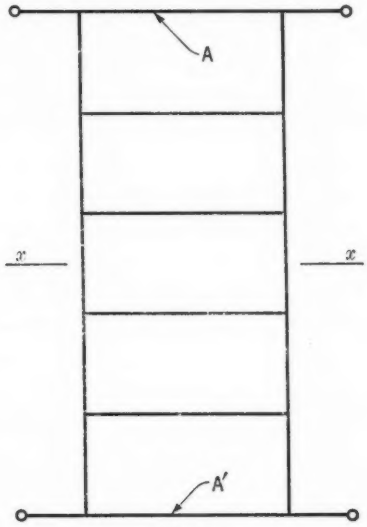

FIG. 2

$$u = \int_a \frac{\bar{M}\,\bar{m}}{E\,I_a}\,dx + \int_b \frac{\bar{M}\,\bar{m}}{E\,I_b}\,dx + \int_c \frac{\bar{M}\,\bar{m}}{E\,I_c}\,dx + \cdots\cdots\cdots\cdots (8)$$

in which the three integrals are taken over girders a, b, and c, respectively. Similar equations can be written down for systems A and B. For system A, $I_b = I_c = \cdots = \infty$, whereas, for system B, $I_a = \infty$. Consequently,

$$u_A = \int_a \frac{\bar{M}\,\bar{m}}{E\,I_a}\,dx \quad \text{and} \quad u_B = \int_b \frac{\bar{M}\,\bar{m}}{E\,I_b}\,dx + \int_c \frac{\bar{M}\,\bar{m}}{E\,I_c}\,dx + \cdots\cdots (9)$$

and, by comparison of Eqs. 8 and 9,

$$u = u_A + u_B \cdots\cdots\cdots\cdots\cdots\cdots\cdots\cdots (10)$$

Because of this relation systems A and B are named "complementary systems."

In the case of symmetrical systems it is necessary to modify the procedure slightly; otherwise the advantage of the symmetry would be lost. In a case

such as that in Fig. 2, system B should be obtained by making $I_A = I'_A = \infty$; system A will have moments of inertia I_A and I'_A at their original values, and in all the other beams the value of I will be ∞. The important relation expressed in Eq. 10 remains true. If the complementary systems are chosen in this way, the two systems A and B remain symmetrical and their normal modes can be separated into symmetrical and asymmetrical ones, which is of considerable advantage.

FIG. 3

Dynamic Reactions.—Except for symmetrical structures, system A consists of only one flexible girder A which supports the masses of the original system by further girders that are assumed rigid. Fig. 3 shows the simplest case possible, in which the flexible girder A supports one rigid girder B. The amplitudes ϕ_A of the normal mode are indicated in this diagram. If the amplitude of the normal mode at point 1 is $\phi_A(1)$, all the amplitudes along girder B can be expressed in the form:

$$\phi_A = \phi_A(1)\,\frac{x}{l} \qquad (11)$$

Assuming the system to be loaded with its inertia forces $\omega^2\,\phi_A\,dm$, the reaction of girder B at point 1 is

$$R_1 = \int \frac{x}{l}\,\omega^2\,\phi_A\,dm = \frac{\omega^2}{l^2}\,\phi_A(1)\int x^2\,dm \qquad (12a)$$

If system A contained a concentrated mass M_1 at point 1, the inertia force exerted by this mass would be

$$R_1 = \omega^2\,\phi_A(1)\,M_1 \qquad (12b)$$

From a comparison of the two values of R_1 in Eqs. 12, girder B is found to cause the same inertia force as a concentrated mass:

$$M_1 = \frac{1}{l^2}\int x^2\,dm \qquad (13)$$

Under the heading, "Fundamental Facts Concerning Oscillations" (Section 1), it has been stated that, when any mechanical system is loaded with the inertia forces $\omega^2{}_i\,m\,\phi_i$ corresponding to a normal mode ϕ_i, the deflection of the system is equal to the normal mode ϕ_i. Therefore, if the inertia force exerted by the fictional mass M_1 is equal to the inertia force exerted by the masses on girder B, it is obvious that the mechanical system A must have the same normal modes and frequencies as a system consisting only of girder A if this girder carries the additional mass M_1 assumed concentrated at point 1. For symbolic purposes the mass M_1 is termed the "dynamic reaction" of girder B.

The value of the dynamic reaction is different from the value obtained by the law of static reactions; the latter, expressed in a form similar to Eq. 13, would have been

$$R = \frac{1}{l}\int x\, dm \qquad (14)$$

For a uniformly distributed mass m the dynamic reaction becomes $m\,\frac{l}{3}$.

In other more complex cases the procedure is similar. The system is loaded with its inertia forces and the reactions of the rigid girders on girder A are replaced by the inertia forces of fictional masses or "dynamic reactions." The use of this concept enables the designer to reduce system A to one single girder, the natural frequencies and normal modes of which can be found by the usual methods.

In certain complicated cases the dynamic reactions become functions of the amplitudes at other points of the girder. An example of this condition is shown in Fig. 4. In system A for this structure the members will have mo-

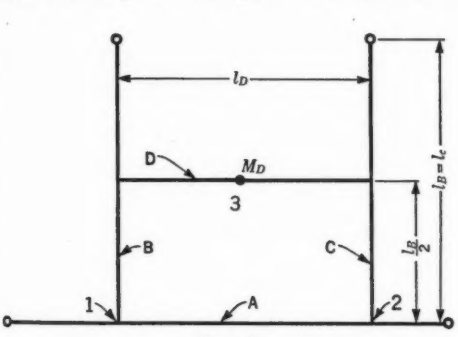

FIG. 4

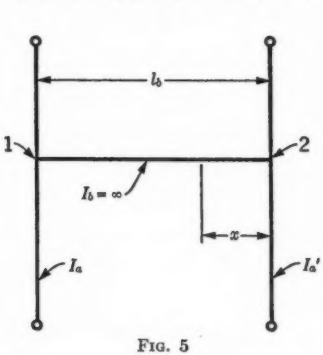

FIG. 5

ments of inertia $I_B = I_C = I_D = \infty$. Girder D carries a concentrated mass M_D in the center, girders B and C carry distributed masses m_B and m_C, respectively.

The amplitudes of girder A at points 1 and 2 are $\phi(1)$ and $\phi(2)$; the dynamic reactions due to the masses on girders B and C are found, as before, to be $\frac{m_B\, l_B}{3}$ and $\frac{m_C\, l_C}{3}$, respectively. The amplitude at point 3 due to the deflection of girder A is $\frac{\phi(1) + \phi(2)}{4}$, which results in an inertia force $\omega^2\, M_D\, \frac{\phi(1) + \phi(2)}{4}$. This force has reactions $\omega^2\, M_D\, \frac{\phi(1) + \phi(2)}{16}$ at both point 1 and point 2. To obtain the dynamic reactions, these values must be divided by $\omega^2\, \phi(1)$ and $\omega^2\, \phi(2)$, respectively. The result gives total dynamic reactions at points 1 and 2 equal to

$$M_1 = \frac{m_B\, l_B}{3} + M_D\, \frac{\phi(1) + \phi(2)}{16\,\phi(1)} = \frac{m_B\, l_B}{3} + \frac{M_D}{16} + \frac{\phi(2)}{\phi(1)} \times \frac{M_D}{16} \qquad (15a)$$

and

$$M_2 = \frac{m_C\, l_C}{3} + M_D \frac{\phi(1) + \phi(2)}{16\,\phi(2)} = \frac{m_C\, l_C}{3} + \frac{M_D}{16} + \frac{\phi(1)}{\phi(2)} \times \frac{M_D}{16} \ldots (15b)$$

This result is not as simple as before, because M_1 and M_2 now depend on the ratio of the amplitudes at points 1 and 2. These "variable" dynamic reactions can be used without difficulty, however, to find the normal modes, applying any of the methods described subsequently in Section 3.

For symmetrical structures system A may consist of two flexible girders, but dynamic reactions can be found in a similar manner if symmetrical and asymmetrical modes are treated separately. For example, to obtain the normal modes of the system shown in Fig. 5 consider first the symmetrical modes only. The amplitudes of both girders a and a′, Fig. 5, must be alike—that is $\phi(1) = \phi(2)$. The amplitudes for all points of girder b, therefore, are $\phi(x) = \phi(1)$. The inertia loading of girder b is $\omega^2\, m\, \phi(x) = \omega^2\, m\, \phi(1)$, and the reactions become

$$R_1 = R_2 = \frac{\omega^2}{l_b}\, \phi(1) \int x\, dm \ldots\ldots\ldots\ldots\ldots\ldots (16a)$$

This reaction is identical with the inertia force of a mass M_1 assumed acting at point 1 and that of a mass M_2 acting at point 2:

$$M_1 = M_2 = \frac{1}{l_b} \int x\, dm \ldots\ldots\ldots\ldots\ldots\ldots (16b)$$

Eqs. 16 are the expressions for the dynamic reactions for symmetrical modes which, in this case, could be derived from the law of static reactions. For asymmetrical modes, $\phi(1) = -\phi(2)$ and the amplitudes of girder b are $\phi(x) = \phi(1) \dfrac{2\,x - l_b}{l_b}$. The reactions of the inertia forces are

$$R_1 = -R_2 = \frac{\omega^2}{l^2_b}\, \phi(1) \int x\, (2\,x - l_b)\, dm \ldots\ldots\ldots\ldots (17a)$$

and the dynamic reactions for asymmetrical modes become

$$M_1 = M_2 = \frac{1}{l^2_b} \int x\, (2\,x - l_b)\, dm \ldots\ldots\ldots\ldots\ldots (17b)$$

Eq. 17*b* is different from the results for symmetrical modes (Eq. 16*b*). If m is equally distributed, Eq. 16*b* yields $M_1 = \dfrac{m\, l_b}{2}$, whereas Eq. 17*b* yields $M_1 = \dfrac{m\, l_b}{6}$.

By using the concept of dynamic reactions any system A can be reduced to a one-beam system, the normal modes of which can be found.

The Normal Modes of the Original System.—Thus far, the paper has shown how a system of girders can be separated into two idealized systems A and B

called "complementary systems." It remains to demonstrate that the frequencies and normal modes of the original system can be built up from those of systems A and B. The deflections of the original system due to any external load are given by Eq. 10. Furthermore, the deflections of any mechanical system can be expressed in terms of its normal modes by Eq. 5. Applying this equation to each of the two systems A and B,

$$u_A = \sum_i c_{iA}\,\phi_{iA} \qquad \text{and} \qquad u_B = \sum_i c_{iB}\,\phi_{iB} \ldots\ldots\ldots\ldots (18)$$

Eq. 18, substituted in Eq. 10, yields

$$u = \sum_i c_{iA}\,\phi_{iA} + \sum_i c_{iB}\,\phi_{iB} \ldots\ldots\ldots\ldots\ldots\ldots (19)$$

Eq. 19 defines the deflections of the original system due to an arbitrary external load. The coefficients c can be determined from Eq. 6; thus,

$$c_{iA} = \frac{1}{\omega^2{}_{iA}} \int \phi_{iA}\,dP \qquad \text{and} \qquad c_{iB} = \frac{1}{\omega^2{}_{iB}} \int \phi_{iB}\,dP \ldots\ldots (20)$$

Any normal mode ϕ of the original system can be considered as the deflection of the system due to the inertia forces $\omega^2\,m\,\phi$. Applying Eqs. 19 and 20 to this loading, Eq. 19 yields

$$\phi = \sum_i c_{iA}\,\phi_{iA} + \sum_i c_{iB}\,\phi_{iB} \ldots\ldots\ldots\ldots\ldots\ldots (21)$$

Substitution of $dP = \omega^2\,\phi\,dm$ in Eq. 20 gives

$$c_{iA} = \frac{\omega^2}{\omega^2{}_{iA}} \int \phi_{iA}\,\phi\,dm \qquad \text{and} \qquad c_{iB} = \frac{\omega^2}{\omega^2{}_{iB}} \int \phi_{iB}\,\phi\,dm \ldots\ldots (22)$$

The amplitude ϕ is now introduced from Eq. 21 except that, to avoid confusion, a subscript k is substituted for i in the summations:

$$c_{iA} = \frac{\omega^2}{\omega^2{}_{iA}} \left(\int \phi_{iA} \sum_k c_{kA}\,\phi_{kA}\,dm + \int \phi_{iA} \sum_k c_{kB}\,\phi_{kB}\,dm \right) \ldots\ldots (23a)$$

and

$$c_{iB} = \frac{\omega^2}{\omega^2{}_{iB}} \left(\int \phi_{iB} \sum_k c_{kA}\,\phi_{kA}\,dm + \int \phi_{iB} \sum_k c_{kB}\,\phi_{kB}\,dm \right) \ldots\ldots (23b)$$

Eqs. 23 can be written in the form:

$$\frac{\omega^2{}_{iA}}{\omega^2}\,c_{iA} = \sum_k c_{kA} \int \phi_{iA}\,\phi_{kA}\,dm + \sum_k c_{kB} \int \phi_{iA}\,\phi_{kB}\,dm \ldots\ldots (24a)$$

and

$$\frac{\omega^2{}_{iB}}{\omega^2}\,c_{iB} = \sum_k c_{kA} \int \phi_{iB}\,\phi_{kA}\,dm + \sum_k c_{kB} \int \phi_{iB}\,\phi_{kB}\,dm \ldots\ldots (24b)$$

The orthogonality relations (Eqs. 4*b* and 4*c*) supply the following equations:

$$\int \phi_{iA}\,\phi_{kA}\,dm = \left\{\begin{matrix} 0 & \text{if} & i \neq k \\ 1 & \text{if} & i = k \end{matrix}\right\} \quad \ldots\ldots\ldots\ldots\ldots\ldots (25a)$$

and

$$\int \phi_{iB}\,\phi_{kB}\,dm = \left\{\begin{matrix} 0 & \text{if} & i \neq k \\ 1 & \text{if} & i = k \end{matrix}\right\} \quad \ldots\ldots\ldots\ldots\ldots\ldots (25b)$$

For simplicity, substitute

$$\beta_{ik} = \int \phi_{iA}\,\phi_{kB}\,dm \quad \ldots\ldots\ldots\ldots\ldots\ldots (26)$$

and the equations for the coefficients c (Eqs. 24) become simply

$$\left(1 - \frac{\omega^2_{iA}}{\omega^2}\right) c_{iA} + \sum_k \beta_{ik}\,c_{kB} = 0 \quad \ldots\ldots\ldots\ldots\ldots\ldots (27a)$$

and

$$\sum_k \beta_{ki}\,c_{kA} + \left(1 - \frac{\omega^2_{iB}}{\omega^2}\right) c_{iB} = 0 \quad \ldots\ldots\ldots\ldots\ldots\ldots (27b)$$

After changing the "dummy" indexes in Eq. 27*b* from k to j and from i to k, the coefficients c_{kB} can be expressed:

$$c_{kB} = \frac{1}{\dfrac{\omega^2_{kB}}{\omega^2} - 1} \sum_i \beta_{jk}\,c_{jA} \quad \ldots\ldots\ldots\ldots\ldots\ldots (28a)$$

and, by substitution in Eq. 27*b*,

$$\left(1 - \frac{\omega^2_{iA}}{\omega^2}\right) c_{iA} + \sum_{j,k} c_{jA}\,\frac{\beta_{ik}\,\beta_{jk}}{\dfrac{\omega^2_{kB}}{\omega^2} - 1} = 0 \quad \ldots\ldots\ldots\ldots\ldots\ldots (28b)$$

There are as many such equations as there are coefficients c_{iA}. Written fully, these equations become for $i = 1, 2, 3, \cdots, j = 1, 2, 3, \cdots$,

$$\left.\begin{aligned} c_{1A}\left(1 - \frac{\omega^2_{1A}}{\omega^2} + \sum_k \frac{\beta^2_{1k}}{\dfrac{\omega^2_{kB}}{\omega^2} - 1}\right) + c_{2A} \sum_k \frac{\beta_{1k}\,\beta_{2k}}{\dfrac{\omega^2_{kB}}{\omega^2} - 1} + \cdots = 0 \\ c_{1A} \sum_k \frac{\beta_{1k}\,\beta_{2k}}{\dfrac{\omega^2_{kB}}{\omega^2} - 1} + c_{2A}\left(1 - \frac{\omega^2_{2A}}{\omega^2} + \sum_k \frac{\beta^2_{2k}}{\dfrac{\omega^2_{kB}}{\omega^2} - 1}\right) + \cdots = 0 \\ \cdots\cdots\cdots\cdots\cdots\cdots\cdots\cdots\cdots\cdots\cdots\cdots \end{aligned}\right\} \quad \ldots (29)$$

Eqs. 29 comprise a system of linear and homogeneous equations for the coefficients c_{iA}. Such equations are capable of solutions other than $c_{iA} = 0$ only if the determinant Δ of their coefficients vanishes; the condition $\Delta = 0$ is therefore the frequency equation.

To obtain Eqs. 28, it was necessary to divide Eq. 27*b* by $1 - \omega^2{}_{kB}/\omega^2$. This procedure is only permissible if that factor does not vanish; in other words, if ω is not equal to ω_{kB}. Therefore, the determinant of Eq. 28*b* or Eqs. 29 is not reliable as far as possible roots $\omega = \omega_{kB}$ are concerned. An investigation shows that $\omega = \omega_{kB}$ will be a frequency if all the values β_{ik} vanish, but this case is trivial and of no importance. The only other possibility that ω_{kB} may become a frequency of the original system is when ω_{kB} is a multiple frequency of system B. If $\omega_{kB} = \omega_{(k+1),B}$, the possibility of this frequency being a root ω must be investigated.

If $\omega = \omega_{kB} = \omega_{(k+1),B}$, Eqs. 27 will be satisfied if all the coefficients c_A and c_B, except c_{kB} and $c_{(k+1),B}$ vanish and provided that

$$\beta_{i,k}\, c_{kB} + \beta_{i,(k+1)}\, c_{(k+1),B} = 0 \qquad (30)$$

The number of equations similar to Eq. 30 is equal to the number of functions ϕ_{iA} used. If there is more than one mode ϕ_{iA}, Eq. 30 has solutions $c_{kB} \neq 0$ and $c_{(k+1),B} \neq 0$ only if

$$\frac{\beta_{1,(k+1)}}{\beta_{1,k}} = \frac{\beta_{2,k}}{\beta_{2,(k+1)}} = \frac{\beta_{3,(k+1)}}{\beta_{3,k}} = \cdots \qquad (31)$$

which is the necessary condition for $\omega = \omega_{kB}$ being a frequency of the system. If only one mode ϕ_A is used, Eq. 31 is automatically satisfied, and then every double root ω_{kB} creates a root of the original system. This root is not given by Eq. 28*b* and can only be deduced by referring to Eqs. 27.

The question of multiple frequencies requires attention in practical cases because similar girders, or similar groups of girders, are sometimes used repeatedly in a structure; and this fact leads to multiple frequencies ω_{kB} of system B. A case of multiple frequencies ω_{kB} is treated subsequently in Section 4.

The Frequency Equation for Special Cases.—In general, there will be as many Eqs. 29 for the coefficients c_{iA} as there are normal modes ϕ_A. As explained in the next two paragraphs, the number of these modes to be considered is only one or two.

System A is equivalent to a girder carrying a certain distribution of mass. If there are n concentrated masses such a system has n different normal modes. In addition, if part of the mass is distributed, the number of normal modes becomes infinite. All these normal modes can be arranged in order of their frequencies $\omega_{1A} < \omega_{2A} < \omega_{3A} < \cdots \omega_{nA}$. For a system consisting of one girder it will be found that ω_{2A} is considerably higher than ω_{1A}; and ω_{3A}, much higher than ω_{2A}; etc. For an equally distributed load alone the sequence of frequencies is $\omega_{1A}:\omega_{2A}:\omega_{3A} = 1:4:9:\cdots$.

If there were many coefficients, c_{iA}, the computation would become cumbersome and impracticable. Luckily, however, the expansions Eq. 21, show marked convergence and the first few terms give excellent approximations. The values of the coefficients decrease quickly due to the factors $\frac{1}{\omega^2{}_{iA}}$ in Eq. 22. For an equally distributed mass these factors decrease in the ratio $\frac{1}{1}:\frac{1}{16}:\frac{1}{81}:\cdots$, and the third one is practically negligible.

A rule presented subsequently under the heading, "Practical Computations, Number of Modes ϕ_A and ϕ_B" (Section 1) can be used to decide how many modes ϕ_{iA} and ϕ_{kB} should be considered to obtain reliable results. In normal cases this rule requires the use of only one or two modes ϕ_{iA}. If, in addition to a number of modes ϕ_{kB}, only one mode ϕ_{1A} is considered, the frequency equation, $\Delta = 0$, becomes simply

$$\sum_k \frac{\beta^2_{1k}}{\frac{\omega^2_{kB}}{\omega^2} - 1} = \frac{\omega^2_{1A}}{\omega^2} - 1 \quad \ldots\ldots\ldots\ldots\ldots\ldots (32)$$

Eq. 28*a* is used to compute the amplitudes of the normal mode corresponding to any one of the roots ω of this equation; thus,

$$c_{kB} = \frac{\beta_{1k}\, c_{1A}}{\frac{\omega^2_{kB}}{\omega^2} - 1} \quad \ldots\ldots\ldots\ldots\ldots\ldots\ldots\ldots (33)$$

By using Eqs. 25 and 26, the normalizing condition can be transformed; thus,

$$\int \phi^2\, dm = \int (c_{1A}\, \phi_{1A} + \sum_i c_{iB}\, \phi_{iB})^2\, dm$$

$$= c^2_{1A} + 2\, c_{1A} \sum_i c_{1B}\, \beta_{1i} + \sum_i c^2_{iB} = 1 \ldots (34)$$

Making further use of Eq. 27*a* the final form of the normalizing condition is

$$\omega^2_{1A}\, c^2_{1A} + \sum_i \omega^2_{iB}\, c^2_{iB} = \omega^2 \quad \ldots\ldots\ldots\ldots\ldots\ldots (35)$$

Eqs. 33 and 35 are sufficient to determine all the values c_{1A} and c_{iB}.

In addition to the roots of Eq. 32, any multiple frequency $\omega_{kB} = \omega_{(k+1),B}$ of system B is a frequency of the original system, $\omega = \omega_{kB}$. To obtain the amplitudes of the mode corresponding to such a frequency, Eqs. 27 must be used, as demonstrated subsequently in Section 4.

Eqs. 32 to 35 enable the designer to compute the modes and frequencies of a system if the modes and frequencies of the simplified systems A and B are known. System A can always be reduced to a simple beam, the modes of which can be found by various methods. For a system B that consists of a number of ordinary beams the modes ϕ_{iB} and frequencies ω_{iB} are the total of the modes and frequencies of the separate parts of the system. If one of these beams has a certain frequency ω_i and a mode ϕ_i, system B as a whole has the same frequency $\omega_{iB} = \omega_i$. The amplitudes for the corresponding mode for any point within the beam in question are $\phi_{iB} = \phi_i$, whereas for any other point $\phi_{iB} = 0$.

If system B is not of such a simple nature but contains beams supporting one another, a preliminary computation of the modes must be made by applying the method of this paper to system B. Through repeated application of this method, one will reach a stage at which system B becomes a number of simple beams the modes of which can be found.

Discussion of the Frequency Equation.—The frequency equation (Eq. 32) can be represented graphically in a very simple and instructive manner. The abscissas in Fig. 6 are the frequencies ω and the ordinates are the values of the left-hand side of Eq. 32. For $\omega = 0$, all terms of the sum vanish; if ω approaches any one of the values ω_{kB}, one term becomes $\pm\infty$. The full curves in Fig. 6 represent the left side of Eq. 32, and the vertical dotted lines are asymptotes to these curves.

The dotted curves marked *I*, *II*, and *III* in Fig. 6 indicate the value of the right side of Eq. 32 for three different values of ω_{1A}. The quantity $\frac{\omega^2_{1A}}{\omega^2} - 1$ begins with an infinite value for $\omega = 0$, vanishes for $\omega = \omega_{1A}$, and then steadily approaches -1 for $\omega = \infty$.

The natural frequencies of the system are represented by the intersection points of the full and of the dotted curves. Fig. 6 shows that there is always one frequency that is lower than any frequency of systems A and B; and there is one frequency between each of the consecutive frequencies ω_{1B}, ω_{2B}, $\cdots$.

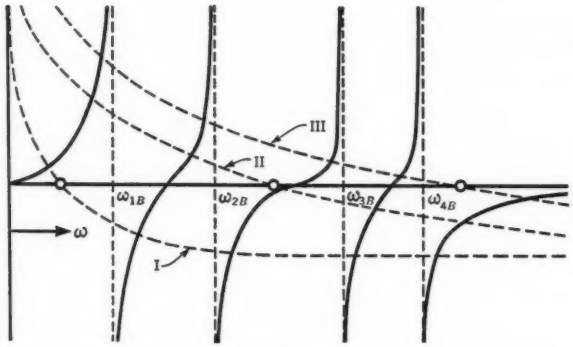

FIG. 6

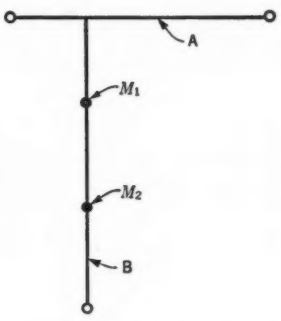

FIG. 7

If there are n frequencies, ω_{iB}, the total number of frequencies will be $n + 1$. This total number can include a trivial root $\omega = \infty$, however, which happens in the special case in which the complete system contains only masses which already form part of system B.

Fig. 7 shows an example of this condition. System B is girder B loaded with two masses. Such a system has two frequencies ω_{1B} and ω_{2B}. System A is girder A loaded with the dynamic reaction of girder B, and has one frequency ω_{1A}. Therefore, the original system should have two plus one, or three, frequencies. The system contains two masses only, however; and it has two degrees of freedom because vertical displacements only are to be counted. For mechanical reasons such a system has two natural frequencies, and no more. The frequency formula (Eq. 32) for this case, therefore, must give two proper roots. The third root must be a trivial root $\omega = \infty$ without physical meaning.

The Flooring.—Thus far only systems of beams supported by one another have been considered. The last element of a floor, however, is the flooring, which may be the open steel type, checker plating, or reinforced concrete slabs,

and it is necessary to show how to introduce the flooring into the computations. Because of the small span between the secondary beams, the flooring will not deflect appreciably from beam to beam, but it must move with the supporting beams and its mass may be a considerable part of the total mass of the structure.

As a first approximation the designer could concentrate the mass of the flooring in the supporting secondary beams; however, to decide if this simplification is justified, it is necessary to make a more precise computation. If the flooring is not continuous over its supporting beams, it can be considered as a number of narrow beams spanning the secondary girders. This assumption reduces the system to a type of structure that has already been treated. In nearly all cases it will be found that the beams that replace the flooring are relatively rigid and have high natural frequencies. It is justifiable, therefore, to regard these beams as entirely rigid—that is, $I = \infty$.

Without presenting details, the result of computations, using finite difference equations, for a structure consisting of n equal secondary beams T_1, T_2, T_3, $\cdots$, T_n, with equal spacing and loading, is as follows: The values of the frequencies are

$$\omega_k = \frac{\pi^2}{l^2}\sqrt{\frac{E\,I}{m_B + \frac{2}{3}\,a\,m_s + \frac{1}{3}\,a\,m_s \cos\frac{k\,\pi}{n+1}}} \quad (k = 1, 2, 3, \cdots, n) \ldots (36)$$

in which m_B is the mass of the beams per unit length; m_s is the mass of the flooring per unit area; l is the span; I is the moment of inertia; and a is the spacing of the beams. The quantity $\cos\frac{k\,\pi}{n+1}$ can vary only between $+1$ and -1 and, therefore, all the frequencies must lie between the limits:

$$\frac{\pi^2}{l^2}\sqrt{\frac{E\,I}{m_B + a\,m_s}} < \omega_k < \frac{\pi^2}{l^2}\sqrt{\frac{E\,I}{m_B + \frac{a\,m_s}{3}}} \ldots\ldots\ldots\ldots (37)$$

To compare Eq. 36 with the frequency obtained if the mass of the flooring is concentrated on the beams, $m_B = m_B + a\,m_s$ and $m_s = 0$ are introduced in Eq. 36; thus,

$$\omega = \frac{\pi^2}{l^2}\sqrt{\frac{E\,I}{m_B + a\,m_s}} \ldots\ldots\ldots\ldots\ldots\ldots\ldots (38)$$

The approximate value ω derived from Eq. 38 is equal to the lower limit for the exact frequencies ω_k. If $n > 2$ or if m_s is small compared to m_B, there will be little difference between the fundamental frequency ω_1 as derived from Eq. 36 and the approximate value of ω derived from Eq. 38.

Therefore, the concentration of the mass of the flooring on the beams is a good approximation for the fundamental frequency if there are more than two secondary beams. If there are two secondary beams, it is still justifiable if $a\,m_s$ is small compared with m_B; but, if higher frequencies are required, a more exact computation must be used. This conclusion remains true if the secondary beams carry unequal masses or are otherwise different.

If the secondary beams are supported by other beams forming part of a more complicated structure, the approximation can still be used as long as the frequencies which are ultimately determined remain below the lowest frequency ω of any of the secondary beams alone. On the other hand, if reliable frequencies higher than the lowest frequency are required, a more exact computation would have to be made. This condition should not occur in practical cases, however, because it would imply that the structure has a considerable number of resonant frequencies within the range of the running frequency which would make the structure unsuitable for its purpose. The difference between the approximate and the more exact solution is shown subsequently in Section 4 for a special case.

Practical Computations.—

Mass Distribution.—To obtain correct results it is of the utmost importance that the mass distribution used for the computation shall represent the actual distribution under working conditions. It would be quite erroneous to include the mass of the accidental live load, as specified for the design, in the customary manner. In most cases only the permanent load needs to be considered; but, if considerable live loads, such as those in water tanks or coal bunkers, can occur at the same time as dynamic forces generated by machines in operation, it becomes necessary to investigate two cases—the structure with live load and the structure without live load.

Another consideration is the matter of accounting for the mass of machines. A machine can usually be regarded as a rigid body supported by the structure at three or more points. Structural engineers are likely to assume that the total mass of such a machine distributes itself over the points of support in the same ratio as the static reactions. This assumption is rarely justified. A correct procedure for replacing a machine by its "dynamic reactions" at the points of support is treated in Section 3.

Number of Modes ϕ_A and ϕ_B.—As stated, it is not necessary to use all the frequencies and normal modes of the complementary systems A and B, but the higher modes can be neglected. The decision as to which modes should be retained depends on the value of the frequencies to be investigated. To be sure that a certain frequency ω_i, found by these computations, is reasonably exact, all the frequencies up to $2\,\omega_i$ should be used. It is quite obvious, furthermore, that at least one mode of each system must be considered. If system B consists of a number of separate girders, one mode of each of these should be retained.

To check the suitability of a structure for a certain frequency ω, only the resonant frequencies up to about $1.5\,\omega$ are required. Then, the limit for the frequencies of the complementary systems is $2 \times 1.5\,\omega = 3\,\omega$. Frequently this rule requires the use of only one mode of system A, and of only one mode of each of the girders forming system B.

Factor of Safety Against Resonance.—After finding the natural frequencies of a system they must be compared with the frequency of the machines carried. If the machines run at variable speed, an entire range of frequencies must be regarded as dangerous. To obtain the smallest possible vibratory deflections and to avoid resonance during the starting of the machines, the running fre-

quency should be sufficiently lower (40% being a safe margin) than the fundamental frequency of the structure.

If this condition cannot reasonably be fulfilled, either because the running speed is high or because the span of the structure is large, the system will still prove satisfactory if the running speed is kept clear of the nearest resonant frequencies. It is essential, however, that as few frequencies as possible be below the running speed.

Concrete and Reinforced Concrete.—If the structure is concrete or if steel beams incased in concrete are used, an uncertainty is introduced because the value of E for concrete varies considerably. The only safe procedure is to determine the frequencies for limiting values of E and to regard the entire range between these frequencies as dangerous. When fixing these limits, it should be kept in mind that vibrations of structures must be restricted to small amplitudes and, therefore, to low vibratory stresses. The value of E for such low stresses is likely to be higher than the values of E used for stress computations.

Subsequent Alteration of Sections.—If the frequencies of a system are found to be unsatisfactory, the moments of inertia of some of the members are altered and the determination of the frequencies is repeated. It is not necessary to repeat the entire computation if the following property of the modes is used:

> Theorem II.—If all the moments of inertia, I, of the beams of a system are changed to αI and if the ratio α is the same for all beams and the mass distribution remains the same, the frequencies $\omega_1, \omega_2, \cdots$, of the original system are changed to $\sqrt{\alpha}\,\omega_1, \sqrt{\alpha}\,\omega_2, \cdots$. The numerical values of the amplitudes of the normal modes $\phi_1, \phi_2, \cdots$, corresponding to these frequencies remain entirely unaffected by such a change.

Theorem II may be applied to any system. It can be useful if changes are made in the moments of inertia which affect only the beams of one of the complementary systems. By the terms of this theorem the modes of this complementary system can be used again, and only the frequencies remain to be adjusted.

Systems That Include Statically Indeterminate Beams.—At the beginning of Section 1 the discussion was restricted to statically determinate arrangements of floors; but the method developed can be applied without modification to floors that include statically indeterminate members as long as the arrangement of the beams is such that the reactions from each beam on the others are statically determinate.

Consider the floor shown in plan in Fig. 1 and assume beam A to be part of a portal frame consisting of beam A and its supporting columns. The structure as a whole is statically indeterminate, but the reactions from the secondary beams on beam A remain statically determinate.

This type of structure can be dealt with by the method of "complementary systems" because the fundamental Eq. 10 applies. By this method it is possible to reduce the floor system gradually to one of the basic types of statically indeterminate structures, like continuous beams or portal frames. Such struc-

tures can be dealt with by known methods—as, for example, those explained in Section 3.

Statically indeterminate floors of other types require different treatment and are considered in Section 2.

2. Theory Applied to Statically Indeterminate Structures

The procedures explained in Section 1 apply only to structures that are statically determinate or that belong to a special type of indeterminate systems mentioned at the very end of Section 1. Frequently beams are continuous because their end connections are rigid and able to transfer bending moments. To estimate the influence of rigid connections and to treat floors that contain continuous beams, or are otherwise indeterminate, the method developed in Section 1 is extended, as follows:

First, imagine that all the continuous beams are cut into simple beams, leaving a floor system of statically determinate elements. Frequencies ω_i and normal modes ϕ_i of such a system can be found by the procedure in Section 1.

Next (as in the theory of statically indeterminate structures), assume that moments X_k act on each of the points k where the continuous beams were cut. Each of the moments $X_k = 1$ acting alone on the statically determinate basic structure creates certain deflections, ψ_k. If a system is symmetrical, it is advantageous to treat symmetrical and asymmetrical modes separately. For symmetrical modes a symmetrical arrangement of moments $X_k = X'_k = 1$ can be selected as statically indeterminate values whereas for asymmetrical modes $X_k = -X'_k = 1$ is a suitable indeterminate value.

Since the deflections u of any statically indeterminate structure are equal to the deflections u_d of the statically determinate basic structure due to the same load, plus the deflections u_X due to the statically indeterminate moments X_k, the former can be expressed by the normal modes of the basic structure $u_d = \sum_i c_i \phi_i$ (see Eq. 5) and the latter are $u_X = \sum_k X_k \psi_k$. The amplitude of the normal mode, ϕ, of the statically indeterminate system can be found as the deflections u of the system due to the inertia loading $\omega^2 \phi \, dm$, from which

$$\phi = \sum_i c_i \phi_i + \sum_k X_k \psi_k \quad \ldots\ldots\ldots\ldots\ldots\ldots (39)$$

The coefficients c_i in this expansion are defined by Eq. 6 which (after introducing $dP = \omega^2 \phi \, dm$) yields

$$c_j = \frac{\omega^2}{\omega^2_j} \int \phi \, \phi_j \, dm = \frac{\omega^2}{\omega^2_j} \sum_i c_i \int \phi_i \, \phi_j \, dm + \frac{\omega^2}{\omega^2_j} \sum_k X_k \int \psi_k \, \phi_j \, dm \ldots (40)$$

Using the orthogonality relations (Eq. 4*b* and Eq. 4*c*) the first sum on the right-hand side can be reduced to c_j. Then, replacing the dummy index j by i and introducing the abbreviation:

$$\beta_{ik} = \int \phi_i \, \psi_k \, dm \quad \ldots\ldots\ldots\ldots\ldots\ldots (41)$$

the resulting form is

$$\left(\frac{\omega^2_i}{\omega^2} - 1\right) c_i = \sum_k \beta_{ik} X_k \ldots\ldots\ldots\ldots\ldots\ldots (42)$$

There are as many such equations as there are coefficients c_i.

Additional relations can be obtained from the theory of statically indeterminate structures. If the moments due to any loading P on a statically indeterminate structure are $\bar{M}_p$ and if the moments created by the action of any statically indeterminate moment $X_j = 1$ on the statically determinate basic structure are $\bar{m}_j$, then the condition—

$$\int \frac{\bar{M}_p \bar{m}_j}{E I} dx = 0 \ldots\ldots\ldots\ldots\ldots\ldots (43)$$

—must be satisfied. The integral has to be applied to all the beams of the system. If Eq. 43 is applied to the present system loaded with the inertia forces $\omega^2 \phi\, dm$, the moment $\bar{M}_p$ can be expressed by second derivative of the deflections ϕ of the system.

$$\bar{M}_p = - E I \phi'' \ldots\ldots\ldots\ldots\ldots\ldots (44a)$$

By definition ψ_j is the deflection of the basic system due to the action of $X_j = 1$. Therefore,

$$\bar{m}_j = - E I \psi''_j \ldots\ldots\ldots\ldots\ldots\ldots (44b)$$

If these values are substituted for $\bar{M}_p$ and $\bar{m}_j$ in Eq. 43,

$$\int E I \phi'' \psi''_j\, dx = 0 \ldots\ldots\ldots\ldots\ldots\ldots (45)$$

Substitution of the expansion (Eq. 39) in Eq. 45 yields

$$\sum_i c_i \int E I \phi''_i \psi''_j\, dx + \sum_k X_k \int E I \psi''_k \psi''_j\, dx = 0 \ldots\ldots\ldots (46)$$

The integral in the first term of Eq. 46 is the well known expression for the virtual work done by the loading $\omega^2_i \phi_i\, dm$, which creates the deflection ϕ_i, if the system undergoes a deflection ψ_j. According to Betti's law this virtual work must be equal to the virtual work done by the moment $X_j = 1$ if the system undergoes a deflection ϕ_i.

The virtual work done by the loads $\omega^2_i \phi_i\, dm$ on the deflection ψ_j is obviously $\int \omega^2_i \phi_i \psi_j\, dm$; and, with reference to Eq. 41, $\int \omega^2_i \phi_i \psi_j\, dm = \omega^2_i \beta_{ij}$. The virtual work done by the moments $X_j = 1$ on the deflection ϕ_i is $1 \times \gamma_{ij} = \gamma_{ij}$, in which γ_{ij} is the angle between the two tangents to the curve ϕ_i at point j. Therefore,

$$\int E I \phi''_i \psi''_j\, dx = \omega^2_i \beta_{ij} = \gamma_{ij} \ldots\ldots\ldots\ldots\ldots (47)$$

The integrals in the second term of Eq. 46 can be interpreted in a similar manner. They represent the angle α_{kj} between the two tangents to ψ_k at point j,

$$\int E\,I\,\psi''_k\,\psi''_j\,dx = \alpha_{kj} \ldots\ldots\ldots\ldots\ldots\ldots (48)$$

The value α_{kj} can easily be computed by differentiation of ψ_k. Substitution of Eqs. 47 and 48 into Eq. 46 yields

$$\sum_i \omega^2_i\,\beta_{ij}\,c_i + \sum_k \alpha_{jk}\,X_k = 0 \ldots\ldots\ldots\ldots\ldots\ldots (49)$$

There are as many such equations as there are statically indeterminate values of X_j. Eqs. 42 and 49 form a set of linear and homogeneous equations for the values of c_i and X_i. Such equations have solutions $c_i \neq 0$ and $X_i \neq 0$ only if the determinant Δ of their coefficients vanishes. The condition $\Delta = 0$ is therefore the frequency equation.

To obtain normalized solutions the coefficients c_i and X_i must be determined in such a way that Eq. 4*b* is satisfied. The normalizing condition can be brought into the form:

$$\sum_i c^2_i\,\omega^2_i - \sum_{j,k} \alpha_{jk}\,X_j\,X_k = \omega^2 \ldots\ldots\ldots\ldots\ldots\ldots (50)$$

To apply the formulas derived in Section 2 it is first necessary to find the values of the coefficients β_{ij} defined by Eq. 41. There would be no fundamental difficulty in computing the value of the integral in Eq. 41, but Eq. 47 gives an alternative relation which avoids the determination of any integral. From the right-hand side of Eq. 47,

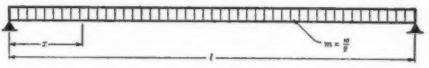

FIG. 8

$$\beta_{ij} = \frac{1}{\omega^2_i}\,\gamma_{ij} \ldots\ldots\ldots\ldots\ldots\ldots\ldots (51)$$

in which γ_{ij} is the angle between the two tangents of ϕ_i at point j. This angle is positive if X_j does positive work during its formation.

3. FORMULAS FOR REFERENCE

Formulas for Frequencies and Modes of Simple Beams.—A beam with distributed mass $m = \frac{w}{g}$, as shown in Fig. 8, has the frequencies:

$$\omega_i = \frac{i^2\,\pi^2}{l^2}\sqrt{\frac{E\,I}{m}} = 25{,}500\,\frac{i^2}{l^2}\sqrt{\frac{I}{w}} \ldots\ldots\ldots\ldots\ldots (52)$$

in which l is measured in feet, I, in inches^4, w, in pounds per foot, and $E = 30{,}000{,}000$ lb per in.^{2}. The normal modes are

$$\phi_i = \sqrt{\frac{2}{m\,l}}\,\sin\frac{i\,\pi\,x}{l}\ (i = 1, 2, 3, \cdots) \ldots\ldots\ldots\ldots\ldots (53)$$

The value of the following integral is frequently required:

$$\int_0^l m \frac{x}{l} \phi_i \, dx = (-1)^{i-1} \frac{\sqrt{2\,m\,l}}{i\,\pi} \quad \ldots\ldots\ldots\ldots\ldots\ldots (54)$$

Beams or Other Structures Carrying a Small Number of Concentrated Masses. —The masses are M_1 at point 1, M_2 at point 2, etc., as shown in Fig. 9. If such a system vibrates with the circular frequency ω and the amplitudes are $y_1, y_2, \cdots$, the inertia forces acting at points 1, 2, $\cdots$ are $\omega^2 M_1 y_1, \omega^2 M_2 y_2$, etc. These inertia forces cause the deflections of the system; and, if the deflections due to these forces are determined, the result must be equal to the original amplitudes y_1, y_2, etc. This relationship can be used to find the natural frequencies and modes of such a system.[3]

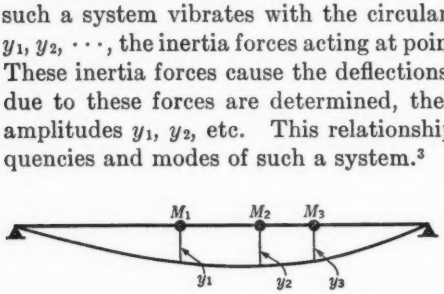

FIG. 9

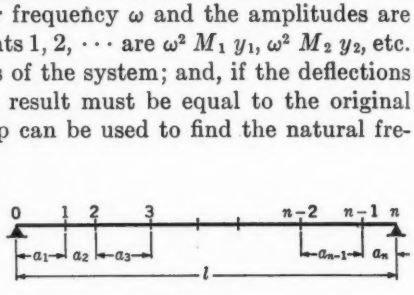

FIG. 10

If the influence numbers δ_{ik} (which indicate the deflection at any point k due to a unit load at point i) are used, the deflection y_1 due to the inertia forces can be expressed in the form:

$$y_1 = \omega^2 M_1 y_1 \delta_{11} + \omega^2 M_2 y_2 \delta_{21} + \omega^2 M_3 y_3 \delta_{31} + \cdots \quad \ldots\ldots\ldots\ldots (55)$$

Eq. 55, and similar equations for points 2, 3, $\cdots$, can be rearranged:

$$\left.\begin{aligned} \left(M_1 \delta_{11} - \frac{1}{\omega^2}\right) y_1 + M_2 \delta_{21} y_2 + \cdots &= 0 \\ M_1 \delta_{12} y_1 + \left(M_2 \delta_{22} - \frac{1}{\omega^2}\right) y_2 + \cdots &= 0 \\ \cdots\cdots\cdots\cdots\cdots\cdots\cdots\cdots & \end{aligned}\right\} \quad \ldots\ldots\ldots\ldots (56)$$

If there are n masses, there are n such equations for the n values of y_i. Eqs. 56 are homogeneous and have only trivial solutions $y_i = 0$ unless the determinant Δ of these equations vanishes. Therefore, $\Delta = 0$ is the frequency equation:

$$\Delta \equiv \begin{vmatrix} M_1 \delta_{11} - \frac{1}{\omega^2} & M_2 \delta_{21} \cdots \\ M_1 \delta_{12} & M_2 \delta_{22} - \frac{1}{\omega^2} \cdots \\ \cdots\cdots\cdots\cdots\cdots & \end{vmatrix} = 0 \quad \ldots\ldots\ldots\ldots (57)$$

Eqs. 57 are of the nth order in terms of $1/\omega^2$ and have n roots which need not all be different. It can be shown that all these roots $1/\omega^2$ are positive and real. Each root can be introduced in Eqs. 56 yielding a set of amplitudes y_i for each frequency ω.

[3] "Mechanical Vibrations," by J. P. Den Hartog, McGraw-Hill Book Co., Inc., New York, N. Y., 2d Ed., 1940, p. 149.

Every set of values y_i can be multiplied by an arbitrary factor. If this factor is suitably chosen, the normalizing condition is satisfied and the amplitudes y_i become the normal mode ϕ. The normalizing condition is

$$\sum_i M_i \phi^2 = 1 \quad \ldots\ldots\ldots\ldots\ldots\ldots\ldots\ldots (58)$$

This method is very suitable for systems with a small number of masses. If the number is high, the computations become rather involved, but approximate solutions can be derived by the matrix method.[4] The latter is not explained in this paper because such cases can be solved by the Stodola-Vianello method, which is based on the same principle. The Stodola-Vianello method is the more advantageous because it is more akin to engineers than the rather mathematical matrix method.

The Method of Stodola-Vianello.—The principle of this method is as follows:

To obtain a series of approximations of the fundamental mode assume a first approximation $y^{(1)}$ by pure guessing. Then, compute the deflections of the system due to the loading $m\, y^{(1)}$. If $y^{(1)}$ were the exact mode ϕ, or a multiple $c\,\phi$ of it, the resulting deflection $y^{(2)}$ would be equal to $\frac{1}{\omega^2} y^{(1)}$, because the deflections of any system due to the inertia loading $\omega^2\, m\, \phi$ corresponding to a normal mode ϕ are equal to this same mode ϕ. Since the amplitude $y^{(1)}$ is somewhat like ϕ, the amplitude $y^{(2)}$ will still be roughly similar in shape to that of $y^{(1)}$ but it will be on a different scale because of the factor $1/\omega^2$.

It can be proved that $y^{(2)}$ is nearer to the correct shape of the principal oscillation than is $y^{(1)}$. If the process is repeated, a series of approximations $y^{(1)}, y^{(2)}, y^{(3)}, \cdots$ are obtained. After a few steps these curves do not differ in shape any more—they differ only in scale and the ratios $y^{(1)}/y^{(2)}, y^{(2)}/y^{(3)}, \cdots$ are approximate values of ω^2. The most exact value is the average value of the last two steps:

$$\omega^4 = \frac{\int [y^{(n-1)}]^2\, dm}{\int [y^{(n)}]^2\, dm} \quad \ldots\ldots\ldots\ldots\ldots\ldots\ldots\ldots (59)$$

Any method, graphical or numerical, can be used to find the consecutive deflections $y^{(1)}, y^{(2)}, y^{(3)}, \cdots$. The foregoing procedure can be applied to statically determinate as well as indeterminate structures.

One suitable method of finding the deflections of beams with either constant or variable moment of inertia I is to divide the beams in a number of short segments a (see Fig. 10) for which the moments of inertia can be assumed to be constant, and to concentrate the masses in the division points 1, 2, 3, $\cdots$. Then, the moments $\bar{M}_i$ at the division points due to the inertia loading are determined.

According to the theorem of "elastic weights" the deflections of a girder are equal to the bending moments in a beam of equal span created by the

[4] "Mathematical Methods in Engineering," by T. von Kármán and M. A. Biot, McGraw-Hill Book Co., Inc., New York, N. Y., 1940, pp. 196–204.

"elastic weights" $w_1, w_2, w_3, \cdots$.[5] Excluding framed structures, these weights w_i are given by the formula:

$$w_i = \frac{a_i}{6\,E\,I_i}(\bar{M}_{i-1} + 2\,\bar{M}_i) + \frac{a_{i+1}}{6\,E\,I_{i+1}}(2\,\bar{M}_i + M_{i+1}) \quad \ldots\ldots (60a)$$

If the intervals a_i and the moments of inertia I_i are constant, Eq. 60*a* becomes

$$w_i = \frac{a}{6\,E\,I}(\bar{M}_{i-1} + 4\,\bar{M}_i + \bar{M}_{i+1}) \quad \ldots\ldots (60b)$$

If this method of "elastic weights" is used, the entire computation can be arranged in tabular form as shown subsequently in Section 4.

Since the masses M_i are now concentrated at the division points, the integrals in Eq. 59 change into sums:

$$\omega^4 = \frac{\sum M_i\,[y^{(n-1)}]^2}{\sum M_i\,[y^{(n)}]^2} \quad \ldots\ldots (61)$$

The amplitudes of the principal mode y are finally multiplied by a factor c and become the normal mode $\phi = c\,y$. This factor c is found from the normalizing condition:

$$\sum_i M_i\,\phi^2 = 1 \quad \ldots\ldots (62)$$

If a system is symmetrical, the method can be used to find the lowest symmetrical and the lowest asymmetrical modes. These two modes are obtained by starting once with a symmetrical curve $y^{(1)}$, and once with an asymmetrical curve $y^{(1)}$.

A Generalization of the Stodola-Vianello Method.—The Stodola-Vianello method can be used to find the fundamental frequency of simple beams but it is possible to extend it further and to determine higher frequencies. Making use of the fact that the fundamental mode ϕ_1 and any higher mode ϕ are orthogonal,

$$\int \phi_1\,\phi\,dm = 0 \quad \ldots\ldots (63a)$$

the designer can find the second mode by the same procedure, if he begins with an assumed first approximation $y^{(1)}$ which is orthogonal to ϕ_1; thus,

$$\int \phi_1\,y^{(1)}\,dm = 0 \quad \ldots\ldots (63b)$$

Functions $y^{(1)}$ which satisfy this condition can be expressed and found by the formula:

$$y^{(1)} = \bar{y} - \phi_1 \int \phi_1\,\bar{y}\,dm \quad \ldots\ldots (64)$$

[5] "Statically Indeterminate Stresses," by J. I. Parcel and G. A. Maney, John Wiley & Sons, Inc., New York, N. Y., 2d Ed., 1936, p. 47.

in which $\bar{y}$ is an arbitrary function. This relation can easily be checked by substituting it in Eq. 63*b*.

Beginning with a function $y^{(1)}$ according to Eq. 64 further approximations can be obtained by following the same procedure as for the first mode. If the first mode is known exactly, it would be sufficient to start with a function $y^{(1)}$ which is orthogonal to ϕ_1 and every subsequent approximation would remain orthogonal to ϕ_1; but ϕ_1 is known approximately only, and, therefore, Eq. 64 gives a function $y^{(1)}$ which is approximately orthogonal in relation to the exact amplitudes ϕ_1. Therefore, it is necessary to insure that $y^{(4)}$ remains orthogonal to ϕ_1 by applying Eq. 64 to the subsequent approximations $y^{(2)}$, $y^{(3)}$, $\cdots$.

If further modes are required the same process can be used, but the normalizing condition—

$$y = \bar{y} - \phi_1 \int \phi_1 \bar{y}\, dm - \phi_2 \int \phi_2 \bar{y}\, dm - \cdots \quad (65)$$

—must be employed. This procedure insures that the approximations are orthogonal to all the lower modes which are already known. The convergence of the process for higher frequencies is not as good as for the fundamental one; but the first four or five frequencies can be computed with reasonable accuracy.

Replacing Rigid Bodies by Their Dynamic Reactions.—The masses supported by a beam frequently comprise machines that can be considered as rigid bodies. For computations it is desirable to replace such bodies by equivalent imaginary masses placed at the points of support. This can be done by using the concept of "Dynamic Reactions" described in Section 1.

A common case is shown in Fig. 11(*b*). The machine is supported at four points 1, 2, 3, and 4 which rest on the girders T_1 and T_2. Such an arrangement is statically indeterminate because a rigid body requires only three supports.

There is an important case in which this difficulty disappears. If axis $y-y$ is an axis of symmetry of the machine and if the amplitudes of girders T_1 and T_2 are equal, or approximately equal, each girder carries one half of the load. The mass supported by girder T_1 is M and equals half the total mass of the machine (see Fig. 11(*a*)); J is the polar moment of the mass M in relation to point O, which is the projection of the center of gravity on the girder axis. If the beam oscillates with amplitudes y_1 and y_2 as shown in (Fig. 11(*a*)), the movement of the machine consists of a vertical movement and of a rotation around point O. Therefore, the inertia forces are a vertical force $\omega^2 M \frac{l_b y_1 + l_a y_2}{l_a + l_b}$ and a couple $\omega^2 J \frac{y_1 - y_2}{l_a + l_b}$. Their reactions at point 1 and point 2 are

$$R_1 = \omega^2 M \frac{l_b^2 y_1 + l_a l_b y_2}{(l_a + l_b)^2} + \omega^2 J \frac{y_1 - y_2}{(l_a + l_b)^2} \quad (66a)$$

and

$$R_2 = \omega^2 M \frac{l_a l_b y_1 + l_b^2 y_2}{(l_a + l_b)^2} - \omega^2 J \frac{y_1 - y_2}{(l_a + l_b)^2} \quad (66b)$$

Imaginary masses at points 1 and 2 would create inertia forces:

$$R_1 = \omega^2 M_1 y_1 \quad \text{and} \quad R_2 = \omega^2 M_2 y_2 \quad (67)$$

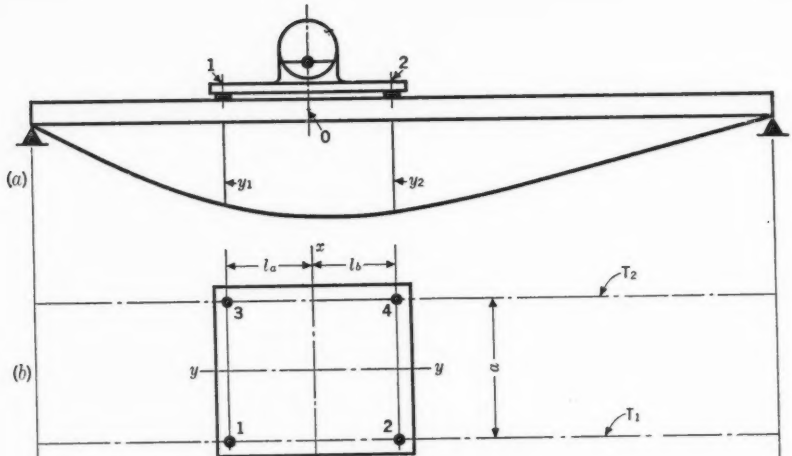
1
2
0
(a)
y_1
y_2
x
l_a
l_b
T_2
3
4
(b)
y
y
a
T_1
1
2
x
x
l_a
l_b
T_2
3
4
5
(c)
y
y
a
1
2
T_1
x

FIG. 11

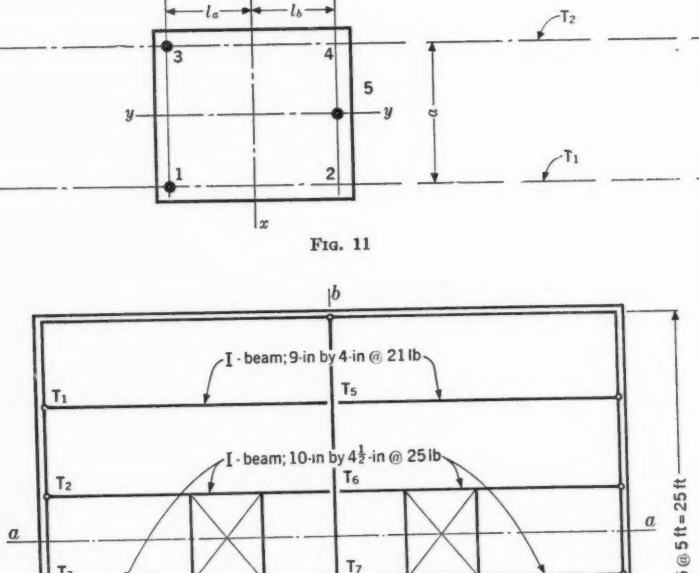
b
I - beam; 9-in by 4-in @ 21 lb
T_1
T_5
I - beam; 10-in by 4½-in @ 25 lb
T_2
T_6
a
a
T_3
T_7
4 ft
4 ft
4 ft
4 ft
I - beam; 9-in by 4-in @ 21 lb
T_4
T_8
I - beam; 20-in by 6½-in @ 65 lb
5 @ 5 ft = 25 ft
16 ft
16 ft
b

FIG. 12

Accordingly, the machine can be replaced by the imaginary masses:

$$M_1 = \frac{l^2_b\, M + J}{(l_a + l_b)^2} + \frac{l_a\, l_b\, M - J}{(l_a + l_b)^2}\,\frac{y_2}{y_1} \quad \ldots\ldots\ldots\ldots\ldots (68a)$$

and

$$M_2 = \frac{l^2_a\, M + J}{(l_a + l_b)^2} + \frac{l_a\, l_b\, M - J}{(l_a + l_b)^2}\,\frac{y_1}{y_2} \quad \ldots\ldots\ldots\ldots\ldots (68b)$$

These fictional masses M_1 and M_2 still depend on the ratio y_1/y_2 but they can, nevertheless, be used for frequency computations without any difficulty (see Section 4). Eqs. 68 apply for the case of equal amplitudes $y_1 = y_2$, in the form:

$$M_1 = M\,\frac{l_b}{l_a + l_b} \qquad \text{and} \qquad M_2 = M\,\frac{l_a}{l_a + l_b} \quad \ldots\ldots\ldots\ldots (69)$$

Eq. 69 indicates a mass distribution according to the law of statical reactions. It is correct to use Eq. 69 only if the amplitudes of the points of support are equal or at least approximately equal.

If the machine is not symmetrical or if the girders T_1 and T_2 do not deflect equally, it is necessary to remove one of the redundant supports, analyze the remaining system, and afterward consider the effect of the reintroduction of this support by the method developed in Section 2 for statically indeterminate structures.

To demonstrate the principle, consider again the machine shown in Fig. 11(*b*). The machine still has the axis of symmetry $y-y$ but the deflections of T_1 and T_2 are assumed to be different.

The total mass of the machine is 2 M and there will be two polar moments J_x and J_y which refer to axes parallel to $x-x$ and $y-y$, respectively. In order not to lose the advantage of the symmetry but still to obtain a statically determinate case, remove the supports at points 2 and 4 and support the machine instead at point 5 halfway between points 2 and 4 by an imaginary rigid girder that rests on girders T_1 and T_2 at points 2 and 4 (see Fig. 11(*c*)).

Expressions for the fictional masses M_1, M_2, M_3, and M_4 as functions of the amplitudes y_1, y_2, y_3, and y_4 can be derived in a manner similar to that used for Eqs. 68. The frequencies and modes of the system carrying these imaginary masses can then be found by the method given in Section 1. The modes of this statically determinate basic system can then be used, as explained in Section 2, to find the frequencies and modes of the actual statically indeterminate system. The statically indeterminate values X defined in Section 2, in this case, are a couple of vertical forces acting at points 2 and 4 on the machine, and an opposite couple of equal size acting at points 2 and 4 on the girders T_1 and T_2. The value of these couples will be such that the imaginary gap between the machine and the supporting girders is closed.

It should be emphasized that, to obtain fairly exact results, it is really necessary to use the procedure indicated in this subsection. To distribute the mass M over the supports simply following the laws of static reactions and to disregard the restraint due to the indeterminate four-point support of machines would lead to considerable errors in the frequencies (particularly in the higher

frequencies) except when the machines represent only a small part of the total mass of the system.

The dynamic reactions thus found are used to replace the actual masses of rigid bodies all through the computations. To determine the value of an expression such as $\int \phi^2\, dm$, the amplitudes y_i in Eqs. 68 must be interpreted to mean the values of ϕ at points i. In the case of an integral $\int \phi_A\, \phi_B\, dm$, the dynamic reactions can be computed by introducing the amplitudes of either ϕ_A or ϕ_B into these equations; but ϕ_A, or ϕ_B, must be used consistently for all dynamic reactions. The final value of the integral does not depend on which of the two is used.

4. Illustrative Example

To demonstrate the application of the theory developed in Section 1, consider a rather simple example which, nevertheless, will serve as a guide to procedure in more complicated cases. The structure is shown in Fig. 12. The 25-ft-span cross girder T_9 supports eight secondary 16-ft-span floor beams T_1 to T_8, which in turn carry open steel flooring $1\frac{1}{2}$ in. deep weighing 14 lb per sq ft. The secondary beams T_2, T_3, T_6, and T_7 carry two identical machines, each weighing 6,720 lb, including the base but without any impact allowance. The beams shown in Fig. 12 are British standard sections, and would be suitable to carry the dead load, the weight of the machines plus 50% impact, and a distributed live load of 100 lb per sq ft. It is desired to investigate whether this structure is safe against resonance if the machines run at 320 rpm.

Only the masses that are on the structure under working conditions should be taken into account. These are the masses of the flooring, of all the beams, and of the machines without impact. Under normal working conditions no appreciable live load occurs and no allowance will be made for it. For the computation of the lowest frequency of a system the distributed mass of the flooring can be assumed concentrated on the secondary floor beams (see Section 1). Making use of this simplification, the system consists of only the nine girders T_1 to T_9.

The system has two axes of symmetry $a-a$ and $b-b$ as indicated in Fig. 12. In general, computations can be simplified by considering symmetrical and asymmetrical modes separately. In this particular case it is advantageous to use the axis of symmetry $a-a$ and the modes which are symmetrical in relation to $a-a$ are considered separately from those which are asymmetrical in relation to $a-a$. For structures that do not contain continuous beams the lowest frequency corresponds, as a rule, to a symmetrical mode and, therefore, the designer needs to compute symmetrical modes only. In computations of this nature it is essential to keep the dimensions uniform. Throughout this example all distances are in inches, weights are in pounds, and time is in seconds —unless definitely stated otherwise. The acceleration of the earth in these dimensions is $g = 386$ in. per sec.^{2}.

Choice of Complementary Systems.—As explained in Section 1, the system is divided into two complementary systems A and B. Girder T_9 (Fig. 12) is the

only one that rests entirely on external supports. To form system B, therefore, assume girder T_9 to have $I_9 = \infty$, all other girders retaining their actual moments of inertia. System A is obtained by leaving the moment of inertia of girder T_9 at its original value, the value of I to be ∞ for all other girders. Referring to system B, the assumption $I_9 = \infty$ transforms all the girders T_1 to T_8 into simple beams on fixed supports. The normal modes of system B, therefore, comprise all the modes of the girders T_1 to T_8. These modes can be found by the methods in Section 3. The choice of complementary systems, in this case, has not been influenced by any consideration of symmetry; these systems can be used for both types of modes, symmetrical and asymmetrical.

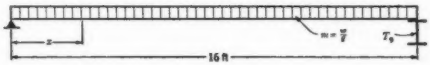

FIG. 13

The Normal Modes of System B.—System B consists of the eight secondary beams which (as a result of the simplification concentrating the mass of the flooring on the beams) oscillate independently from each other. The four girders T_1, T_4, T_5, and T_8 (see Fig. 13) are mechanically alike and carry an equal mass. Their frequencies and modes must be identical. The equally distributed load w is $5 \times 14 + 21 = 91$ lb per ft. The total mass per girder is $m\,l = \frac{w\,l}{g} = \frac{91 \times 16}{386} = 3.77 \frac{\text{lb-sec}^2}{\text{in.}}$. The moment of inertia is $I = 81.13$ in.^{4} For $i = 1$, Eq. 52 gives the fundamental frequency of these beams as: $\omega_{1B} = \omega_{4B} = \omega_{5B} = \omega_{8B} = \frac{25{,}500}{16^2}\sqrt{\frac{81.13}{91}} = 94.0$. The amplitudes of the modes are given by Eq. 53: $\phi_{1B} = \phi_{4B} = \phi_{5B} = \phi_{8B} = \sqrt{\frac{2}{m\,l}} \sin \frac{\pi\,x}{l} = 0.728 \sin \frac{\pi\,x}{l}$. From Eq. 54, $\int_0^l m \frac{x}{l} \phi_{1B}\,dx = \int_0^l m \frac{x}{l} \phi_{4B}\,dx = \int_0^l m \frac{x}{l} \phi_{5B}\,dx = \int_0^l m \frac{x}{l} \phi_{8B}\,dx = \frac{\sqrt{2\,m\,l}}{\pi} \times \frac{\sqrt{2 \times 3.77}}{\pi} = 0.874$. The dynamic reactions of each of these beams on girder T_9 are: $M_1 = M_4 = M_5 = M_8 = \frac{m\,l}{3} = \frac{3.77}{3} = 1.26$.

To decide if higher modes of these beams are required the rule given in Section 1—that only frequencies below $3\,\omega$ need to be considered—is applied. The machines run at 320 rpm which yields $\omega = \frac{2\,\pi \times 320}{60} = 33.5$; and, consequently, modes corresponding to frequencies greater than $\omega = 100$ can be neglected. As the fundamental frequency of these beams is already 94, no higher modes are required, and the designer can proceed to the more complicated task of finding the modes of the girders T_2, T_3, T_6, and T_7. These latter girders are again equal in dimensions and mass and must have identical frequencies and modes.

Each machine is carried by two secondary girders. The arrangement is symmetrical, and the computation is concerned with modes that are symmetrical to axis $a-a$. Section 3 describes how such a machine should be

replaced by concentrated masses; and the present case is one to which Eqs. 68 apply.

As shown in Fig. 14(*a*), each of these girders carries distributed load and one half of a machine. The moment of inertia of these girders is $I = 122.3$ in.^{4} The distributed weight is $w = 5 \times 14 + 25 = 95$ lb per ft, the mass is $m = \frac{95}{386} = 0.246 \frac{\text{lb-sec}^2}{\text{in-ft}}$. The weight of each machine is 6,720 lb, of which one half is carried by each girder. The mass, therefore, is $M = \frac{6{,}720}{2 \times 386}$ $= 8.70 \frac{\text{lb-sec}^2}{\text{in.}}$. To replace the machine by its dynamic reactions at the points of support A and B, the polar moment J of the machine is required. If this

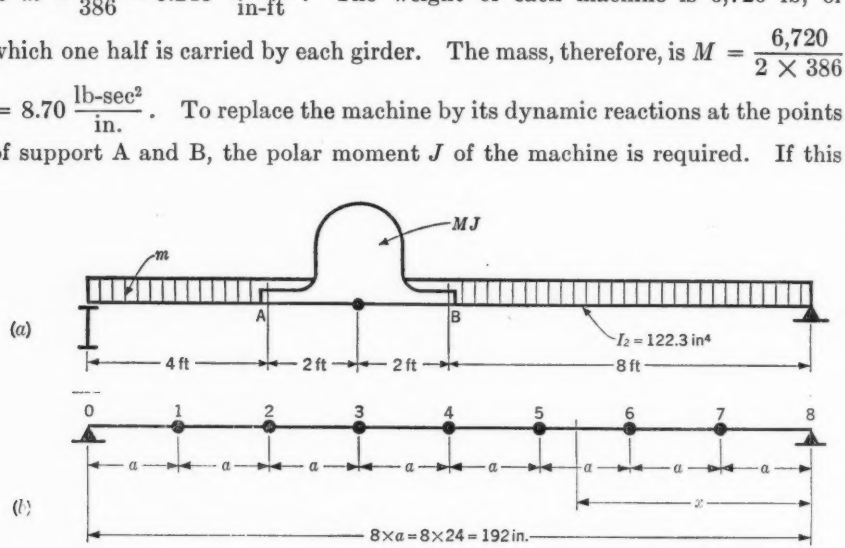

FIG. 14

polar moment for the entire machine is 5,376 lb-ft^2, the polar moment J per beam is equal to $\frac{5{,}376}{2 \times 386} = 6.96 \frac{\text{lb-sec}^2\text{-ft}^2}{\text{in.}}$. Substituting these values in Eqs. 68 the dynamic reactions are

$$M_A = \frac{2^2 \times 8.70 + 6.96}{4^2} + \frac{2 \times 2 \times 8.70 - 6.96}{4^2} \frac{y_B}{y_A} = 2.61 + 1.74 \frac{y_B}{y_A} \quad (70a)$$

and

$$M_B = \frac{2^2 \times 8.70 + 6.96}{4^2} + \frac{2 \times 2 \times 8.70 - 6.96}{4^2} \frac{y_A}{y_B} = 2.61 + 1.74 \frac{y_A}{y_B} \quad (70b)$$

Application of the Stodola-Vianello Method to the Determination of the Mode of T_2.—As shown in Fig. 14(*b*) the span is divided into eight equal parts and the masses are concentrated at the division points. The choice of the division points has been made in such a way that important and large concentrated masses, such as the dynamic reactions M_A and M_B coincide with division points. The masses at these points $\left(\text{in } \frac{\text{pound-second}^2}{\text{inches}} \right)$ are: $M_0 = M_8 = \frac{1}{2} \times 2 \times 0.246 = 0.25$ and $M_1 = M_3 = M_5 = M_6 = M_7 = 2 \times 0.246 = 0.49$.

Also

$$M_4 = 2 \times 0.246 + 2.61 + 1.74 \frac{y_2}{y_4} = 3.10 + 1.74 \frac{y_2}{y_4} \ldots\ldots (71a)$$

and

$$M_2 = 2 \times 0.246 + 2.61 + 1.74 \frac{y_4}{y_2} = 3.10 + 1.74 \frac{y_4}{y_2} \ldots\ldots (71b)$$

Points A and B in Fig. 14(*a*) are points 2 and 4 in Fig. 14(*b*), therefore, $y_A = y_2$ and $y_B = y_4$. As explained in Section 3 the Stodola-Vianello method makes it possible to obtain the normal modes by successive approximation. The first approximation $y^{(1)}$ is found by guessing only; then, the beam is loaded with the inertia forces corresponding to $y^{(1)}$ and the deflections are determined. These deflections are the next approximation $y^{(2)}$ of the mode; the process is then repeated as often as required.

TABLE 1.—STODOLA-VIANELLO METHOD, FIRST STEP

Point (Fig. 14)	$y^{(1)}$	Mass M	$M \times [y^{(1)}]^2$	Inertia Loading			Elastic Weights			$\frac{M (E I)^2}{a^6} \times [y^{(2)}]^2$	$\omega^2 y^{(2)}$
				$M y^{(1)}$	Shear V	Moment $\frac{M}{a}$	$\frac{E I}{a^2} w$	Shear $\frac{E I}{a^2} V$	Moment $\frac{E I}{a^2} y^{(2)}$		
(1)	(2)	(3)	(4)	(5)	(6)	(7)	(8)	(9)	(10)	(11)	(12)
0	0	0.25	0	0	5.998	0	1.00	35.412	0	0	0
1	0.45	0.49	0.10	0.22	5.778	5.998	5.96	29.452	35.412	615	0.40
2	0.80	5.19	3.32	4.15	1.628	11.776	11.08	18.372	64.864	23,012	0.731
3	1.00	0.49	0.49	0.49	1.138	13.404	13.32	5.052	83.236	3,396	0.93
4	0.95	4.57	4.12	4.34	−3.202	14.542	13.82	−8.768	88.288	34,145	0.994
5	0.75	0.49	0.28	0.37	−3.572	11.340	11.28	−20.048	79.520	3,100	0.89
6	0.50	0.49	0.12	0.25	−3.822	7.768	7.73	−27.778	59.472	1,733	0.67
7	0.25	0.49	0.03	0.12	−3.942	3.946	3.92	−31.698	31.694	492	0.36
8	0	0.25	0	0		0.004	0.66		−0.006	0	0
Σ...	....	....	8.46	9.94	....	....	....	....	....	66,493	....

Table 1 shows the arrangement of the computations for the first step. Cols. 2, 3, and 4, Table 1, contain the values of the assumed amplitudes $y^{(1)}$, the masses M, and $M [y^{(1)}]^2$. To obtain the numerical values of the masses M at points 2 and 4, it must be carefully remembered that the ratios $\frac{y_4}{y_2}$ and $\frac{y_2}{y_4}$ in the expressions for these masses refer to the amplitudes just considered and that, therefore, $y_2 = 0.80$ and $y_4 = 0.95$ (see Col. 2, Table 1) which yields $M_2 = 3.10 + 1.74 \frac{0.95}{0.80} = 5.19$; and $M_4 = 3.10 + 1.74 \frac{0.80}{0.95} = 4.57$.

Cols. 5, 6, and 7 are headed "Inertia Loading" and contain the inertia load $M y^{(1)}$, the shear forces due to these loads, and, finally, the moments. After

the reactions at point 0 are found, the shear forces are determined, one by one, by subtracting the point load from the shear in the preceding panel. Since the panel length is constant, $a = 24$ in., the values of the moment $\frac{\bar{M}}{a}$ can be found, step by step, by adding the shear force to the moment in the preceding panel point, starting with $\bar{M} = 0$ for point 0.

Cols. 8, 9, and 10, Table 1, are headed "Elastic Weights" and contain the values w_i found from Eq. 60*b*, the shear, and the moments due to the loads w_i—all with suitable multipliers. Col. 10 is the approximation $y^{(2)}$ of the fundamental mode.

Col. 11 gives the values of $M\,[y^{(2)}]^2$ which are required to find the frequency from Eq. 61: $\omega^4 = \frac{8.46 \times E^2 I^2}{66{,}493 \times a^6}$; $\omega^2 = \sqrt{\frac{8.46}{66{,}493}} \times \frac{E\,I}{a^3} = 0.01126 \times \frac{30 \times 10^6 \times 122.3}{24^3} = 2{,}990$; and $\omega = 54.7$. To obtain the values in Col. 11, the masses at points 2 and 4 must be recomputed, using the values of $y_2 = 64.864$ and $y_4 = 88.288$; thus, $M_2 = 3.10 + 1.74\,\frac{88.288}{64.864} = 5.47$; and $M_4 = 3.10 + 1.74\,\frac{64.864}{88.288} = 4.38$.

Col. 12, Table 1, finally, contains the values:

$$\omega^2\,y^{(2)} = \sqrt{\frac{8.46}{66{,}493}} \times \frac{E\,I}{a^3}\,y^{(2)} = 0.01126\,\frac{E\,I}{a^3}\,y^{(2)} \ldots\ldots\ldots (72)$$

If $y^{(1)}$ had been the correct mode, $\omega^2\,y^{(2)}$ would have been exactly equal to $y^{(1)}$, and the actual differences enable the designer to judge the degree of approximation. As this is only the first step, there are still noticeable differences.

The computation is now repeated, beginning with the values $y^{(2)}$ just found. A principal mode can always be multiplied by a factor; it is therefore permissible to start the next step with the values $\omega^2\,y^{(2)}$. This procedure is convenient because otherwise the numbers in the tables would increase after every step. It is not necessary to reproduce the computation for the further steps since the tables are quite similar to Table 1. The results of the first three steps are shown in Cols. 2, 3, and 4, Table 2.

The result $\omega^2\,y^{(3)}$ of the second step (Col. 3) differs very little from $\omega^2\,y^{(2)}$ (Col. 2) and the third step (Col. 4) produces no change. The result of the third step, therefore, is selected as final. The values in Table 2 represent the amplitudes of a principal mode and therefore contain an arbitrary factor. To find the normal mode this factor must be chosen to satisfy the normalizing condition Eq. 62:

$$\sum M\,\phi^2 = 1 \ldots\ldots\ldots\ldots\ldots\ldots\ldots\ldots (73)$$

The quantity $\sum M y^2 = 8.39$ has been computed in Col. 6, Table 2, and the normalizing condition will be satisfied by

$$\phi = \frac{y}{\sqrt{\sum M y^2}} = \frac{y}{\sqrt{8.39}} = 0.345\, y = 0.345\, \omega^2 y^{(4)} \ldots\ldots\ldots (74)$$

Col. 9, Table 2, contains the value of $\sum M \frac{x}{l} \phi_{2B}$ which will be required subsequently.

The result of all these computations can be summarized as follows:

$$\omega_{2B} = \omega_{3B} = \omega_{6B} = \omega_{7B} = 54.6;$$

and

$$\sum M \frac{x}{l} \phi_{2B} = \sum M \frac{x}{l} \phi_{3B} = \sum M \frac{x}{l} \phi_{6B} = \sum M \frac{x}{l} \phi_{7B} = 2.034.$$

The exact value of the next frequency of these beams is not known without further computation, but it will be at least four times the fundamental frequency—that is, more than 200. As this value is greater than the previously explained limit of $\omega = 100$, further modes of these beams need not be considered.

TABLE 2.—STODOLA-VIANELLO METHOD, RESULT OF ADDITIONAL STEPS, AND FINAL MODE ϕ_{2B}

Line	First step $\omega^2 y^{(2)}$	Second step $\omega^2 y^{(3)}$	Third step $\omega^2 y^{(4)}$	Normal Mode					Dynamic Reaction R_2		
				M	$M y^2$	ϕ_{2B}	$\frac{x}{l}$	$M \frac{x}{l} \phi_{2B}$	$\frac{x}{l}$	M	$M \frac{x^2}{l^2}$
(1)	(2)	(3)	(4)	(5)	(6)	(7)	(8)	(9)	(10)	(11)	(12)
0	0	0	0	0.25	0	0	1	0	1.000	0.25	0.25
1	0.40	0.396	0.396	0.49	0.08	0.137	0.875	0.059	0.875	0.49	0.375
2	0.731	0.727	0.727	5.48	2.90	0.251	0.750	1.032	0.750	4.26	2.395
3	0.93	0.934	0.934	0.49	0.43	0.322	0.625	0.099	0.625	0.49	0.19
4	0.994	0.993	0.993	4.37	4.31	0.343	0.500	0.750	0.500	5.71	1.43
5	0.89	0.896	0.896	0.49	0.39	0.309	0.375	0.057	0.375	0.49	0.07
6	0.67	0.672	0.672	0.49	0.22	0.239	0.250	0.029	0.250	0.49	0.03
7	0.36	0.358	0.358	0.49	0.06	0.124	0.125	0.008	0.125	0.49	0.01
8	0	0	0	0.25	0	0	0	0	0	0.25	0
Σ...	....	....	....	....	8.39	....	....	2.034	....	....	4.75
ω...	54.7	54.6	54.6	...	....	....	....	....	....	....	....

The dynamic reactions of these girders on the main girder T_9 are given by the integral formula Eq. 13. For concentrated masses M this equation yields

$$\frac{1}{l^2} \int x^2\, dm \equiv \sum M \frac{x^2}{l^2} \ldots\ldots\ldots\ldots\ldots\ldots (75)$$

The computation of this sum is shown in Col. 12, Table 2. In accordance with Fig. 3 the dimension x must be measured from the far end of the girder—that is, in this case from point 8, as shown in Fig. 14(*b*). When determining

the masses M in Col. 11, Table 2, for points 2 and 4, the amplitudes y at these points are required. (Amplitudes y always refer to the amplitudes under consideration, which are, in this case, $y_2 = 0.75\ y_0$ and $y_4 = 0.50\ y_0$.)

Finally, the dynamic reactions of these girders are: $R_2 = R_3 = R_6 = R_7 = 4.75 \frac{\text{lb-sec}^2}{\text{in.}}$.

The Normal Modes of System A.—System A consists of girder T_9, which has a moment of inertia $I_9 = 1{,}226$ in.^{4}, and of eight imaginary beams T_1 to T_8 which are assumed to be rigid, $I = \infty$.

As explained in Section 1, such a system can be replaced by girder T_9 alone, carrying (in addition to the actual masses) further imaginary masses which are termed the dynamic reactions of the omitted girders.

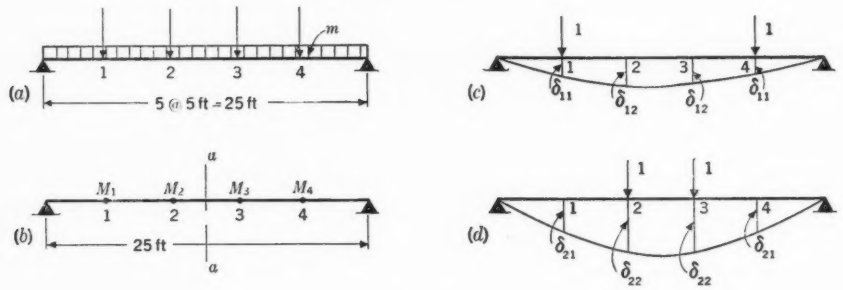

FIG. 15

Fig. 15(a) shows girder T_9 and its mass distribution. The weight of the girder, 65 lb per ft corresponds to a mass $m = \frac{65}{386} = 0.168 \frac{\text{lb-sec}^2}{\text{in-ft}}$. The additional mass at point 1 is the sum of the dynamic reactions of the beams T_1 and T_5 which have already been found equal to $R_1 = R_5 = 1.26 \frac{\text{lb-sec}^2}{\text{in.}}$. The additional masses at point 2 are $R_2 = R_6 = 4.75 \frac{\text{lb-sec}^2}{\text{in.}}$. By symmetry, the masses at points 3 and 4 are equal to those at points 2 and 1.

For the computation, concentrate the comparatively small distributed mass at points 1 to 4 and thus obtain the mass distribution shown in Fig. 15(b):

$$M_1 = M_4 = 5 \times 0.168 + 2 \times 1.26 = 3.36 \frac{\text{lb-sec}^2}{\text{in.}}$$

and

$$M_2 = M_3 = 5 \times 0.168 + 2 \times 4.75 = 10.34 \frac{\text{lb-sec}^2}{\text{in.}}$$

Because of the small number of masses the use of influence numbers (explained in Section 3) gives the quickest result. For the present only the modes that are symmetrical to axis $a-a$ are of interest; and to take full advantage

of this symmetry the influence numbers δ_{ik} are defined in a special way. Numbers δ_{11} and δ_{12} are the deflections at points 1 and 2 as a result of the symmetrical arrangement of unit loads shown in Fig. 15(*c*). Because of symmetry, $\delta_{13} = \delta_{12}$ and $\delta_{14} = \delta_{11}$. Similarly δ_{21} and δ_{22} are the deflections due to the two unit loads shown in Fig. 15(*d*). The numerical values of these influence numbers are (in inches per pound): $\delta_{11} = 0.108 \times 10^{-4}$; $\delta_{12} = \delta_{21} = 0.166 \times 10^{-4}$; and $\delta_{22} = 0.274 \times 10^{-4}$.

The amplitudes of the principal modes are $y_1 = y_4$ and $y_2 = y_3$. By using the same reasoning that led to Eqs. 56 in Section 3 two equations are obtained for the amplitudes y_1 and y_2 which are identical to Eqs. 56. Substituting the numerical values for M and δ in Eqs. 56,

$$\left(0.363 \times 10^{-4} - \frac{1}{\omega^2}\right) y_1 + 1.717 \times 10^{-4}\, y_2 = 0 \ldots\ldots\ldots (76a)$$

and

$$0.558 \times 10^{-4}\, y_1 + \left(2.835 \times 10^{-4} - \frac{1}{\omega^2}\right) y_2 = 0 \ldots\ldots\ldots (76b)$$

Eqs. 76 have only the trivial solution $y_1 = y_2 = 0$ unless their determinant Δ vanishes. Therefore, $\Delta = 0$ is the frequency equation:

$$\Delta = \left(\frac{10^4}{\omega^2}\right)^2 - 3.198\,\frac{10^4}{\omega^2} + 0.071 = 0 \ldots\ldots\ldots\ldots (77)$$

There are two roots: $\frac{10^4}{\omega^2} = 3.176$ and 0.022 or $\omega = 56.1$ and $\omega = 725$. The higher value of ω is beyond the limit $\omega = 100$ and only one root remains: $\omega_A = 56.1$ and $\omega^2{}_A = 3{,}149$. To find the amplitudes of the normal mode, introduce this frequency in Eqs. 76 both of which give the identical result $y_1 = 0.610\, y_2$. A further relation is the normalizing condition (Eq. 58) which, for the present case, reads

$$M_1 y^2{}_1 + M_2 y^2{}_2 + M_3 y^2{}_3 + M_4 y^2{}_4 = 1 \ldots\ldots\ldots\ldots (78)$$

Substituting $y_1 = y_4 = 0.610\, y_2$ and $y_3 = y_2$, $2\,(3.36 \times 0.610^2 + 10.34)\, y^2{}_2 = 1$; and finally $y_2 = 0.207$ and $y_1 = 0.610 \times 0.207 = 0.127$. To express the fact that these are the amplitudes of the normal modes of system A one may write $\phi_A(1) = \phi_A(4) = 0.127$; and $\phi_A(2) = \phi_A(3) = 0.207$.

These are the values of ϕ_A at the four points where concentrated masses occur. The next step is to find the amplitudes of the mode ϕ_A for points situated along the secondary beams. Since in system A these beams are rigid, they must also remain straight. At the ends where these beams are supported by girder T_9 the amplitudes are $\phi_A = 0.127$ for girders T_1, T_4, T_5, and T_8 and $\phi_A = 0.207$ for girders T_2, T_3, T_6, and T_7; at the other ends ϕ_A must vanish. Therefore, the linear expressions are: For beams T_1, T_4, T_5, and T_8—

$$\phi_A = 0.127\,\frac{x}{l} \ldots\ldots\ldots\ldots\ldots\ldots (79a)$$

and, for beams T_2, T_3, T_6, and T_7,

$$\phi_A = 0.207 \frac{x}{l} \quad \text{.....(79b)}$$

In Eqs. 79, x is the coordinate of the point considered measured from the external support of each girder.

Computation of the Coefficients β_{ik}.—The frequency equation, Eq. 32, contains the coefficients β_{ik} which are yet to be found. Eq. 26 defines these coefficients. In this example one mode ϕ_{1A} and eight modes ϕ_{kB} (k = 1 to 8) occur. There are, therefore, eight values of β_{1k} (k = 1 to 8).

The integrals in the equations for β_{ik} must be taken over all the masses of the system. Because system B consists of a number of separate beams, any value of ϕ_{kB} vanishes for all points except those lying on beam T_k. Each integral, therefore, needs to be taken over the masses of beam T_k only.

To find β_{11} the value of

$$\beta_{11} = \int_{T_1} \phi_A \, \phi_{1B} \, dm \quad \text{.....(80)}$$

must be found. Substituting $\phi_A = 0.127 \frac{x}{l}$ (which is valid for points on beam T_1) and remembering that $dm = m \, dx$,

$$\beta_{11} = 0.127 \int \frac{x}{l} \phi_{1B} \, dm = 0.127 \int m \frac{x}{l} \phi_{1B} \, dx \quad \text{.....(81)}$$

The value of the last integral in Eq. 81 has already been found, together with the mode ϕ_{1B}, and $\beta_{11} = 0.127 \times 0.874 = 0.111$. The values of β_{1k} for girders T_4, T_5, and T_8 must be the same as those for T_1; thus, $\beta_{11} = \beta_{14} = \beta_{15} = \beta_{18} = 0.111$.

In the same manner, $\beta_{12} = \beta_{13} = \beta_{16} = \beta_{17} = \int_{T_2} \phi_A \, \phi_{2B} \, dm = 0.207 \times \int_{T_2} \frac{x}{l} \phi_{2B} \, dm = 0.207 \sum M \frac{x}{l} \phi_{2B} = 0.207 \times 2.034 = 0.423$.

The Frequency Equation.—If the numerical values β_{ik} and the values of the frequencies—$\omega^2_A = 3{,}149$; $\omega^2_{1B} = \omega^2_{4B} = \omega^2_{5B} = \omega^2_{8B} = 8{,}836$; $\omega^2_{2B} = \omega^2_{3B} = \omega^2_{6B} = \omega^2_{7B} = 2{,}980$—are substituted into Eq. 32, the frequency equation assumes the form:

$$\frac{0.049}{\frac{8{,}836}{\omega^2} - 1} + \frac{0.716}{\frac{2{,}980}{\omega^2} - 1} = \frac{3{,}149}{\omega^2} - 1 \quad \text{.....(82)}$$

Fig. 16, with ω as variable, gives the values of the left-hand side of Eq. 82 as solid lines and the values of the right-hand side as dotted lines. The intersection points are the frequencies of the system. The roots of the frequency equation, found by trial and error, are: ω^2 = 1,654, 7,950, and 26,000 or ω = 40.7, 89.2, and 161.

It has been shown in Section 1 that Eq. 32 does not give all the frequencies of a system if some of the values ω_{iB} are alike. This occurs in this example: $\omega_{1B} = \omega_{4B} = \omega_{5B} = \omega_{8B} = 94.0$ and $\omega_{2B} = \omega_{3B} = \omega_{6B} = \omega_{7B} = 54.6$. Every multiple frequency of system B remains a frequency of the complete system and there are, therefore, two additional frequencies, $\omega = 54.6$ and $\omega = 94$.

All the frequencies found correspond to modes that are symmetrical to axis $a-a$, and these frequencies, arranged in order of increasing magnitudes, are: $\omega_1 = 40.7$, $\omega_2 = 54.6$, $\omega_3 = 89.2$, $\omega_4 = 94$, and $\omega_5 = 161$.

To enable the designer to appreciate the meaning of these results the amplitudes of the modes corresponding to these frequencies were computed. This procedure will give some enlightening information on the frequencies ω_2 and ω_4 which would otherwise not be quite clear.

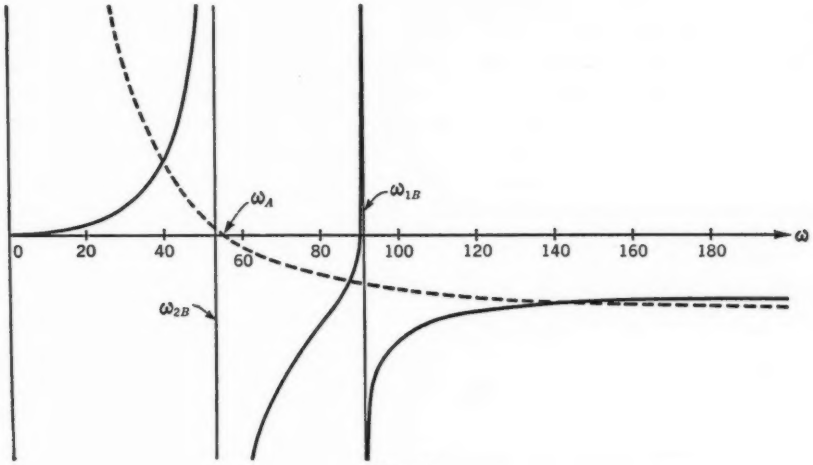

FIG. 16

Determination of the Modes ϕ_1, ϕ_3, and ϕ_5.—To compute the amplitudes of these modes which belong to the roots of the frequency equation (Eq. 32), Eqs. 33 and 35 were used.

The amplitudes of the modes ϕ_1, ϕ_3, and ϕ_5 are illustrated in Fig. 17(a), 17(c), and 17(e). Referring to the axes $a-a$ and $b-b$ shown in Fig. 12 these modes are symmetrical not only for axis $a-a$ but also for axis $b-b$.

Determination of the Modes ϕ_2 *and* ϕ_4.—To find the modes ϕ_2 and ϕ_4 refer to Eqs. 27 which now become

$$\left(1 - \frac{\omega^2_A}{\omega^2}\right) c_A + \sum_{k=1}^{8} \beta_{1k}\, c_{kB} = 0 \quad \ldots\ldots\ldots\ldots\ldots\ldots (83a)$$

and

$$\beta_{1k}\, c_A + \left(1 - \frac{\omega^2_{kB}}{\omega^2}\right) c_{kB} = 0 \quad (k = 1, 2, \cdots, 8) \quad \ldots\ldots\ldots (83b)$$

Eq. 83b represents eight equations because k can be any number from 1 to 8.

Investigating the root $\omega_4 = \omega_{1B}$, Eq. 83*b* gives (for $k = 1$, 4, 5, or 8) simply $\beta_{1k}\, c_A = 0$—or $c_A = 0$. For $k = 2$,

$$\beta_{12}\, c_A + \left(1 - \frac{\omega^2_{2B}}{\omega^2_{1B}}\right) c_{2B} = 0 \qquad (84)$$

and, because $c_A = 0$, $c_{2B} = 0$. Similarly, $c_{3B} = c_{6B} = c_{7B} = 0$. Introduce these results in Eq. 83*a* (remembering that $\beta_{11} = \beta_{14} = \beta_{15} = \beta_{18}$), only four terms of this equation remain; thus, $c_{1B} + c_{4B} + c_{5B} + c_{8B} = 0$. Since the mode is symmetrical to the $a-a$ axis, $c_{1B} = c_{4B}$ and $c_{5B} = c_{8B}$; or $c_{1B} + c_{5B} = 0$.

The numerical values of c_{1B} and c_{5B} are computed from the normalizing condition (Eq. 35)— $c_{1B} = c_{4B} = 0.500$ and $c_{5B} = c_{8B} = -0.500$. The amplitudes of the mode are illustrated in Fig. 17(*d*). A similar computation for $\omega_2 = \omega_{2B}$ gives the analogous result—$c_A = 0$; $c_{1B} = c_{4B} = c_{5B} = c_{8B} = 0$; $c_{2B} = c_{3B} = 0.500$; and $c_{6B} = c_{7B} = -0.500$—as illustrated in Fig. 17(*b*).

These two modes (Figs. 17(*b*) and 17(*d*)) are still symmetrical to axis $a-a$ but they are asymmetrical to axis $b-b$. The significance of these two modes now becomes quite clear; each group of secondary beams can oscillate without interference by the other beams, because the girders on both sides of T_9 move in opposition; girder T_9 remains stationary because there are no loads on girder T_9, which is due to the fact that the reactions for each pair of secondary beams T_1 and T_5, T_2 and T_6, etc., balance each other.

TABLE 3.—COMPARISON OF FREQUENCIES

Line	ω_1	ω_2	ω_3	ω_4	ω_5
1.....	40.7	54.6	89.2	94	161
2.....	40.7	54.6	88.7	94	158
3.....	41.0	55.4	104.5	109	166
4.....	41.0	55.4	104.3	109	162

Reliability of Frequencies.—The mechanical system shown in Fig. 12 includes some distributed masses. Therefore, it has an infinite number of degrees of freedom. Such a system has an infinite number of frequencies as well. The present study has revealed only five frequencies corresponding to symmetrical modes because the frequencies of the complementary systems greater than $\omega = 100$ have been neglected, thus artificially reducing the number of degrees of freedom.

The limit $\omega = 100$ has been selected to insure that frequencies up to approximately $\omega = 50$ will be correct; greater frequencies may contain some error. For example, in Table 3 (a comparison of frequencies), line 1 shows the results of the foregoing computations; and line 2, the frequencies obtained by doubling the number of modes of the complementary systems. The first two frequencies remain entirely unaltered, which is better than could be expected.

There is another simplifying assumption that affects the frequencies—the mass of the flooring has been concentrated on the secondary beams. According to the rule given in Section 1, this is a good approximation as long as the result

remains below the lowest frequency of the secondary girders themselves. In the present example this lowest frequency is $\omega_{2B} = 54.6$. Therefore, ω_1 and ω_2 are good approximations, whereas the higher frequencies are not reliable. As

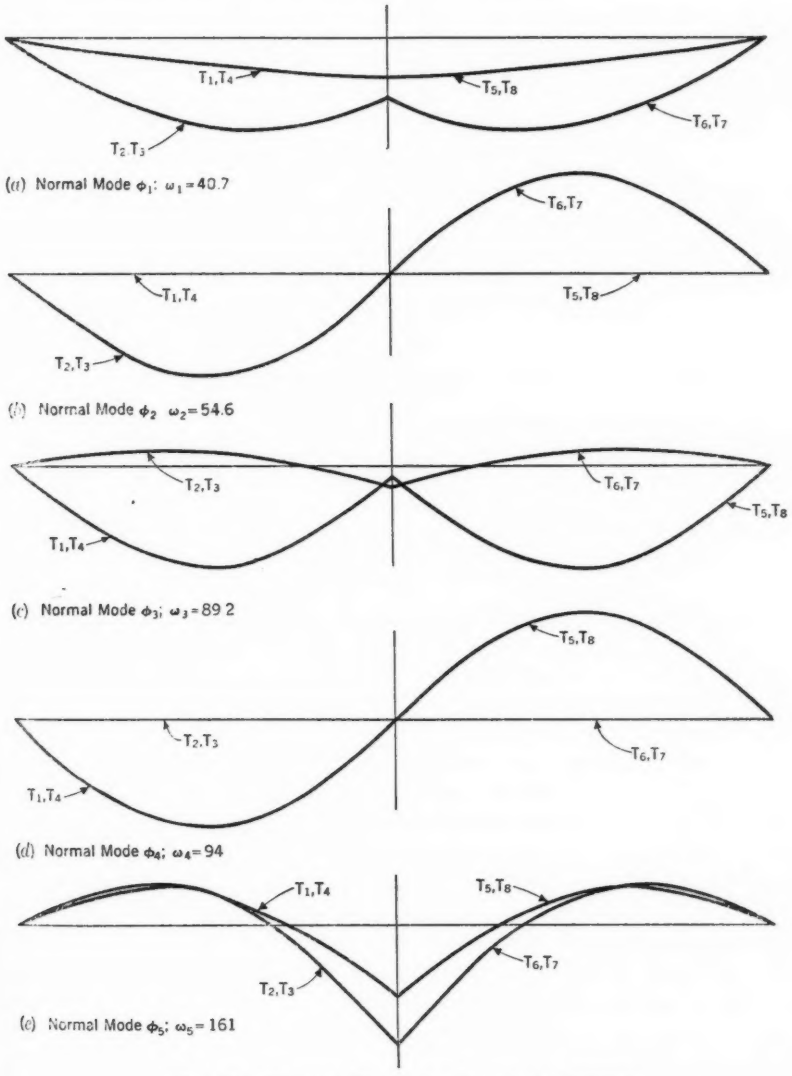

FIG. 17.—(VERTICAL SCALE OF *c*, *d*, AND *e*, REDUCED)

a check on this rule, line 3, Table 3, shows the result of a more exact computation taking into account the effect of the flooring. Line 4, gives the result obtained if the same number of modes is employed as for line 2. The more

exact results in line 4 differ from line 1 only by 0.75% for the fundamental frequency and by 1.75% for the next frequency, which is quite sufficient for all practical purposes, and justifies the rules given in Section 1.

In the foregoing computations all the connections of the secondary beams have been assumed entirely hinged. In actual practice these beams will be at least partly restrained and this restraint will tend to increase the frequencies. To obtain an estimate of the effect of partial fixation, the fundamental frequency of the system with fully continuous secondary beams was determined by the method explained in Section 2. The fundamental frequency was found to be 43.8—8% higher than that without continuity. The effect of partial restraint, therefore, will be less than 8%.

Factor of Safety.—The higher frequencies and the shape of the modes have been discussed to gain a better understanding; but for practical purposes the value of the fundamental frequency $\omega = 40.7$ is all that is required. The machines run at 320 rpm, the circular frequency being $\omega = \frac{2\pi \times 320}{60} = 33.5$. The factor of safety against resonance therefore is $\frac{40.7}{33.5} = 1.21$. This result is not quite satisfactory. Considering that a certain margin of error in computations of this kind must be expected, one should attempt to obtain a factor of safety of 1.40 whenever possible. The structure shown in Fig. 12 therefore is not quite suitable for the contemplated purpose and should be strengthened. To secure a factor of safety of 1.40 the fundamental frequency must be raised to $1.40 \times 33.5 = 46.9$.

Alteration of the Moments of Inertia.—To find the moments of inertia required to give the fundamental frequency $\omega = 46.9$, it is not necessary to repeat the entire computation. Assuming that the mass of the structure is not altered by the change in I, which is approximately correct, it will be seen that nearly all the original computations can be used.

The most economical method of obtaining the small required increase in the frequency is to alter only the beam, or beams, with the lowest frequency ω_A or ω_B. Thus, in the present case only beams T_2, T_3, T_6, and T_7 need to be altered. This alteration does not affect the modes and frequencies of system A. Even the modes ϕ_{1B}, ϕ_{4B}, ϕ_{5B}, and ϕ_{8B} and their frequencies which originate from girders T_1, T_4, T_5, and T_8, remained unaltered.

To obtain the new modes ϕ_{2B}, ϕ_{3B}, ϕ_{6B}, and ϕ_{7B} and their frequencies, theorem II, Section 1, is used. It states that the normal modes of a system remain unaltered if all the moments of inertia are changed, proportionately, from I into αI; such a change, however, alters the frequencies ω_i, which become $\sqrt{\alpha}\,\omega_i$.

If theorem II is applied to each of the separate girders T_2, T_3, T_6, and T_7, their moments of inertia are increased from I_2 to αI_2. This increase alters their frequencies to $\sqrt{\alpha}\,\omega_{2B}$, $\sqrt{\alpha}\,\omega_{3B}$, $\sqrt{\alpha}\,\omega_{6B}$, and $\sqrt{\alpha}\,\omega_{7B}$, but leaves the amplitudes ϕ_{2B}, ϕ_{3B}, ϕ_{6B}, and ϕ_{7B} unchanged. As the numerical values of none of the modes have varied, the numerical values of all the coefficients β_{ik}

remain the same. Thus, the frequency equation can be written without further computations because it is only the frequencies ω_{2B}, ω_{3B}, ω_{6B}, and ω_{7B} that need to be adjusted:

$$\frac{0.049}{\frac{\omega^2_{1B}}{\omega^2} - 1} + \frac{0.716}{\frac{\alpha\,\omega^2_{2B}}{\omega^2} - 1} = \frac{\omega^2_A}{\omega^2} - 1 \qquad (85)$$

The effect of the change of sections on the frequency equation is only the introduction of the coefficient α. Since the desired frequency ω is known, this equation can be used in the reverse to determine the required value of α. Substituting $\omega^2 = 46.9^2 = 2{,}200$ in Eq. 85 gives $\frac{0.049}{\frac{8{,}836}{2{,}200} - 1} + \frac{0.716}{\frac{2{,}980}{2{,}200}\alpha - 1} = \frac{3.149}{2{,}200} - 1$ and $\alpha = 2.01$.

Originally, $I_2 = 122.3$ and now it is required that $I_2 = 122.3 \times 2.01 = 246$ in.^{3}.

Conclusion

The method presented in this paper permits the determination of the resonant frequencies of complicated structures. It makes possible a comparison of the values of the operating frequencies of machinery with the values of resonant frequencies of a supporting floor. If any danger of resonance is found, appropriate changes can be made before the beginning of actual construction.

The author has applied the method successfully to the frequency analysis of the complicated fan floors of boilerhouses and, on one occasion, to the frequency analysis of a high radio tower on the roof of a multiple-story building.

AMERICAN SOCIETY OF CIVIL ENGINEERS

Founded November 5, 1852

PAPERS

ROADS AND PAVEMENTS, SAMPSON NAVAL TRAINING STATION

BY JACOB FELD,[1] M. ASCE

SYNOPSIS

During World War II, the design and construction of temporary access and permanent roads, walks, and paved training areas was one phase of the emergency provision for the United States Navy personnel training facilities at Sampson, N. Y., on the east shore of Seneca Lake. Unfavorable soil conditions, absence of any local suitable base or aggregate materials, limited transportation facilities into the site, and unusually severe weather conditions made necessary a flexible program. The construction methods for almost 65 lane miles of roads within 6 months, with little time for preparation, and with keen competition for labor and equipment, and yet at a reasonable cost, are recorded because of the extremely low maintenance required in 4 years of concentrated use as a training station followed by 3 years of use as a temporary college. Some of the procedures deviated considerably from previously established practice and are suggested as proper methods of design and construction for roads in fine-grained plastic soil areas. Design was predicated on the availability of materials and equipment and followed the actual purchase of the materials.

INTRODUCTION

Extent of Project.—An area of 2,500 acres, adjacent to the east shore of Seneca Lake in New York, with about 5 miles of lake frontage, was to be converted into a training station for Navy personnel. The basic training areas (six in number) consisted of a rectangular 15-acre sodded drill field, with a paved drill area 50 ft wide on three sides. All six fields with barracks and service buildings were connected by paved roads and paths. Each area had an average of 1.5 miles of main road and a training strip about 0.5 mile long. A number of special service areas (for advanced training, administration, warehousing, civilian housing, and a hospital) accounted for almost as much paving as in the six training areas.

As a total, the equivalent of 51 miles of roads 22 ft wide was surfaced. The roads comprised (in million square yards): Primary road paving, 394; secondary

NOTE.—Written comments are invited for immediate publication; to insure publication the last discussion should be submitted by March 1, 1950.

[1] Cons. Engr., New York, N.Y.

road paving, 158; concrete paving, 48; gravel surfacing, 17; and resurfacing existing roads, 49. About 95% of the paved area required an 8-in. stabilized gravel subbase, which with shoulders involved almost 300,000 tons of gravel. Crushed stone base was placed on all main roads. Hot lay tar concrete was used to surface all primary, secondary, and existing road areas. Penetration and seal coats required about 800,000 gal of tar, and the hot mix required 900,000 gal of tar.

Land was acquired in early June, 1942, before any surveys or plans had been executed. Construction was well under way by the end of July, and in spite of weather conditions, all road excavation and subbase were completed by December 15, with about 60% of the tar concrete in place. The station was "established" on October 17 and all areas were occupied by the end of 1942. Some 440,000 sailors received their basic training at this station.

Local Geology and Topography.—The entire work was within the strip of Hamilton shale exposure (Devonian period) (see Fig. 1). The surface soil is a Dunkirk silty clay loam (New York State Agricultural Classification), also designated as a Honeoye silty clay loam. It seemed to have only two qualities —tough gummy clay when wet, and gaseous dust when dry. Soft shale was found everywhere within a depth of 3 ft. This soil is very difficult to drain, quite unstable when wet, and readily subject to frost heave. It gives a slightly alkaline reaction. Known also as "Seneca County clay," it is considered the worst soil for highway work in New York State.

The developed land strip was about 6,000 ft wide, generally sloping uniformly toward the lake shore. Fig. 2 is a part reproduction of the Ovid quadrangle Geological Survey (United States Department of the Interior) map containing the area occupied by the Sampson Training Station. The edge 500 ft has a drop of 60 ft, the next 1,500 ft has a drop of 40 ft, and there is a drop of 100 ft in the easterly 4,000 ft. The land was divided by a series of sharply sloping gulleys, running normal to the lake shore, approximately 2,000 ft apart. Natural runoff had eroded these channels from 20 ft to 25 ft in depth; and, as far as possible, they were left undisturbed. With the watershed area limited in extent, a water level rise of almost 10 ft was measured in one gulley in less than 30 min during a thunderstorm. Runoff was almost 100%. Vegetation consisted of some tile drained grape and apple orchards, and small isolated fields of flax and buckwheat. Most of the area, however, was abandoned submarginal farmland.

Any rainfall in excess of 0.1 in. stopped rubber-tired vehicles on unpaved areas. A heavy rainfall stopped all operations for 3 days. At all other times, continuous sprinkler wagon coverage on all traveled ways was absolutely essential. During dry periods, the dust cloud was visible 10 miles away, and it was not unusual for automobiles to drive with full headlights in broad daylight.

Weather Conditions.—Local experience indicated that most of the work must be performed before the usual, heavy, early fall rains. The year 1942 did not agree with local experience, however. In July and again in August, there were 10 days in which precipitation exceeded 0.1 in. In September and October, there were only 5 such days each month. Normal construction season in this

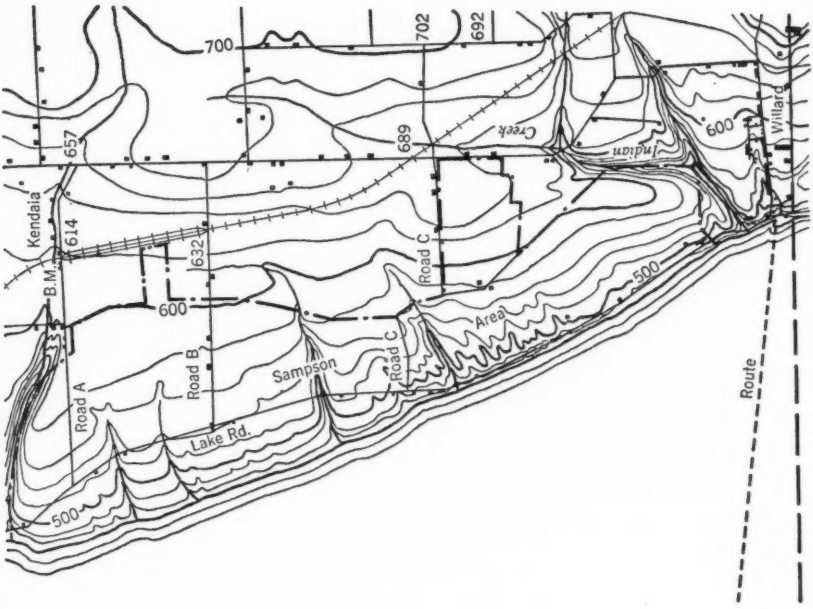

FIG. 2.—TOPOGRAPHIC MAP OF AREA

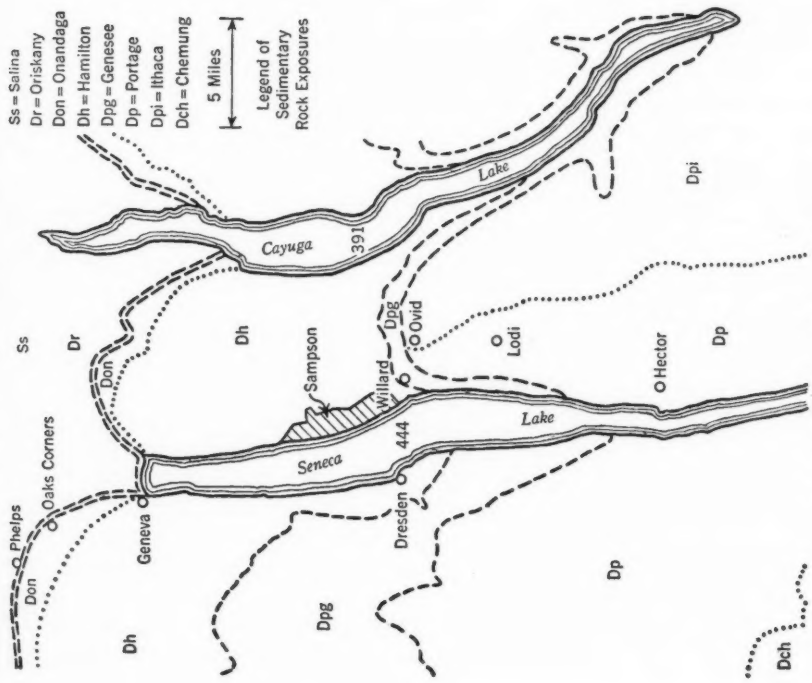

FIG. 1.—GEOLOGICAL MAP OF AREA

area is less than 6 months; the last frost was on May 11, and winter arrived with a snowfall of 1.7 in. on October 26. Considerable subzero weather was experienced in December.

Construction Materials

Available Materials.—In the immediate vicinity, the only stone found was a soft shale, which slaked easily and rapidly upon exposure. The nearest hard shale quarry, near Hayt Corners, N. Y. (a 10-mile haul each way), had been abandoned and required a full complement of tools and equipment. Lack of time prevented its development. Good limestone and some dolomite was available from Oaks Corners, N. Y., 6 miles north of Geneva, N. Y. (a 22-mile haul to the station). This rock was selected for railroad ballast, road base, pavement concrete aggregate, and tar concrete aggregate.

Some granular bank material was found near the local drainage gulleys, but in such small and uncertain volumes that only one area was actually placed into production. A few days of work depleted the entire area. Good sand and gravel deposits were being worked along the contact between the limestone and shale outcrops, chiefly at Oaks Corners and Phelps, N. Y., about 24 miles from the work.

The Oaks Corners pit produced a clean, fine, mason sand—double washed. The glacial deposits at Phelps gave a satisfactory run-of-bank sandy gravel suitable for road subbases, with no processing or blending. A fine sand was obtained from a deposit at Junius, N. Y., containing considerable lime intrusion from outwash seepage. Adjacent to this deposit was a sandy gravel deposit (54% retained on the No. 4 mesh, and 4% passing the No. 100 mesh) which was developed to produce 2,500 tons per day. Transportation bottlenecks and depletion of exposures in this area north of Geneva forced prospecting toward the south, and in October, a run-of-bank gravel pit was opened at North Hector, N. Y.—about a 16-mile haul to the area. Several feet of overburden was blended into the gravel and much large stone had to be "scalped" from the roads when this material was spread. The finer graded materials were more suitable and gave better results with less effort.

Transportation Facilities.—The only road feeding this area is New York route 96A, which was then a concrete pavement 16 ft wide. The lake road (see Fig. 2) was a black-top light traffic by-pass branch of route 96A. Railroad connections were built as an early part of the program, but there was little space on cars for anything beyond lumber and metal materials.

By careful scheduling of truck movements over the one road access (using about 110 trucks on the day shift and 50 trucks at night) more than 100,000 tons of sand, stone, and gravel were brought into the site per month. To permit higher speed and to increase safety, the road was widened by paving with one course of hot lay tar concrete a 3-ft strip on each side of the 16-ft concrete strip. No trucks were permitted on the lake road, and trucks were required to keep off the main road for 30 min, morning and evening, during the peaks of worker travel. Almost 10,000 people, about 90% in private cars (fully loaded), came into the station within a 30-min period at the beginning

of the day shift. About 8,500 came from the north, with traffic congestion of major proportions.

Existing Roads and Temporary Facilities.—Three east and west roads were found crossing the station area (see Fig. 2). Road A was a built-up surfaced farm road, consisting of a cobblestone bed 8 in. deep over part of the width, the remainder being 6 in. of loose crushed soft shale. On this bed had been placed several layers of bituminous penetrated crushed limestone (probably a tar binder and 1 in. of unscreened stone), making up a 6-in. thickness. The total surfaced width was 16 ft, bounded by steep ditches.

Road B consisted of a 6-in. bed of soft shale with a 2-in. covering of penetrated screenings. This was also 16 ft wide. Road C was similar but the screenings had not been penetrated. Locally, these roads are known as "shuck" roads and are made by spreading crushed shale directly on the natural clay soil and letting traffic iron out the aggregate into a pavement. Later, screenings are added to fill out the ruts; and, when traffic warrants it, especially to reduce the dust in dry periods, a penetrated surface is added. The roads shed water very readily, are not slippery, and permit a 35-mile speed for all types of passenger and light truck traffic. Roads of this type were used for hauling several hundred truck loads of sod (from 3-ton loads to 5-ton loads) per day, in addition to the normal local use, with little damage to the surface of the compressed soft shale.

To widen these roads required digging new ditches and filling in the existing drainage channels. There was no time for such a major change. Ditches were cleaned and the road surfaces were scarified 1 in. deep, penetrated with grade RT-4 tar, and covered with $\frac{1}{2}$ in. of stone screenings. No added surface layer could be applied because the resulting road width decrease was not considered safe.

In the middle of each road length, a traffic circle was constructed to permit reversal of direction. The radius of this circle was 30 ft. These traffic "turnarounds" provided space for trucks to pull out while waiting orders and also to unload part loads into smaller vehicles which could move on the natural soil. Eventually, after construction was almost completed, these roads were widened and resurfaced and became part of the completed road system.

Generally, permanent roads were graded and covered with a 4-in. layer of the gravel subbase for use as temporary access roads. A continuous maintenance gang of from 10 to 25 men, with a grader, a bulldozer, and 2 trucks kept all roads available for construction traffic, while also operating 3 water sprinkler wagons to keep the dust within some control.

All-weather parking and bus terminal areas were built by preparing sand-clay compacted surfaces. The procedure was to scarify the soil about 3 in. deep, cover with a 2-in. layer of fine dusty sand from the limestone outwash area, harrow and disk the mixture to a uniform color, and roll the surface. Water was added from a sprinkler truck. Control of water and of rolling was in accordance with a simple instruction: When a light private car left tire marks, more rolling was needed; when the tires raised dust, more water was needed. These parking areas were maintained by adding stone chips as low spots developed. There was no subsurface drainage and the surfaces were sloped at

about 1 on 200 toward a ditch. The main parking areas were 200 ft wide, and held up remarkably well; 4 years of further use as public parking areas and bus terminals still left them in fairly good condition.

Grading Excavation.—In general all excavation and shaping of the subgrade was by tractor scrapers; fifteen such units of 12-cu-yd size, aided by 60-hp bulldozers in tough ground areas, each moved from 600 cu yd to 700 cu yd daily to build up grade and cut ditches. The work was then finished by patrol graders so that practically no handwork was needed. The road cuts were first made 5½ in. below final grade between ditch slopes and then "boxed" out 8 in. deep for the gravel subbase. For primary roads, approximately 500,000 sq yd of grading was required; and, for secondary road areas, 200,000 sq yd. Peak

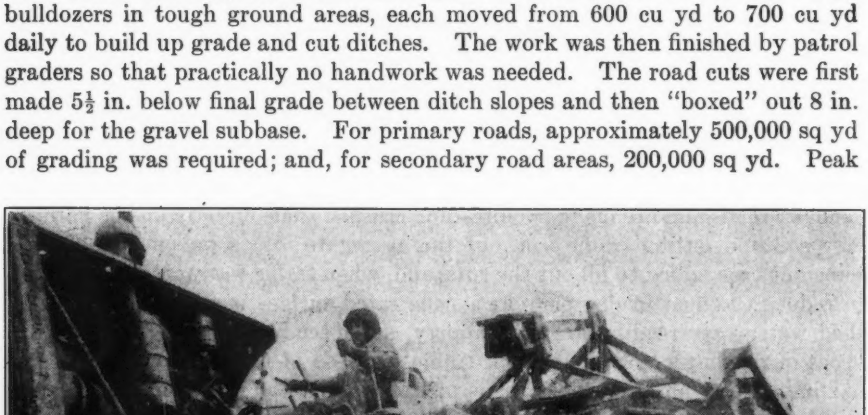

FIG. 3.—GRADING WORK AFTER A RAIN

production occurred in the month of September when 143,000 sq yd was graded and prepared for gravel subbase. Most of the excavation volume came from the drainage ditches. This excavation was expedited to provide gravity drainage for all road excavation. To drain the box trench excavated for the road pavement bleeder trenches were cut 75 ft apart and 2 ft wide, on each side into the open ditches, and filled with broken stone. Working conditions after a rainy spell are shown by Fig. 3.

The same labor-equipment group prepared subgrades, finished slopes of ditches, and placed the gravel subbase (from 2,000 tons per day to 4,000 tons per day) for roads and shoulders. The typical size of this group usually operating at six locations was as follows: 9 tractor scrapers, 2 bulldozers, 11 motor graders, 8 rollers, and from 150 men to 185 men including foremen.

To expedite the road preparation work, some wheel-propelled scrapers were brought to the site in October because no additional tractors were obtainable. The soil conditions made these scrapers useless since the ground was too hard to cut without the help of double bulldozers and the slightest rain eliminated all traction. The additional equipment was then used chiefly for spreading gravel from stock pile and other comparatively easy excavation.

Drainage Pipe.—Open ditches at road junctions, and across paved plazas, were connected by concrete drain pipe. The size of pipe varied from 8 in. to 48 in., the average diameter being 20½ in. Small sizes were laid with open joints and trenches were backfilled with broken stone and large gravel. The total length of all drain pipes used was 71,000 ft, with about 10,000 tons of stone fill. Maximum production in pipe laying was 25,600 ft in October, about half of which was laid in trenches dug by back hoes; the remainder was laid in sections of open ditches prepared by the road gang. In both September and November more than 15,000 ft of pipe was laid.

Design Problems and Their Solution (Specification Requirements)

Pavement Design.—The general schedule for road construction planned all permanent road work for September, October, and November to permit the buildings, railroads, and subsurface utilities to have a good start in June, July, and August. Although the size of the project was almost doubled, no extra time for road construction was possible because of weather conditions. Some work was performed in December, but about a third of the final road surface was postponed to the following spring.

All pavements were to be placed above a subbase of stabilized gravel. There were three pavement classes:

a. Primary or main roads, consisting of 8 in. of gravel, 24 ft wide at the top; a 3-in. stone base, penetrated[2] with RT-12, 24 ft wide at the bottom; a 1½-in. binder course and a 1-in. wearing course of plant mixed tar concrete, 22 ft wide; and 6-in. gravel shoulders, 9 ft wide on each side.

b. Secondary roads, paved 11 ft for single-lane traffic with the six assembly areas 50 ft wide, consisting of a 6-in. gravel subbase; a prime coat (0.4 gal per sq yd) of RT-3, allowed to soak in; a tack coat (0.25 gal per sq yd) of RT-2, or RT-3; and a 1½-in. binder course and a 1-in. wearing course of plant mixed tar concrete. On the narrow roads, gravel shoulders were 5 ft wide on each side.

c. Tertiary pavement on paths and light traffic areas, consisting of a 6-in. gravel subbase; a prime coat of RT-3 (0.4 gal per sq yd); and a 1½-in. binder course (rolled with a "pup" roller) of plant mixed tar concrete.

All subgrade excavations were crowned, allowing for a final 3-in. crown on the 22-ft-wide roads. To discourage high speeds, no superelevation was provided at curves. The foregoing designs were agreed upon late in July, after alternate estimates of cost and labor requirements eliminated the possibility of concrete roads, and material controls prohibited the use of asphalt in any form.

Subbase Course.—Daily subbase gravel deliveries averaged more than 2,500 cu yd with maximum deliveries at about 4,500 cu yd per day in October, so that

[2] "Military Roads in Forward Areas," *ASCE Manual of Engineering Practice No. 23*, New York, N. Y., 1941, p. 10, Table 1.

stock pile of more than 32,000 tons was ready for use when weather slowed both gravel production and trucking.

Bids had been asked for the following items:

1. Run-of-bank gravel, maximum size 2½ in., with more than 30% passing the ¼-in. screen;
2. Run-of-crusher limestone-dolomite, passing a 2½-in. screen to dust;
3. Run-of-crusher hard shale, passing a 2½-in. screen to dust, and of a quality that will not weather or soften when exposed to air; and
4. Slag from industrial furnaces, all passing a 2½-in. screen.

Each vender was to agree to furnish 50,000 cu yd and to deliver at a rate of 2,000 cu yd per day of 20 hours. A theoretical preferred specification was prepared as follows:

Sieve size	Passing by weight (%)
3 in.	96
2 in.	94
1½ in.	70 to 95
1 in.	55 to 85
¾ in.	50 to 80
⅜ in.	40 to 70
No. 4	30 to 60
No. 10	20 to 50
No. 40	10 to 30

The fraction passing the No. 200 mesh was specified to be between 5% and 15%, less than half of the fraction passing the No. 40 mesh. The binder includes any blended binder passing No. 40 mesh with a liquid limit less than 25 and a plasticity index of less lhan 6.

Actually, local field inspectors roughly checked the production at each pit and the acceptability of the gravel shipped was determined by the men placing it into the subbase. Considerable gravel from different sources was blended at the site to reduce the necessary blading and rolling, for proper compaction.

The cost varied from $1.45 per cu yd to $1.75 per cu yd delivered to the site, measured in trucks upon delivery. As the previously developed pits were depleted, prices went up to compensate for the purchase of land and for stripping and exploratory expenses. Hauling costs remained stable during the entire period at approximately 5¢ per cu-yd mile hauled, with no allowance for the return trip. Practically every available truck within 50 miles of the station was employed in this haulage, as subcontractors to the gravel venders. As an average, a ton of gravel yielded 2.67 sq yd of subbase, compacted to a thickness of 8 in. This is equivalent to a density of 125 lb per cu ft.

On main and secondary road areas, a layer of fine sand was first spread, from 1 in. to 2 in. thick, to seal the clay, before placing the gravel unless the gravel as delivered contained a surplus of fines. In the first training area built, the subgrade was covered with straw cut from the area. This straw was laid about 2 in. to 3 in. high and the gravel was dumped on it. Objections to this

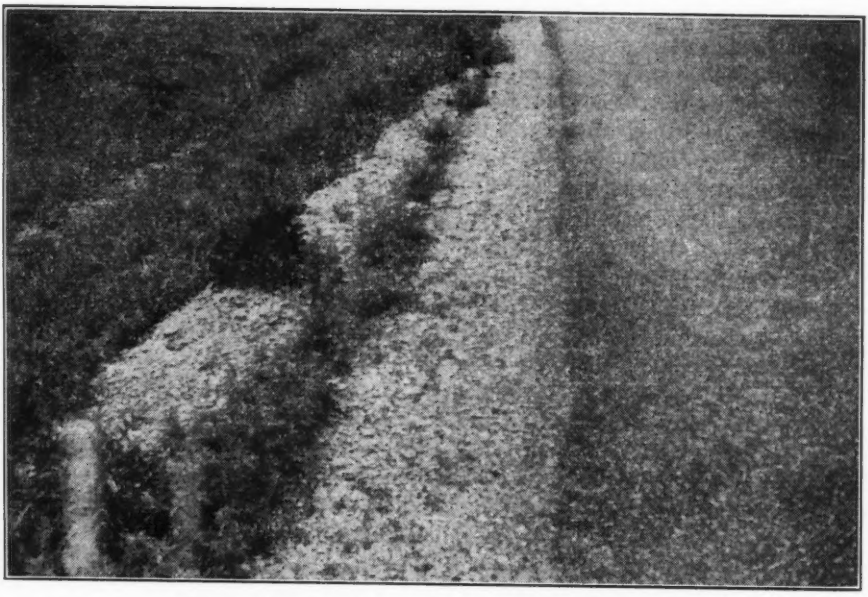

FIG. 4.—DETAIL OF SHOULDER OF MAIN CONNECTING ROAD

FIG. 5.—SPREADING AND SEALING STONE BASE

procedure resulted in the change to the fine run-of-bank silty sand as a screen on the clay subgrade. Inspection of one of the earliest roads built, after 1 year of use and after 3 years of use, indicated that the straw had served its purpose. No clay had worked up through any of these roads. The other roads, with the sand screen, also stood up very well; curves, grades, and crown remained in excellent shape. The volume of the sand used is included in the quantities listed as gravel. The satisfactory behavior of the subbase is partly explained by the screen layer placed on the subgrade. Shoulders of gravel remain in good shape (Fig. 4) although weed growth was not controlled.

Stone Base.—The contractor began work in the stone base and penetration on September 1, 1942 (Fig. 5). The stone used was crushed dolomite, delivered by rail and distributed from the siding by trucks. The grading specification required: 100% passing a 2½-in. screen, 90% to 100% passing a 1⅞-in. screen, and 0% to 15% passing a 1-in. screen. After spreading and rolling to the desired crown, hot tar (RT-11 or RT-12 depending upon air temperatures) was applied by pressure distributers, 1.25 gal per sq yd. The surface was then covered with 50 lb per sq yd of from ⅜-in. stone to ½-in. stone, rolled, and broom dragged until the base stone was well chinked. This was followed by a second application of hot tar (0.50 gal per sq yd) and the surface was covered with 10 lb per sq yd to 15 lb per sq yd of screenings and broom dragged. The totals were from 330 lb to 335 lb of stone and 1.75 gal of tar per sq yd.

After a week of trial, it was found expedient to apply the stone base in two layers, which reduced the total rolling time. On November 20, the tar was changed to RT-10 because of low temperatures, and work continued through most of December. The original plan was to allow an interval of at least a week between the completion of the gravel subbase and the application of the stone. After November 1 (with freezing weather starting on October 27), with the danger of rain freezing within the gravel, the stone was applied soon after the gravel had been shaped. This required some extra stone, since traffic had usually pounded out some depressions in the gravel subbase which were refilled with stone.

Total amounts used approximated 60,000 tons of No. 3-A stone; 10,000 tons of No. 1 stone, No. 1-A stone, and No. 1-B stone; 1,000 tons of No. 3 stone for drains in shoulders; and almost 700,000 gal of tar (RT-12, RT-11, and RT-10).

A typical gang consisted of 30 men with 2 spreader boxes, 2 rollers, and 2 shapers, and they used about 400 tons of stone to cover 900 ft of road 24 ft wide. At full speed, five gangs were operating. Stone was delivered to the work by 15 trucks, and 2 cranes unloaded the cars. The stone cost 27¢, the placing cost 70¢, and the tar cost 21¢ per sq yd of base. The stone delivered to the site on cars cost $1.68 per ton.

Black-Top Pavement.—A premixed tar concrete test road section, 12 ft by 250 ft long, was laid on a gravel subbase to test the feasibility of this material for the intended traffic. Even though no base was laid down, heavy trucking did not seriously damage the test strip. Upon deciding to use tar mix (asphalt was not available), it was imperative to move a suitable plant to the site. Approximately 75,000 tons were required and the congestion of traffic on the

access roads would seriously handicap any attempted delivery schedule of hot mix from locations outside the station.

Fortunately, a complete premix plant, built in 1941, and used for only 1,000 tons was located, and it was moved bodily to the site. A contractor was engaged to produce all binder and top course material at $7.65 per ton complete in place. This price covered all materials, equipment, and labor, except that a railroad siding was provided to the contractor without charge. About 20 men including truck drivers (the average haul distance was 3 miles) were employed at the plant.

The plant was an integrated mixing unit with feed bin and reciprocating feeder. Two aggregate driers, equipped with oil burners and a cyclone dust collector were set up in tandem, with hot and dust elevators. Screens in the mixing tower unit were 2 in., $\frac{5}{8}$ in., $\frac{3}{8}$ in., and $\frac{1}{8}$ in. The mixer was a 4,000-lb-capacity twin pug mill, equipped with 5,000-lb aggregate batch scale and 500-lb tar bucket scale. Storage of aggregate was in a 50-ton bin with four compartments. Tar storage was in tank cars with a 10,000-gal reserve storage tank. Steam generated by a 150-hp locomotive steam boiler was used in the tar heating kettle and in the jackets surrounding the tar lines and mixer box. The mixing cycle, electrically controlled, was 45 sec, including dry and wet mix. Temperatures of the mix leaving the plant were from 180° F to 200° F for the binder and from 200° F to 230° F for the top course. Plant production averaged 100 tons of binder and 80 tons of top course per hour.

The tar concrete was mixed, laid, and rolled according to New York State Highway Specifications.[3] The specification for binder and top course were in conformity with the following limitations:

Passing screen size	Binder course (%)	Top course (%)
1½ in.	100	....
1 in.	70 to 100	....
½ in.	20 to 60	100
⅜ in.	....	85 to 100
No. 4	5 to 20	55 to 80
No. 8	0 to 5	35 to 65
No. 40	....	14 to 34
No. 100	....	6 to 20
No. 200	....	5 to 15

The aggregate sizes used in the mix were of New York State highway designation and were of the following description:

The No. 2, No. 1, and No. 1-A sizes, which were limestone, as well as the stone, sand, or limestone screenings, were shipped by rail. The sand was trucked in from a pit 22 miles distant. The proportions of each aggregate were set up to provide a dense, impervious, surface course, retaining nonskid features.

[3] "Hot Lay Tar Concrete Pavement—Two Course Construction Mixing Method—Type 6," N. Y. State Highway Specification, Albany, N. Y., 1939.

The mixing formulas, adopted after some trial proportions were laid and modified, were as follows (Table 1):

TABLE 1.—MIXING FORMULAS FOR BLACK-TOP PAVEMENTS

Passing sieve:	Retained on sieve:	BINDER TO NOVEMBER 19		BINDER AFTER NOVEMBER 19		TOP	
		%	Pounds	%	Pounds	%	Pounds
(1)	(2)	(3)	(4)	(5)	(6)	(7)	(8)
2 in.	½ in.	....	....	39	1,560	....	....
2 in.	½ in.	60	2,400	....	....	....	....
½ in.	⅜ in.	....	....	24	960	14	560
½ in.	⅜ in.	15	600	....	....	....	....
⅜ in.	⅛ in.	16	640	28	1,120	37	1,480
⅛ in.	....	6	240	6	235	42	1,680
Tar	....	3	120	3¼	125	7	280
Total	....		4,000	....	4,000	....	4,000

The tar binder used was RT-12. As the weather became colder, RT-11 was substituted for RT-12. Check analyses were made daily of samples from the bins and of the mixed product. Where it was not possible, due to construction scheduling, to cover the binder course within 2 days, the binder mix (Col. 5, Table 1) was changed. This denser binder mix withstood construction traffic better than the more open mix. The better practice is to cover the binder course the same day with top mix, but in order to keep traffic flowing, and to avoid changing from binder mix to top mix at the plant during the middle of the day, the binder course was left uncovered for periods as long as 3 days or more in some few instances. When cold weather arrived all the binder was of the denser mix.

Tar mix production began on September 15 and closed down on December 9 for the winter, after 40,000 tons had been placed. An illustrated progress report of this work to this period was published[4] in January, 1943. The plant was opened again in May and completed the remaining 35,000 tons by the middle of July, 1943. At first the work progressed on a 10-hour day, 7-day-per-week basis, and changed to a 12-hr day, partly after nightfall. Only the binder mix was laid under artificial light. Production of 1,300 tons in a 12-hr day was not unusual.

The Navy's order to stop all binder placing when the temperature fell below 32° F and top course when it was below 35° F was only generally followed. The mean recorded temperatures were 54° F for October (with more than 2 in. of snow) and 41.7° F for November (with almost 5 in. of snow and 7 days with precipitation greater than 0.1 in.). With below zero weather early in December, it was impossible to continue the surfacing.

The contractor placed the tar mix using 4 paving machines to spread and finish the surface. The mix was fed from dump trucks into the hoppers of the paving machines which pushed the trucks ahead. Additional equipment used included 8 rollers, 21 trucks, 1 grader, 2 bulldozers, 1 power broom, and 1 gang broom. About 90 men were used for this work.

[4] *Construction Methods*, January, 1943, p. 62.

Surfaces were rolled with 10-ton to 12-ton, 3-wheel rollers, or 8-ton to 10-ton tandem rollers, to produce a compression of 250 lb per in. of tread width. Surface tolerances were $\frac{1}{4}$ in. from crown template and $\frac{1}{4}$ in. from a 10-ft straightedge parallel to the axis of the road. It was pointed out by the vender in the middle of October that tar mix was being placed with air temperatures far below the 50° limit specified by the N. Y. State Highway Department and that the base was often in rather soft condition. In many cases, a 2-ton roller was used for compacting the base course to prevent undue deflections, especially when work was continued immediately after heavy rains. At times, the spreader had to be pulled forward by the trucks delivering the mix (instead of the spreader pushing the trucks) to pass through soft spots. In spite of all these conditions, the road surfaces held up very well, the gravel subbase drained

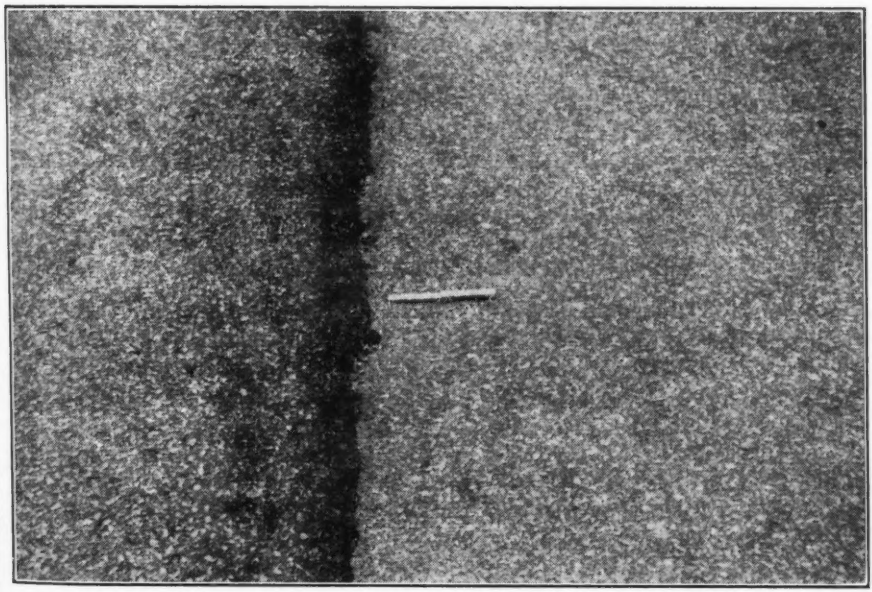

FIG. 6.—TEXTURE OF ROAD SURFACE (RIGHT) AND ASSEMBLY AREA (RULE IS 8 IN. LONG)

out the excess moisture, and the roads were used for 4 years with practically no maintenance. An illustration of the pavement surfaces photographed in 1946 is shown in Fig. 6.

Theoretical yield was 7.0 sq yd per ton as compared with an actual yield of about 6.5 sq yd. The binder course of $1\frac{1}{2}$ in. compacted gave 10.93 sq yd per ton and the topping course of 1 in. compacted gave 15.61 sq yd per ton. The density of the top mix, as tested from samples in place, was 141.1 lb per cu ft. The yields include the losses in material at soft spots and the filling of ruts in the stone base from traffic. The total cost of primary pavement surface was $1.08 per sq yd.

Concrete Pavement.—Concentrated trucking and vehicle servicing was expected in the warehouse and repair shop areas and pavements were designed

with a concrete surface. Concrete design was specified in accordance with the N. Y. State Highway (1939) requirements for plain concrete, permitting crushed gravel as coarse aggregate. Cement content was 6 bags of Portland and 1 bag (80 lb) of natural cement per cu yd. With a water content of 5.5 gal per bag of cement, the slump was held to 2 in. When the central concrete plant was not being run to full capacity by the other operations, transit mix concrete was used for road construction. To prevent stoppage of work, a small batch bin was set up and a paver mixer, with cement in bags, was used to maintain continuous concreting. No reinforcement was used in the 6-in.-thick slab, with transverse joints filled with cane asphalt premolded strips, $\frac{3}{4}$ in. by $5\frac{1}{2}$ in., and transverse dummy joints $1\frac{1}{2}$ in. deep spaced not more than 20 ft apart.

About 50,000 sq yd of concrete pavement was placed before cold weather forced a change to black-top pavement for the remainder of the area. Water for the mix came from Seneca Lake and during the period of water main sterilization with chlorine, very rapid setting of the concrete mix was noted. With a residual of 5 ppm of chlorine in the water, concrete had to be spread and finished within 20 min of mixing, even with air temperatures between 45° F and 55° F. Little surface spalling was found in this concrete paving after 4 years of use and exposure. Paved surfaces were cured with straw covering and the work was done by an experienced concrete road gang.

Personnel and Acknowledgment

All work was under the direction of Capt. J. C. Gebhard, M. ASCE, (CEC), U. S. Navy, with the firm of Shreve, Lamb and Harmon associated with Gilmore D. Clarke, M. ASCE, Michael Rapuano, and Malcolm Pirnie, M. ASCE, as architect-engineer. The planning of the roads and pavements was assigned to Ralph MacDonald of Mr. Clarke's office. Contractors were the John A. Johnson Contracting Company and the Mount Vernon Contracting Company. The latter firm executed all road construction work. The Dale Engineering Company supplied the complete premix plant for the construction of the black-top pavement, including the production of all binder and top course material. The material, equipment, and labor for the stone base tar mix and penetration phase of the construction were supplied by A. L. Blades Company as the subcontractor for the Dale Company. The writer was site project manager in direct charge of the performance of all site work operations. Pavement construction planning and performance was directed by Richard Halton, superintendent of paving.

Acknowledgment is made of the able assistance of P. F. Phelan, Assoc. M. ASCE, of the Koppers Company, Incorporated, in the planning, design, and control of the tar concrete mixes.

AMERICAN SOCIETY OF CIVIL ENGINEERS

Founded November 5, 1852

PAPERS

AERODYNAMIC THEORY OF BRIDGE OSCILLATIONS

By D. B. Steinman,[1] M. ASCE

Synopsis

General equations are derived, expressing the aerodynamic forces of lift and torque on any oscillating section of two independent degrees of freedom. The parameters representing the distinctive aerodynamic characteristics of the section and the coefficients representing the variation with wind velocity are derived from static wind-tunnel tests on straight and curved section models. The effects of vertical velocity, angular displacement, and angular velocity are included, as well as the effects of the angle of incidence. The complete expressions for the aerodynamic forces are equated to the corresponding expressions for the dynamic forces acting on the section, including elastic (and gravitational) restoring force, inertia, and damping. The resulting general equations yield solutions for all practical problems of vertical, torsional, and coupled oscillations, including analytical determination and prediction of frequencies, critical velocities, instability response (rate of amplification), and amplitude response.

Numerical examples are given, to illustrate the practical application of the derived relations and to confirm the validity of the underlying theory. Graphic methods are presented to facilitate application and visualization.

Introduction

A primary requisite for a comprehensive solution of all problems in aerodynamic oscillations is the writing of the general "aerodynamic" equations for the forces (L and M) acting on any section, together with the general "dynamic" equations for the same forces. Once these general equations are correctly set up, the rest is simple algebra—to determine frequencies, critical velocities, amplification or damping, limiting (maximum or minimum) amplitudes, amplitude response curves, and other relations for vertical, angular, and coupled oscillations.

Note.—Written comments are invited for immediate publication; to insure publication the last discussion should be submitted by **March 1, 1950.**

[1] Cons. Engr., New York, N. Y.

For the complete solution, the aerodynamic equations must include the effects of vertical velocity, angular position, and angular velocity of the section.

The dynamic equations must include the elastic (and gravitational) resistance to displacement, the inertia resistance to acceleration, and the damping force or resistance (in phase with the velocity).

Theoretical equations for the limiting case of a flat plate or streamline airfoil have been derived by Theodore Theodorsen,[2] R. Kassner and H. Fingado,[3] H. Glauert,[4,5,6] H. G. Küssner,[7] Herbert Wagner,[8] Theodor von Kármán, M. ASCE, and J. M. Burgers,[9] and others, using the methods of classical aerodynamic theory (based on potential flow and the application of the Kutta condition).

For the more general case of bridge sections and other nonstreamline sections for which the Kutta condition is not applicable, it appears impossible to write the aerodynamic equations by purely theoretical derivation. Some of the necessary coefficients must be supplied by experiment.

Consequently, for a practically feasible solution to cover all cases, it is necessary to deduce rationally the correct general form of the aerodynamic equations, with the unknown coefficients or parameters (representing the distinctive characteristics of different sections) to be supplied experimentally.

Since only the aerodynamic characteristics of the section need to be determined experimentally, full-scale models incorporating the dynamic characteristics of the complete structure are unnecessary; simple section models suffice. Moreover, to the extent that static wind-tunnel tests reveal the distinctive aerodynamic characteristics of a section, oscillating model tests are not required. The thesis that the distinctive aerodynamic characteristics of oscillating sections can be mathematically predicted from the known or measurable aerodynamic characteristics of stationary section models has now received cumulative and consistent confirmation.

Notation.—The letter symbols used in this paper follow customary notation as far as practicable.

Vertical vectors are measured positive upward; angular vectors are measured positive clockwise; wind velocity is to the right, and wind inclination is measured positive upward.

As used in this paper, b is the chord or width of the section (in feet), and the dynamic parameters, w, m, and K, are per full width.

---

[2] "General Theory of Aerodynamic Instability and the Mechanism of Flutter," by Theodore Theodorsen, *Technical Report No. 496*, National Advisory Committee for Aeronautics, Washington, D. C., 1935.

[3] "Das ebene Problem der Flügelschwingung," by R. Kassner and H. Fingado, *Luftfahrtforschung*, November 20, 1936, pp. 374–387. ("The Two-Dimensional Problem of Wing Vibration," by R. Kassner and H. Fingado, *Journal*, Royal Aeronautical Soc., Vol. 41, 1937, pp. 921–944.)

[4] "The Accelerated Motion of a Cylindrical Body Through a Fluid," by H. Glauert, *Reports and Memoranda No. 1215*, British Aeronautical Research Committee, 1928–1929, Vol. 1, January, 1929, pp. 118–127.

[5] "The Lift and Pitching Moment of an Aerofoil Due to a Uniform Angular Velocity of Pitch," by H. Glauert, *Reports and Memoranda No. 1216*, British Aeronautical Research Committee, 1928–1929, Vol. 2, January, 1929, pp. 636–644.

[6] "The Force and Moment on an Oscillating Aerofoil," by H. Glauert, *Reports and Memoranda No. 1242*, British Aeronautical Research Committee, 1929–1930, Vol. 2, March, 1929, pp. 742–758.

[7] "Zusammenfassender Bericht über den instationären Auftrieb von Flügeln," by H. G. Küssner, *Luftfahrtforschung*, December 20, 1936, pp. 410–424.

[8] "Ueber die Entstehung des dynamischen Auftriebes von Tragflügeln," by Herbert Wagner, *Zeitschrift für angewandte Mathematik und Mechanik*, February, 1925, pp. 17–36.

[9] "General Aerodynamic Theory—Perfect Fluids," by Theodor von Kármán and J. M. Burgers in "Aerodynamic Theory" (W. F. Durand, editor), Springer, Berlin, 1935, Vol. 2.

Numeral subscripts distinguish corresponding parameters for vertical and torsional oscillations: ω_1, K_1, δ_1, g_1, s_1 (and s_3) for vertical oscillations; ω_2, K_2, δ_2, g_2, s_2 (and s_4) for torsional oscillations.

Use of Stationary Section Models

Use of Curved Models.—By a principle of relativity, the motion of the section (regarded as an immersed boundary surface) may be translated into a relative tilt or distortion of the flow lines in the fluid, or into a contrary relative tilt or distortion of the boundary surface, so that in either case the boundary surface may then be treated as stationary.

For parallel vertical motion of the section with downward velocity v, the graphic representation (Fig. 1) consists of the simple composition of horizontal

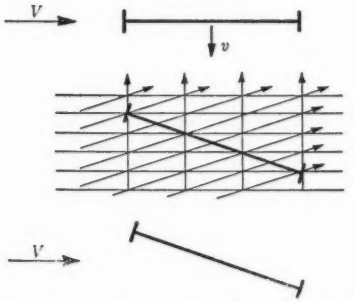

Fig. 1.—Tilting of Field of Flow for Vertical Motion of Section

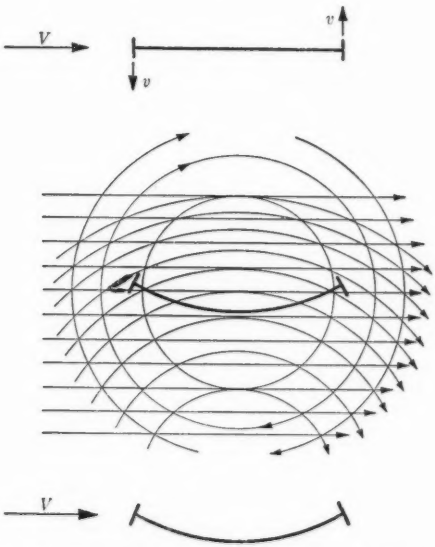

Fig. 2.—Curving of Field of Flow for Angular Motion of Section

flow lines with spacing $1/V$ and relative (upward) vertical flow lines with spacing $1/v$. By this graphic composition, the horizontal flow lines in the fluid are simply tilted up to a positive angle of incidence v/V. Instead of tilting the horizontal flow lines upward, an equivalent procedure is to tilt the section downward the same angle v/V; this is also given (Fig. 1) by the graphic composition of the same superimposed flow lines with the direction of the vertical lines reversed. Accordingly:

Analogy 1.—The tilting of the stationary model in a wind tunnel takes the place of a vertical velocity of the section.

When the same procedure is applied to angular velocity of the section, the graphic representation (Fig. 2) consists of the simple composition of the horizontal flow lines with spacing $1/V$ and a series of concentric circular flow lines

with graduated spacing $\frac{1}{2}\, b/(c\, v)$—in which v is the linear downward velocity at the leading edge and c is the distance of any flow filament from the center. This graphic composition yields a series of concentric circular flow lines, convex upward. The angular velocity of the section is thus translated into a curved field of flow, as in an arching wind tunnel, with the immersed section model kept stationary and unchanged. Instead of curving the field of flow, an equivalent procedure is to curve the immersed section model an equal and opposite amount. This curvature is also given (Fig. 2) by the graphic composition of the same superimposed flow lines with the direction of the rotational flow lines reversed. The equivalent warping of the immersed section model is symmetrical about the center of angular rotation, with horizontal tangent at this center and with slope change v/V at each end; the radius of curvature is $\frac{1}{2}\, b\, V/v$. Accordingly:

> Analogy 2.—The curvature of the stationary model in a wind tunnel takes the place of an angular velocity of the section.

With a curved section model, as in the more familiar tilted section model, the added angle of incidence at the leading edge remains $-v/V$.

For wind-tunnel duplication of this condition, the section model must be warped to the circular (or parabolic) curvature indicated above, with horizontal tangent at the center of rotation and the curvature changed for different desired values of the slope β at the leading edge (angle of incidence at the leading edge equivalent to angular velocity of section). This curvature is called the "dynamic camber."

The first wind-tunnel tests on curved models of bridge sections were made in 1947 at the Virginia Polytechnic Institute at Blacksburg by F. J. Maher, in cooperation with the writer. The results yield the needed additional data for the analysis of torsional instability.

In the absence of such tests on curved models, the analysis for the effect of angular velocity has previously been based on the static torque graphs obtained from straight section models (simply tilted instead of curved). Qualitatively, the results and conclusions should be substantially unchanged, since the major disturbance of the incident stream flow is determined by the effective angle of incidence at the leading girder. Quantitatively, the indicated correction from straight section models to curved section models is in the direction of reducing stability torque or intensifying instability torque.

It should be noted that the straight, tilted section model has a dual significance. It represents the effect of angular position, α, also the identical effect of vertical velocity, v. Accordingly, in aerodynamic formulas, the two are interchangeable; the conversion relation is simply $\alpha = -v/V$. The two contributions may be bracketed, as $(\alpha - v/V)$, with the same factors and coefficients applied to both.

The curved section model represents solely the effect of angular velocity, $\dot{\alpha}$. The conversion relation is $\beta = -v/V = -b\,\dot{\alpha}/(2\,V)$.

For ordinary values of β, it is sufficiently accurate to use a circular or parabolic arc for the curvature of the model. For higher values of β, the curve is more accurately a catenary, to keep the elements of the section width unchanged

in length. For the limiting case of $V = 0$, yielding $\beta = -90°$, the catenary becomes a folded straight line (zero span, and sag = $b/2$).

Curvature of the section model in static wind-tunnel tests, as the equivalent of angular velocity of the section, is (for this application) a new concept introduced by the writer. A search of aerodynamic literature reveals that a similar idea has been applied in the study of curvilinear flight of airships.[10] The same idea, but intended to be applied analytically instead of experimentally, is also briefly suggested by Messrs. Kassner and Fingado,[3] who state that one of the terms of the lift force due to angular velocity of an airfoil "could be deduced by replacing the rotating airfoil by a correspondingly cambered airfoil." This relationship is also confirmed by comparing the respective aerodynamic formulas.[9] A simple analytic derivation yields a parabola for the dynamic camber.

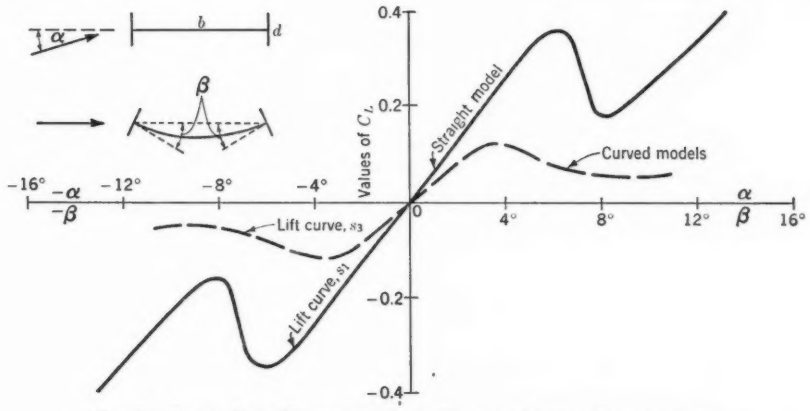

FIG. 3.—STATIC LIFT GRAPHS FOR STRAIGHT AND CURVED MODELS OF AN H-SECTION ($d/b = 0.20$)

Lift and Torque Graphs from Curved Models.—Fig. 3 shows the static lift graphs obtained from straight and curved section models, respectively, for an H-section of section ratio $d/b = 0.20$ (approximately the section of the original Tacoma (Wash.) bridge). The respective slopes are $s_1 = +4.00$ for the straight model (corrected for drag) and $s_3 = +2.00$ (approximately) for the curved model. Accordingly, for this section, the vertical lift resultant produced by a given β (at the leading edge) due to angular velocity is approximately one half the vertical lift resultant produced by an equal α due to vertical velocity or to angular position ($q_3 = s_3/s_1 = 0.50$).

Fig. 4 shows the static moment graphs obtained from the same straight and curved section models. The respective slopes are $s_2 = -0.50$ for the straight model and $s_4 = -1.00$ for the curved model (corrected for drag). Accordingly, for this section, the aerodynamic instability torque produced by β (at the leading edge) is twice the aerodynamic instability torque produced by an equal α due to vertical velocity or to angular position ($q_4 = s_4/s_2 = 2.0$).

[10] "Method of Curved Models and Its Application to the Study of Curvilinear Flight of Airships," by G. A. Gourjienko, *Technical Memorandum No. 829* (Pt. 1) and *Technical Memorandum No. 830* (Pt. 2), National Advisory Committee for Aeronautics, Washington, D. C., 1937.

Since the lift is halved and the torque is doubled, the eccentricity of the resultant (or center of pressure) on the curved model is four times as great as on the straight model, the respective values for this section being $e_4 = s_4/s_3 = -0.50$ (placing the resultant at the leeward edge of the section) and

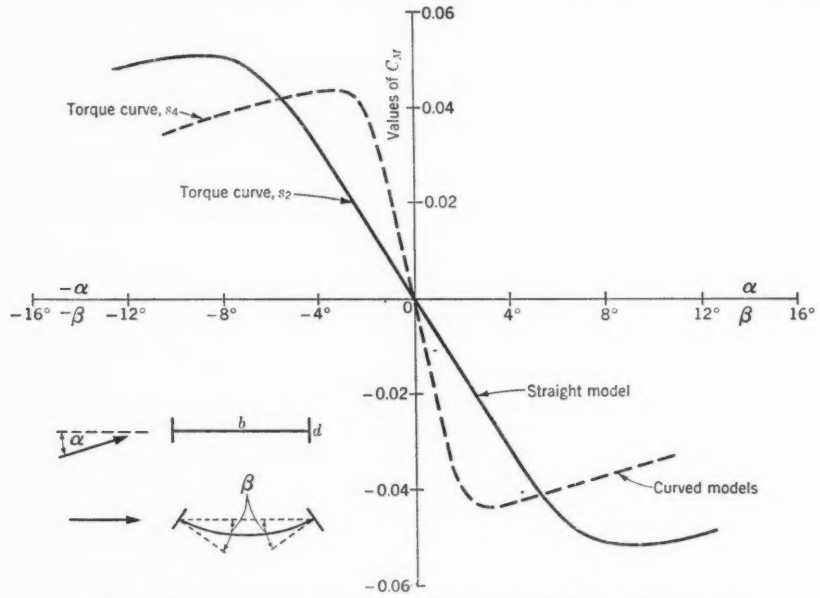

FIG. 4.—STATIC TORQUE GRAPHS FOR STRAIGHT AND CURVED MODELS OF AN H-SECTION ($d/b = 0.20$)

$e_2 = s_2/s_1 = -0.125$. Accordingly, the ratio M/L for angular velocity is not the same as for vertical velocity or angular position. The resultant center of pressure does not remain stationary (along the section) during a cycle of angular oscillation, nor during a cycle of coupled vertical and angular oscillations.

As shown by the positive value of s_1 and the negative values of s_2 and s_4, the section $d/b = 0.20$ is vertically stable and torsionally unstable. For such sections, the curved model yields increased negative slope of torque graph ($q_4 > 1$), representing intensified torsional instability.

TABLE 1.—GRAPH SLOPES FROM STRAIGHT AND CURVED SECTION MODELS

Section (d/b)	s_1	s_2	s_3	s_4	e_2	e_4	q_3	q_4
0 (theoretical).....	6.28	1.57	−3.14	0	0.25	0	−0.50	0
0.02 (test).....	5.25	1.10	−1.75	0.55	0.21	−0.31	−0.33	0.50
0.20 (test).....	4.00	−0.50	2.00	−1.00	−0.125	−0.50	0.50	2.00

For torsionally stable sections, as typified by a flat plate, the curved model yields a reversed slope of lift graph (Fig. 5) and a reduced slope of torque graph (Fig. 6). For comparison, the slopes and their respective ratios, for $d/b = 0$ (ideal flat plate), $d/b = 0.02$ (flat plate tested), and $d/b = 0.20$, are collated in Table 1.

FIG. 6.—STATIC TORQUE GRAPHS FOR STRAIGHT AND CURVED MODELS OF A FLAT PLATE ($d/b = 0.02$)

FIG. 5.—STATIC LIFT GRAPHS FOR STRAIGHT AND CURVED MODELS OF A FLAT PLATE ($d/b = 0.02$)

General Aerodynamic Equations

For Oscillating Sections.—For the derivation of the following aerodynamic equations, let:

α_i = initial angle of incidence (for the section at rest);
L_i = initial static lift at α_i;
M_i = initial static torque at α_i;
η = vertical displacement;
$\dot{\eta} = d\eta/dt$ = vertical velocity;
$\ddot{\eta} = d^2\eta/dt^2$ = vertical acceleration;
α = angular displacement;
$\dot{\alpha} = d\alpha/dt$ = angular velocity; and
$\ddot{\alpha} = d^2\alpha/dt^2$ = angular acceleration.

Then the general aerodynamic force equations for a moving or oscillating section are

$$L = L_i + L(\alpha) + L(\dot{\eta}) + L(\dot{\alpha}) + L(\ddot{\eta}) + L(\ddot{\alpha}) \ldots\ldots\ldots (1a)$$

and

$$M = M_i + M(\alpha) + M(\dot{\eta}) + M(\dot{\alpha}) + M(\ddot{\eta}) + M(\ddot{\alpha}) \ldots\ldots\ldots (1b)$$

in which $L(\alpha)$, $L(\dot{\eta})$, ..., denote the contributions to L due to α, $\dot{\eta}$, ...; and $M(\alpha)$, $M(\dot{\eta})$, ... denote the corresponding contributions to M. All moments are taken about the midpoint of the width b.

The angular displacement α is measured from the initial angle of incidence α_i. The slopes s_1 and s_2 are measured at α_i (for small displacements).

For vertically symmetrical sections, as a flat plate or an H-section, in horizontal wind, $\alpha_i = 0$; $L_i = 0$; and $M_i = 0$.

The ordinates of the static lift and torque graphs are C_L and C_M, respectively, defined by: $L = (\frac{1}{2}\rho V^2 b)\, C_L$; and $M = (\frac{1}{2}\rho V^2 b^2)\, C_M$.

The slopes of the static lift and torque graphs are as follows:

s_1 = slope of static lift graph, straight model = $\partial C_L/\partial\alpha$
s_2 = slope of static torque graph, straight model = $\partial C_M/\partial\alpha$
s_3 = slope of static lift graph, curved model = $\partial C_L/\partial\beta$
s_4 = slope of static torque graph, curved model = $\partial C_M/\partial\beta$

The contributions due to angular displacement α will then be

$$C_L = s_1\,\alpha \qquad \text{and} \qquad C_M = s_2\,\alpha$$

Similarly, the contributions due to vertical velocity $\dot{\eta}$ will be

$$C_L = s_1\,(-\dot{\eta}/V) \qquad \text{and} \qquad C_M = s_2\,(-\dot{\eta}/V)$$

since α and $(-\dot{\eta}/V)$ are equivalent in aerodynamic effect.

Similarly, from the slopes s_3 and s_4 of the static lift and torque graphs obtained from the curved model, the contributions due to angular velocity $\dot{\alpha}$ will be

$$C_L = s_3\,\beta \qquad \text{and} \qquad C_M = s_4\,\beta$$

in which $\beta = -\frac{1}{2} b \dot{\alpha}/V$. For this case, however, one correction is required. Referring to Fig. 2, the curved model, held stationary in horizontal wind, is equivalent to a straight model held stationary in an opposite curving airflow, or to a straight model moving in an opposite curvilinear path in a straight airflow. In each case the radius of curvature is $R = V/\dot{\alpha}$. This introduces a radial acceleration or centrifugal force involving the mass m_a of the cylinder of air enveloping the section. This radial acceleration is $V^2/R = V\dot{\alpha}$, and the resulting inertia force is $-m_a V\dot{\alpha}$. Since this is an extra force created by the curvilinear flow or motion represented by the curved model, it must be subtracted (algebraically) from the lift L given by the curved model. It does not affect the moment $M(\dot{\alpha})$, since this lift correction is centered at the midpoint $(b/2)$. Consequently the sole effect of this correction for centrifugal force is to augment $L(\dot{\alpha})$ by $\Delta L\,(\dot{\alpha}) = m_a V\dot{\alpha}$.

The contributions due to vertical acceleration $\ddot{\eta}$ are

$$L(\ddot{\eta}) = -m_a \ddot{\eta} \qquad \text{and} \quad M(\ddot{\eta}) = 0$$

The contributions due to angular acceleration $\ddot{\alpha}$ are

$$L(\ddot{\alpha}) = 0 \qquad \text{and} \quad M(\ddot{\alpha}) = -I_a \ddot{\alpha}$$

in which I_a is the effective polar moment of inertia of the enveloping cylinder of air.

Collecting the component values of L and M and substituting in Eqs. 1*a* and 1*b*,

$$L = L_i + \tfrac{1}{2}\rho V^2 b\left[C_1 s_1\left(\alpha - \frac{\dot{\eta}}{V}\right) - C_3 s_3\left(\frac{b\dot{\alpha}}{2V}\right)\right] + m_a(V\dot{\alpha} - \ddot{\eta}) \quad ..(2a)$$

and

$$M = M_i + \tfrac{1}{2}\rho V^2 b^2\left[C_2 s_2\left(\dot{\alpha} - \frac{\ddot{\eta}}{V}\right) - C_4 s_4\left(\frac{b\dot{\alpha}}{2V}\right)\right] - I_a\ddot{\alpha} \quad ..(2b)$$

in which C_1, C_2, C_3, and C_4 are phase-correction factors for the effect of time lag between any change in attitude or motion of the section and the resulting pressures across the width of the section. The inertia forces are instantaneous with the accelerations that produce them; hence, the terms containing m_a and I_a contain no phase-lag factors. Similarly initial or constant contributions, like L_i and M_i, contain no C-factors.

Eqs. 2 are of fundamental importance. They are the pivotal formulas of the analysis presented. Theories for evaluating the coefficients C_1, C_2, C_3, and C_4 vary; but, whatever evaluation of those coefficients is adopted, the basic validity of the general equations (Eqs. 2) is an independent proposition.

The applicability of Eqs. 2 is without restriction as to the form of the section and without restriction as to the nature of the motion or oscillation of the section (uniform, irregular, or harmonic). Moreover, the section may be horizontally stationary in a steady wind (as in the case of a bridge) or moving horizontally relative to the wind (as in the case of an airplane); V is the relative wind velocity.

In the case of harmonic oscillations, the coefficients C_1, C_2, C_3, and C_4, are functions of the velocity ratio $\frac{V}{N\,b}$ $\left(\text{or of } k = \frac{\omega\,b}{2\,V} = \frac{\pi\,N\,b}{V}\right)$. In such case, the C-coefficients are of the vector form, $C = F - i\,G$, representing an angle of lag equal to $\tan^{-1} G/F$. As derived subsequently, the values of F and G may be calculated and plotted from the pressure distribution graphs for the section (F_1, F_2, G_1, and G_2 from the straight model; F_3, F_4, G_3, and G_4, from the curved model).

In Eqs. 2 all the terms and parameters within the brackets are dimensionless. The outside terms may also be written in terms of $\rho\,V^2\,b$ or $\rho\,V^2\,b^2$ and dimensionless factors.

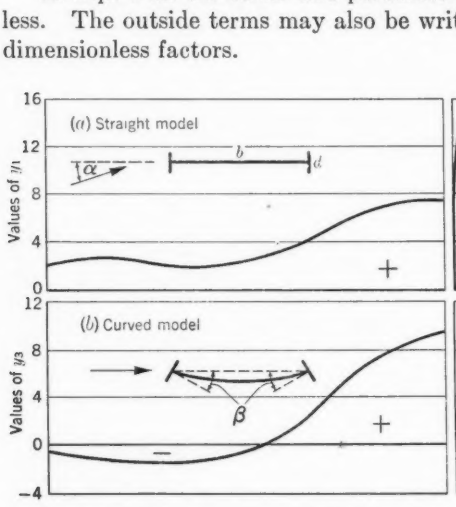

FIG. 7.—PRESSURE DISTRIBUTION GRAPHS FOR STRAIGHT AND CURVED MODELS OF AN H-SECTION (d/b = 0.20)

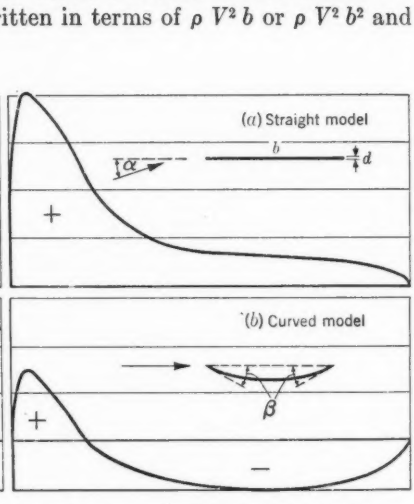

FIG. 8.—PRESSURE DISTRIBUTION GRAPHS FOR STRAIGHT AND CURVED MODELS OF A FLAT PLATE (d/b = 0.02)

For a thin flat plate ($d/b = 0$), the mass of the enveloping cylinder of air is $m_a = \frac{\pi}{4}\rho\,b^2$. For deeper sections (**H**, deck, or through sections), the corresponding indicated value is $m_a = \frac{\pi}{4}\rho\,r_1\,b^2$, in which $r_1 = 1 + (d/b)^2$, which reduces to $r_1 = 1$ for the thin plate.

By aerodynamic theory, for a thin flat plate, $I_a = \frac{b^2}{32}\,m_a = \frac{\pi}{128}\rho\,b^4$. This value of I_a is one fourth of the polar moment of inertia of the air cylinder, or one half of the moment of inertia about the vertical axis. For deeper sections, with sufficient accuracy, also, $I_a = \frac{b^2}{32}\,m_a = \frac{\pi}{128}\rho\,r_1\,b^4$. (This last formula considers that the effective radius of gyration is based on b and not on $\sqrt{r_1}\,b$.)

Because the mass m_a of the enveloping cylinder of air is small in comparison with the mass m of the bridge section, the terms representing the effects of acceleration ($\ddot{\eta}$ and $\ddot{\alpha}$) may be omitted. The correction (if desired) is easily made by simply including m_a and I_a of the circumscribing cylinder of air in

the values of m and I, respectively. This implies that the frequencies N_1 and N_2 are the natural frequencies in still air, not in a vacuum. The fractional additive corrections to m and I are given by $\frac{m_a}{m} = \frac{\pi}{4}\mu r_1 \approx 0.02$; and $\frac{I_a}{I} = \frac{\pi}{32}\mu\frac{r_1}{a_1} \approx 0.005$.

Pressure Distribution Graphs.—Fig. 7 shows typical pressure distribution graphs for a straight and a curved model, respectively, for the section $d/b = 0.20$, as obtained by manometer readings in static wind-tunnel tests. Fig. 8 shows the corresponding pressure distribution graphs for a flat plate ($d/b = 0.02$). Fig. 8(a) is similar to the curve of pressure distribution by aerodynamic theory,[2] except for the correction to zero pressure at the leading edge; aerodynamic theory fails to provide this correction. For the curved model, Fig. 8(b) differs from the (symmetrical) curve of pressure distribution yielded by aerodynamic theory, particularly in the region near the leading edge, where aerodynamic theory is known to be defective and inconsistent.

The ordinates of the respective graphs are designated by y_1 for the straight model and y_3 for the curved model. By definition: $y_1 = \frac{\Delta p}{0.5\,\rho\,V^2\,\alpha}$; and $y_3 = \frac{\Delta p}{0.5\,\rho\,V^2\,\beta}$. Integrating across the width b (or from $x = 0$ to 1),

$$s_1 = \int_0^1 y_1\,dx \qquad (3a)$$

$$s_2 = \int_0^1 y_1\,(\tfrac{1}{2} - x)\,dx \qquad (3b)$$

$$s_3 = \int_0^1 y_3\,dx \qquad (3c)$$

and

$$s_4 = \int_0^1 y_3\,(\tfrac{1}{2} - x)\,dx \qquad (3d)$$

These values of s_1, s_2, s_3, and s_4, refer to the stationary section, and should be identical with the slopes of the static lift and torque graphs (as in Figs. 3 and 4, or Figs. 5 and 6).

Effect of Phase Lag Across the Width of the Section.—Let ϕ_1 = total phase lag across the width b; ϕ = phase lag at any element dx of the width b, and x = abscissa along the width b (taken as unity). Then, in the case of harmonic oscillations of frequency N,

$$\phi_1 = \frac{2\,\pi\,N\,b}{V} = \frac{\omega}{V} = 2\,k \qquad (4a)$$

and

$$\phi = x\,\phi_1 = 2\,k\,x \qquad (4b)$$

Each pressure ordinate, y_1 or y_3, lags an amount ϕ behind the respective displacement or velocity vector that produces it. Hence, for the oscillating section, the static ordinates y_1 and y_3 are replaced by the lagging values—$y_1 e^{-i\phi} = y_1 (\cos \phi - i \sin \phi)$; and $y_3 e^{-i\phi} = y_3 (\cos \phi - i \sin \phi)$—and the static values s_1, s_2, s_3, and s_4 are replaced by the modified lagging values:

$$C_1 s_1 = \int_0^1 y_1 e^{-i\phi} \, dx \ldots\ldots\ldots\ldots\ldots\ldots\ldots\ldots (4c)$$

$$C_2 s_2 = \int_0^1 y_1 e^{-i\phi} \left(\tfrac{1}{2} - x\right) dx \ldots\ldots\ldots\ldots\ldots\ldots\ldots (4d)$$

$$C_3 s_3 = \int_0^1 y_3 e^{-i\phi} \, dx \ldots\ldots\ldots\ldots\ldots\ldots\ldots\ldots (4e)$$

and

$$C_4 s_4 = \int_0^1 y_3 e^{-i\phi} \left(\tfrac{1}{2} - x\right) dx \ldots\ldots\ldots\ldots\ldots\ldots\ldots (4f)$$

For each force or moment vector $C s$, $F s$ is the cosine component and $-i G s$ is the sine component. The angle of lag of the resultant force or moment vector is $\tan^{-1} (G/F)$. Accordingly, for the force vectors,

$$F_1 = \frac{\int_0^1 y_1 \cos \phi \, dx}{\int_0^1 y_1 \, dx \; (= s_1)}; \qquad G_1 = \frac{\int_0^1 y_1 \sin \phi \, dx}{\int_0^1 y_1 \, dx \; (= s_1)}; \qquad C_1 = F_1 - i G_1 \ldots (5a)$$

$$F_3 = \frac{\int_0^1 y_3 \cos \phi \, dx}{\int_0^1 y_3 \, dx \; (= s_3)}; \qquad G_3 = \frac{\int_0^1 y_3 \sin \phi \, dx}{\int_0^1 y_3 \, dx \; (= s_3)}; \qquad C_3 = F_3 - i G_3 \ldots (5b)$$

and, for the moment vectors,

$$F_2 = \frac{\int_0^1 y_1 \left(\frac{1}{2} - x\right) \cos \phi \, dx}{\int_0^1 y_1 \left(\frac{1}{2} - x\right) dx \; (= s_2)}; \; G_2 = \frac{\int_0^1 y_1 \left(\frac{1}{2} - x\right) \sin \phi \, dx}{\int_0^1 y_1 \left(\frac{1}{2} - x\right) dx \; (= s_2)}; \; C_2 = F_2 - i G_2 . \; (5c)$$

$$F_4 = \frac{\int_0^1 y_3 \left(\frac{1}{2} - x\right) \cos \phi \, dx}{\int_0^1 y_3 \left(\frac{1}{2} - x\right) dx \; (= s_4)}; \; G_4 = \frac{\int_0^1 y_3 \left(\frac{1}{2} - x\right) \sin \phi \, dx}{\int_0^1 y_3 \left(\frac{1}{2} - x\right) dx \; (= s_4)}; \; C_4 = F_4 - i G_4 . \; (5d)$$

In Eqs. 5 the denominators (by Eqs. 3) represent s_1, s_2, s_3, and s_4 and the numerators represent $F_1 s_1$, $F_2 s_2$, $F_3 s_3$, and $F_4 s_4$, and $G_1 s_1$, $G_2 s_2$, $G_3 s_3$, and $G_4 s_4$. For all cases of F, G, and C,

$$\text{Limit}_{k=0} F = 1 \qquad \text{limit}_{k=0} G = 0 \qquad \text{limit}_{k=0} C = 1$$

For infinite V or zero N,

$$\frac{V}{N b} = \infty \qquad \phi = 0 \qquad k = 0$$

Hence, $F = 1$; $G = 0$; $C = 1$; and $C s = s$. All phase difference vanishes, and the forces and moments acting on the section coincide in phase with their respective causative displacement or velocity vectors, and coincide in magnitude with the values given directly by the static lift and torque graphs (for the straight and curved models) without any correction for phase lag.

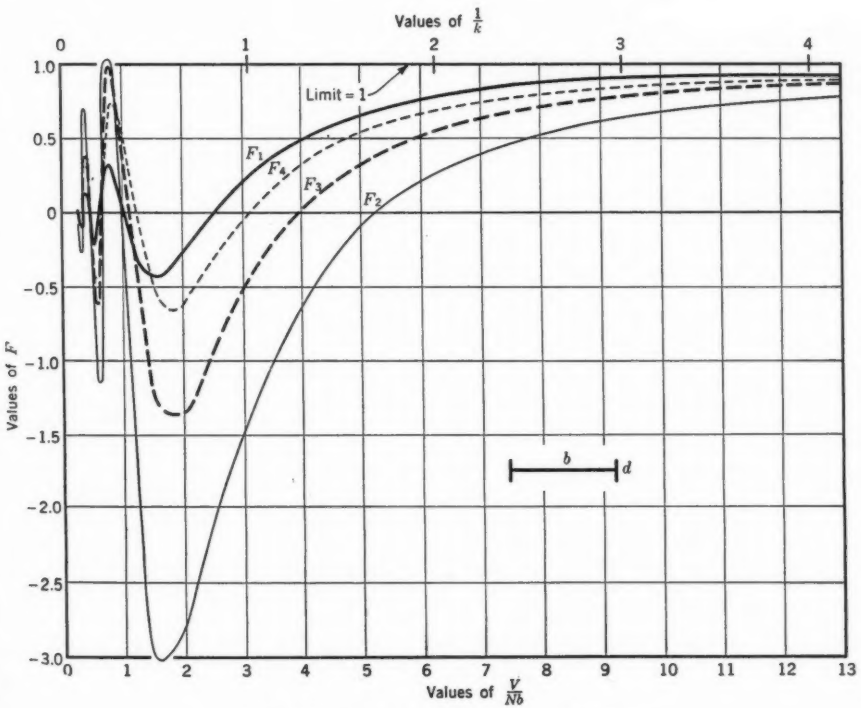

FIG. 9.—*F*-GRAPHS FOR AN H-SECTION ($d/b = 0.20$)

The *F*-graphs and *G*-graphs for the H-section of $d/b = 0.20$, computed by Eqs. 5 from the pressure distribution graphs of Fig. 7, are plotted in Figs. 9 and 10; and the *F*-graphs and *G*-graphs for the flat plate of $d/b = 0.02$, computed by Eqs. 5 from the pressure distribution graphs of Fig. 8, are plotted in Figs. 11 and 12.

General Dynamic Equations

For Oscillating Sections.—The general dynamic equations for a symmetrical oscillating section are

$$L = (L_i) + m\,\ddot{\eta} + c_1\,\dot{\eta} + K_1\,\eta \quad \ldots\ldots (6a)$$

and

$$M = (M_i) + I\,\ddot{\alpha} + c_2\,\dot{\alpha} + K_2\,\alpha \quad \ldots\ldots (6b)$$

in which η and α are measured from the initial static η_i and α_i, K_1, and K_2 are the spring constants or restoring-force coefficients, and c_1 and c_2 are the

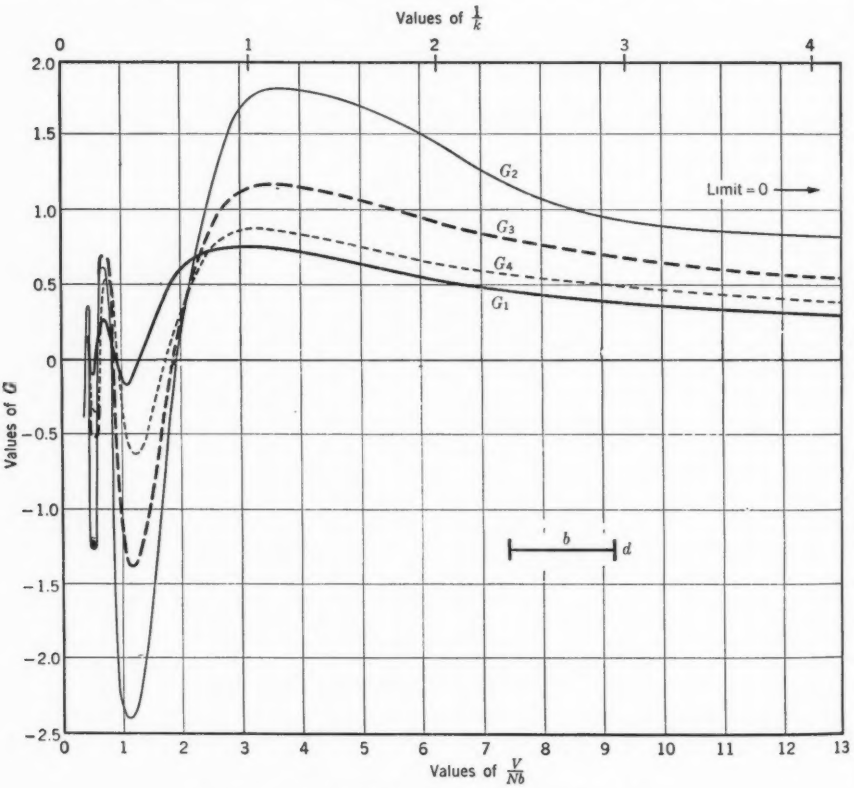

Fig. 10.—*G*-Graphs for an H-Section ($d/b = 0.20$)

damping coefficients. The terms L_i and M_i are canceled by the identical terms in the aerodynamic equations. For the uncommon case of unsymmetrical bridge sections, Eqs. 6 require modification by including the lateral eccentricity of the center of gravity and of the stiffness axis.

If η_o and α_o are the vertical and angular amplitudes, respectively,

$$\eta = \eta_o\, e^{i(\omega t + \psi)} \quad \ldots\ldots (7a)$$

and

$$\alpha = \alpha_o\, e^{i\omega t} \quad \ldots\ldots (7b)$$

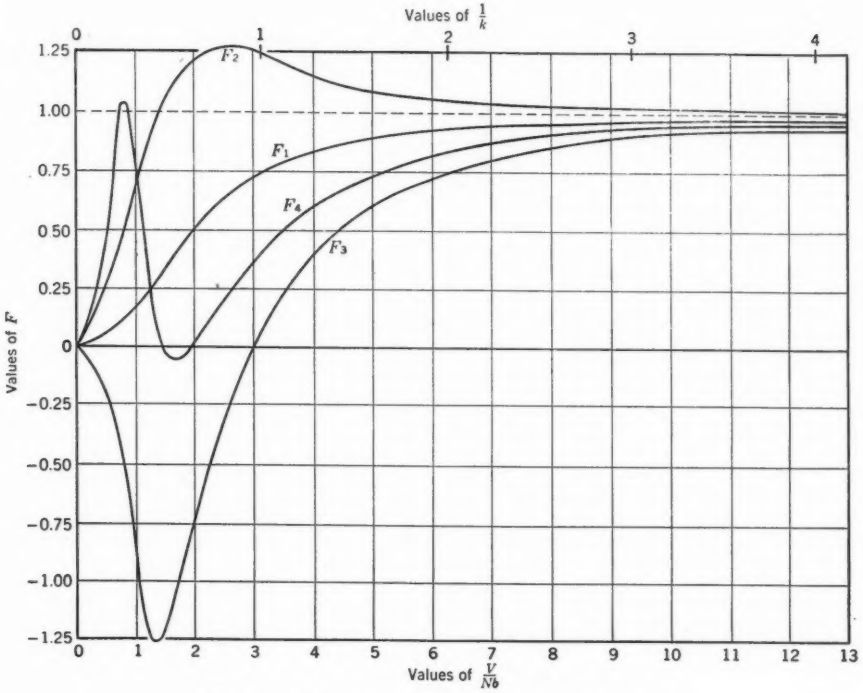

FIG. 11.—*F*-GRAPHS FOR A FLAT PLATE ($d/b = 0.02$)

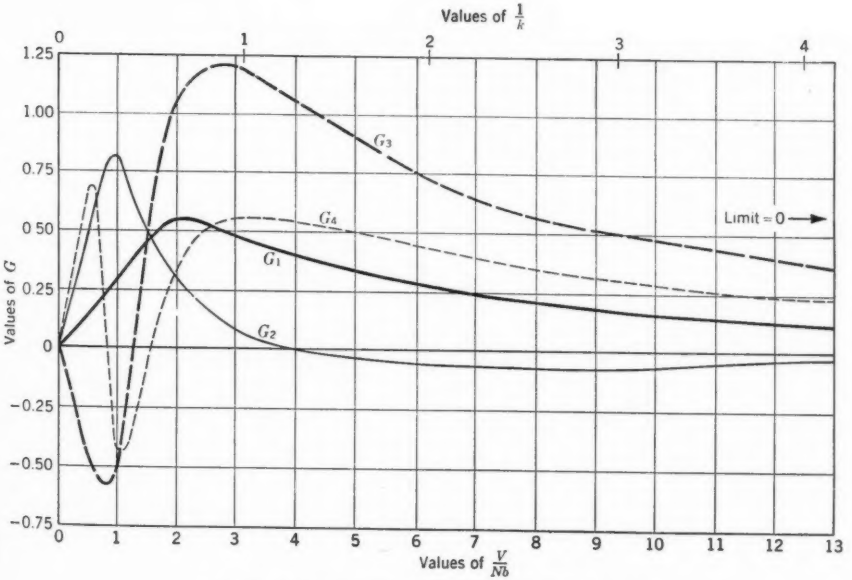

FIG. 12.—*G*-GRAPHS FOR A FLAT PLATE ($d/b = 0.02$)

in which ψ is the phase difference (angle of lead of the vertical oscillations) in coupled vertical and angular oscillations. Eqs. 7 yield

$$\dot{\eta} = i\,\omega\,\eta \qquad \ddot{\eta} = -\,\omega^2\,\eta$$
$$\dot{\alpha} = i\,\omega\,\alpha \qquad \ddot{\alpha} = -\,\omega^2\,\alpha$$

On substituting,

$$K_1 = m\,\omega^2{}_1 \qquad \frac{c_1}{m\,\omega} = g_1 = \frac{\delta_1}{\pi}$$

$$K_2 = I\,\omega^2{}_2 \qquad \frac{c_2}{I\,\omega} = g_2 = \frac{\delta_2}{\pi}$$

Eqs. 6 reduce to

$$L = L_i + m\,\omega^2\left[\left(\frac{\omega_1}{\omega}\right)^2 + i\,g_1 - 1\right]\eta \quad \ldots\ldots\ldots\ldots (8a)$$

and

$$M = M_i + I\,\omega^2\left[\left(\frac{\omega_2}{\omega}\right)^2 + i\,g_2 - 1\right]\alpha \quad \ldots\ldots\ldots\ldots (8b)$$

The structural damping (within a cycle of oscillation) can be represented as a force in phase with the velocity but of a magnitude proportional to the restoring force (corresponding to ω^2). Mr. Theodorsen and I. E. Garrick[11] suggest the form: $m\,\omega^2{}_1\,(1 + i\,g_1)\,\eta$ and $I\,\omega^2{}_2\,(1 + i\,g_2)\,\alpha$, but this would not yield $g_1 = \delta_1/\pi$ and $g_2 = \delta_2/\pi$ for the general case. The form used in Eqs. 8 meets the indicated requirements.

Combined Force Equations for Oscillating Sections.—Equating the aerodynamic forces given by Eqs. 2 with the dynamic resisting forces given by Eqs. 8, the general force equations for an oscillating section are obtained; thus,

$$m\,\omega^2\left[\left(\frac{\omega_1}{\omega}\right)^2 + i\,g_1 - 1\right]\eta = \tfrac{1}{2}\,\rho\,V^2\,b\left[C_1\,s_1\left(\alpha - \frac{\dot{\eta}}{V}\right) - C_3\,s_3\left(\frac{b}{2\,V}\,\dot{\alpha}\right)\right] + m_a\,V\,\dot{\alpha} \quad \ldots (9a)$$

and

$$I\,\omega^2\left[\left(\frac{\omega_2}{\omega}\right)^2 + i\,g_2 - 1\right]\alpha = \tfrac{1}{2}\,\rho\,V^2\,b^2\left[C_2\,s_2\left(\alpha - \frac{\dot{\eta}}{V}\right) - C_4\,s_4\left(\frac{b}{2\,V}\,\dot{\alpha}\right)\right] \quad \ldots (9b)$$

The $\ddot{\eta}$-terms and $\ddot{\alpha}$-terms are canceled by including m_a and I_a in m and I.

On substituting, $\mu = \rho\,b^2/m$; $I = m\,r^2$; $\dot{\eta} = i\,\omega\,\eta$; $k = \omega\,b/(2\,V)$; $a_1 = 4\,r^2/b^2$; and $\dot{\alpha} = i\,\omega\,\alpha$—Eqs. 9 reduce to

$$\frac{4}{\mu}\left[\left(\frac{\omega_1}{\omega}\right)^2 + i\,g_1 - 1\right]\frac{2\,\eta}{b} = \left[\frac{1}{k^2}\,C_1\,s_1\,\alpha - \frac{i}{k}\,C_1\,s_1\,\frac{2\,\eta}{b} + \frac{i}{k}\,(\pi\,r_1 - C_3\,s_3)\,\alpha\right] = \frac{C_L}{k^2} \quad \ldots (10a)$$

[11] "Mechanism of Flutter: A Theoretical and Experimental Investigation of the Flutter Problem," by Theodore Theodorsen and I. E. Garrick, *Technical Report No. 685*, National Advisory Committee for Aeronautics, Washington, D. C., 1940.

and

$$\frac{2\,a_1}{\mu}\left[\left(\frac{\omega_2}{\omega}\right)^2 + i\,g_2 - 1\right]\alpha = \left[\frac{1}{k^2}C_2\,s_2\,\alpha - \frac{i}{k}C_2\,s_2\frac{2\,\eta}{b} - \frac{i}{k}C_4\,s_4\,\alpha\right] = \frac{C_M}{k^2} \quad \ldots(10b)$$

All the terms are in dimensionless form.

Eqs. 10 are the key equations for solving the various problems of aerodynamic oscillations.

Initial Static Lift and Torque.—The initial static values of lift and torque (L_i and M_i) at zero amplitude are given by the ordinates $(C_L)_i$ and $(C_M)_i$ of the straight model static lift and torque graphs, respectively, at the angle of incidence α_i. This angle of incidence is given by

$$\alpha_i = \alpha_w + \alpha_d \quad \ldots(11a)$$

in which α_w is the angle of inclination of the wind and α_d is the static pitch or static angular displacement produced by M_i. By definition,

$$L_i = \tfrac{1}{2}\,\rho\,V^2\,b\,(C_L)_i = K_1\,\eta_d \quad \ldots(11b)$$

$$M_i = \tfrac{1}{2}\,\rho\,V^2\,b^2\,(C_M)_i = K_2\,\alpha_d \quad \ldots(11c)$$

and

$$(C_L)_i = (C_L)_w + s_1\,\alpha_d \quad \ldots(11d)$$

$$(C_M)_i = (C_M)_w + s_2\,\alpha_d \quad \ldots(11e)$$

From Eqs. 11c and 11e,

$$\alpha_d = \frac{(C_M)_w}{K_2/(\tfrac{1}{2}\,\rho\,V^2\,b^2) - s_2} \quad \ldots(11f)$$

By Eqs. 11 a positive initial torque M_i augments the apparent angle of incidence α_w by the amount α_d to yield the corrected angle of incidence α_i. This α_d-correction, commonly overlooked, should be considered in experimental determinations of critical angles of incidence. The K_1-relations and K_2-relations in Eqs. 11 are written for a section model (uniform L, M, η, and α). For a bridge or a scale model of a bridge, α_d has sinusoidal variation and the mean value of α_d is reduced. Consequently, section models and complete scale models yield different apparent values of critical angles of incidence. Inconsistent results, inadequately explained by the induced angle correction for aspect ratio, may be explained by the α_d-correction.

The initial torsion α_d and its accompanying vertical deflection η_d are functions of V and α_w. This explains how a change in velocity or in inclination of the wind may initiate the oscillations of a structure.

The values of L_i and M_i are aerostatic forces and are balanced by the equilibrating deflections and restoring forces ($K_1\,\eta_d$ and $K_2\,\alpha_d$) evoked in the structure. Their sole influence in aerodynamic relations is in determining the true angle of incidence α_i from which the angular displacements α are measured and at which the slopes s_1 and s_2 are taken.

Angle of Incidence: Numerical Example.—Given: $\alpha_w = +5°$; $(C_M)_w = +0.070$; $s_2 = +1.00$; $K_2 = 60{,}000$ ft-lb; $b = 50$; and $V = 100$ (= 68 miles per hr). Then $\frac{1}{2}\rho V^2 b^2 = 30{,}000$ ft-lb. By Eq. 11*f*, $\alpha_d = +0.07 = +4°$. Hence, $\alpha_i = 5° + 4° = +9°$. The initial static torque, in this case, increases the angle of incidence from $\alpha_w = +5°$ to $\alpha_i = +9°$; half of the increase is due to the positive slope, s_2. The static torque is thereby increased from $M_w = 2{,}100$ ft-lb to $M_i = 4{,}200$ ft-lb. (All moments are "moments per foot of length.")

Vertical Instability

Vertical Oscillations.—For pure vertical oscillations (single degree of freedom, or torsional oscillations either not initiated or damped out), with $\alpha = 0$ and $\dot{\alpha} = 0$, Eq. 10*a* reduces to

$$\frac{4}{\mu}\left[\left(\frac{\omega_1}{\omega}\right)^2 + i\,g_1 - 1\right] = -\frac{i}{k}(F_1 - i\,G_1)\,s_1 \quad \ldots\ldots\ldots (12)$$

The imaginary terms furnish the equation: $\frac{4}{\mu} g_1 = -\frac{1}{k} F_1 s_1$; whence,

$$\delta_1 = -\frac{\mu}{4}(F_1 s_1)\frac{V}{N b} \quad \ldots\ldots\ldots\ldots\ldots\ldots\ldots (13)$$

in which $\mu = \rho b^2/m \approx 0.0766\, b^2/w$. Eq. 13 is identical with the equations previously published for δ in vertical oscillations,[12,13,14,15] with F_1 written for the identical β-function, and with w, m, and K now taken per full width. The real terms of Eq. 12 furnish the equation: $\frac{4}{\mu}\left[\left(\frac{\omega_1}{\omega}\right)^2 - 1\right] = -\frac{1}{k}(G_1 s_1)$, whence,

$$\left(\frac{N_1}{N}\right)^2 = \left(\frac{\omega_1}{\omega}\right)^2 = 1 - \frac{\mu}{4\pi}(G_1 s_1)\frac{V}{N b} \quad \ldots\ldots\ldots\ldots (14)$$

Eq. 14 gives the modified frequency (N or ω) of aerodynamic vertical oscillations in terms of the natural frequency (N_1 or ω_1) at $V = 0$. For positive $G_1 s_1$, $N > N_1$. This modification of vertical frequency increases with $V/(N b)$, but is only a small percentage change—usually negligible.

Vertical Instability: Numerical Examples.—For an H-section of $d/b = 0.20$, with $b^2/w = 0.268$ (hence $\mu = 0.0206$), and $s_1 = +4.00$, and using the ordinates of the F_1-graph presented in Fig. 9, Eq. 13 yields the vertical instability graph plotted in Fig. 13. The highest instability range (at zero structural damping) extends from $V/(N b) = 1.08$ to 2.57, with lower ("subharmonic") instability ranges at $V/(N b) = 0.50$ to 0.68, 0.33 to 0.40, etc. (In the original Tacoma Narrows Bridge, with $d/b = 0.205$, the corresponding ranges of re-

[12] "Rigidity and Aerodynamic Stability of Suspension Bridges," by D. B. Steinman, *Transactions*, ASCE, Vol. 110, 1945, p. 450, Eqs. 29.

[13] *Ibid.*, p. 558, Eq. 158*a*.

[14] *Ibid.*, p. 563, Eq. 164*a*.

[15] "Simple Model Tests Predict Aerodynamic Characteristics of Bridges," by D. B. Steinman, *Civil Engineering*, January, 1947, p. 21, Eqs. 2 and 3.

corded oscillations were $V/(N\,b) = 0.93$ to 2.35, 0.53 to 0.89, 0.37 to 0.43, etc., representing substantial agreement subject to admitted inaccuracy in the original observations.) As shown by the graph in Fig. 13, this section is a vertically "stable" section—that is, one that is stable in the high velocity (or "catastrophic") range, as predicted from the positive slope of the lift graph (Fig. 3). The maximum value of δ (the logarithmic increment) occurs at $V/(N\,b) = 1.7$ (= 6 miles per hr for the original Tacoma bridge) and amounts to 0.0152; all ordinates of the δ-graph would be proportionately increased for a higher value of b^2/w.

At $V/(N\,b) = 1.7$, representing maximum vertical instability for this section, the graph recorded in Fig. 10 gives $G_1 = +\,0.46$. With these values, Eq. 14 yields $N = 1.0026\,N_1$, an almost negligible increase above the natural frequency N_1.

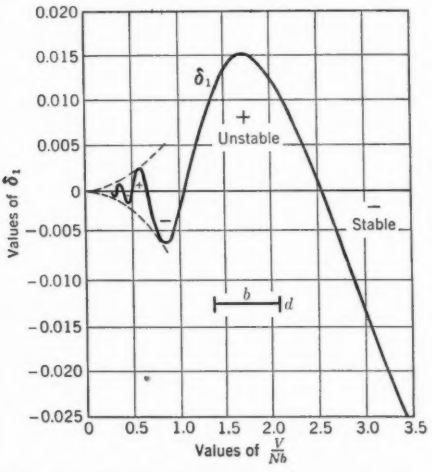

FIG. 13.—VERTICAL INSTABILITY GRAPH FOR AN H-SECTION ($d/b = 0.20$)

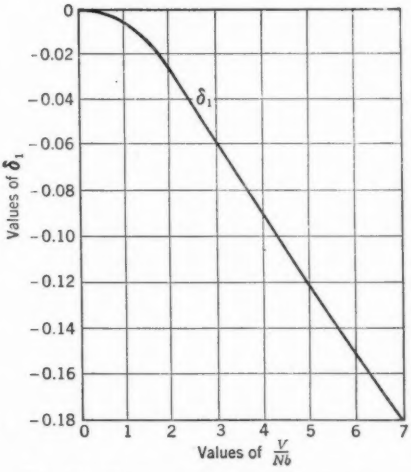

FIG. 14.—VERTICAL STABILITY GRAPH FOR A FLAT PLATE ($d/b = 0.02$)

For a flat plate of $d/b = 0.02$, with $s_1 = +\,5.25$ and $b^2/w = 0.268$, and using the ordinates of the F_1-graph represented in Fig. 11, Eq. 13 yields the vertical instability graph plotted in Fig. 14. With all ordinates negative, this graph shows vertical stability at all wind velocities.

TORSIONAL INSTABILITY

Torsional Oscillations.—For pure angular oscillations (single degree of freedom, or vertical oscillations either not initiated or damped out), with $\dot{\eta} = 0$, Eq. 10*b* reduces to

$$\frac{2\,a_1}{\mu}\left[\left(\frac{\omega_2}{\omega}\right)^2 + i\,g_2 - 1\right] = \frac{1}{k^2}\,C_2\,s_2 - \frac{i}{k}\,C_4\,s_4 \ldots\ldots\ldots\ldots (15)$$

The imaginary terms furnish the equation: $\frac{2\,a_1}{\mu}\,g_2 = -\,\frac{1}{k^2}\,G_2\,s_2 - \frac{1}{k}\,F_4\,s_4$;

whence,

$$\delta_2 = -\frac{\mu}{2\,a_1}\left(\frac{G_2}{k}\,s_2 + F_4\,s_4\right)\frac{V}{N\,b} \quad \ldots\ldots\ldots\ldots\ldots\ldots (16)$$

in which $\mu = \rho\,b^2/m \approx 0.0766\,b^2/w$, and $a_1 = 4\,r^2/b^2$.

Eq. 16 is identical with the equations previously published for δ in torsional oscillations,[16,17,18,19] except that $(\beta\,s_2)$ is now represented by the amplified expression: $\beta\,s_2 = \left(\frac{G_2}{k}\,s_2 + F_4\,s_4\right)$; in which β was the prior symbol for the phase-lag factor. This last expression is significant. The first term represents the integrated effect of angular position, a contribution previously overlooked or dismissed as apparently canceling out over the cycle. The second term represents the integrated effect of angular velocity, but is now based on static wind-tunnel tests on curved section models. At high wind velocities, although G_2 approaches zero as a limit, $\text{limit}_{k=0}\ \frac{G_2}{k} \leqq 2$; and $\text{limit}_{k=0}\ F_4 = 1$. Hence, for sections yielding $s_4 \approx 2\,s_2$, $\text{limit}_{k=0}\ \beta\,s_2 = \left(\frac{G_2}{k}\,s_2 + F_4\,s_4\right) \leqq 4\,s_2$.

It was previously known[20] that a value of $\beta \leqq 4$ at high wind velocities was needed in order to check the known test results on torsional oscillations. The foregoing amplification of the theory supplies this missing factor of 4, and yields a perfect check on the recorded results of oscillating model tests.

The real terms of Eq. 15 furnish the equation: $\frac{2\,a_1}{\mu}\left[\left(\frac{\omega_2}{\omega}\right)^2 - 1\right] = \frac{1}{k^2}F_2\,s_2 - \frac{1}{k}G_4\,s_4$; whence,

$$\left(\frac{N_2}{N}\right)^2 = \left(\frac{\omega_2}{\omega}\right)^2 = 1 + \frac{\mu}{2\,\pi\,a_1}\left(\frac{F_2}{k}\,s_2 - G_4\,s_4\right)\frac{V}{N\,b} \quad \ldots\ldots (17)$$

As a rule, for negative $F_2\,s_2$ (torsional instability), $N > N_2$. At high wind velocities, this increase in torsional frequency may be substantial. (In catastrophic vertical oscillations, the corresponding effect would be a small reduction in frequency.)

Torsional Instability: Numerical Examples.—For an H-section of $d/b = 0.20$ —with $s_2 = -0.50$, $s_4 = -1.00$, $b^2/w = 0.238$, and $a_1 = 0.476$, and using the F_4-values and G_2-values represented in Figs. 9 and 10, respectively—Eq. 16 yields the torsional instability graph plotted in Fig. 15. This graph shows catastrophic instability starting at a critical velocity ratio of $V/(N\,b) = 2.50$. For comparison, Fig. 15 also shows the torsional instability graph recorded by

[16] "Rigidity and Aerodynamic Stability of Suspension Bridges," by D. B. Steinman, *Transactions*, ASCE, Vol. 110, 1945, p. 460, Eqs. 51.

[17] *Ibid.*, p. 559, Eq. 160*a*.

[18] *Ibid.*, p. 563, Eq. 164*b*.

[19] "Simple Model Tests Predict Aerodynamic Characteristics of Bridges," by D. B. Steinman, *Civil Engineering*, January, 1947, p. 21, Eqs. 4 and 5.

[20] "Rigidity and Aerodynamic Stability of Suspension Bridges," by D. B. Steinman, *Transactions*, ASCE, Vol. 110, 1945, pp. 463–465.

Louis G. Dunn[21] in 1941 from oscillating tests on a section model of the same d/b and b^2/w. With an indicated vertical shift of the experimental graph to correct for a residual positive damping that was overlooked by the investigators,[22] the two graphs compared in Fig. 15 are found to be almost identical. Without the indicated correction, Mr. Dunn's graph showed a critical $V/(N\,b)$ of 3.33, which is now known to have been too high. More recent tests (1945–1946) on oscillating models of the Tacoma section yield values of critical $V/(N\,b)$ of 2.50 (at the California Institute of Technology in Pasadena) and from 2.43 to 2.56 (at the University of Washington in Seattle), confirming the correctness of the theoretical graph in Fig. 15 and the validity of the theory

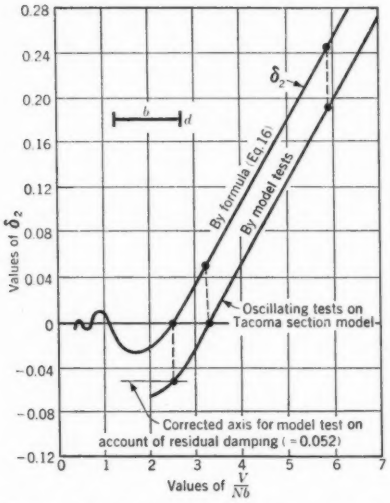

FIG. 15.—TORSIONAL INSTABILITY GRAPH FOR AN H-SECTION ($d/b = 0.20$)

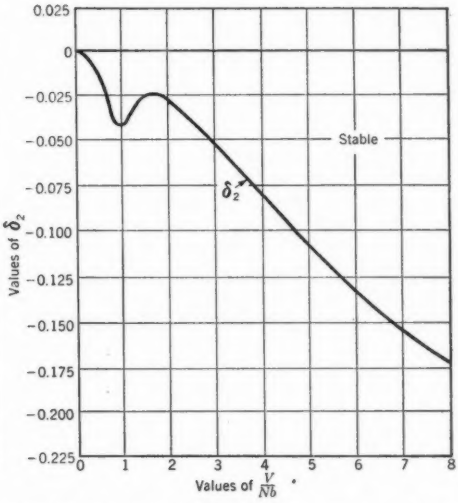

FIG. 16.—TORSIONAL STABILITY GRAPH FOR A FLAT PLATE ($d/b = 0.02$)

represented by Eq. 16. The striking agreement of the slopes of the two graphs in Fig. 15 is further confirmation of the correctness of the theory here presented. Without the angular position term and the use of the curved model for the angular velocity term in Eq. 16, the slopes and the ordinates of the computed δ-graph would be only one fourth as large. If instability graphs can be predicted scientifically, as in Fig. 15, without expensive and time-consuming oscillating model tests, the theory is justified.

The indicated critical $V/(N\,b) = 2.50$, applied to the original Tacoma bridge, represents a critical wind velocity of only 13.3 miles per hr (at zero damping) for catastrophic torsional instability. Such earlier torsional oscillations of the span in the first asymmetric mode were prevented by the midspan stays until the latter failed.

[21] "The Failure of the Tacoma Narrows Bridge," a report to the Hon. John M. Carmody, Administrator of the Federal Works Agency, Washington, D. C., March 28, 1941, by a Board of Engineers consisting of O. H. Ammann, Theodor von Kármán, and Glenn B. Woodruff, Appendix VIII, Fig. VIII-2.

[22] "Rigidity and Aerodynamic Stability of Suspension Bridges," by D. B. Steinman. *Transactions* ASCE, Vol. 110, 1945, p. 569.

At $V/(N\,b) = 7.5$ (corresponding to the wind velocity of 40 miles per hr that destroyed the Tacoma span), the graphs in Figs. 9 and 10 give $F_2 = +0.48$ and $G_4 = +0.59$. With these values and $b^2/w = 0.268$ (or $\mu = 0.0206$) and $a_1 = 0.476$, Eq. 17 yields $N = 0.9995\,N_2$, which is an almost imperceptible decrease below the natural frequency N_2. For the same section, at $V/(N\,b) = 18.75$ (corresponding to 100 miles per hr for the same assumed value of N), $F_2 = +0.91$ and $G_4 = +0.26$, and Eq. 17 yields $N = 1.21\,N_2$, which is a 21% increase above the natural frequency.

For a flat plate of $d/b = 0.02$, using the F_4-graphs and G_2-graphs represented in Figs. 11 and 12, with $s_2 = +1.10$, $s_4 = +0.55$, $b^2/w = 0.268$, and $a_1 = 0.333$, Eq. 16 yields the torsional instability graph plotted in Fig. 16. With all ordinates negative, this graph shows torsional stability at all wind velocities.

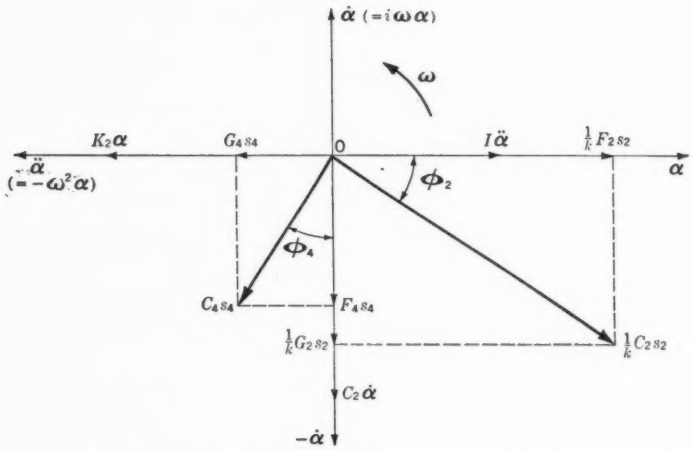

FIG. 17.—VECTOR DIAGRAM FOR TORSIONAL OSCILLATIONS (DRAWN FOR $s_2 = +$, $s_4 = +$)

Vector Diagram for Torsional Oscillations.—The terms in Eqs. 2*b*, 9*b*, and 10*b*, representing the aerodynamic moments in angular oscillations, are shown in vector relationship in Fig. 17 $\left(C\ s\text{-vectors} = \frac{1}{k}\,\frac{M}{\frac{1}{2}\rho V^2 b^2 \alpha}\right)$. The $(C_2\,s_2)$-moment, due to an angular position α, lags an amount ϕ_2 behind α. The $(C_4\,s_4)$-moment, due to an angular velocity $\dot{\alpha}$, lags an amount ϕ_4 behind $-\dot{\alpha}$. The components along the vertical (imaginary) axis yield $\left(\frac{1}{k}G_2\,s_2 + F_4\,s_4\right)$, opposing $\dot{\alpha}$. Therefore they represent positive damping if $G_2\,s_2$ and $F_4\,s_4$ are positive, and negative damping (amplification) if $G_2\,s_2$ and $F_4\,s_4$ are negative—all in accordance with Eq. 16. The components along the horizontal (real) axis yield $\left(\frac{1}{k}F_2\,s_2 - G_4\,s_4\right)$ opposing $K_2\,\alpha$. Therefore they represent a reduction in frequency if $F_2\,s_2$ is positive, and an increase in frequency if $F_2\,s_2$ is negative, unless outweighed by the term $G_4\,s_4$—all in accordance with Eq. 17.

Limiting Amplitudes and Amplitude Response Curves

Effect of Curvature of the Static Lift Graph.—The equation of the static lift graph, straight model, with origin assumed at α_i, may be written in the general form: $C_L = A_o + A_1\,\alpha + A_2\,\alpha^2 + A_3\,\alpha^3 + \cdots$, in which A_o is the ordinate (C_L) and A_1 the slope (s_1) at α_i. If η_o is the amplitude of vertical oscillations, and α_o the equivalent abscissa,

$$\eta = \eta_o \sin(\omega\,t) \qquad \alpha_o = -\,\omega\,\eta_o/V$$
$$\dot{\eta} = \omega\,\eta_o \cos(\omega\,t) \qquad \alpha = -\,\dot{\eta}/V = \alpha_o \cos(\omega\,t)$$

The work done in a cycle is $\Delta W = F_1 \int_0^{2\pi/\omega} L\,\dot{\eta}\,dt = -\,F_1\,V \int_o^{2\pi/\omega} [L\,\alpha_o \times \cos(\omega\,t)]\,dt$. Substituting the expressions for L, C_L, and α, and performing the integration, $\Delta W = F_1 \left(\frac{\pi}{2}\rho\,V^2\,b\right) \eta_o \left[A_1\,\alpha_o + \frac{3}{4}A_3\,\alpha^3{}_o + \frac{15}{24}A_5\,\alpha^5{}_o + \cdots\right]$. For constant slope s_1, $\Delta W = F_1 \left(\frac{\pi}{2}\rho\,V^2\,b\right) \eta_o\,(s_1\,\alpha_o)$. Hence, for the curving graph,

$$\text{Equivalent } s_1 = A_1 + \frac{3}{4}A_3\,\alpha^2{}_o + \frac{15}{24}A_5\,\alpha^4{}_o + \cdots \qquad (18)$$

Equating this expression to zero determines the limiting amplitude.

If the equation of the C_L-curve (in the range traversed) is a cubic or quartic equation, or if terms in that equation of higher order than α^4 may be dropped, then (for zero structural damping) the limiting amplitude, defined by equivalent $s_1 = 0$, will be given by Eq. 18 as

$$\alpha_m = \text{limiting } \alpha_o = \sqrt{-\frac{4}{3}\frac{A_1}{A_3}} = \sqrt{-\frac{4}{3}\frac{s_1}{A_3}} \qquad (19a)$$

Hence,

$$\eta_m = \text{limiting } \eta_o = \frac{V}{\omega}\sqrt{-\frac{4}{3}\frac{A_1}{A_3}} = \frac{V}{\omega}\sqrt{-\frac{4}{3}\frac{s_1}{A_3}} \qquad (19b)$$

If the slope ($F_1\,s_1$) at α_i is negative, representing instability, Eqs. 19 define a maximum limiting amplitude, terminating the instability range. If the slope at α_i is positive, representing stability, Eqs. 19 define a minimum limiting amplitude, beyond which potential instability commences. For real values, in either case, by Eqs. 19, $A_1\,(=s_1)$ and A_3 must be opposed in sign. The usual identification is a section of the graph curving away from the vertical axis. A section of the graph curving toward the vertical axis will not yield a limiting (maximum or minimum) amplitude.

By Eq. 19*b*, the limiting vertical amplitude η_m increases with V; but by Eq. 19*a*, the range α_m along the graph, defining the limiting vertical amplitude η_m, is independent of V but depends only upon the geometry of the graph.

Extending the ΔW-integration over a segment of the span, using the sine-curve wave form, and equating to zero, the limiting vertical amplitude at

midsegment is

$$\eta_{ms} = \sqrt{\frac{4}{3}}\,\eta_m = \frac{4}{3}\,\frac{V}{\omega}\sqrt{-\frac{s_1}{A_3}} \quad \ldots\ldots\ldots\ldots\ldots\ldots (19c)$$

Eqs. 19 are in agreement with corresponding equations previously published.[23]

Limiting Amplitudes of Torsional Oscillations.—The equation of the static torque graph, straight model, with origin assumed at α_i, may be written in the general form, $C_M = A_o + A_1\,\alpha + A_2\,\alpha^2 + A_3\,\alpha^3 + \cdots$, in which A_o is the ordinate (C_M) and A_1 the slope (s_2) at α_i; and the equation of the static torque graph, curved model, with origin at $\beta = 0$, may be written similarly, $C_M = B_o + B_1\,\beta + B_2\,\beta^2 + B_3\,\beta^3 + \cdots$, in which B_o is the ordinate (C_M) and B_1 the slope (s_4) at $\beta = 0$. By the same integration as used above for vertical oscillations,

$$\text{Equivalent } s_2 = A_1 + \frac{3}{4}\,A_3\,\alpha_o^2 + \frac{15}{24}\,A_5\,\alpha_o^4 + \cdots\cdots\cdots (20a)$$

and

$$\text{Equivalent } s_4 = B_1 + \frac{3}{4}\,B_3\,\beta_o^2 + \frac{15}{24}\,B_5\,\beta_o^4 + \cdots\cdots\cdots (20b)$$

in which α_o is the angular amplitude and β_o is the corresponding abscissa of the β-torque graph. For zero damping (defining the limiting amplitude), by Eq. 16, $\left(\frac{1}{k}\,G_2\,s_2 + F_4\,s_4\right) = 0$. Substituting equivalent s_2 and equivalent s_4, dropping the terms of fourth and higher order, and noting that $\beta_o = k\,\alpha_o$,

$$\alpha_m = \text{limiting } \alpha_o = \sqrt{-\frac{4}{3}\,\frac{A_1\,G_2 + k\,B_1\,F_4}{A_3\,G_2 + k^3\,B_3\,F_4}} \quad \ldots\ldots\ldots (21a)$$

With $A_1 = s_2$, $B_1 = s_4$, $G_2/k \approx 2$, $F_4 \approx 1$, and with the negligible k^3-term dropped, Eq. 21*a* may be written:

$$\alpha_m = \text{limiting } \alpha_o \approx \sqrt{-\frac{4\,(s_2 + \frac{1}{2}\,s_4)}{3\,A_3}} \quad \ldots\ldots\ldots\ldots (21b)$$

Analogous to Eq. 19*c*, the limiting angular amplitude at midsegment of a span will be

$$\alpha_{ms} = \sqrt{\frac{4}{3}}\,\alpha_m \approx \frac{4}{3}\sqrt{-\frac{s_2 + \frac{1}{2}\,s_4}{A_3}} \quad \ldots\ldots\ldots\ldots\ldots (21c)$$

Eqs. 21 correspond to equations previously published,[24] with $\frac{1}{2}\,s_4$ now added to s_2. For $s_4 \approx 2\,s_2$, the calculated value of the limiting amplitude in torsion is thereby multiplied by $\sqrt{2}$. This supplies a factor previously missing in checking the theory against recorded oscillations and adds new confirmation of the basic validity of the theory.

[23] "Rigidity and Aerodynamic Stability of Suspension Bridges," by D. B. Steinman, *Transactions*, ASCE, Vol. 110, 1945, p. 452, Eqs. 34*a* and 34*b*.

[24] *Ibid.*, p. 461, Eqs. 54*a* and 54*b*.

For $d/b = 0.20$, the static torque curves (Fig. 4) yield $s_2 = -0.50$, $s_4 = -1.00$, and $A_3 = +3.7$. Hence, by Eq. 21*c*, the limiting segment amplitude is $0.70 = 40°$, which checks the reported value for the Tacoma bridge failure.

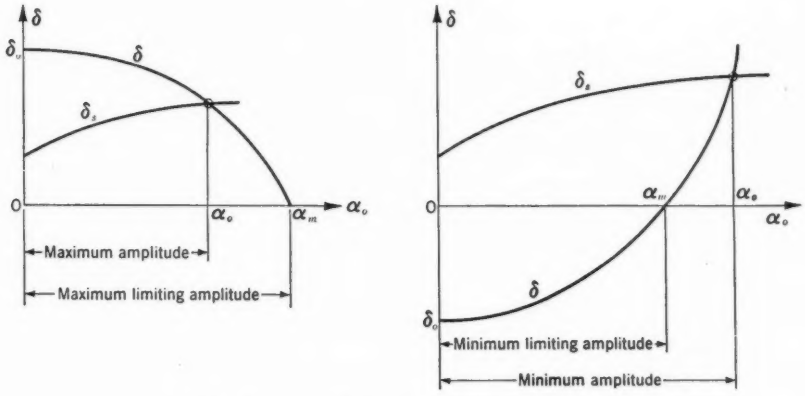

FIG. 18.—LIMITING, MAXIMUM, AND MINIMUM AMPLITUDES

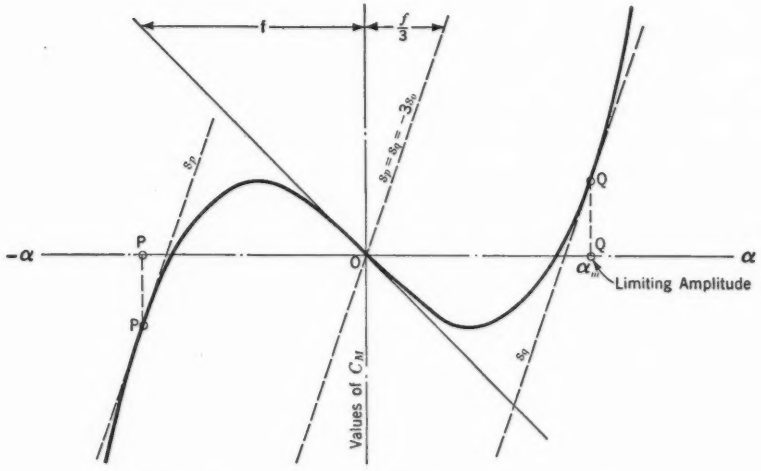

FIG. 19.—GRAPHIC METHOD FOR LIMITING AMPLITUDES

The limiting amplitudes defined by Eqs. 19 and 21 are for zero positive damping. Positive damping δ_s (structural and friction) will reduce the maximum amplitudes and raise the minimum amplitudes. This is illustrated in Fig. 18.

Graphic Methods for Limiting Amplitudes.—In any lift or torque graph, let s_o, s_p, and s_q be the respective slopes at the center O and the ends, P and Q, of any range of oscillation, and let s_e be the equivalent slope over the range PQ as

affected by the curvature of the graph. Then, by Eqs. 18 and 20, very closely,

$$s_e \approx \tfrac{3}{4}\, s_o + \tfrac{1}{8}\, s_p + \tfrac{1}{8}\, s_q \ldots\ldots\ldots\ldots\ldots\ldots\ldots\ldots (22)$$

This yields a simple graphic method (Fig. 19) for plotting limiting vertical amplitudes, defined by $s_e = 0$. The two points P and Q, marking the limits of the range and spaced at equal horizontal distances α_m from 0, are given by their slopes:

$$s_p = s_q = -\,3\, s_o \qquad \text{or} \qquad \tfrac{1}{2}\,(s_p + s_q) = -\,3\, s_o \ldots\ldots\ldots\ldots (23)$$

The limiting amplitudes η_m will then be $(V/\omega)\ \alpha_m$. Fig. 19 yields a maximum limiting amplitude, and the inverted reflection of Fig. 19 would yield a minimum limiting amplitude.

The approximate value of the coefficient A_3, for substitution in Eqs. 19, may be similarly obtained from the geometry of the lift graph:

$$A_3 \approx \frac{s_p + s_q - 2\, s_o}{6\ \alpha^2{}_o} \ldots\ldots\ldots\ldots\ldots\ldots\ldots\ldots (24)$$

in which α_o is any convenient assumed amplitude. The same geometric relation applied to the two torque graphs yields the corresponding coefficients A_3 and B_3 for substitution in Eqs. 21.

Eqs. 19 and Eqs. 21 to 24 are approximate short cuts which may be sufficiently accurate for practical requirements. For more accurate determinations of limiting amplitudes, Eqs. 18 and 20 should be used.

Use of Slope Graphs.—Since the significant feature of static lift and torque graphs appearing in the foregoing equations (Eqs. 18 to 24) is the magnitude and variation of the slope of the graphs, a directly indicated geometric device is the construction and application of slope graphs. By plotting the slopes of any lift or torque graph as the ordinates of a new curve, the corresponding slope graph is obtained (Fig. 20). Any range below the zero axis represents instability. The four respective slope graphs for any section will be referred to as the s_1-graph, s_2-graph, s_3-graph, and s_4-graph. If the lift or torque graph is antisymmetrical, the slope graph will be symmetrical. If the lift or torque graph is a cubic equation, the slope graph will be a parabola.

The center of oscillation O is marked on the curve, at α_i for the s_1-graph and the s_2-graph, and at $\beta = 0$ for the s_3-graph and the s_4-graph.

In Fig. 20(a), for any assumed amplitude α (or β), the terminal points P and Q are marked on the curve at equal horizontal distances $\pm\,\alpha$ (or $\pm\,\beta$) from O. The ordinates of O, P, and Q are s_o, s_p, and s_q. The midpoint M of the chord PQ is on the vertical through O, and MO is the middle ordinate of the arc PQ. By Eq. 24, $A_3 = \frac{1}{3}\frac{\overline{\text{MO}}}{\alpha^2}$; and $B_3 = \frac{1}{3}\frac{\overline{\text{MO}}}{\beta^2}$, yielding A_3 or B_3, positive if the chord PQ is above O. By Eq. 22, $s_e = s_o - \frac{1}{4}\,\overline{\text{MO}}$—yielding the equivalent slope for the curving range PQ.

From the horizontal line through O, lay off the ordinates $\frac{1}{4}\,\overline{\text{OM}}$ on the respective Q-verticals. The curve thus obtained is the s_e-graph, showing the variation of equivalent slope s_e with amplitude. Since δ is proportional to s_e,

this is also the δ-amplitude graph, showing the variation of δ with amplitude. The limiting amplitude occurs where this δ-amplitude graph crosses the zero horizontal axis; this is the point of demarcation between stability and instability. It is given directly by $\overline{MO} = 4\,s_o$.

Fig. 20(a) shows the construction for the general case, with the center of oscillation O off center, at an angle of incidence α_i.

For the symmetrical case, with the center of oscillation O at zero and the slope curve symmetrical, the construction is simplified (Fig. 20(b)). The ordinates of the δ-amplitude graph (from the horizontal line through O) are simply one fourth of the corresponding ordinates of the slope graph.

Figs. 20(a) and 20(b) are drawn for an unstable range, yielding a maximum limiting amplitude. If Figs. 20(a) and 20(b) are inverted, stability and instability are reversed and the intercepted amplitudes are minimum limiting amplitudes.

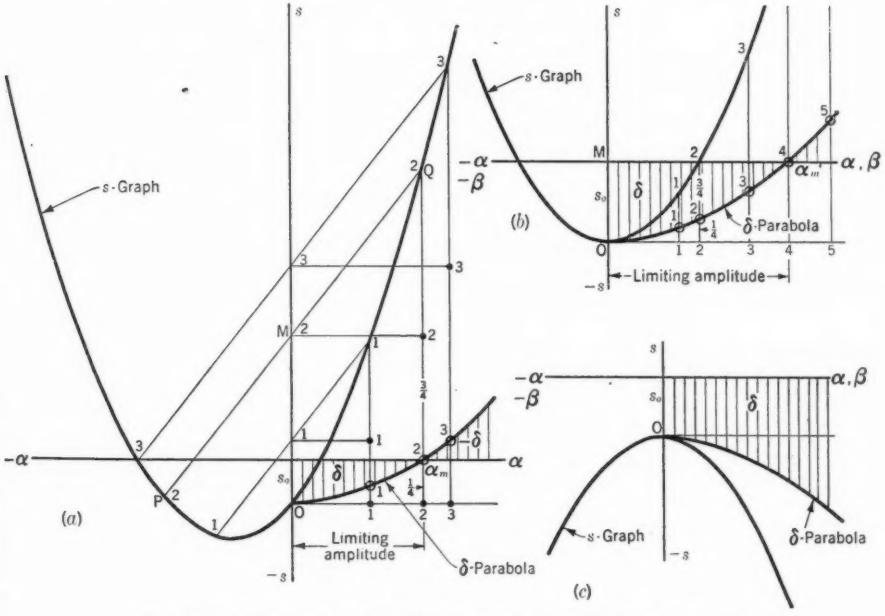

FIG. 20.—CONSTRUCTION OF δ-AMPLITUDE GRAPHS FROM SLOPE GRAPHS

For all practical purposes, the δ-amplitude graph, as a rule, may be taken as a parabola; accordingly, for convenient identification, it will be referred to as the "δ-parabola." The base is the limiting amplitude (given by the foregoing formulas or graphic constructions) and the altitude is δ_o, the value of δ at zero amplitude.

In Fig. 20, the δ-values (varying with amplitude) are represented by the ordinates between the δ-parabola and the horizontal zero axis of the slope graph. If the zero axis is on the convex side of the δ-parabola (Fig. 20(c)) the δ-ordinates increase with amplitude and there is no limiting (maximum or minimum)

amplitude. In such case, a δ-parabola below the zero axis will represent catastrophic instability of unlimited amplitude, and a δ-parabola above the zero axis (Fig. 20(*c*) inverted) will represent unlimited stability.

Graphic Construction of Amplitude Response Curves.—Fig. 21 shows a simple graphic procedure for plotting an amplitude response curve from a given δ-graph

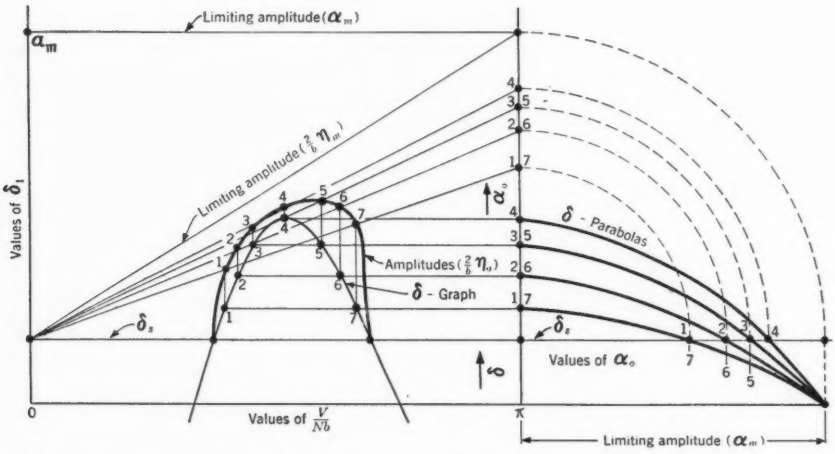

FIG. 21.—CONSTRUCTION OF VERTICAL AMPLITUDE RESPONSE CURVE FOR CONSTANT DAMPING

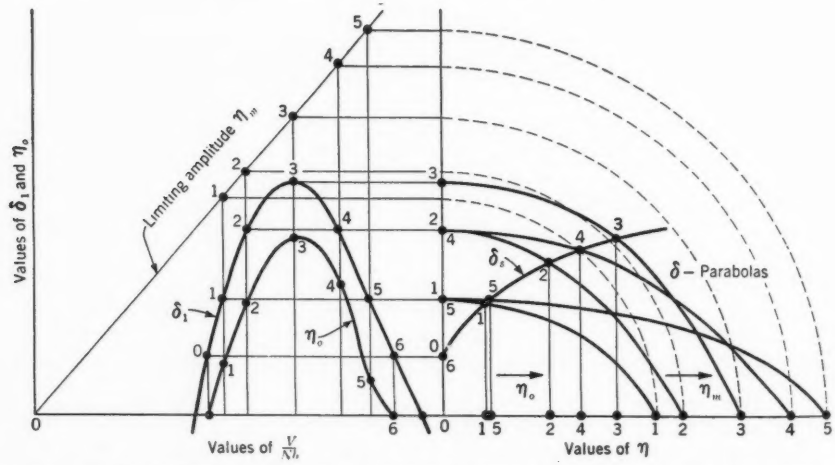

FIG. 22.—CONSTRUCTION OF VERTICAL AMPLITUDE RESPONSE CURVE FOR VARIABLE DAMPING

(for vertical oscillations). The points of the δ-graph are projected horizontally to give the altitudes of the δ-amplitude curves. These parabolic curves have a common base—namely, the limiting amplitude α_m, determined as in Fig. 19 or Fig. 20; and they may be drawn as simple parabolas or, for greater accuracy, their form (with proportional ordinates) is determined as in Fig. 20. A line

representing the positive damping (δ_s) is drawn across the curves, horizontally if the positive damping is assumed constant (independent of amplitude). The points where this transversal cuts the parabolas give the respective amplitudes α_o. Using a vertical axis at $V/(N\,b) = \pi$ (or any convenient multiple of π), each ordinate α_o is multiplied geometrically by $\dfrac{V/(N\,b)}{\pi} = \dfrac{1}{k} = 2\,\dfrac{V}{\omega\,b}$ to give the ordinates $2\,\eta_o/b$ of the required η_o-response graph.

If the positive damping δ_s increases with amplitude, the graphic construction illustrated in Fig. 21 requires corresponding modification. A convenient graphic solution is illustrated in Fig. 22. The constant α_m is translated graphically into the linear variable η_m (increasing with $V/(N\,b)$), and η_m is used as the base of the δ-parabola. The intersection of this parabola by the δ_s-graph gives directly the amplitude response, η_o.

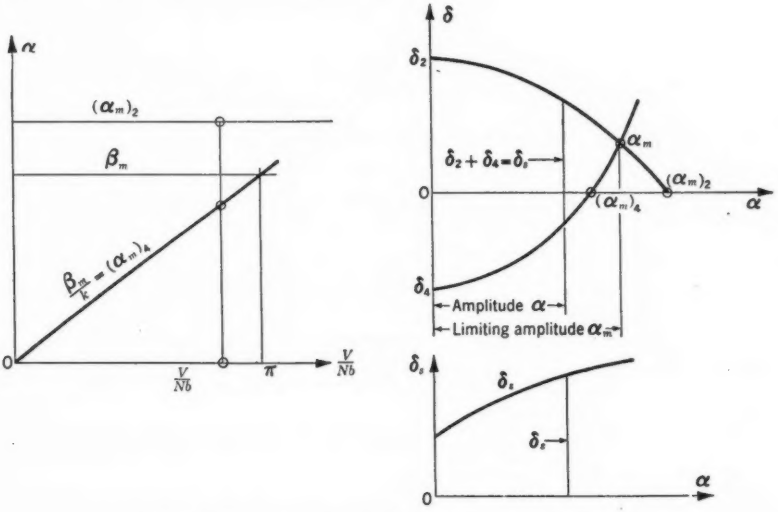

FIG. 23.—GRAPHIC METHOD FOR TORSIONAL AMPLITUDE RESPONSE

Comparison of Figs. 21 and 22 with known amplitude response curves indicates that the positive damping δ_s is not constant, but increases (at a diminishing rate) with amplitude. Increase with the square root of the amplitude is suggested.

The corresponding graphic construction for angular amplitudes is illustrated in Fig. 23. In this case, by Eq. 16, δ has two components—the contribution $G_2\,s_2$, here denoted by δ_2, and the contribution $F_4\,s_4$, denoted by δ_4—so that $\delta = \delta_2 + \delta_4$. The corresponding limiting amplitudes are the constant $(\alpha_m)_2$ and the linear varying $(\alpha_m)_4$, the latter given (Fig. 23(*a*)) by β_m/k. With $(\alpha_m)_2$ and $(\alpha_m)_4$ as the respective bases, the δ_2-parabola and δ_4-parabola are drawn additively (Fig. 23(*b*)); their intersection gives the resultant limiting amplitude α_m. The vertical intercept equal to the corresponding ordinate of the δ_s-graph determines the required amplitude response, α_o.

The amplitudes given by Figs. 18 to 23, inclusive, are for a section model, or the mean amplitudes over a segment of a span. Multiply by $\sqrt{4/3}$ to obtain the corresponding amplitude at midsegment.

Coupled Oscillations

Vertical and Torsional Oscillations, with Damping Included.—Let:

$$X_1 = \frac{4}{\mu\, s_1}\left[\left(\frac{\omega_1}{\omega}\right)^2 - 1\right] \qquad X_2 = \frac{2\, a_1}{\mu\, s_2}\left[\left(\frac{\omega_2}{\omega}\right)^2 - 1\right]$$

$$q_3 = \frac{s_3}{s_1} \qquad q_4 = \frac{s_4}{s_2}$$

$$d_1 = \frac{4}{\mu\, s_1} g_1 \qquad d_2 = \frac{2\, a_1}{\mu\, s_2} g_2$$

Then Eqs. 10 reduce to

$$\left(X_1 + i\, d_1 + \frac{i}{k} C_1\right)\frac{2\,\eta}{b} = \left[\frac{1}{k^2} C_1 - \frac{i}{k} q_3 \left(C_3 - \frac{\pi\, r_1}{s_3}\right)\right]\alpha \ldots (25a)$$

and

$$\left(\frac{i}{k} C_2\right)\frac{2\,\eta}{b} = \left(-X_2 - i\, d_2 + \frac{1}{k^2} C_2 - \frac{i}{k} q_4\, C_4\right)\alpha \ldots\ldots (25b)$$

Apply the determinant, substitute $C = F - i\,G$, and $F'_3 = F_3 - \pi\, r_1/s_3$, and separate the real and imaginary terms. The imaginary terms yield

$$X_2 = H_2 - H_1\, X_1 \ldots\ldots\ldots\ldots\ldots\ldots (26a)$$

in which $H_1 = \dfrac{J_1}{F_1 + k\, d_1}$; $J_1 = q_4\, F_4 + \dfrac{G_2}{k} + k\, d_2$; $J_2 = \dfrac{F_2}{k} - q_4\, G_4$; and

$$H_2 = \frac{\frac{q_3}{k}(F_2\, G_3 + F'_3\, G_2) - \frac{q_4}{k}(F_1\, G_4 + F_4\, G_1) + d_1\, J_2 - d_2\, G_1}{F_1 + k\, d_1}.$$

The real terms yield

$$2\, X_1 = -H_3 \pm \sqrt{H^2_3 - 4\, H_4} \ldots\ldots\ldots\ldots\ldots (26b)$$

in which $H_3 = \dfrac{G_1}{k} + \dfrac{1}{H_1}\left(\dfrac{J_2}{k} - H_2\right)$; and $H_4 = \dfrac{1}{k\, H_1}\left[-G_1\, H_2 + \dfrac{q_4}{k}(F_1\, F_4 - G_1\, G_4) - \dfrac{q_3}{k}(F_2\, F'_3 - G_2\, G_3) + d_1\, J_1 + d_2\, F_1\right]$.

Let $a_2 = a_1\,(\omega_2/\omega_1)^2$. By definition of X_1 and X_2, and from Eq. 26*a*,

$$(a_2 - a_1) = (\tfrac{1}{2}\, s_2\, X_2 - \tfrac{1}{4}\, a_2\, s_1\, X_1)\,\mu \ldots\ldots\ldots\ldots (27a)$$

$$\left(\frac{\omega_1}{\omega}\right)^2 = 1 + \frac{\mu\, s_1}{4} X_1 \ldots\ldots\ldots\ldots\ldots (27b)$$

$$\left(\frac{\omega_2}{\omega}\right)^2 = 1 + \frac{\mu\, s_2}{2\, a_1} X_2 \ldots\ldots\ldots\ldots\ldots (27c)$$

and

$$\left(\frac{\omega_1}{\omega}\right)^2 = \frac{2\,a_1/s_2 + 4\,H_1/s_1 + \mu\,H_2}{2\,a_2/s_2 + 4\,H_1/s_1} \quad \ldots\ldots\ldots\ldots (27d)$$

in which the last term $\mu\,H_2$ is relatively negligible. By Eq. 27*d*, the coupled frequency ω will normally have an intermediate value between ω_1 and ω_2.

With a few trial values of k and interpolating, the values of X_1 and X_2 are found to satisfy Eq. 27*a*, and the coupled frequency ω is then given by any of the remaining Eqs. 27. The critical (flutter) velocity is then given by

$$V_c = \frac{\omega\,b}{2\,k} \quad \ldots\ldots\ldots\ldots\ldots\ldots\ldots\ldots (28)$$

The amplitude ratio (including the phase difference ψ) is given by Eqs. 25, yielding

$$\frac{2\,\eta}{\alpha\,b} = \frac{C_1/k - i\,q_3\,(C_3 - \pi\,r_1/s_3)}{k\,X_1 + i\,C_1 + i\,k\,d_1} = \frac{1}{C_2}\,(-\,q_4\,C_4 + i\,k\,X_2 - k\,d_2) - \frac{i}{k} \quad \ldots (29)$$

For zero damping, the foregoing solution is simplified by dropping the d_1-term and the d_2-term from the equations.

Coupled Oscillations with Damping: Numerical Example.—As shown by Figs. 14 and 16, the flat plate ($d/b = 0.02$) is a stable section against both vertical and torsional oscillations. Such sections have potential instability in coupled oscillations.

The following data are assumed:

$\omega_1 = 0.867$	$a_1 = 0.625$	$\mu = 0.0318$	$s_1 = 5.25$	$s_3 = -1.75$	$q_3 = -0.33$
$\omega_2 = 1.552$	$a_2 = 2.00$	$b = 60$	$s_2 = 1.10$	$s_4 = 0.55$	$q_4 = 0.50$

Let the structural damping (in both types of oscillations) be $\delta_s = 0.05$. Hence, $g_1 = g_2 = 0.016$, $d_1 = 0.383$, and $d_2 = 0.571$. The damping raises V_c, and therefore lowers k.

Estimating k by short-cut formulas (subsequently presented), the F-values and G-values in Table 2(*a*) are read from Figs. 11 and 12, adding $-\pi\,r_1/s_3 = 1.80$ to the F_3-values to obtain F'_3. The computation of X_1 and X_2 by Eqs. 26 is recorded in Table 2(*b*). To satisfy Eq. 27*a*, $X_2 - 4.77\,X_1 = 78.62$. Hence, by interpolation in Table 2,

$k = 0.349$	$X_1 = -14.97$	$H_1 = 0.504$
	$X_2 = 7.36$	$H_2 = -0.159$

By any of Eqs. 27*b*, 27*c*, and 27*d*, $\omega = 1.41$. Hence, $V_c = 121 = 83$ miles per hr. By either of Eqs. 29, the amplitude ratio is $2\,\eta/(\alpha\,b) = -0.546 - 0.182\,i = -0.58e^{0.32i}$. The angular oscillation dominates. The vertical oscillation leads by $\psi = 0.32 = 0.051$ cycle. The center of oscillation is shifted $0.58\,\frac{b}{2}$ toward the leading edge. The complete solution is self-checking when the two Eqs. 29 yield identical values of $2\,\eta/(\alpha\,b)$.

For the case of zero damping, the solution is similar, but with the d_1-term and the d_2-term dropped from the equations. Somewhat higher values of k are used as trial values ($k = 0.45$, 0.475, and 0.50). The solution yields

$$k = 0.462 \qquad \begin{matrix} X_1 = -15.59 & H_1 = 0.347 & \omega = 1.46 \\ X_2 = 4.26 & H_2 = -1.144 & V_c = 65 \text{ miles per hr.} \end{matrix}$$

Again by Eqs. 29, the amplitude ratio is $2\eta/(\alpha b) = -0.314 - 0.081\,i = -0.32\,e^{0.25i}$.

TABLE 2.—NUMERICAL EXAMPLE;

Ratio, k	(a) From Figs. 11 and 12								J_1
	F_1	F_2	F'_3	F_4	G_1	G_2	G_3	G_4	
0.30	0.970	1.015	2.690	0.935	0.170	−0.025	0.475	0.285	0.556
0.35	0.963	1.023	2.668	0.917	0.197	−0.037	0.534	0.323	0.552
0.40	0.953	1.032	2.633	0.895	0.224	−0.050	0.600	0.364	0.551

Coupled Oscillations: Simplified Approximate Formulas and Short Cuts.— Eq. 27*a* may be written in the form:

$$X_2 = A\,X_1 + B \qquad (30)$$

in which A and B are known constants of the section; thus, $A = \frac{a_2\,s_1}{2\,s_2}$ and $B = \frac{2\,(a_2 - a_1)}{\mu\,s_2}$. From Eqs. 26*a* and 30,

$$X_1 = \frac{H_2 - B}{A + H_1} \qquad (31a)$$

With H_2 generally negligible in comparison with B, Eq. 31*a* may be reduced to

$$X_1 \approx \frac{-B}{A + H_1}; \qquad X_2 \approx -H_1 X_1 \qquad (31b)$$

Without requiring the final value of k, Eqs. 31 offer an abridged solution, yielding values of X_1 and X_2 that are fairly constant over a substantial range of values of k. With X_1 and X_2 known, the frequency ω is given by Eqs. 27. Dropping the small H_2-term, Eq. 27*d* yields, with sufficient accuracy,

$$\left(\frac{\omega}{\omega_1}\right)^2 = \frac{H_1 + A}{H_1 + \frac{a_1}{a_2}A} \qquad (32a)$$

and

$$\left(\frac{\omega}{\omega_2}\right)^2 = \frac{H_1 + A}{\frac{a_2}{a_1}H_1 + A} \qquad (32b)$$

—requiring only H_1 for the determination of ω, and yielding a fairly constant value of ω over a substantial range of values of k.

To test the practical accuracy of the abridged solutions given by Eqs. 30 to 32, they are applied to the data of the preceding numerical example (using $A = 4.77$ and $B = 78.62$) and the results are given in Table 3.

If H_3 and H_4 are known for different values of k, and with X_1 known from Eq. 31*a* or Eq. 31*b*, the true value of k is given, with sharp definition, by ap-

(*b*) By Eqs. 26									Ratio, k
J_1	J_2	H_1	H_2	H_3	H_4	X_1	X_2	$X_2 - 4.77\ X_1$	
0.556	3.241	0.514	−0.031	21.71	33.80	−20.02	10.27	105.77	0.30
0.552	2.763	0.504	−0.162	16.56	25.92	−14.81	7.30	77.94	0.35
0.551	2.398	0.499	−0.269	13.12	20.22	−11.33	5.38	59.42	0.40

plying the relation (from Eq. 26*b*):

$$f(X_1) = X_1 + H_3 + \frac{H_4}{X_1} = 0 \qquad (33)$$

This computation is illustrated in Table 4(*a*) by application to the data of the preceding numerical example, from which the true value is found to be $k = 0.349$.

TABLE 3.—Coupled Oscillations with Damping, Simplified Approximate Methods

Trial k	H_1	X_1, Eq. 31*b*	X_2, Eq. 31*b*	ω, Eqs. 32	H_2	X_1, Eq. 31*a*	X_2, Eq. 30	ω, Eqs. 27
0.30	0.514	−14.88	7.65	1.41	−0.031	−14.91	7.50	1.41
0.35	0.504	−14.91	7.52	1.41	−0.162	−14.94	7.36	1.41
0.40	0.499	−14.92	7.45	1.41	−0.269	−14.97	7.21	1.42
True value: 0.349	0.504	−14.94	7.36	1.41	−0.159	−14.94	7.36	1.41

TABLE 4.—Computation of the Frequency Ratio, k

Trial k	(*a*) True Value by Eq. 33				(*b*) Approximate Value by Eqs. 35				
	H_3	H_4	X_1, Eq. 31*a*	$f(X_1)$	F_1	$F_1 + k\,d_1$	F_2	X_2, Eq. 31*b*	k, Eq. 35*a*
0.30	21.71	33.80	−14.91	4.54	0.970	1.085	1.015	7.65	0.344
0.35	16.56	25.92	−14.94	−0.11	0.963	1.097	1.023	7.50	0.346
0.40	13.12	20.22	−14.97	−3.20	0.953	1.106	1.032	7.45	0.346

Dropping the relatively small term H_4/X_1, Eq. 33 yields, approximately,

$$X_1 \approx -H_3 \approx \frac{H_2 - J_2/k}{H_1} \qquad (34)$$

Upon substituting the expressions for H_2 and J_2, and dropping the minor terms, Eq. 34 yields

$$k^2 \approx \frac{F_1 F_2}{X_2 (F_1 + k\, d_1)} \ldots\ldots\ldots\ldots\ldots\ldots\ldots\ldots (35a)$$

which, for zero damping, reduces to

$$k^2 \approx \frac{F_2}{X_2} \ldots\ldots\ldots\ldots\ldots\ldots\ldots\ldots\ldots\ldots (35b)$$

Eqs. 35 offer a short cut for preliminary approximate estimates of k. For the data of the preceding examples, the results are listed in Table 4(*b*). With $\omega = 1.41$, the approximate value of $k = 0.346$ (instead of the true value of $k = 0.349$) yields $V_c = 83.5$ miles per hr (instead of the true value of 83 miles per hr).

Eqs. 35 may be written in terms of the ratio of vertical to torsional instability (or stability), δ_1/δ_2, as given by Figs. 14 and 16. By Eqs. 13 and 16, for zero structural damping,

$$H_1 = \frac{J_1}{F_1} = A \frac{a_1}{a_2} \frac{\delta_2}{\delta_1} \ldots\ldots\ldots\ldots\ldots\ldots\ldots\ldots (36)$$

Substituting Eq. 36 in the expression for X_2 of Eq. 31*b*, Eq. 35*b* becomes

$$k^2 \approx \frac{F_2}{B} \left(1 + \frac{a_2}{a_1} \frac{\delta_1}{\delta_2} \right) \ldots\ldots\ldots\ldots\ldots\ldots\ldots\ldots (37a)$$

With damping included,

$$k^2 \approx \frac{F_2}{B} \left(1 + \frac{a_2}{a_1} \frac{\delta_1}{\delta_2} \right) \frac{F}{F_1 + k\, d_1} \ldots\ldots\ldots\ldots\ldots\ldots\ldots\ldots (37b)$$

The added factor indicates the reduction of k (increase of V_c) by structural damping.

For the physical significance of the ratio a_1/a_2, recurring in these formulas, by definition, $\frac{a_1}{a_2} = \left(\frac{\omega_1}{\omega_2} \right)^2$. Hence, for a section with $\omega_1 = \omega_2$, the foregoing approximate formulas yield $B = 0$, $k = \infty$, and the critical velocity $V_c = 0$; such section would be unstable (for coupled oscillations) at all wind velocities. As the difference between the frequencies $(\omega_2 - \omega_1)$ is reduced, the critical velocity is lowered. Actually the lower limit of V_c is given by the discriminant of Eq. 26*b*, $H^2_3 - 4\, H_4 = 0$, or $2\, X_1 = -\, H_3$. This occurs with ω_2 slightly exceeding ω_1. If the differences between the frequencies were reversed, with ω_1 exceeding ω_2, then B would be negative and, by Eqs. 37, k would be imaginary, indicating that the section would be stable, with no critical velocity at which self-excited coupled oscillations could develop.

Coupled Oscillations: Comparison with the Theodorsen Equations.—For the same applications to coupled oscillations, Mr. Theodorsen's equations yield lower values of k and corresponding higher values of the critical velocity V_c. Part of the difference is due to the application to a real section $(d/b = 0.02)$,

instead of an idealized case with $s_1 = 2\pi$ and $s_2 = \pi/2$. If, however, the Theodorsen coefficients $\left(C,\ C,\ C,\ \frac{1-C}{2q_4}\right)$ are substituted for the writer's general coefficients (C_1, C_2, C_3, and C_4), and the classical values of s_1, s_2, s_3, and s_4 are used, a perfect check is obtained. The writer's equations for coupled oscillations (both exact and simplified) provide a convenient and completely generalized solution for the application of any of the theories. With the other sets of coefficients substituted, their unifying relations and identities permit a still further simplification of the writer's formulas, yielding solutions of maximum simplicity for the problem of coupled oscillations, a problem commonly regarded as recondite and formidable.

Instability Graph for Coupled Oscillations.—The critical velocity yielded by the equations for coupled oscillations is the wind velocity of zero net amplification or damping, represented by $\delta - \delta_s = 0$, or $\delta = \delta_s$. Consequently, the critical velocity computed for any given value of the (positive) structural damping δ_s is also the wind velocity that produces an equal negative damping or potential amplification ratio δ. By calculating the critical velocities for different values of δ, the instability curve for coupled oscillations is obtained.

TABLE 5.—Numerical Example, Construction of Instability Graph

δ	k	ω	V_c	$V/(N\,b)$
0	0.462	1.46	65	6.81
0.05	0.349	1.41	83	9.02
0.10	0.304	1.39	93	10.37
0.15	0.274	1.38	102	11.48
0.20	0.254	1.36	109	12.39
0.25	0.237	1.35	116	13.28
0.30	0.223	1.34	122	14.10

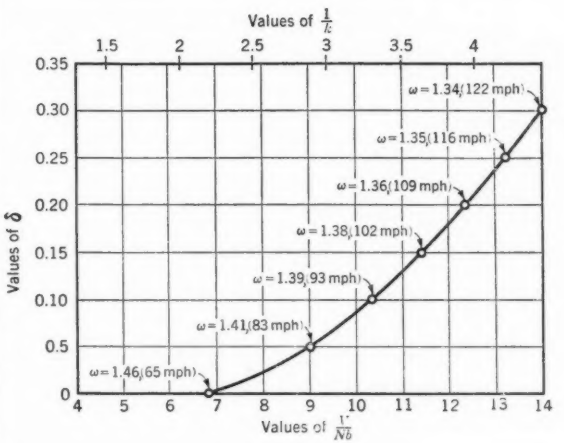

As shown in the preceding section, the approximate short cut, Eq. 35*a*, yields a solution very close to the exact values. This provides a quick method for computing and plotting the instability graph (or negative damping curve) for coupled oscillations.

Coupled Oscillations: Instability Graph (Numerical Example).—For the same section ($d/b = 0.02$) and data as in the preceding examples, with trial $k = 0.30$ for the new values, Eq. 35*a* yields the values of k shown in Table 5, for the different values of δ, and Eqs. 32 yield the corresponding values of ω. Plotting

these values, the instability graph for coupled oscillations will be as shown in the table.

Coupled Oscillations in Spans with Vertical and Torsional Modes Dissimilar.—The preceding analysis for coupled oscillations, derived for a unit section, is valid for a complete bridge provided the vertical and torsional wave forms are practically similar over the span or spans, with common nodes, so that the amplitude ratio η/α is uniform throughout the length. If the vertical and torsional modes differ materially, a correction is required in the analysis.

The two force equations for a unit section, such as Eqs. 10 or 25, may be represented in abbreviated form as $(A_1)\frac{2\eta}{b} + (A_2)\alpha = 0$; and $(B_1)\frac{2\eta}{b} + (B_2)\alpha = 0$—for the vertical and torsional forces, respectively.

Let $2\eta/b = u_1\phi_1(x)$; and $\alpha = u_2\phi_2(x)$, in which u_1 and u_2 are time functions, and ϕ_1 and ϕ_2 are the respective (dissimilar) wave forms (along the span or spans). The virtual work done by the vertical and torsional forces, respectively (in an element of time), over the spans will then be

$$\delta W = A_1 u_1 \delta u_1 \int_0^L \phi_1 \phi_1 \, dx + A_2 u_2 \delta u_1 \int_0^L \phi_1 \phi_2 \, dx = 0$$

and

$$\delta W = B_1 u_1 \delta u_2 \int_0^L \phi_1 \phi_2 \, dx + B_2 u_2 \delta u_2 \int_0^L \phi_2 \phi_2 \, dx = 0$$

Write the numerical expressions for $u_1\phi_1$ and $u_2\phi_2$ in normalized form so as to make $\int_0^L \phi_1\phi_1\,dx = 1$; $\int_0^L \phi_2\phi_2\,dx = 1$; and $\int_0^L \phi_1\phi_2\,dx = U$. The virtual work equations then reduce to $(A_1)u_1 + (A_2)U u_2 = 0$; and $(B_1)U u_1 + (B_2)u_2 = 0$. Substituting the expressions represented by A_1, A_2, B_1, and B_2 from Eqs. 25,

$$\left(X_1 + i\,d_1 + \frac{i}{k}C_1\right)u_1 = \left(\frac{1}{k^2}C_1 - \frac{i}{k}q_3 C_3\right)U u_2 \ldots\ldots (38a)$$

and

$$\left(\frac{i}{k}C_2\right)U u_1 = \left(-X_2 - i\,d_2 + \frac{1}{k^2}C_2 - \frac{i}{k}q_4 C_4\right)u_2 \ldots\ldots (38b)$$

Proceeding as with the solution of Eqs. 25, a duplication of Eqs. 26 to 28 is obtained, with U-terms added in the expressions for H_2 and H_4 (also in Eq. 29) as the sole modifications:

$$H_2 = \frac{\frac{q_2}{k}U^2(F_2G_3 + F'_3G_2) - \frac{q_4}{k}(F_1G_4 + F_4G_1) + d_1J_2 - d_2G_1 + \frac{1}{k^2}(1-U^2)(F_1F_2 - G_1G_2)}{F_1 + k\,d_1} \ldots (39a)$$

and

$$H_4 = \frac{1}{k\,H_1}\Big[-G_1H_2 + \frac{q_4}{k}(F_1F_4 - G_1G_4) - \frac{q_3}{k}U^2(F_2F'_3 - G_2G_3) + d_1J_1 + d_2F_1 + \frac{1}{k^2}(1-U^2)(F_1G_2 + F_2G_1)\Big] \ldots (39b)$$

—and Eq. 29 is replaced by

$$\frac{u_1}{u_2} = \left(\frac{C_1/k - i\, q_3\, (C_3 - \pi\, r_1/s_3)}{k\, X_1 + i\, C_1 + i\, k\, d_1} \right) U$$

$$= \frac{1}{U} \left(\frac{-\, q_4\, C_4 + i\, k\, X_2 - k\, d_2}{C_2} - \frac{i}{k} \right) \ldots (40)$$

For the case in which vertical and torsional modes are similar, $U = 1$, and Eqs. 39 and 40 reduce to the simpler ones previously derived.

Coupled Oscillations with Dissimilar Modes: Numerical Example.—Let the span lengths equal $l = 2{,}800$; $l_1 = 1{,}100$; and $(L = l + 2\, l_1)$; and let the wave forms be

Vertical mode—main span:	$\phi_1 = \alpha_1\, (\sin \pi\, x/l - 0.113 \sin 3\, \pi\, x/l)$
Vertical mode—side spans:	$\phi_1 = \alpha_1\, (0.740 \sin \pi\, x/l_1)$
Torsional mode—main span:	$\phi_2 = \alpha_2\, (\sin \pi\, x/l - 0.493 \sin 3\, \pi\, x/l)$
Torsional mode—side spans:	$\phi_2 = \alpha_2\, (0.493 \sin \pi\, x/l_1)$

To normalize these expressions:

$$\int_0^L \phi_1\, \phi_1\, dx = 1; \qquad \text{hence, } \alpha_1 = \frac{0.830}{\sqrt{0.5\, l}}$$

$$\int_0^L \phi_2\, \phi_2\, dx = 1; \qquad \text{hence, } \alpha_2 = \frac{0.835}{\sqrt{0.5\, l}}$$

Hence, $U = \int_0^L \phi_1\, \phi_2\, dx = 0.932.$

For the section data of the preceding examples $(d/b = 0.02)$, with zero damping, the solution including the U-correction, using Eqs. 39 and 40, yields $k = 0.43$, $\omega = 1.46$, $V_c = 69$ miles per hr, and $u_1/u_2 = -0.34 - 0.089\, i = -0.35\, e^{0.26 i}$.

Conclusion

General expressions have been derived for the aerodynamic forces on any oscillating section and for the opposing dynamic forces. The resulting general equations yield solutions for all problems of vertical, torsional, and coupled oscillations, including analytical determination and prediction of frequencies, critical velocities, rate of amplification, and limiting amplitudes. Maximum simplicity and practical applicability have been the governing considerations. Numerical applications, graphic methods, and simplifying short cuts have been included.

The methods of classical aerodynamic theory are limited to idealized streamline sections and are not applicable to other sections, such as practical bridge sections. In order to overcome this limitation and to secure complete generality of application to any form of section whatsoever, the unknown parameters and coefficients in the aerodynamic equations are supplied by static wind-tunnel tests on section models, using tilted straight models to represent the effects of

vertical velocity and angular position, and horizontal curved models to represent the effects of angular velocity. With the use of curved models and the added consideration of the effects of varying angular position, the results of prior analysis of the problem of bridge oscillations have been extended and amplified toward greater finality and verified validity.

The coefficients representing the correction for phase lag have been derived in simple, general form from the pressure distribution graphs for the straight and curved models, by simply applying to the pressure ordinates the progressive phase difference across the width of the section. In classical aerodynamic theory, the corresponding coefficients (for the limited case of an ideal flat plate or streamline airfoil) are derived from the theoretical discontinuity or vortex sheet extending from the trailing edge of the section to infinity, so that the coefficients theoretically represent a function of the complete past history of the motion of the oscillating section. The coefficients derived by the two different concepts are not identical. The classical derivation is not applicable to nonstreamline sections, and no method of adapting it so as to fit the known behavior of nonstreamline sections is apparent. The coefficients derived by the simpler concept do fit the known behavior of nonstreamline sections. The equations of this paper, however, are written in completely general form so as to retain their usefulness and validity for any substitution of coefficients derived by other theories, existing or anticipated.

The analysis here submitted is believed to be the first generalized aerodynamic theory of oscillating sections, not limited to sections of any one type. It is also believed to constitute the aerodynamic theory of bridge oscillations brought to greater completeness and generality than any prior presentation. It is submitted to the profession in order that constructive review and discussion may further advance the solution of the problem toward definitive completeness and finality.

AMERICAN SOCIETY OF CIVIL ENGINEERS

Founded November 5, 1852

DISCUSSIONS

THE RELATION OF URBAN EXPRESSWAYS TO MASS TRANSPORTATION FACILITIES

Discussion

BY CURTIS G. BRADFIELD

CURTIS G. BRADFIELD,[8] M. ASCE.—It is gratifying to the writer to have had such learned discussions of this paper and to find that the little valid adverse comment must indicate rather general assent to the basic premise.

Mr. Steigelman presents an interesting but somewhat extreme projection of the basic theory advanced in the paper when he recommends prohibiting all private passenger cars from the congested areas, and proposes the erection of radial artery perimeter parking facilities as the innermost limits of private vehicular travel. Mr. Steigelman would place these travel termini around the edge of the downtown zone and suggests either walking or surface mass transportation equipment to accomplish circulation within the critical area. At first, this would appear to be a radical step to insure freeing streets from congestion. However, in view of the steady, inexorable increase in motor car registration, who can deny that some day such a drastic move may be necessary?

At any rate, although scarcely necessary now or in the foreseeable future (since such problems have a way of solving themselves), the possibility that some kind of prohibition ultimately may be required should be kept in mind by all city planners and devisers of traffic corrective measures. Incidentally, it is a strong argument against a too-liberal provision of urban expressways for local traffic when such facilities are not carefully balanced with adequate mass transportation.

The excellent discussion by Mr. Lewis adds greatly to the paper. The only comments the writer believes justified are the following:

1. The third paragraph, under the heading, "Relief for Intercity Traffic," was intended to convey the thought that the urban expressways needed for intercity traffic would automatically be valuable for much cross-the-city traffic and, similarly, for intracity vehicular movements. In any case, the writer agrees heartily with Mr. Lewis' statement: "* * * the inner sections

NOTE.—This paper by Curtis G. Bradfield was published in December, 1948, *Proceedings*. Discussion on this paper has appeared in *Proceedings*, as follows: April, 1949, by Elmer F. Steigelman, and Harold M. Lewis; May, 1949, by Joseph Barnett; and September, 1949, by Ralph Wesley Jones.

[8] Public Works Officer, U. S. Coast Guard Yard, Curtis Bay, Md.

of such [expressway] routes should be so designed that they can also take care of intracity traffic * * *."

2. As stated in the paper (under the heading, "Relief for Local Traffic"), the writer believes all curb parking should be prohibited during business hours in the congested zone. Meter controlled parking, as suggested by Mr. Lewis, is as much a traffic flow deterrent as unlimited curb parking and there is no justification for such retarding influences.

3. The writer feels it is not putting "the cart before the horse" to state that the cities with the most centralization have the most extensive mass transportation systems. Cities become large for economic reasons, not because of local mass transportation facilities. In such cities, business people tend to group together in the smallest possible cluster of centers because, up to now, no communication device ever used is as satisfactory, in the final analysis, as personal face-to-face contact when consummating, or arriving at, an agreement. Somewhat belatedly, transportation usually follows this grouping to move the workers in and out of these trade or profession centers. The centralization originates first and then transportation somehow blunders along to at least partial adequacy. If, by chance, adequate transportation should fail to evolve, obviously the entire scheme would bog down, decentralization would result, and large investments in downtown properties would be depreciated in an unreasonably short time. This process is now occurring in too many cities.

The only method of maintaining the value (and taxable assessment) of the downtown area is to improve the mass transportation service to that area in keeping with the demands of the greatest number of people desiring to move in and out of the district.

No discussion of urban expressways and urban mass transportation facilities could be considered complete without the comments of Mr. Barnett to provide the reaction of those who lean toward a liberal provision of expressways. Mr. Barnett's statement that there are about fifteen cities with combined city and satellite populations of 1,000,000 or more is, of course, accurate. However, when it is realized that the total population of these metropolises is approximately a fourth of the total population of the entire United States, the urgency of solving the transportation problem properly is readily apparent. Eleven of these fifteen cities do not now have off-the-surface mass transportation of any consequence. If these cities, which are of the utmost importance to the national economy, fail to meet the demand for adequate transportation or incur huge indebtedness for a type of facility which does not halt the too-rapid tendency toward blight in their downtown areas, disastrous municipal financial conditions could easily arise.

As Mr. Barnett so clearly indicates, surface mass transit is in a vicious cycle leading only to ultimate strangulation and, seemingly, is not the answer to the problem. It certainly follows that, if planners make it still easier and more attractive for the motorist to bring his car into the zone of congestion, such a policy can only accelerate this eventual strangulation. The inescapable fact is that the greatest number of people desiring to enter and leave the downtown

areas daily would use mass transportation facilities if the service were adequate. These are the people who must be considered, and whether they should be encouraged to use private motor cars by building a network of expressways or whether, instead, they should be discouraged from the use of automobiles by furnishing adequate mass, rapid transit, is the crux of this entire discussion.

It is not the occasional traveling salesman, the service mechanic, or the insurance collector who congests cities when he brings his very necessary car downtown. Instead, it is the intolerably large number of people who merely drive to and from their place of employment and leave their cars idle all day. They are the motorists that must be either accommodated or discouraged.

The writer gathers from the comments of Mr. Jones that the paper was not sufficiently lucid. At least, there was no intention that it should be interpreted as meaning all downtown vehicular traffic is unnecessary as Mr. Jones states. Instead, the paper seemed to the writer to be clear in remarking that much of the downtown vehicular traffic arising from motorists merely going to places of employment or keeping business appointments was not really mandatory and these people could be served by adequate mass transportation.

Again, the paper would be quoted more accurately if Mr. Jones' discussion read "many" instead of "most" when commenting on the number of cities with imperfect grid patterns of street layout.

Still again, the writer is unable to find in the paper any statement which could be commented on, thus: "Surely, the author's statement that expressways are unnecessary inside cities, but are needed between cities is debatable." Instead, the writer tried to state an opinion that expressways were needed in cities for intercity and cross-the-city traffic (and such incidental local traffic as could advantageously use the facilities), but that the immediate need for expressways for purely local shuttle traffic could not be determined accurately or positively until all possible methods of handling this movement volume by improved mass transportation facilities had been thoroughly exploited.

Mr. Jones further states: "* * * nor should the author confine his planning to circumferential expressway belts as the only geometric pattern." No part of this paper recommends any expressway pattern. Incidentally, the more important expressways Mr. Jones describes as "radial" are actually "tangential," as the writer recommends, and are basically for intercity or satellite community traffic.

The paper should not have given the impression that the writer proposed prohibiting the taxpayer from using his downtown streets. It did recommend discouraging the use of these thoroughfares unless the need was actually mandatory—a quite different approach. In this connection, there seems to be no impropriety in a policy of discouraging taxpayers from using various tax-supported facilities unless they have an urgent need for them. Cases in point are old people's homes, welfare clinics, and mental hospitals.

Unfortunately, Mr. Jones assumed the writer's statement "* * * the elevated trackage along Market Street (Philadelphia, Pa.) * * *" as meaning the Market Street Elevated (rapid transit) west of the Schuylkill River. Instead, the elevated trackage (railroad) along Market Street between the

Schuylkill River and Broad Street Station was the intended example of an element of interference with consistent city growth. The cited example (a railroad fill) is known in Philadelphia as the "Chinese Wall" and the need for its removal has long been a familiar source of complaint on the part of most Philadelphians.

Other comments the writer feels may be justified when considering Mr. Jones' discussion are:

1. Citing an accident frequency table to contradict the statement that timid drivers avoid high-speed expressways does not appear germane.

2. Mr. Jones' criticism that streets projected over filled in harbor indentations, as recommended by the writer, would be objectionable appears to be hypercritical.

3. Despite Mr. Jones' skepticism, the writer believes it is self-evident that the net cost to the taxpayer of off-the-surface mass transportation facilities confined to the downtown district, even if not entirely self-liquidating, will be measurably less than the tremendous, nonrecapturable outlay required for an extensive network of urban expressways covering every part of a city except the downtown district. Expressways cost about $5,500,000 per mile and subways approximately $7,500,000 per mile. Obviously, the first cost of central zone subways will be immeasurably less than a city-wide network of expressways, and even the most skeptical cannot help but admit that some revenue will be collected to defray part of the rapid transit cost. On the other hand, the expressways will return nothing and will entail a constantly growing unliquidated maintenance cost.

4. The writer agrees with Mr. Jones that "Cities must be planned today * * * for the forseeable needs" but cannot agree that "* * * they always have been * * *." There is little evidence that past city planning has been any more than an unrelated series of expedient measures arising from waves of indignant pressure on political groups. Furthermore, the writer doubts that the future definitely indicates a return to a modern version of the personal horse and buggy—the personal automobile—and the gradual atrophy of mass transportation. There is little place in modern metropolitan areas for personal luxury transportation—antiquated or modern versions—and the only feasible, sound, procedure for moving large volumes of people from place to place is by mass transportation equipment.

5. Mr. Jones' analogy of a hand pump compared to a modern municipal water supply supports the writer's contention. The hand pump was the personal facility—personal transportation, albeit either horse and buggy or automobile—and the municipal water supply is the mass facility—mass transportation.

6. There seems to be little evidence to support Mr. Jones' contention that subways cannot accommodate all mass transportation equipment. There are relatively few surface transit vehicles operating on Manhattan (New York, N. Y.) streets and the subways, although often overcrowded, successfully bear well-nigh the entire transportation burden.

7. Despite Mr. Jones' statement, the writer does not recommend that: "* * * all vehicles [should be] * * * taken from the streets * * *." He did

suggest, however, that unnecessary surface traffic be reduced and that mass transportation be measurably improved. If this is done, it is quite possible that Mr. Jones' remark—"* * * expressways will be uneconomic; expressways will also be unnecessary * * *"—may prove to be true.

If the paper was not entirely clear in all respects, or if erroneous impressions were given, a brief restatement may be justified. The paper was, in essence, a plea for moderation in current city planning—an admonition that broad thinking on the entire subject, not just the motorists' woes, might be indicated before arbitrary steps are taken.

The United States is largely a nation of extremists. Its citizens will endure and tolerate a condition for far too long and then, suddenly, wish to alter the entire situation immediately.

Most cities are already burdened with a heavy tax load brought about, in many instances, by past inadequate expediencies or hastily planned measures which failed to cope with overevaluated or underevaluated problems.

This traffic problem and its effect on the economic well-being of cities in the United States is a matter of great concern. A proper solution of the dilemma must be found. The cost of either an expressway network or a composite system with some expressways and some intensively redeveloped mass transportation facilities will be huge and, if the wrong decision is made, there could be serious economic repercussions.

Some guidance may be found from past experience. There was a time when personal transportation, in the form of a horse and buggy, threatened to drive the lumbering omnibus from the city streets. However, instead of this, the horse car and cable car (the rapid transit of their day) were provided and the seeds of the present growth of modern downtown districts sown. Again there has arisen a form of personal transportation that is strangling the existence of the lumbering buses and street cars. The writer believes it is quite possible that the wiser course would be to concentrate planning efforts on rectifying the shortcomings of mass transportation and redeveloping it to the utmost before saddling the taxpayers with still more debt largely for the benefit of people who desire a luxury type of transportation to their places of employment.

AMERICAN SOCIETY OF CIVIL ENGINEERS

Founded November 5, 1852

DISCUSSIONS

EFFECT OF DRIVING PILES INTO SOFT CLAY

Discussion

BY STUART B. AVERY, JR., AND STANLEY D. WILSON, AND GEORGE L. FREEMAN AND JAMES D. PARSONS

STUART B. AVERY, JR.,[29] AND STANLEY D. WILSON,[30] ASSOC. M. ASCE.—Factual data, on a subject that has long been controversial, are contained in this paper; and the authors are to be commended for initiating a type of investigation that, if conducted systematically on various types of clay, will furnish much needed information.

The investigation reported was made at the site of a structure supported by point-bearing piles driven through a clay of low plasticity and slight sensitivity, to hardpan. Under these conditions it is difficult to conceive detrimental effects caused by pile driving. The writers' interpretation of the data differs from that presented by the authors.

Effect of Disturbance on Consolidation and Strength Characteristics of Clays.—It is well established that structural disturbance of a mass of undisturbed, sedimentary clay changes its consolidation characteristics. This is illustrated by Fig. 28. Typical void ratio-pressure curves and corresponding shear strength-pressure curves for a sensitive clay in undisturbed, badly disturbed, and laboratory remolded states are shown in Fig. 28(*a*).

Driving piles into a fully saturated clay, without pre-excavation, causes the total foundation volume to increase by the volume of the piles. In addition, the following effects will result in a clay having a sensitive structure:

(1) At least a portion of the clay is badly disturbed at unchanged water content. This means that the effective stress in the clay moves from point A to point B, Fig. 28(*a*). In this condition the clay is only partly consolidated under its own weight.

(2) The shear strength is correspondingly reduced from point C to point D.

NOTE.—This paper by A. E. Cummings, G. O. Kerkhoff, and R. B. Peck was published in December, 1948, *Proceedings*. Discussion on this paper has appeared in *Proceedings*, as follows: May, 1949, by Leonardo Zeevaert, Jacob Feld, Joseph C. Fegan, and Gregory P. Tschebotarioff; June, 1949, by Philip C. Rutledge, A. W. Skempton, James R. Schuyler, and B. A. Kantey; and September, 1949, by D. P. Krynine, and Robert F. Leggett.

[29] Cons. Engr., Cambridge, Mass.

[30] Asst. Prof. of Soil Mechanics and Foundation Eng., Harvard Univ., Cambridge, Mass.

(3) The badly disturbed clay immediately begins to reconsolidate under its own weight and would reach full consolidation at point E. However, if a part of the weight of the overlying clay is supported by negative skin friction, between the piles and the clay, the consolidation would stop at an intermediate point F, corresponding to full consolidation under the decreased load. (The term "negative skin friction" was first introduced by Karl Terzaghi,[31] Hon. M. ASCE, in 1935.)

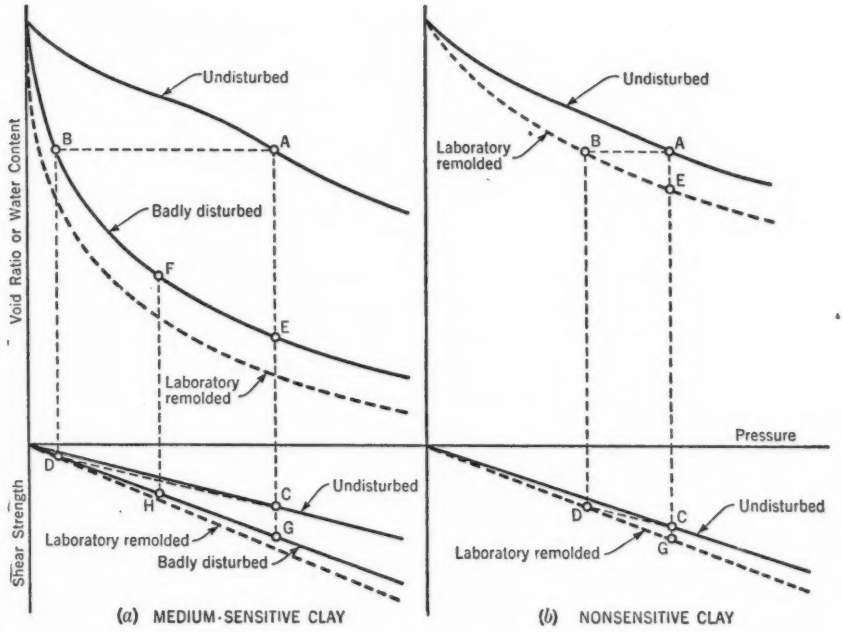

FIG. 28.—LABORATORY TESTS ILLUSTRATING EFFECT OF DISTURBANCE ON CONSOLIDATION AND STRENGTH CHARACTERISTICS OF SEDIMENTARY CLAYS

(4) The shear strengths corresponding to points E and F are shown graphically by points G and H, respectively. It should be noted that the disturbed clay, after 100% consolidation under its own weight, has a higher shear strength than the original undisturbed clay.

The same relationships for a nonsensitive clay are shown in Fig. 28(*b*), from which it can be seen that even complete laboratory remolding would have little effect on either the strength or the consolidation characteristics of such a material.

It was from an analysis of such laboratory test curves that A. Casagrande,[4] M. ASCE, in 1932, warned that increased settlements may result from driving

[31] "Die Setzung der Fundierungen und ihre Wirkung auf den Oberbau," by Karl Terzaghi, *De Ingenieur*, 1935, Nos. 50 en 51.

[4] "The Structure of Clay and Its Importance in Foundation Engineering," by A. Casagrande, *Journal*, Boston Soc. of Civ. Engrs., April, 1932.

friction piles, closely spaced, into a sensitive clay. His conclusion applied only to the case of floating, or friction, piles, and the writers question the applicability of the following statement of the authors (under the heading, "Conclusions"):

> "The preceding information indicates that the driving of piles at the site where the investigation was made did not have the detrimental effects which were forecast on the basis of soil tests on undisturbed and remolded samples and the theory of consolidation as applied by Mr. Casagrande."

This statement could easily be misunderstood by a reader to mean that Mr. Casagrande had forecast detrimental effects for point-bearing piles driven through a nonsensitive clay under conditions similar to those at the particular project for which the authors have conducted their investigation. The writers maintain that such a "forecast" could not be made on the basis of Mr. Casagrande's paper. In order to bring out differences between the two cases, the writers propose to discuss the four distinct types of pile foundations illustrated in Fig. 29.

Case I. Point-Bearing Piles Driven Through Nonsensitive Clay.—In this case, the ground surface will heave simultaneously with driving, the volume of this heave being equal to the volume displaced by the piles. The clay being nonsensitive, there will be little tendency for reconsolidation, and only a negligible settlement of the ground surface will occur even if the clay is badly disturbed by the pile driving operation.

Case II. Point-Bearing Piles Driven Through Sensitive Clay.—As in case I, the ground surface will heave simultaneously with driving, but the disturbed clay will immediately start to reconsolidate under its own weight. The consolidation continues until sufficient friction has developed to carry the weight of the clay between the piles by negative skin friction. The final elevation of the ground surface will depend on the sensitivity of the clay, the degree of disturbance, the diameter of the piles, and their spacing. The more sensitive the clay, the greater will be the volume of water lost as a result of complete reconsolidation under the existing overburden. Although with increased pile spacing the disturbance is less, the percentage of the soil weight between the piles that can be carried by negative skin friction is also reduced. Therefore, the greater the pile spacing the greater will be the effective load under which the disturbed clay must reconsolidate. The writers' experience indicates that even in extreme cases the settlements due to consolidation are less than the heave that had resulted from the volume displacement of the piles. Hence, a net heave is to be expected in any case.

In cases I and II no detrimental effects can result, unless in case II the soil between the piles is supporting a part of the structure, or the piles are designed with so low a factor of safety that they settle or fail under the additional load of the weight of some of the soil between the piles.

Case III. Friction Piles Driven Into Nonsensitive Clay.—As in case I, the ground surface will heave simultaneously with driving and the volume of heave will be equal to the volume displaced by the piles. When the load is applied,

the piles and the ground surface will settle together because of the consolidation of the lower part of the clay stratum under the additional load of the structure.

Case IV. Friction Piles Driven Into Sensitive Clay.—As in case II, the ground surface will heave simultaneously with driving and the disturbed clay

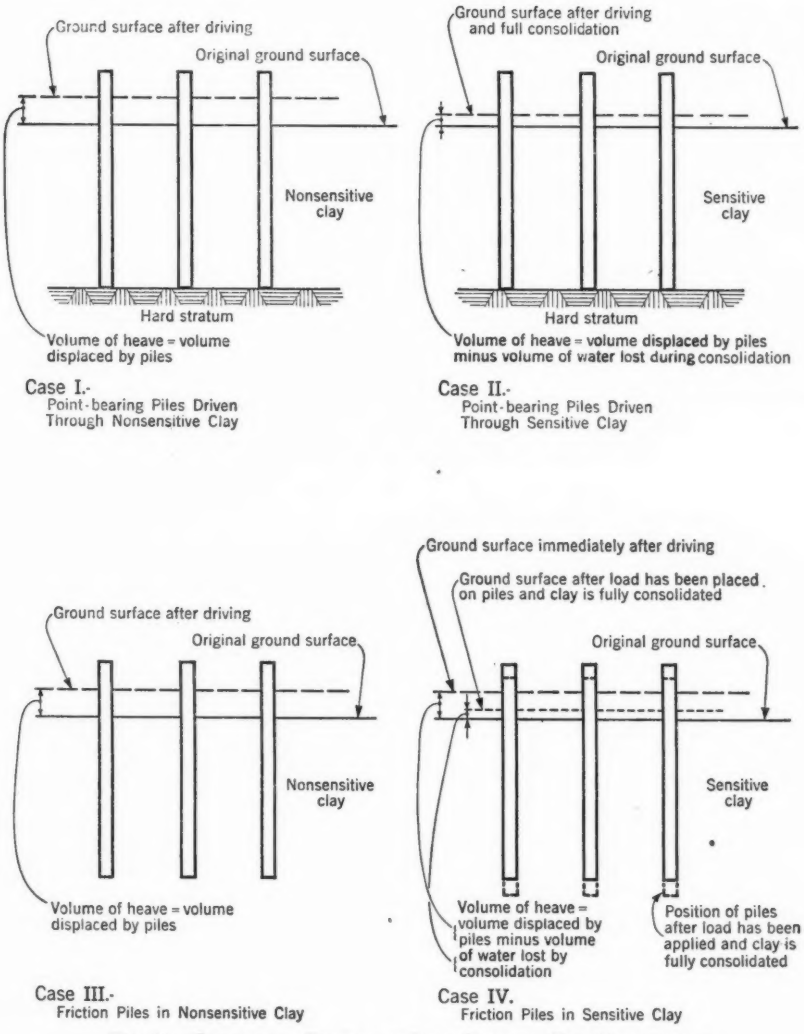
Ground surface after driving
Original ground surface
Nonsensitive clay
Hard stratum
Volume of heave = volume displaced by piles
Case I.-
Point-bearing Piles Driven Through Nonsensitive Clay
Ground surface after driving and full consolidation
Original ground surface
Sensitive clay
Hard stratum
Volume of heave = volume displaced by piles minus volume of water lost during consolidation
Case II.-
Point-bearing Piles Driven Through Sensitive Clay
Ground surface after driving
Original ground surface
Nonsensitive clay
Volume of heave = volume displaced by piles
Case III.-
Friction Piles in Nonsensitive Clay
Ground surface immediately after driving
Ground surface after load has been placed on piles and clay is fully consolidated
Original ground surface
Sensitive clay
Volume of heave = volume displaced by piles minus volume of water lost by consolidation
Position of piles after load has been applied and clay is fully consolidated
Case IV.
Friction Piles in Sensitive Clay

FIG. 29.—SETTLEMENT EFFECTS IN FOUR CASES OF PILE FOUNDATIONS

will begin to reconsolidate under its own weight. However, the skin friction will soon build up to a value which will enable it to carry the weight of the clay between the piles by negative skin friction. In case IV this condition will develop only along the upper part of the pile, whereas along its lower part

this clay load will be transferred into the adjacent clay by means of positive skin friction. Eventually a condition of equilibrium will be established such that the upper part of the clay will carry only a small part of its own weight. In this condition, if the piles are loaded, the load will be transmitted by skin friction into the clay along the lower part of the piles, which then must start a new cycle of consolidation. If the skin friction along the lower part of the piles is not sufficient to carry the new load, plus the clay load, the piles would actually fail by slipping. Otherwise, all clay between the piles will develop additional consolidation which will produce settlements of the piles. In addition, the clay stratum underlying the points of the piles will consolidate under the net increase in load.

In case III one should expect that the settlements would not be larger, and often smaller, than if the structure had been supported by spread footings. In case IV, however, the settlements in a very sensitive clay may well be considerably larger than if no piles had been used.

Experiences in Driving Piles Into Boston Blue Clay.—The foundation of the new John Hancock Building[32] in Boston, Mass., is an example of case II, Fig. 29. The soil conditions at the site are as follows: 20 ft of sand and gravel fill, 20 ft of organic clay, 13 ft of medium stiff clay, 80 ft of soft clay, 10 ft of hardpan, and then bedrock. The organic clay is known locally as Charles River silt and, with a liquid limit of about 50, has physical properties comparable to those of a very soft clay. The soft clay is typical Boston Blue clay with a medium sensitivity. The foundation consisted of 14-in., 117-lb H-piles, with an average spacing of about 5 ft, driven from slightly above the surface of the organic clay to bedrock. Steel H-piles, rather than a full displacement type of pile, were used on this project specifically to reduce to a minimum all undesirable effects. If full displacement piles had been used, an adjacent building would first have been subjected to sharp differential heaving and later to settlements that would have certainly caused structural damage to the adjacent section of the building. A follower was used to drive each pile the last 20 ft. The first 20 ft of excavation preceded pile driving, whereas the remaining 25 ft followed pile driving.

A record of the vertical movement of the surface of the foundation clay at the middle of the site is shown in Fig. 30, together with a cumulative record of pile driving operations. The parabolic curve is the estimated heave due to the excavation of about 20 ft of soil.

By the time the second stage of excavation began approximately 80% of the piles had been driven. With full displacement, this corresponds to a computed heave of about 6 in., whereas the observed heave attributed to pile driving amounted to only about $3\frac{3}{4}$ in. The main reason for this difference is believed to be the consolidation of the clay caused by the disturbance of the clay structure during pile driving. This is indicated by the settlement Δ_1 of the observation points (see Fig. 30) from August 1 to August 13 when the driving operations were suspended, by which time no piles had been driven

[32] "The Pile Foundation for the New John Hancock Building in Boston," by A. Casagrande, *Journal*, Boston Soc. of Civ. Engrs., October, 1947, p. 297.

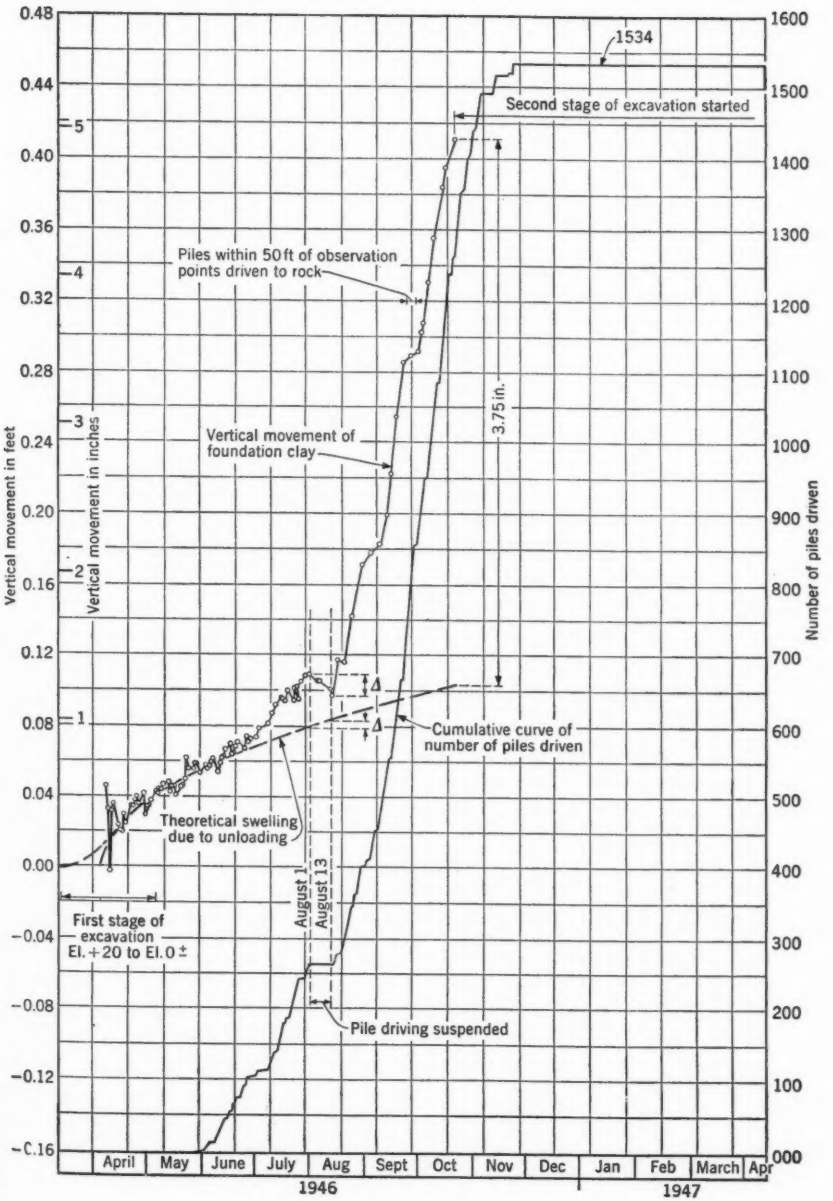

FIG. 30.—VERTICAL MOVEMENT OF FOUNDATION CLAY COMPARED WITH NUMBER OF PILES DRIVEN

closer than 50 ft from the observation points. Whereas one should have expected, during this period to observe only the slight heave Δ_2 from the swelling of the clay caused by the unloading, the points actually settled. From this unexpected observation it is concluded that even the small displacement and small strains caused by driving steel H-piles into a sensitive clay cause additional consolidation.

If this conclusion is correct, it would follow that little or no swelling pressure would develop against the bottom of the foundation slab. To date (August, 1949), the observed soil pressures beneath the foundation slab have ranged between zero and about 7 lb per sq in., confirming this conclusion.

The New England Mutual (NEM) Building[33] in Boston in the vicinity of the John Hancock (JH) Building, has similar soil conditions but is supported on a floating foundation without piles. The settlements of the adjacent streets during construction of the NEM building were neglibible, whereas those adjacent to the JH building were large. Most of these settlements occurred after pile driving and before installation of internal bracing. It is believed that they are chiefly due to disturbance to the organic clay, caused by pile driving, and, to some degree, to disturbance of the soft clay.

In his discussion of the Casagrande paper,[4] H. A. Mohr, M. ASCE, described another point-bearing pile foundation in the Boston Blue clay where the clay suffered large disturbances although all pile holes were partly pre-excavated with an auger 22 in. in diameter. The foundation consisted of pre-cast concrete piles 20 in. square, driven on 3-ft centers. Because of the close spacing it was decided to auger every other hole, drive these piles, and then repeat the procedure on the intermediate holes. No trouble was encountered in the augering operation until after the first group of piles had been driven; but, immediately after driving this group of piles, augering of holes, even at a considerable distance from the driven piles, and removal of material from the auger, became extremely difficult.

Disturbance of Clay During Construction of Chicago (Ill.) Subway.—Interesting observations on the settlements caused by disturbance to the clay structure in the construction of the Chicago subway have been published by Mr. Terzaghi,[34] who stated: "The tunnel lining * * * is surrounded by a layer of completely remolded clay, several feet thick." This badly disturbed clay has caused substantial street settlements.

Overloading of Piles Resulting from Disturbance of Sensitive Clays.—The additional soil load which point-bearing piles are called upon to carry, as a result of reconsolidation, may become critical for long slender piles driven through sensitive clay. An extreme example of this situation is in Mexico City (Mexico), where the foundation soil is an extremely sensitive and compressible bentonitic clay. Point-bearing piles are often driven through this clay to a sand layer at a depth of about 100 ft. As a result of general lowering of the piezometer surface in the clay because of pumping from lower strata, the clay is consolidating causing continual subsidence of the ground surface.

[33] "Application of Soil Mechanics in Designing Building Foundations," by A. Casagrande and R. E Fadum, *Transactions*, ASCE, Vol. 109, 1944, pp. 383–490.

[34] "Shield Tunnels of the Chicago Subway," by Karl Terzaghi *Journal*, Boston Soc. of Civ. Engrs. July, 1942, pp. 163–210.

In connection with a foundation project in Mexico City, pile pulling tests were performed to determine if negative skin friction would develop to a magnitude sufficient to carry the load of the clay, and also to determine the rate at which it would develop. The clay at the site of the test is of volcanic origin. It had a liquid limit of about 400, a plastic limit of about 100, and a natural water content at or slightly below the liquid limit (void ratio about 8.0). The unconfined compressive strength of undisturbed samples of this clay was about 0.3 ton per sq ft.

The test piles, in groups of four, on 3-ft centers, drove very easily, showing only a slight increase in resistance with increasing depth. The results of pulling tests showed that, only 2 hours after driving, the shearing force required to break the piles loose was at least 0.15 ton per sq ft, which is of the same order of magnitude as the shear strength of the undisturbed clay. This shearing strength is more than ample, at normal pile diameter and spacing, to carry the entire weight of the clay between the piles. Furthermore, the shearing strength of the reconsolidated clay, after the piles were broken loose, was found to be at least one half of its maximum value, in contrast to the negligible shear strength of the clay when freshly remolded.

These tests explain why the ground surface does not subside between piles, even though the ground surface in the immediate vicinity of a structure is subsiding. However, overloading of the piles may develop even if the clay between the piles is not in the least disturbed except for a few inches surrounding the piles. It is conceivable that under these conditions long, slender piles could actually fail in the course of time.

Disturbance of Clay at Detroit (Mich.) Investigation.—The clay described by the authors falls somewhere between cases I and II (Fig. 29). In view of the preceding discussion it is apparent that no detrimental effects could possibly occur, providing the piles are sufficiently strong to withstand the additional load of the clay between the piles as well as of the structure.

Clay with a liquid limit of about 30, a plastic limit of about 19, and a natural water content midway between these two values, together with the modest overburden, indicates two possibilities: (1) The clay is well overconsolidated, probably by drying; or (2) The clay has relatively little sensitivity to remolding. In either case one would expect that pile driving would have little effect in increasing the settlements from disturbance to the clay. Some settlement must have occurred due to reconsolidation of disturbed clay as evidenced by the fact that computed heave corresponding to full displacement is about 4 ft, whereas measured heave was only about 2 ft.

The authors state, under the heading, "Results of Tests":

> "In the homogeneous clay layer constituting the lower part of the deposit the effect of pile driving appears to have been negligible. There is no essential difference between the average compressive strength of the soil before and after pile driving."

This statement refers to the strengths obtained from boring P-1, taken 1 month after pile driving. From Fig. 9 it is obvious that the water content decreased appreciably during this period, and the writers have computed that

more than 50% of the reconsolidation had already taken place. This would correspond approximately to points F and H in Fig. 28(*a*). During the following 10 months, the clay further consolidated to some point between F and E, resulting in an even higher shear strength than that of the original undisturbed material.

Under the heading, "Interpretation of Results," the authors state:

> "Since the water appears to have migrated exclusively in a horizontal direction, the process of consolidation initiated by driving friction piles into the clay would not ordinarily result in settlement."

The direction of the flow will depend largely on the relative permeabilities vertically and horizontally, but this has no effect on the ultimate settlement. Probably the excess water resulting from disturbance to the clay structure will first drain away from the vicinity of the pile in horizontal direction (unless the pile itself permits drainage). This lateral drainage may well cause slight swelling in the immediately surrounding mass of clay. However, eventually the excess water must be drained off to enable the grain structure to carry the loads, and this drainage must result in settlements, unless the piles are essentially point-bearing piles. Mr. Casagrande,[35] in discussing skin friction on floating piles, stated.

> "Unless the piles themselves facilitate the drainage, the consolidation will proceed from the surface downward, so that the shearing resistance of the clay, and therefore the skin friction along the upper portion of the piles, will increase before a similar increase can take place along the lower section of the piles."

In contrast to this, the reported results indicate that, in this case, the reconsolidation of the badly disturbed clay surrounding the pile proceeded at the same rate along the entire length of the pile. However, since the excess water must eventually find its way to the surface, or to a more pervious stratum, and since it is the escape of this water that causes the settlements, the writers disagree with the statement in the "Conclusions" that:

> "The assumption that the settlement would proceed as a result of vertical migration of the water out of the clay, which formed the basis of the Casagrande settlement forecast, is not in agreement with the observations made in the investigation."

In this connection it should be noted that in the early nineteen thirties it was still generally assumed that drainage during consolidation developed mainly in a vertical direction. The original, one-dimensional theory of consolidation by Mr. Terzaghi includes this as one of the basic assumptions. Experience has since shown that lateral drainage is in many cases more important than vertical drainage. That applies particularly to settlements of buildings having a width of the same order of magnitude as the thickness of the clay layers. If water can drain horizontally more readily than vertically, it will speed up the consolidation process, but it will of course have no influence on the final value of the settlements.

[35] "The Structure of Clay and Its Importance in Foundation Engineering," by A. Casagrande, *Journal*, Boston Soc. of Civ. Engrs., April, 1932, p. 187.

Comparison of settlements under a relatively small loaded area with those under a large area, with identical foundation conditions and loads, was afforded in connection with settlement analyses of the Logan Airport[36] in Boston. These observations proved conclusively that, under an area comparable in size to an average building, consolidation proceeded much faster than when a similar load was distributed over a very large area.

Conclusion.—The writers believe that experience to date, including that reported by the authors, indicates that pile driving in a sensitive, sedimentary clay will badly disturb the clay immediately surrounding the pile and that even at a considerable distance from the piles, where the strain due to deformation is quite small, there can be sufficient disturbance to the clay structure to cause additional settlements.

In 1932 Mr. Casagrande visualized that large distortions are required to disturb clay structures sufficiently to cause additional settlements. Evidence which has accumulated since shows that even minor strains may cause sufficient disturbance to some sensitive, sedimentary clays so as to result in additional settlements. Thus, the effects of disturbance are in some cases more serious than one would be justified to assume on the basis of the Casagrande paper.[4] Certainly, a conclusion that the effects of disturbance are of small import and perhaps entirely nonexistent, as implied by the authors, is not warranted either on the basis of their investigation, or in the light of other available evidence.

Additional investigations are required to determine the limits of the zone of disturbance. The writers do not believe that the authors' investigation warrants the conclusion that "* * * the region of disturbance is limited to a zone within a few inches of the pile * * *." Until more data are available, designers would do well to make conservative assumptions regarding the possible effects of this disturbance on pile foundations in sensitive, sedimentary clay.

With this investigation the authors have pioneered in a new, but long overdue branch of foundation investigation. It is hoped that this work will be followed by similar tests in more sensitive clays of greater plasticity. In such investigations it would be well also to include both consolidation tests and pore pressure measurements in the clay before and after driving of the piles (perhaps the piezometers could be built into the sides of the piles) to furnish additional information on the amount of disturbance and on the additional consolidation that is taking place in the clay between the piles.

GEORGE L. FREEMAN,[37] M. ASCE, AND JAMES D. PARSONS,[38] ASSOC. M. ASCE.—Interesting information has been made available in this paper, although the writers are not in agreement with the conclusions derived from the data. They believe that the situation would have been entirely different had the piles not penetrated the uniform soft clay bed into the underlying sand and gravel.

[36] "Analysis of Pore Pressure and Settlement Observations at Logan International Airport," by J. P. Gould, thesis presented to Harvard Univ., at Cambridge, Mass., in 1949, in partial fulfilment of the requirements for the degree of Doctor of Science.

[37] Partner, Moran, Proctor, Freeman & Mueser, New York, N. Y.

[38] Associate Partner, Moran, Proctor, Freeman & Mueser, New York, N. Y.

A. Casagrande,[4] M. ASCE, provided the profession with a sound explanation of what had been previously observed relative to the detrimental effects of driving piles into soft clays. His paper has done much to curb the indiscriminate use of friction piles as a structural support in such soils.

The conclusions of the authors are based largely on the laboratory results of tests made on samples recovered from the uniform soft blue clay, persisting from about El. +505 to El. +550, through which the point-bearing piles were driven. The average unconfined compression strengths and water contents of the bed as a whole for the several periods considered were as shown in Table 4.

An examination of Fig. 5 indicates that the 2-in. samples suffered some distortion during sampling, and a similar distortion is noted in the samples shown in Fig. 7. It is assumed that the 2-in. samples were entirely subjected to unconfined compression tests and that the "drag" which is evident around the periphery of the samples was not trimmed off before testing. It is further

TABLE 4.—RELATIVE CHARACTERISTICS OF UNIFORM SOFT CLAY, IN RELATION TO TIME OF PILE DRIVING

Months from driving	AVERAGE WATER CONTENT (PERCENTAGES)		AVERAGE COMPRESSIVE STRENGTH (TONS PER SQUARE FOOT)	
	Adjacent to piles (P borings)	Midway between piles (C borings)	Adjacent to piles	Midway between piles
Before driving.....	24.7[a]	24.7[a]	0.61[a]	0.61
1 month after.....	22.8	23.8	0.56	0.56
11 months after.....	22.0	24.4	0.75	....[b]

[a] Boring A. [b] This value is mentioned by the authors but not given in the paper.

assumed that all the "undisturbed" samples tested had suffered a degree of disturbance similar to that evident in Figs. 5 and 7. Examination of the soil surrounding the pile, as shown in Fig. 4, indicates very substantial remolding of the soil extending away from the pile surface for at least the diameter of the pile itself. Although samples secured adjacent to the pile, shown in Fig. 6, did retain their "laminated structure," to some extent, they are visibly much disturbed and their strengths, as determined from tests, are the strengths of considerably remolded soils. Had the samples from boring A been truly undisturbed, their compressive strengths would no doubt have been substantially more than shown by the tests, and there should have been a greater difference between the strengths of undisturbed samples and samples recovered from the P borings and C borings.

The degree of disturbance midway between the piles must have been nearly the same as at the pile periphery, because the compressive strengths 1 month after pile driving are the same in both cases. With regard to the upper laminated clay, the authors state (see "General Soil Conditions") that:

> "In their undisturbed state, the samples had an unconfined compressive strength approximately eight times that of the same samples when remolded in the laboratory at their natural water content."

This difference is not apparent in Fig. 8, except in the upper few feet of the laminated clay. The same reduction in soil strength after 1 month, in the samples adjacent to, and midway between, the piles, may be purely a coincidence; and the test results certainly do not warrant the assumption that the disturbed soil zone is limited to within a few inches of the pile.

The limited scope of the investigation, and the scattered results of the few tests made, do not warrant the conclusions presented in the paper. Certainly more than one boring of each type should have been made before and after driving piles. It would also be interesting to know the results of unconfined compression tests on the samples from boring C-11. The addition of consolidation tests to the test program might have yielded valuable information regarding the relative strengths and degree of disturbance of the soil in different locations.

The authors state that, as a result of the pile driving operations, the ground surface between the piles heaved about 2 ft. Piles driven in similar soil formations frequently cause adjacent piles to heave, sometimes enough to require redriving. When the piles are point bearing and closely spaced the resulting settlement of the soil between the piles may be negligible, even when significant heaving has been noted, because of the transfer of soil weight to the pile surfaces through friction. The resulting arching effect between piles is sufficient to restrain the natural tendency for the remolded or disturbed soil to reconsolidate. The foregoing observed phenomena, however, cannot properly be construed to indicate that, if the piles were not point bearing and were in effect friction piles, they, or the soil between the piles, would not settle as a result of the remolding effect and added load. On the contrary, settlements should be expected and in all probability would occur. The authors' conclusions would be far more convincing had the authors determined from actual level observations whether the soil did or did not settle after pile driving.

Although the degree of restraint against settlement afforded by the piles depends (among other things) on the physical properties of the clay penetrated, such restraint has been observed to occur in some of the softest of soils. At LaGuardia Field, in New York, N. Y., for example, where the soft organic silt is approximately 60 ft thick, settlements of the order of 5 ft have been observed since 1937 when about 20 ft of ash fill was placed over much of the site. On the other hand, in areas where structures had been supported on end bearing piles penetrating the fill and mud and supported in the underlying sand, observed settlements between the piles have been of the order of 1.5 ft for the same period. Obviously, it cannot be concluded that, if the structures had been built on friction piles supported in the organic silt, settlements of the lower order would have resulted, or that friction piles would be beneficial to the situation.

Neither the evidence of Fig. 4 nor the evidence of the writers' frequent observations supports the statement (see "Conclusions") that: "* * * the region of disturbance is limited to a zone within a few inches of the pile and the main volume of the clay mass is apparently undisturbed." As early as 1915, Karl Zimmerman[39] reported on the influence of pile size and shape on dis-

[39] "Die Rammwirkung im Erdreich," by Karl Zimmerman, *Versuche auf neuer Grundlage*, Berlin, 1915.

turbance to the surrounding soil, and pointed out that both factors are influenced by the type of soil involved. In varved soils where the distortion of the soil may be readily seen it is not uncommon to observe severely disturbed zones extending at least a diameter beyond the face of the piles.

In most instances the observed effects of driving piles into soft clay formations are more pronounced than stated by the authors. The disturbance exhibited in Fig. 31 was a matter of considerable concern in one such instance

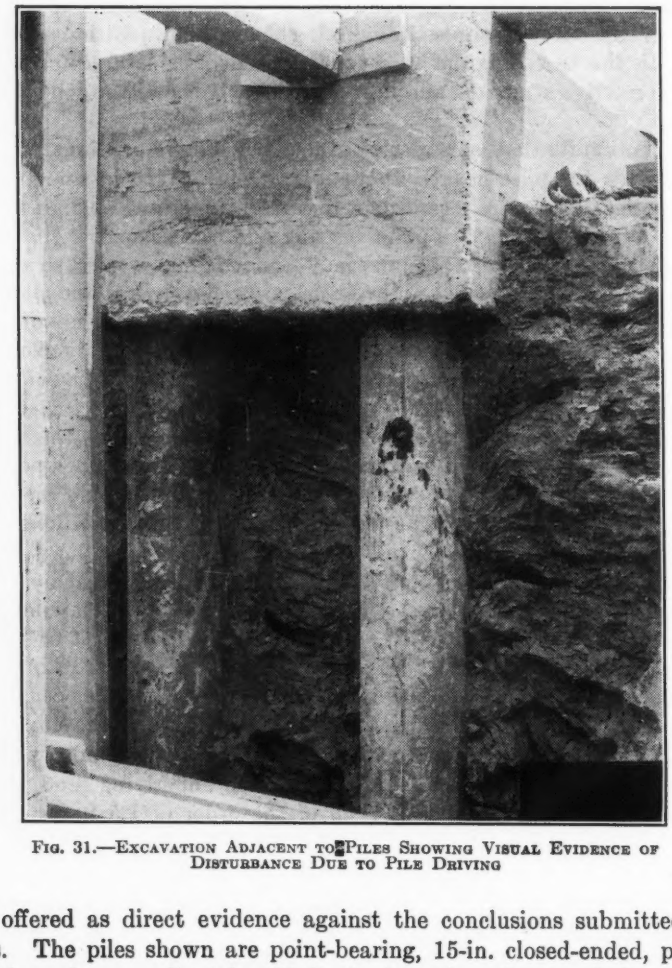

FIG. 31.—EXCAVATION ADJACENT TO PILES SHOWING VISUAL EVIDENCE OF DISTURBANCE DUE TO PILE DRIVING

and is offered as direct evidence against the conclusions submitted by the authors. The piles shown are point-bearing, 15-in. closed-ended, pipe piles, driven through approximately 100 ft of relatively soft varved clay, of glacial origin, into an underlying compact sand and gravel stratum. The structure supported by the piles is shown in plan in Fig. 32 and may be described as a heavy ornamental type of building. Its entire weight, with the exception of the ground floor partitions and slab, is carried by the piles. It was considered

unnecessary to support either the ground floors or the partitions since they imposed no additional weight on the underlying formation because it was necessary to excavate more than their weight in soil to reach the grade established for the floors. The general grades of the ground surface and floor, together with the soil formations, are shown in Fig. 33. The piles are on a considerably wider spacing than those described by the authors; and the footings are spaced 10 ft on centers along the foundation walls.

Piles were driven from June to August, 1940, and the ground floor was laid in November and December, 1940. Shortly before the building was completed and ready for occupancy, cracks appeared in the ground floor parti-

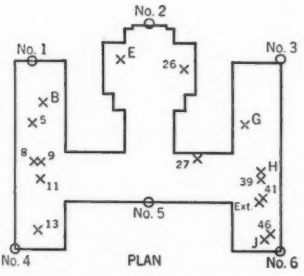

FIG. 32.—PLAN SHOWING LOCATION OF BORINGS AND SETTLEMENT OBSERVATION POINTS IN FLOOR

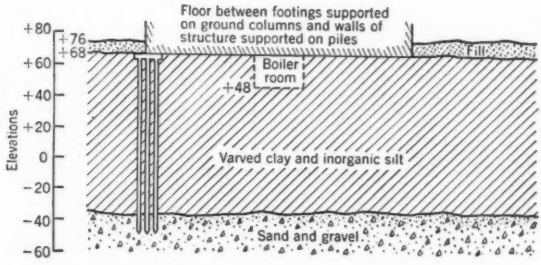

FIG. 33.—COMPOSITE VERTICAL SECTION OF SOIL UNDERLYING BUILDING

tions and slab and it was found that the ground between the pile clusters was settling. The settlements could be traced to no other cause than the disturbance of the soft varved clay produced by driving pipe piles through this formation.

As a temporary solution, underfloor grouting or "mud jacking" was done and holes were drilled through the floor in August, 1941, for the purpose of establishing settlement observation points in the surface of the underlying varved clay bed. The locations of these observation points are shown in Fig. 33, and the settlements that were observed are plotted against the square root of elapsed time in Fig. 34. Because of the straight-line relationship so established it was possible to estimate, for comparison with observed settlements in the floor, the amount of settlement previous to the installation of the settlement observation points. These settlements occurred in spite of an actual net decrease in load on the underlying clay formation that was responsible for the settlements.

Conclusions.—The writers believe that the authors' conclusions regarding the effect of driving piles into soft clays are consistent neither with the data presented, nor with current experience, for the following reasons:

1. The conditions investigated by the authors are not analogous to the situation in which friction piles have been supported in clay;

2. Had the piles in this case been supported by friction in the clay bed, settlement of both the piles and the surrounding ground would have occurred;

3. Laboratory test data submitted by the authors, and their own statements, indicate a loss of strength in the clay both adjacent to and between the driven piles;

4. Illustrations presented by the authors indicate some disturbance of the soil even in "undisturbed" samples, and great disturbance in the samples secured from the region adjacent to the piles;

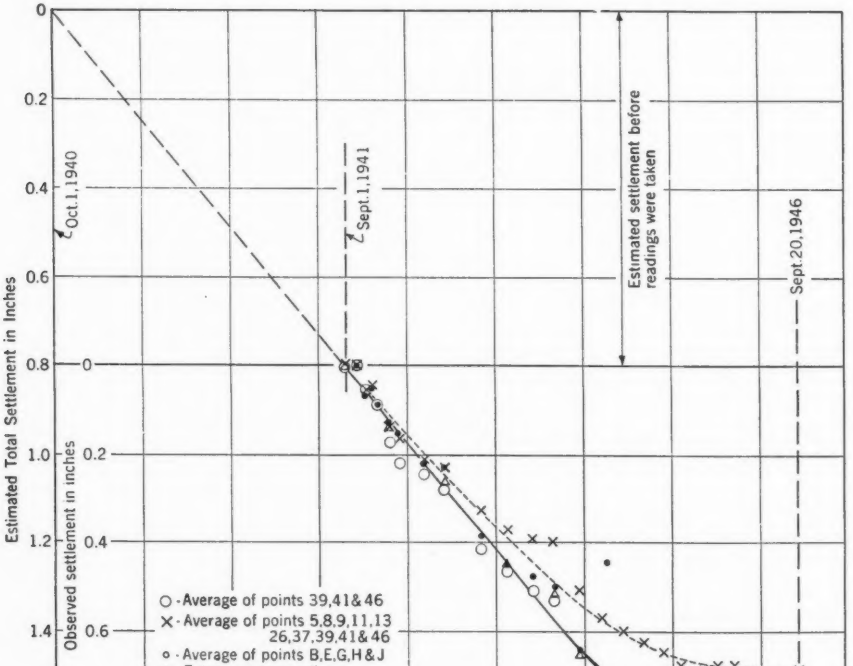
Estimated Total Settlement in Inches
Observed settlement in inches
Square Root of Time in Months
Oct.1,1940
Sept.1,1941
Estimated settlement before readings were taken
Sept.20,1946
○ - Average of points 39,41&46
× - Average of points 5,8,9,11,13 26,37,39,41&46
o - Average of points B,E,G,H&J
△ - Extensometer readings

FIG. 34.—SETTLEMENTS INDUCED BY REMOLDING RESULTING FROM PILE DRIVING

5. The data presented in no way contradict the original contentions of Mr. Casagrande[4] regarding the remolding effect of piles driven into soft clay; and

6. To substantiate the authors' conclusions more borings and more laboratory tests are required, including tests of the soil midway between piles. The simple level observations required to prove the settlement or nonsettlement of the ground surface should be included in any further similar investigations.

AMERICAN SOCIETY OF CIVIL ENGINEERS

Founded November 5, 1852

DISCUSSIONS

MODERN CONCEPTS APPLIED TO CONCRETE AGGREGATE

Discussion

BY HERBERT K. COOK, THOMAS B. KENNEDY, AND BRYANT MATHER

HERBERT K. COOK,[3] THOMAS B. KENNEDY,[4] AND BRYANT MATHER.[5]—The paper by Mr. Blanks, describing the extremely interesting studies of concrete aggregate which have been made in recent years by the Bureau of Reclamation, United States Department of the Interior, is a valuable contribution to concrete research and will be studied by workers in this field for many years. The emphasis that he has placed on the importance of studying aggregate materials as components of concrete rather than as isolated unconfined rock and mineral particles is perhaps the most important concept developed from recent research on aggregates. The importance of this approach has been recognized by the Concrete Research Division of the Waterways Experiment Station (Clinton, Miss.), and its work likewise has been directed toward developing suitable procedures for evaluating materials in accordance therewith. The automatic accelerated freezing-and-thawing apparatus for concrete which was described in 1945 (39)(40)[5a] was recommended as a method of testing aggregate, among other reasons, "because it permits materials for concrete to be tested in concrete" (39*a*). It is suggested, however, that in emphasizing this point and stating that "* * * experience shows that good rocks do not always produce superior concrete, and weak rocks do not always cause deterioration," Mr. Blanks may have implied, more strongly than the data permit, that the reverse is frequently true. The reviews of the significance of the standard tests of aggregates (41)(42) suggest that, in the absence of information such as revealed by the more recently developed procedures discussed by Mr. Blanks, the standard tests will generally provide a satisfactory method of separating good aggregates from bad aggregates. Also, as stated by Harold S. Sweet, Jun. ASCE (42*a*): "* * * it is pertinent that these classical tech-

NOTE.—This paper by R. F. Blanks was published in April, 1949, *Proceedings*.

[3] Chf., Concrete Research Div., Waterways Experiment Station, Clinton, Miss.

[4] Chf., Physical Test Branch, Concrete Research Div., Waterways Experiment Station, Clinton, Miss.

[5] Chf., Special Investigations Branch, Concrete Research Div., Waterways Experiment Station, Clinton, Miss.

[5a] Numerals in parentheses, thus: (39), refer to corresponding items in the Bibliography (see Appendix of the paper and at the end of the discussion in this issue).

niques be recognized in that they may serve as guides for further aggregate research."

In his discussion of the effects of thermal expansivity of aggregates on concrete, Mr. Blanks has suggested that great differences in the thermal coefficient between aggregate particles and cement paste may cause failure in concrete. Studies conducted at the Concrete Research Division have suggested that such differences, when considered as occurring between coarse aggregate particles and the mortar matrix of the concrete, may provide a more useful index than is provided by considerations of aggregate-cement paste relationships. A large number of studies, involving determinations of the linear coefficient of thermal expansion of rocks used as coarse aggregates and of cement mortars containing different natural and manufactured sands as fine aggregate, and accelerated freezing and thawing tests of concretes composed of such coarse aggregate-mortar combinations, have provided the basis for statistical analysis which has yielded a strong inverse correlation between thermal coefficient differences and resistance of concrete to accelerated freezing and thawing. The results of this study have not been published in detail but are mentioned briefly in the papers by J. R. Gilbert (43) and Bryant Mather (44). Mr. Gilbert has stated (43*a*).

> "It must be concluded, therefore, that a large difference between these coefficients [of expansion of the coarse aggregates and mortars] should be avoided since the stresses set up at the interfaces of coarse aggregate particles and mortar can be sufficient to cause loss of bond and cracking from the interface which will eventually destroy watertightness in hydraulic structures."

Mr. Blanks has stated that specific heat and heat conductivity of aggregates strongly affect the rate of temperature change in concrete and the rate at which heat is transmitted through concrete. He then states that these factors are of limited significance for small structural members. In an investigation conducted at the Concrete Research Division (45) it was found that differences in thermal diffusivity between coarse aggregate and mortar appeared to be responsible for differences in resistance of concretes to accelerated freezing and thawing.

Mr. Blanks' discussion of alkali-aggregate reaction is extremely interesting and valuable particularly in view of the fact that his laboratory has, perhaps, done more work in this field than any other. His statement (under the heading, "Research on Concrete Aggregates: Research on Alkali-Aggregate Reaction"):

> "Acid to intermediate volcanic rocks are present in some of these areas and, where significant quantities of these rocks have been used as aggregate in combination with high-alkali cements, deterioration caused by alkali-aggregate reaction is certain to occur."

—appears, however, to be somewhat more positive and inclusive than the data warrant. It is believed that more than an editorial modification would be involved if this statement were changed so that it would read

> "Acid to intermediate volcanic rocks, containing significant quantities of siliceous volcanic glass, are present in some of these areas and, where significant quantities of these rocks have been used as aggregate in combination with high-alkali cements, deterioration caused by alkali-aggregate reaction may be expected to occur."

The sentence should also be qualified by a further statement, such as the following which is taken from a previous paper (46)(46*a*):

> "The possibility that the expected reaction will not occur or that it may be forestalled—as a result of proper attention to the chemical composition of the cement, the use of an inhibitor, the fact that the deleterious constituent is present in an amount much greater than or much less than the 'pessimum' amount, or the favorable location and exposure of the structure, should always be borne in mind * * * However, in the present state of our knowledge these are mere possibilities—none can be counted on to give a safe guarantee of freedom from trouble if reactive materials are in the aggregate."

What is sorely needed by the materials-testing profession is a series of accelerated performance tests to evaluate the behavior of proposed aggregates in concrete. One such test is the accelerated freezing-and-thawing test previously referred to in this discussion. Another is a nonfreezing weathering test, by which the influences of temperature and moisture-content changes could be studied. A number of combinations of influences such as alternate wetting and drying, alternate heating and cooling, and more complex conditions (such as heating-wetting with cooling-drying and heating-drying with cooling-wetting appear to play an important part in the deterioration of concrete. Aggregates that will produce concrete of satisfactory durability when exposed to a nonfreezing natural environment, such as is found in the southern United States, may not produce satisfactory concrete if exposed to freezing and thawing.

C. H. Scholer, M. ASCE (47), has been pioneering in the development of nonfreezing testing techniques for concrete. The Concrete Research Division and the division concrete laboratories of the Corps of Engineers have developed equipment which shows great promise in testing the aggregates, or cement, in concrete, under the influences of heating-wetting with cooling-drying and of heating-drying with cooling-wetting.

The device described by Mr. Blanks for measuring the rate of evaporation from saturated specimens and the force associated with capillary movement of water into the material has promise of becoming a valuable tool in helping to find the reasons for the lack of durability exhibited by some materials. In its present state of development the device appears to have the limitation of being used with only a relatively small specimen (1.5 in. in diameter and 1 in. thick). Although the results obtained from such tests may be valid when the specimen is representative of a material of constant pore characteristics, the interpretation of the data obtained by testing specimens from a heterogeneous gravel deposit or quarry, or from concrete specimens containing such materials, rapidly becomes more complex; and the usefulness of the data in terms of establishing an index of durability for such materials becomes a matter of the

adequacy of the sampling and the number of tests made. The question is also raised as to the validity of application of the data obtained on a specimen of the size used in the test to mass concrete containing aggregate 6 in. in size.

The writers agree with the statements made by Mr. Blanks in the "Conclusions" that, at the present state of knowledge of the evaluation of concrete aggregates, the petrographic examination may serve to establish the testing program necessary for each aggregate. The petrographic examination, for example, would be valuable in determining the number of pressure-deficiency tests which might be required in the investigations of the heterogeneous materials referred to in the preceding paragraph.

The general acceptance of air entrainment in concrete may eventually lead to a general overhauling of current concepts of aggregate suitability and method of aggregate testing; also, the increasing use of manufactured sand with crushed stone as aggregate for concrete may necessitate modifications of present-day concepts of what are suitable gradations and test limitations.

Bibliography.—

(39) **"Automatic Accelerated Freezing-and-Thawing Apparatus for Concrete,"** by Charles E. Wuerpel and Herbert K. Cook, *Proceedings*, A.S.T.M., Vol. 45, 1945, p. 813. (*a*) p. 823.

(40) **Automatic Accelerated Freezing-and-Thawing Apparatus for Testing the Durability of Concrete and Concrete Materials,"** by Herbert K. Cook, *Bulletin No. 30*, Waterways Experiment Station, Vicksburg, Miss., 1947, p. 19.

(41) **"Report on Significance of Tests of Concrete and Concrete Aggregates,"** A.S.T.M., 1943, p. 92.

(42) **"Physical and Chemical Tests of Mineral Aggregates and Their Significance,"** by Harold S. Sweet, *Special Technical Publication No. 83*, A.S.T.M., 1948, p. 49. (*a*) p. 69.

(43) **"The U. S. Corps of Engineers Approach to More Durable Concrete,"** by Jesse R. Gilbert, *The Crushed Stone Journal*, June, 1949, p. 3. (*a*) p. 8.

(44) **"The Testing of Aggregates in Air-Entrained Concrete,"** by Bryant Mather, *Bulletin No. 30*, Waterways Experiment Station, Vicksburg, Miss., 1947, p. 41.

(45) **"A Study of the Influence of Thermal Properties on the Durability of Concrete,"** by Albert Weiner, *Proceedings*, A.C.I., Vol. 43, 1947, p. 997.

(46) **"Petrographic Identification of Reactive Constituents in Concrete Aggregate,"** by Bryant Mather, *Proceedings*, A.S.T.M., Vol. 48, 1948, p. 1120. (*a*) p. 1122.

(47) **"A Wetting-and-Drying Test for Predicting Cement-Aggregate Reaction,"** by C. H. Scholer, *ibid.*, Vol. 49, 1949 (1949 Preprint No. 46, June, 1949).

AMERICAN SOCIETY OF CIVIL ENGINEERS

Founded November 5, 1852

DISCUSSIONS

AN ENGINEERING CONCEPT OF FLOW IN PIPES

Discussion

BY RALPH W. POWELL, J. C. STEVENS, GEORGE A. WHETSTONE, G. H. HICKOX, AND JAMES F. HALSEY AND WILLIAM M. OWEN

RALPH W. POWELL,[25] M. ASCE.—To present the more recent knowledge regarding the loss of head in pipes, in a form that the practicing engineer can understand and use, is most commendable. The writer finds much in the paper with which he is in entire agreement including several worthwhile original ideas. The point that old experiments contained many more values at low velocities than at high velocities, and that this led to the notion that f always decreased with increasing velocity, is very good. Fig. 5 certainly shows the short-comings of the "exponential" formulas that resulted.

The explanation as to why the "dip" at the transition from smooth to rough pipe flow, which J. Nikuradse found with uniform roughness, does not occur in "natural" pipes, is praiseworthy; but, the author's idea that most pipes with which engineers deal are like the pipes in Tables 1 and 3, is questionable. Apparently these pipes reported in the paper had roughness particles of varying sizes, but with the variation very uniformly distributed along the length. As the author shows, this leads to a sudden change from smooth pipe flow to rough pipe flow at a certain critical Reynolds number, which is simultaneous throughout the pipe. Mr. Harris points out that, if certain reaches of the pipe are rougher than others, the total drop in head for the entire length will indicate a friction, f, intermediate between the f-values of the separate reaches, and therefore will show a transition such as found by C. F. Colebrook.[26] Assuming that this is the correct explanation, many pipes used in water supply and other fields must then have this unequally distributed roughness because the experiments of John R. Freeman,[27] Past-President and Hon. M. ASCE, and many

NOTE.—This paper by Charles W. Harris was published in May, 1949, *Proceedings*. Discussion on this paper has appeared in *Proceedings*, as follows: September, 1949, by E. L. Harrington.

[25] Prof. of Mechanics, Ohio State Univ., Columbus, Ohio.

[26] "Turbulent Flow in Pipes, with Particular Reference to the Transition Region Between the Smooth and Rough Pipe Laws," by C. F. Colebrook, *Journal*, Inst. C. E., Vol. 11, 1938–1939, pp. 133–156.

[27] "Experiments Upon the Flow of Water in Pipes and Pipe Fittings Made at Nashua, New Hampshire, June 28 to October 22, 1892," by John R. Freeman, A.S.M.E., New York, N. Y., 1941.

others show such a transition. It seems, therefore, that engineers should be conservative and use graphs[28,29] based on Mr. Colebrook's transition—

$$\frac{1}{\sqrt{f}} = 1.74 - 2\log_{10}\left(\frac{2\epsilon}{D} + \frac{18.7}{\mathbf{R}\sqrt{f}}\right) \ldots\ldots\ldots\ldots\ldots (7)$$

—for naturally roughened pipe, until this transition region has been investigated further. (In Eq. 7 ϵ represents the equivalent sand size roughness, originally called k by Mr. Nikuradse, and must be in the same units as D.)

If ϵ in Eq. 7 is made equal to zero, Eq. 7 becomes the Nikuradse formula for smooth pipes. Eq. 1 is in remarkable agreement with this formula for all values of **R** from 36,000 to 3,000,000, the maximum difference in the value of f by the two formulas being 0.0002; but they begin to deviate rapidly for higher values of **R**. The author states that the present knowledge extends only to a Reynolds number equivalent to a velocity of 5 ft per sec in an 8-ft pipe, which at 58° F gives a Reynolds number of 3,200,000; but Fred C. Scobey,[18] M. ASCE, has reported tests on the Ontario Power Tunnel at Niagara Falls in Canada at 20 ft per sec and in 18-ft-diameter pipe. Assuming a temperature of 55° F, this gives a Reynolds number of 27,500,000 and f was found to be 0.00694. The Nikuradse formula gives 0.00703 and the Harris formula, 0.00792. Therefore, Eq. 1 should not be used for Reynolds numbers greater than 3,000,000 and, since a graph will be ordinarily used rather than a formula, it would seem that the Nikuradse formula is the best. Fig. 15 gives a plotting of Mr. Nikuradse's formula in the middle part of the range. If an algebraic formula is desired, the writer suggests

$$f = 0.0049 + \frac{0.42}{\mathbf{R}^{0.3}} \ldots\ldots\ldots\ldots\ldots\ldots\ldots (8)$$

The author seems troubled by the fact that the Nikuradse formula gives a zero value of f for an infinite value of **R**. There is something logically disturbing in this fact, but when one computes that it is necessary to go up to a Reynolds number of about five hundred million to bring f down to 0.005, and to nearly a million million to bring it down to half that amount, the practical engineer need not be greatly worried.

The derivation of Eq. 3 is based on the assumption that the "index" velocity, V_t, which divides smooth pipe flow from rough pipe flow, is the same for all diameters of pipe as long as the absolute roughness remains the same. This fact, according to the author, was shown "substantially" by the experiments listed in Table 3—that is, the "breakaway point" came at "somewhat less than 4 ft per sec." In Eq. 7, let $\mathbf{R} = \infty$ and divide by 2, then:

$$\frac{1}{2\sqrt{f}} = 0.87 - \log_{10}\frac{2\epsilon}{D} \ldots\ldots\ldots\ldots\ldots\ldots (9a)$$

[28] "Friction Loss in Pipes," by Ralph W. Powell, *Experiment Station News*, Ohio State Univ., Columbus, Ohio, April, 1946, p. 16.

[29] "Elementary Fluid Mechanics," by Hunter Rouse, John Wiley & Sons, New York, N. Y., 1946, p. 211.

[18] "The Flow of Water in Concrete Pipe," by Fred C. Scobey, *Bulletin No. 852*, U.S.D.A., Washington, D. C., 1924, p. 95.

which is Mr. Nikuradse's equation for rough pipes. On the other hand, making $\epsilon = 0$ and simplifying,

$$\frac{1}{2\sqrt{f}} = \log_{10} \mathrm{R}\sqrt{f} - 0.40 \quad \ldots\ldots\ldots\ldots\ldots\ldots (9b)$$

which is the Nikuradse equation for smooth pipes. Solving Eqs. 9 simultaneously to determine the critical point where smooth pipe flow changes to rough pipe flow if there is no transition,

$$\mathrm{R}_t = \frac{9.31\ \mathrm{D}}{\epsilon\sqrt{f}} \quad \ldots\ldots\ldots\ldots\ldots\ldots\ldots (10a)$$

or

$$V_t = \frac{9.31\ \nu}{\epsilon\sqrt{f}} \quad \ldots\ldots\ldots\ldots\ldots\ldots\ldots (10b)$$

Hence, with constant absolute roughness and viscosity, V_t varies inversely as the square root of f. Thus, if V_t is 3.50 ft per sec for the 1-in. pipe in Table 3, it would be $3.50\sqrt{0.0247/0.0360} = 2.90$ ft per sec for the ¼-in. pipe and $3.50\sqrt{0.0247/0.0183} = 4.06$ ft per sec for the 4-in. pipe. This is too much variation to be ignored. From this point of view Eq. 4 changes to

$$V_{t2} = \nu\left(\frac{0.55}{f_1 - 0.0061}\right)^3\sqrt{\frac{f_1}{f_2}} \quad \ldots\ldots\ldots\ldots\ldots\ldots (11)$$

J. C. STEVENS,[30] PAST-PRESIDENT, ASCE.—The writer is glad to find that the old and tried Chezy formula still has a champion. In this phase of hydraulics much confusion has resulted from the use of many exponential formulas, some of which have become so entrenched in current thinking that it will be difficult to eradicate them, but eradicate them we must if progress is to be made. Empiricism must give way to rationality and the complex concept to the simpler concept.

Of special interest to the writer were the head measurements in Table 1 wherein differential water levels were determined to 0.00037 ft. Such refinement is not at all impossible; remote registering instruments in which water surfaces are recorded within an error of ±0.006 in. (0.0005 ft) by electronic probes have been specified for the Waterways Experiment Station at Vicksburg, Miss. The probe system itself is sensitive to 0.002 in.

It is the twilight zone between nonturbulent flow and fully turbulent flow that has given rise to these many exponential formulas. For nonturbulent flow, wherein lost head varies with the first power of the velocity and the velocity distribution is parabolic, the Poiseuille formula is mathematically correct and needs no empirical coefficients. For fully turbulent flow, the Darcy-Weisbach variation of the fundamentally correct Chezy formula has extreme simplicity in its favor. The use of a specific friction factor which

[30] Cons. Engr. (Stevens & Koon), Portland, Ore.

depends solely on roughness and is independent of pipe diameter is a novel concept. If it was originated by the author he surely deserves signal credit for it. The next step follows logically; the friction factor for the particular pipe in question is readily found from the specific friction factor and the pipe diameter. It may be obtained directly from Fig. 17.

The imperfect or partial turbulent phase embraces most of the pipe flows in actual use. It is the transitional nature of flow in pipes that has given rise to so many empirical exponential formulas that are applied quite indiscriminately, far beyond the limits of the experimental data on which they are based. This can readily become a most inaccurate expedient, as illustrated in Fig. 5, for values beyond the velocity that indexes fully turbulent flow. This example, however, appears to be an extreme case.

TABLE 4.—LOST HEAD h_f IN ONE THOUSAND FEET OF NEW CAST-IRON PIPE

Line	Authority	Lost head, h_f, in feet,[a] equals:	INSIDE DIAMETERS, D, IN INCHES		
			12	36	36
1	....	Velocity, in feet per second	3.0	2.0	10.0
2	Williams-Hazen...	$\left(\frac{V}{1.318 \times 130 \times r^{0.63}}\right)^{1/0.54}$	2.8	0.36	7.3
3	Tutton.....	$\left(\frac{V}{140\, r^{0.65}}\right)^{1/0.51}$	3.2	0.31	7.3
4	Unwin.....	$0.0215 \frac{L}{D^{1.156}} \frac{V^{1.95}}{2g}$	2.8	0.36	8.1
5	Scobey[b].....	$\frac{V^2}{0.345^2 D^{1.25}}$	3.4	0.37	9.25
6	Barnes.....	$0.000343 \frac{L}{D^{1.172}} V^{1.953}$	2.9	0.37	8.5
7	Lea.....	$0.00036 \frac{L}{D^{1.25}} V^{1.93}$	3.0	0.35	7.8
8	Manning.....	$2.87 \times 0.012^2 \times \frac{L}{D^{4/3}} V^2$	3.7	0.38	9.5
9	Harris.....	$f \frac{L}{D} \frac{V^2}{2g}$	3.2	0.37	9.25
10	Percentage range of diversion from the Harris formula		0 to +15	0 to −16	0 to −21

[a] In addition to the notation of the paper, r = radius = $D/2$. [b] For smooth pipe.

The writer was mildly surprised to find that for the velocity ranges normally encountered in engineering practice the many formulas give results not too far apart for a given pipe. To satisfy his curiosity in this regard he tabulated the flow for eight formulas for new cast-iron pipe, two diameters, and three velocities. The results are give in Table 4. The percentage range of divergence from the Harris formula (line 9, Table 4) is compared in line 10, Table 4.

GEORGE A. WHETSTONE,[31] Assoc. M. ASCE.—Under the heading, "Artificial Roughness Versus Natural Surfaces: Uniform Sand Grains," the author states:

> "Since the tendency to dip occurs at higher velocities for the smaller elements, it follows that only when many roughness elements are of one size does the dip become perceptible * * *."

With this statement and its elucidation the author has resolved the long-standing conflict between the painstaking and undeniably accurate work of Mr. Nikuradse, and its equally obvious failure to accord with experience on commercial pipe.

In addition to this fundamental contribution to the basic understanding of flow, the author has rendered a service to engineering by his consolidation of known results, by his establishment of a criterion (his value of R_t) for the transition point to purely turbulent flow, and by his discovery of the "specific roughness coefficient."

Without commenting on the relative merits of Eq. 1 and the more usual Blasius expression for this range (a close examination of the experimental data being necessary to do this justly), it would seem to the writer that the author's pattern of reorganization and simplification of pipe friction data into three lines on a ($\log f - \log R$)-graph, two of them universal and the other a horizontal line with its ordinate depending on the specific roughness coefficient, deserves to become the standard in engineering practice. It may be that the factor 0.0061 or some of the values of f_1 in the tabulation under the heading, "Diagrams for Smooth and Rough Pipes: Specific Roughness Coefficients for Pipes," may be subject to change under closer scrutiny; that is a small matter. The important thing is that designers now have a definite rational basis for the engineering treatment of pipe friction.

G. H. HICKOX,[32] M. ASCE.—In promoting the use of the Weisbach formula for head loss in fluid flow, as opposed to empirical formulas, Mr. Harris has done the engineering profession a service. The empirical formulas are based on experiments covering a limited range of flow conditions; and, although they are undoubtedly correct within this range, they are not correct when extrapolated far beyond it. For this reason the use of the Weisbach formula with friction coefficients depending on the type of surface and the Reynolds number should be encouraged. However, there are a number of items in the paper with which the writer disagrees. Although some of these undoubtedly result from personal viewpoints, others seem to be of such fundamental importance as to warrant discussion.

The author's concept of viscosity does not appear to be in harmony with the kinetic theory. Since viscosity is that property of a fluid which enables it to transmit a shearing stress, the supposition of a fluid resistance existing in a fluid of zero viscosity, or of zero shear, is simply a contradiction of terms. The "mechanical interlocking" at the wall is merely momentum exchange

[31] Associate Prof., Dept. of Civ. Eng., Texas Technological College, Lubbock, Tex.
[32] Associate Director, Eng. Experiment Station, Univ. of Tennessee, Knoxville, Tenn.

caused by molecular activity. The concept of zero viscosity implies the complete absence of momentum interchange by molecular action; and, consequently, the complete absence of shearing resistance, both in the interior of the fluid and at the boundary. Accordingly, the concept of a zero friction factor at an infinite Reynolds number caused by zero viscosity is not at all inconsistent.

Furthermore, Eq. 1 is not supported by actual test data. Reference is made to data for a bituminous-coated steel pipe presented by the writer[33] in which f was about 0.0082 at a Reynolds number of 10,000,000. Eq. 1 yields $f = 0.0087$. Reference is also made to the data presented by J. N. Bradley, Assoc. M. ASCE, and S. P. Wing,[34] M. ASCE, which show values of f for the tunnel of the Ontario Power Company at Niagara Falls in Canada, a tunnel of a power plant at Livenza, Italy, and the conduit of Englewood Dam in Ohio. The Reynolds number for all these data ranges between 3,000,000 and 40,000,000. The values of f are lower than those given by Eq. 1 but are in substantial agreement with the von Kármán-Prandtl smooth pipe curve.

It is difficult to understand the author's conclusion that complete turbulence exists as soon as the condition for smooth pipe flow is no longer fulfilled. To arrive at this conclusion, it is necessary to ignore the work of J. Nikuradse,[35] of C. F. Colebrook[26] and C. M. White,[36] and of the writer.[33] Test data presented by each of these indicate a zone between the region of smooth pipe flow and that of complete turbulence where the friction is not constant, but varies according to some law not yet fully understood.

The author's statement (under the heading, "General Principles") that "* * * viscosity plays no part in the loss of head in the fully turbulent flow most frequently encountered in moderately rough pipes and channels" is somewhat misleading. The flow most frequently encountered is not fully developed turbulence with a constant friction factor. Most of the test data presented by the many experimenters in the field of fluid friction show a friction factor f varying with Reynolds number. This result holds true for all the empirical formulas in which the exponent of the velocity is other than 2. Most of the empirical formulas that have been presented are correct for the data on which they were based, and to dismiss them as inadequate because they do not represent a constant factor is at least arbitrary. It is quite possible to accept these equations for what they are, explaining their divergences, and assigning them their proper place in the general field of pipe friction knowledge.

The author also states (under the heading, "Rough Pipes of Same Material and Various Diameters: Open Channels in Relation to Closed Pipes") that: "Hydraulic radius is not used for pipes because it is an unsatisfactory correlating factor." Throughout the paper he has used diameter for correlating

[33] "Friction Coefficients in a Large Tunnel," by G. H. Hickox, A. J. Peterka, and R. A. Elder, *Transactions*, Vol. 113, 1948, pp. 1027–1046.

[34] *Ibid.*, p. 1066.

[35] "Laws of Fluid Flow in Rough Pipes," by J. Nikuradse, English translation in *The Petroleum Engineer*, March, 1940, pp. 164–166; May, 1940, pp. 75, 78, 80, and 82; June, 1940, pp. 124, 127–128, and 130; July, 1940, pp. 38, 40, and 42; and August, 1940, pp. 83–84 and 87.

[36] "Reduction of Carrying Capacity of Pipes with Age," by C. F. Colebrook and C. M. White, *Journal* Inst. C. E., No. 9, 1937–1938, pp. 381–399.

pipe flows; and, since the hydraulic radius of a pipe is simply one fourth of its diameter, it is equally as good a correlating factor.

The author would be helpful if he explained how to differentiate between a series of localized losses and a rough pipe. If the writer's understanding of the paper is correct, a smooth pipe may become a rough pipe if there are enough localized disturbances. The dividing line between these two concepts is not clear.

JAMES F. HALSEY,[37] JUN. ASCE, AND WILLIAM M. OWEN.[38]—A simplifying unification, in Mr. Harris' opinion, of existing methods of analyzing flow in closed conduits has been presented in this paper. The author's concept of this problem, in which three distinct types of flow are characterized by straight line functions of friction factor, f, versus the Reynolds number, **R**, on a logarithmic plot, as shown in Fig. 18, can be examined further in the light of additional data not included in the paper.

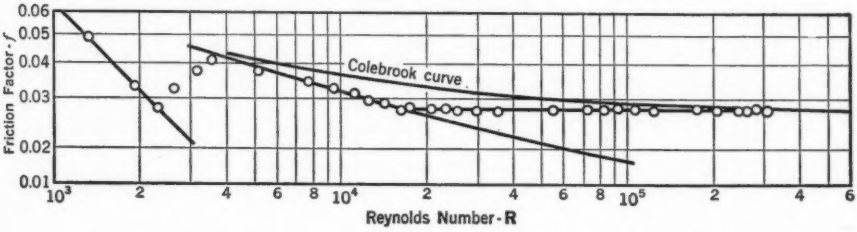

FIG. 18.—FRICTION FACTORS FOR THREE TYPES OF FLOW IN A 2-IN. STEEL PIPE

The three modes of flow represented in Fig. 18—those of nonturbulent or laminar flow, partly turbulent flow, and fully turbulent flow—were first noted by J. Nikuradse[39] and are now generally accepted by the profession. (The limits of the three types in Fig. 18 are up to **R** = 2,000, from **R** = 2,000 to **R** = 16,200, and greater than **R** = 16,200, respectively.) As stated by the author, nonturbulent or laminar flow is subject to rational analysis, partly turbulent flow is governed by the smooth pipe law which has been well established experimentally, and full turbulence is characterized by a constant friction factor.

The author's experimental evidence indicates that these three types of flow were obtained in 2-in. and 4-in. pipes. However, his data show an abrupt transition from partial turbulence (that is, smooth pipe curve) to full turbulence (that is, constant f).

This manner of transition does not agree with the published work of C. F. Colebrook,[26] Hunter Rouse,[40] M. ASCE, and Lewis F. Moody,[41] all of whom present a gradual transition curve between partial and full turbulence ex-

[37] Research Asst. Prof. of Fluid Mechanics, Univ. of Illinois, Urbana, Ill.

[38] Research Asst. Prof. of Theoretical and Applied Mechanics, Univ. of Illinois, Urbana, Ill.

[39] *Forschungsheft*, Verein Deutscher Ingenieure, No. 361, 1933.

[40] "Evaluation of Boundary Roughness," by Hunter Rouse, *Proceedings*, 2d Hydraulics Conference, *Bulletin No. 27*, Univ. of Iowa Studies in Eng., Iowa City, Iowa, 1943.

[41] "Friction Factors for Pipe Flow," by Lewis F. Moody, *Transactions*, A.S.M.E., Vol. 66, 1944, p. 671.

tending over a considerable range of the Reynolds number. The Colebrook function[26]—

$$\frac{1}{\sqrt{f}} = -2 \log \left(\frac{k}{3.7\,D} + \frac{2.51}{\mathbf{R}\sqrt{f}} \right) \ldots\ldots\ldots\ldots\ldots\ldots (12)$$

(in which k is the wall particle size and the other terms are as previously defined)—was plotted in Fig. 18 to show the generally accepted gradual transition from partial to full turbulence. The value of k/D (the relative roughness factor, in Eq. 12) was determined by substitution of the averages value of $f = 0.0278$ as obtained from values greater than $\mathbf{R} = 16{,}200$ in Table 1 in the von Kármán-Prandtl equation—

$$\frac{1}{\sqrt{f}} = 2 \log 3.7 \frac{D}{k} \ldots\ldots\ldots\ldots\ldots\ldots\ldots\ldots (13)$$

—for fully developed turbulent flow in rough pipes. It will be noted that the Colebrook function as applied to the author's data does not agree with the straight line curve used by the author until a Reynolds number of more than 300,000 is approached. This finding is consistent with those of other investigators—namely, Mr. Rouse,[40] who shows full turbulence to be developed when

$$\frac{\mathbf{R}\sqrt{f}}{D/k} = 200 \ldots\ldots\ldots\ldots\ldots\ldots\ldots\ldots (14)$$

When applied to the author's data for a 2-in. pipe, Eq. 14 gives $\mathbf{R} = 321{,}000$ as the point at which full turbulence may be expected to be developed.

Since the author's data and curves did not agree with other investigations,[26,40,41] the writers undertook to clarify the 2-in. pipe curves by making tests on a 30-ft section of moderately rusty 2-in. steel pipe. This pipe has been in place in the Hydraulics and Fluid Mechanics Laboratory at the University of Illinois in Urbana since 1928. The test section was preceded by a straight section 28 ft long and followed by another straight section with a minimum length of 60 ft. The head loss was measured with a 5-ft differential gage using mercury, carbon tetrachloride, or a mixture of carbon tetrachloride and gasoline (specific gravity, 1.067) as the gage fluid. Test runs were overlapped so that any error in reading small gage differences with a heavy gage fluid was compensated for by large differences with a lighter gage fluid. The discharge was measured by weight, with a filling time of 3 min or longer for nearly all runs. The results of these tests are plotted as Fig. 19.[41a]

An abrupt change from partial to full turbulence, such as the author obtained, is not present in Fig. 19. A few minor deviations appear, but it is believed that these may be attributed to experimental error. From values of $\mathbf{R} = 334{,}500$ to $\mathbf{R} = 465{,}000$, the friction factor, f, has a range of only 1% from the average value of $f = 0.0256$ for full turbulence (see Table 5).

[41a] For a copy of these tests data address the writers at 121 Talbot Laboratory, Univ. of Illinois, Urbana, Ill.

Using the value of $f = 0.0256$, Eqs. 12 and 13 were solved and the Colebrook function for the writers' data was plotted in Fig. 19. The Colebrook curve falls below the writers' curve, merging with it at a value of **R** of approximately 350,000. The application of Eq. 14 to the writers' data gave a value of **R** = 450,000 as the point at which full turbulence was developed.

TABLE 5.—TEST DATA FROM A 2-IN. STANDARD STEEL PIPE; D (ACTUAL) = 2.06 IN.

Run No.	Velocity (ft per sec)	Measured head h_f (ft)	Reynolds number (R)	Friction factor (f)	Run No.	Velocity (ft per sec)	Measured head h_f (ft)	Reynolds number (R)	Friction factor (f)
(1)	(2)	(3)	(4)	(5)	(1)	(2)	(3)	(4)	(5)
1	24.75	41.95	465,000	0.0252	44	5.95	2.680	108,200	0.0279
2	24.10	40.40	454,000	0.0256	45	5.70	2.490	108,200	0.0282
3	23.95	39.60	451,000	0.0254					
4	23.80	38.70	447,000	0.0252	46	5.69	2.515	108,000	0.0286
5	23.30	37.42	438,000	0.0254	47	5.35	2.215	101,600	0.0285
					48	5.16	2.045	97,300	0.0283
6	22.90	36.00	430,000	0.0253	49	5.08	2.020	96,600	0.0288
7	22.25	34.60	418,000	0.0257	50	4.79	1.800	91,000	0.0290
8	21.92	33.30	412,000	0.0256					
9	21.35	31.50	401,000	0.0255	51	4.41	1.525	83,900	0.0288
10	20.75	29.60	390,000	0.0254	52	4.38	1.514	83,200	0.0291
					53	3.88	1.191	73,500	0.0292
11	20.15	28.00	379,000	0.0255	54	3.88	1.207	73,500	0.0296
12	19.75	27.25	366,000	0.0258	55	3.77	1.159	71,600	0.0300
13	19.70	27.15	372,000	0.0258					
14	19.62	26.55	371,000	0.0254	56	3.37	0.922	64,000	0.0299
15	19.59	26.75	363,000	0.0258	57	3.36	0.906	63,900	0.0295
					58	2.995	0.735	56,600	0.0302
16	19.45	26.35	368,000	0.0256	59	2.62	0.576	49,800	0.0308
17	19.40	26.25	361,000	0.0258	60	2.61	0.575	49,600	0.0311
18	19.15	25.65	355,000	0.0258					
19	19.00	25.10	359,000	0.0256	61	2.12	0.389	40,300	0.0318
20	18.90	24.95	357,000	0.0258	62	2.115	0.384	40,100	0.0316
					63	1.83	0.2915	34,800	0.0320
21	18.80	24.70	348,000	0.0258	64	1.750	0.272	33,100	0.0327
22	18.05	22.80	334,500	0.0258	65	1.635	0.238	31,100	0.0328
23	17.81	22.15	337,000	0.0257					
24	16.95	20.25	320,000	0.0259	66	1.631	0.237	31,000	0.0328
25	16.58	19.40	313,000	0.0260	67	1.63	0.2395	31,000	0.0332
					68	1.478	0.200	27,900	0.0338
26	15.40	16.81	291,000	0.0261	69	1.362	0.1724	25,900	0.0342
27	14.82	15.60	280,000	0.0261	70	1.219	0.139	23,100	0.0346
28	14.10	14.11	266,000	0.0261					
29	12.92	11.90	244,000	0.0263	71	1.142	0.1246	21,700	0.0351
30	11.63	9.76	220,000	0.0265	72	1.078	0.1128	20,500	0.0358
					73	0.978	0.0936	18,550	0.0360
31	10.58	8.11	200,000	0.0268	74	0.854	0.0730	16,200	0.0368
32	10.02	7.31	190,500	0.0268	75	0.744	0.0560	14,100	0.0373
33	9.94	7.20	188,000	0.0269					
34	9.10	6.04	173,000	0.0269	76	0.660	0.0457	12,550	0.0386
35	8.19	4.94	155,500	0.0272	77	0.569	0.0353	10,760	0.0402
					78	0.495	0.0270	9,400	0.0466
36	7.89	4.64	149,000	0.0273	79	0.417	0.0197	7,890	0.0418
37	7.34	3.97	139,500	0.0273	80	0.3685	0.0163	7,000	0.0442
38	7.16	3.79	130,200	0.0274					
39	6.85	3.53	124,700	0.0278	81	0.337	0.01392	6,360	0.0452
40	6.79	3.46	129,000	0.0284	82	0.3065	0.01152	5,840	0.0451
					83	0.2760	0.00951	5,220	0.0460
41	6.75	3.475	123,000	0.0281	84	0.2285	0.00710	4,350	0.0500
42	6.40	3.110	116,500	0.0280	85	0.1568	0.00368	2,960	0.0553
43	6.03	2.745	114,500	0.0278					

The fact that the Colebrook curve falls above the curve presented by Mr. Harris and below that in Fig. 19 must not be considered a defect as there is a considerable variation in the roughness and transition curves in each class of pipe. The Colebrook function is meant to be the average of many pipes in

the same class. The variation of roughness and transition curve in any one class of pipe precludes the use of the curve in the paper since it is obvious that any standard of design having wide application would necessitate the use of an average curve. The writers believe that the author's method of analyzing flow in closed conduits represents an oversimplification that can result in large

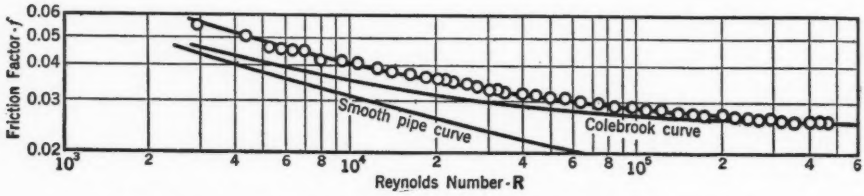

FIG. 19.—FRICTION FACTORS FOR A MODERATELY RUSTY 2-IN. STEEL PIPE

errors when predicting the flow in pipes in the transition region between partial and full turbulence. This oversimplification is not desirable since most flow problems in engineering practice occur in the transition region bounded by the smooth pipe curve for partial turbulence and the curve of Eq. 14 for full turbulence.

AMERICAN SOCIETY OF CIVIL ENGINEERS

Founded November 5, 1852

DISCUSSIONS

CONTINUOUS ARCHES AND BENTS ANALYZED BY COLUMN ANALOGY

Discussion

BY LESLIE J. MESZAROS, A. A. EREMIN, AND J. J. POLIVKA

LESLIE J. MESZAROS,[10] Assoc. M. ASCE.—Mr. Yu has developed a more direct and easily understood approach to a problem that has been solved in several ways. Among such treatments, for the record, a parallel development by Hardy Cross,[11,12] Hon. M. ASCE, the work of Mr. Cross with N. D. Morgan,[13] M. ASCE, and the work of Alexander Hrennikoff,[14] Assoc. M. ASCE, should be given.

A. A. EREMIN,[15] Assoc. M. ASCE.—In this paper the author has developed the column analogy method of stress analysis in continuous rigid frames and arches. The advantage of the method is that it eliminates a solution of simultaneous equations. It is regrettable that, in illustrating the method, the author has introduced a rigid frame with straight members which may be solved with less effort by various graphical or analytical methods. To illustrate this point, and also to check the method, the writer has solved the frame in Fig. 4 ("Example 1") by the graphical distribution of moments.

The distance a to the point of inflection (in Fig. 9) is determined by

$$a = s\,L \ldots\ldots\ldots\ldots\ldots\ldots\ldots\ldots\ldots\ldots (14)$$

in which s is a constant that varies with the shape and elastic properties of members and can be computed analytically[16] or graphically.[17] The moments

NOTE.—This paper by T. M. Yu was published in February, 1949, *Proceedings*. Discussion on this paper has appeared in *Proceedings*, as follows: June, 1949, by Jack R. Benjamin.

[10] Civ. Engr., Piedmont, Calif.

[11] *Transactions*, ASCE, Vol. 88, 1925, pp. 1196–1206.

[12] *Ibid.*, Vol. 90, 1927, pp. 1137–1145.

[13] "Continuous Frames of Reinforced Concrete," by Hardy Cross and N. D. Morgan, John Wiley & Sons, Inc., New York, N. Y., 1932, p. 227 and p. 316 et seq., particularly p. 338.

[14] "Analysis of Multiple Arches," by Alexander Hrennikoff, *Transactions*, ASCE, Vol. 101, 1936, p. 388.

[15] Associate Bridge Engr., California State Highways, Bridge Dept., Sacramento, Calif.

[16] *Transactions*, ASCE, Vol. 111, 1946, p. 887.

[17] "Simplified Graphical Distribution of Moments in Rigid Frames," by A. A. Eremin, Sacramento, Calif., 1948.

in the frame with the joints restrained from translation were constructed by cross lines in Fig. 9.

The basic moments in a member, produced by the transverse displacement of a joint, are

$$M = 6\,r\,N\,a \qquad (15)$$

in which $N = \dfrac{1}{L\,(L - a_1 - a_2)}$; $r = \dfrac{1}{L}$; and $E = 1$. The moments produced by the horizontal displacement of joint D after distribution are shown in Fig. 10. The final moments are obtained by superposing the moments in Figs. 9 and 10, which are close to the moments computed by the author.

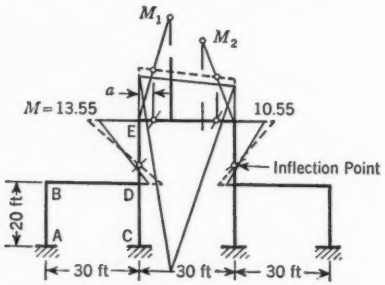

FIG. 9.—DIAGRAM OF BENDING MOMENTS (KIP-FEET)

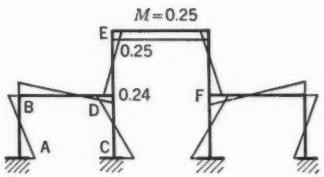

FIG. 10.—EFFECT OF SIDESWAY AT POINTS D AND F

The advantage of the column analogy method applied to a single span is in the simplicity of the rule of signs. In Mr. Yu's method, applied to continuous frames, the rule of signs is quite involved and therefore his method is more complex than other methods in common use.

J. J. POLIVKA,[18] M. ASCE.—As an effort to simplify the analysis of structures that are statically indeterminate to a high degree, this paper is a valuable contribution. It constitutes an extension of the column analogy method to structures of more than three redundant elements by replacing all parts adjacent to a selected span (or to a structural part) with three or less redundant elements—substituting members of definite elastic properties. As a refinement of the column analogy method, this procedure is new; but the principles enumerated by the author in the "Synopsis" (steps (*a*) to (*d*)) have been available since 1920.[19] Furthermore, the column analogy method is basically an adaptation of the ellipse of elasticity method introduced and developed by C. Culmann[20] in 1875 and W. Ritter[21] in 1888. The author limits his application to a general solution of continuous arches and bents and the tracing of influence lines, whereas a more basic approach[19] will permit the solution of cases in which the effect of shear and direct stress on elastic deformations is to be appraised.

---

[18] Cons. Engr., Berkeley, Calif.

[19] "Continuous Arches on Elastic Supports (Elastic Foundations)," by J. J. Polivka, *Der Brueckenbau*, Heidelberg, 1920, Vols. 4, 5, and 6.

[20] "Graphic Statics," by C. Culmann, Zurich, 2d Ed., Meyer & Zeller, 1875.

[21] "Application of Graphic Statics," by W. Ritter, Meyer & Zeller, Zurich, 1888.

In the paragraph preceding Example 1, Mr. Yu states that: " * * * it is not necessary (nor is it possible) to know even the location of * * *" the axis of the substitute member. That it is possible to know the location of this axis is demonstrated by Fig. 11, which represents the central frame DEGF in Fig. 4. This free body rests on elastic foundations at points D and F,

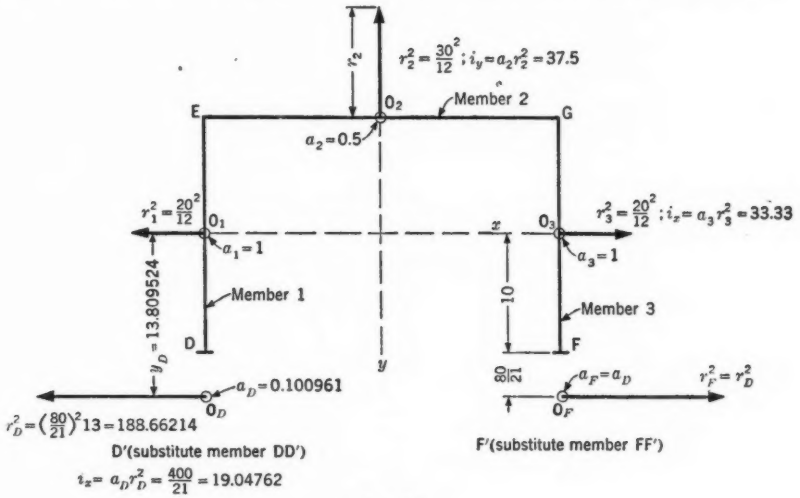

FIG. 11

which have been replaced by the substitute members DD′ and FF′. The elastic area a_d—that is, the elastic weight of the substitute member DD′—is equal to 21/208 = 0.100961. (The author computed 0.1005.) It is concentrated at the centroid O_D, along the vertical axis of the supporting column CD (Fig. 4), the ordinate y_D being equal to $-290/21 = -13.80952$. This value can be computed from Table 3*A*. For example, the second moment $a\,y^2$ of the substitute member DD′ is 19.1. Since $a_D\,y^2_D = 19.1$, $y_D = \sqrt{19.1/0.1005} = 13.785$, which checks the author's computation. Similarly, from Fig. 11, $r^2_D = (80/21)^2 \times 13 = 188.66214$, checking with the author's value of 19.1/0.1005 = 190.04975.

In introducing Fig. 1, the author states: "The extension [of the column analogy] is not applicable to frames with closed panels * * *." Fig. 12 demonstrates the analysis of a two-story frame with rectangular panels ABEGDC, one of which is closed. A horizontal force $H = 1$ acts at point E, as shown. The characteristics of the substitute members BB′ and DD′ can be computed from data in Table 2*C*. In this case also, a more accurate result is obtained by ratios. For example, referring to Fig. 10, $a_B = a_D = (17 - 9)/104 = (30 - 22)/104 = 1/13 = 0.0769231$. The author reports: 0.163 − 0.087 = 0.076. Since 17 − 9 = 30 − 22, the elastic centroids of the substitute members are at the midpoints of columns AB and CD.

The second moment, i_x, of the elastic area is equal to $a_B\,r^2_B$. The displacement δ_{xx} along BD is equal to $\frac{400}{3} - \frac{1,200}{13} = \frac{1,600}{39} = 41.025641$,

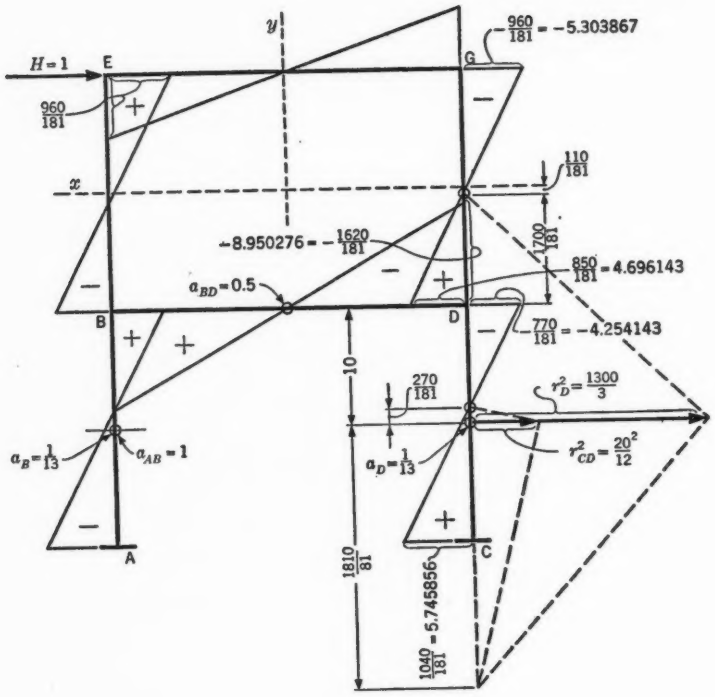

FIG. 12

TABLE 6.—ELASTIC LOAD AND FORMULA FOR m_i, EXAMPLE 3

Bar	a	x	y	ax	ay	ax^2+i_y	ay^2+i_x	P	x	y	Px	Py
BE	1.00	−15	0	−15	0	225	$\frac{100}{3}$	−10	−15	$-\frac{10}{3}$	+150	$+\frac{100}{3}$
EG	0.50	0	+10	0	+5	37.5	50	...	...	...	...	...
GD	1.00	+15	0	+15	0	225	$\frac{100}{3}$	...	...	...	...	...
BB′	$\frac{1}{13}$	−15	−20	$-\frac{15}{13}$	$\frac{20}{13}$	$\frac{225}{13}$	$+\frac{400}{13}+\frac{100}{3}$	$-\frac{30}{13}$	−15	$-\frac{310}{9}$	$+\frac{450}{13}$	$+\frac{3,100}{39}$
DD′	$\frac{1}{13}$	+15	−20	$+\frac{15}{13}$	$-\frac{20}{13}$	$\frac{225}{13}$	$+\frac{400}{13}+\frac{100}{3}$	...	...	...	...	...
Σ	$\frac{69}{26}$	0	$\frac{50}{69}$	0	$\frac{25}{13}$	$\frac{13,575}{26}$	$\frac{9,550}{39}$	$-\frac{160}{13}$	...	...	$+\frac{2,400}{13}$	$+\frac{4,400}{39}$
Correction to centroidal axis.....						...	$-\frac{1,250}{897}$	...	...	$+\frac{8.000}{897}$	...	$+\frac{500}{69}$ $+\frac{1.500}{897}$
Corrected values to centroid.....						...	$+\frac{5,600}{23}$	...	...	...	...	$+\frac{2.800}{23}$

Moments of internal stresses (forces): $m_i = -\frac{320}{69}+\frac{64}{181}x+\frac{1}{2}y$

as compared with $2 \times 20.5 = 41$ in Table 2*C*. With the knowledge that $\delta_{zz} = 1 \times 10 \times a_B \times d$, and $(d - 10)\ 10 = r^2_D$, one can compute: $d = 160/3$; $r^2_B = 1{,}300/3$; and $i_x = 100/3$. The complete analysis of the two-story frame is given in Tables 6 and 7. Table 6 is similar to Table 3*A*.

TABLE 7.—MOMENTS $M = m_s - m_i$, EXAMPLE 3

Moment	x	y	m_s	m_i	$M = m_s - m_i$
M_{EB}.....	−15	$+\frac{640}{69}$	0	$-\frac{960}{181}$	$+\frac{960}{181}$
M_{BE}.....	−15	$-\frac{740}{69}$	−20	$-\frac{2{,}770}{181}$	$-\frac{850}{181}$

$$M_{BA} = \frac{60}{13} - \frac{850}{181 \times 13} = +\frac{770}{181}\,; \quad M_{AB} = -\frac{70}{13} - \frac{850}{181 \times 13} = -\frac{1{,}040}{181}$$

Another example of a continuous frame with closed panels is the Vierendeel open web truss (see Fig. 13). The characteristics of the substitute members are $r^2_B = 64/3$; i_x, the second moment, is 4/3; and, a, the elastic area concen-

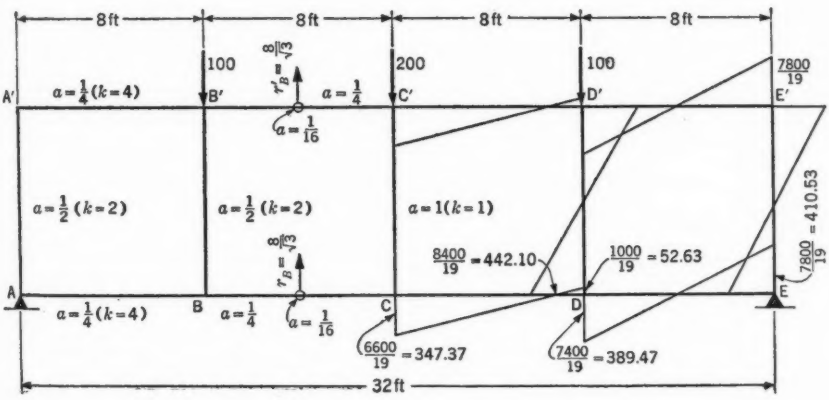

FIG. 13

trated at the midpoints of the chords, is 1/16. The analysis is similar to that in Fig. 12, and the results in Fig. 13 check the solution of this problem presented by A. Amirikian, M. ASCE, in 1942.[22]

Corrections for *Transactions:* In February, 1949, *Proceedings*, on pages 173 and 174: In Table 2*B*, center diagram, reverse the direction of the vertical and horizontal force arrows and change the corresponding minus sign to plus. For the vertical force $Y = 1$ in Table 2*B*, under the columns for P, M_y, and M_x, reverse the signs; and in line 6, under $Y = 1$, reverse the signs of each quantity except 0. In Table 2*C*(*a*), under $Y = 1$, change the minus signs to plus in four places.

[22] "Analysis of Rigid Frames (An Application of Slope Deflection)," by A. Amirikian, U. S. Govt. Printing Office, Washington, D. C., 1942, p. 129.

AMERICAN SOCIETY OF CIVIL ENGINEERS

Founded November 5, 1852

DISCUSSIONS

APPLIED COLUMN THEORY

Discussion

BY JACOB KAROL

JACOB KAROL,[30] M. ASCE.—This comprehensive paper by Mr. Shanley is an admirable presentation of the theory underlying the present methods of stress analysis of compression members in aircraft design. The mathematical development of the nondimensional stress-strain diagrams and column curves may seem somewhat "impractical" to the civil engineer who uses allowable stresses in the design of columns of steel, concrete, or timber that are fixed by the design specifications at values well within the elastic range. In aircraft structures, however, the design stresses are in the inelastic range. Since airplanes are generally static tested for full design loads, it was necessary for the stress analyst to develop a design theory which, in the ideal case, would result in a structure that failed at slightly beyond the design load. Therefore, the detailed study, by the author, of the several phases of applied column theory is undeniably "practical."

The writer will confine his discussion to Sections 6 and 7.

The method of correcting test data to "standard," as indicated in Fig. 12, is correct only for columns that fail by primary instability, since the affinely related column curves are derived from the tangent modulus. The horizontal scale marked "not used" is designated as "effective L/ρ" in the original Lockheed report (see Fig. 12). This value is actually the important variable in the general case, as will be evident subsequently.

It is supposed that a series of compression tests of sheet stiffener combinations have been made. Since the sheet and stiffener may each be subject to local buckling, the column curve plotted from the test data will not be affinely related to the tangent modulus column curve of the specimen material. It may be noted in passing that determination of f_c and L/ρ for a sheet stiffener combination is quite a problem in itself, but it is assumed that they have been determined somehow. It is desirable to plot the test data on a graph, which also has the Euler curve plotted thereon, to determine the point of intersection.

NOTE.—This paper by F. R. Shanley was published in June, 1949, *Proceedings*. Discussion on this paper has appeared in *Proceedings*, as follows: September, 1949, by William R. Osgood, and J. V. du Plessis.

[30] Design Engr., Howard-Needles-Tammen & Bergendoff, Kansas City, Mo.

The procedure for correcting the data for a test stress f_2 to standard is as follows:

Let: f_o be the yield strength for standard material; $K f_o$ be the yield strength for specimen material; f_1 be the stress for $(L/\rho)_1$, as reduced to standard; f_2 be the stress for $(L/\rho)_1$, read from the curve; and f_3 be the stress for $(L/\rho)_3 = (L/\rho)_1/\sqrt{K}$, read from the curve. Then, for the ratio $(L/\rho)_1$,

$$f_1 = \frac{f_3}{K} \quad \ldots\ldots\ldots\ldots\ldots\ldots\ldots\ldots\ldots\ldots (48)$$

The foregoing procedure is merely a verbal statement of the mathematics expressing the affine relationship between the test column curve and the derived column curve for the standard material. The interested reader can readily prove this for himself by assuming that the test column curve is mathematically expressible in terms of f_o and $K f_o$, as indicated elsewhere,[15] and by calculating the stresses f_1, f_2, and f_3. Hence, in the general case, correction to standard is a function of the shape of the test column curve, the yield strength ratio, and L/ρ.

The author's extended treatment of the effects of eccentricity in pin-ended columns is undoubtedly an indication of the importance of the subject. After rejecting the secant formula as inapplicable to materials not having a pronounced yield point, he suggests using interaction curves to solve the problem, and presents in Fig. 15 such a series of curves for axial loading and bending due to third-point loading. He assumes correctly that, for an initial moment due to constant eccentricity, the sag would be greater. He further states that the shape of these curves may be primarily a function of the kind of loading involved, which is also true. Hence, a number of sets of interaction curves would be necessary in design, unless there is some other approach to the problem.

After following the author's lead and verifying the statements referred to in the preceding paragraph, it occurred to the writer that the problem could be generalized so that one interaction curve would apply for various loadings, and perhaps for any shape of cross section and any type of stress-strain diagram. The reasoning was extremely simple. For any column subject to combined bending and compression, the maximum stress on the section is the sum of the axial stress and the total bending stress. The total bending stress is itself the sum of the primary bending stress and the secondary bending stress due to lateral deflection. By using the total bending stress as a parameter, the type of loading is automatically cared for. If the total stress on the section is known, then, by deducting the axial stress, the total bending stress is obtained. The primary bending stress can then be determined by using the available theories of secondary bending.

The problem resolved itself into finding an expression which would equal the critical column stress for pure compression and the modulus of rupture for pure bending. The expression was originally determined to fit the test data in Fig. 14 for the entire range of R'_c and $L/\rho = 30$. It was later found that the same expression checked quite well any point taken at random from Fig. 14. This might be considered as an indication of its possible generality.

[15] "Strength of Metal Aircraft Elements," *ANC-5*, Army-Navy-Civil Committee on Aircraft Design Criteria, U. S. Govt. Printing Office, Washington, D. C., 1942.

The total stress in combined compression and bending is given by the expression:

$$f_c + f_{bt} = f_{cr}\,[1 + (m - 1)\,(0.839 \tan \theta)] \quad \ldots\ldots (49)$$

in which

$$m = \frac{f_{bo}}{f_{cr}} \quad \ldots\ldots (50a)$$

and

$$\theta = \frac{5}{9} \text{ arc tan } \frac{f_{bt}}{f_c} \quad \ldots\ldots (50b)$$

Dividing through both sides of Eq. 49 by f_{cr},

$$\frac{f_c}{f_{cr}} + \frac{f_{bt}}{f_{cr}} = 1 + (m - 1)\,(0.839 \tan \theta) \quad \ldots\ldots (51)$$

The stress ratios are

$$R'_c + m\,R_{bt} = 1 + (m - 1)\,(0.839 \tan \theta) \quad \ldots\ldots (52)$$

in which

$$\theta = \frac{5}{9} \text{ arc tan } \frac{m\,R_{bt}}{R'_c} \quad \ldots\ldots (53)$$

Eq. 52 is plotted in Fig. 20(*a*) for various values of m. Since m is known for a particular problem—

$$R_{bt} = \frac{f_{bt}}{f_{bo}} = \frac{M_{bt}}{M_o} \quad \ldots\ldots (54)$$

—can be determined for any value of

$$R'_c = \frac{f_c}{f_{cr}} = \frac{P}{P_{cr}} \quad \ldots\ldots (55)$$

—and vice versa.

The remaining problem is to determine the primary bending stress f_b from the total bending stress f_{bt}. For any distributed loading (including the test third-point loading), as well as for initial curvature, the stress is given accurately enough by

$$f_b = (1 - \alpha)\,f_{bt} \quad \ldots\ldots (56a)$$

and, for constant eccentricity of axial load,

$$f_b = \frac{1 - \alpha}{1 + 0.272\,\alpha}\,f_{bt} \quad \ldots\ldots (56b)$$

in which

$$\alpha = \frac{f_c}{f_E} = \frac{P}{P_E} = \frac{f_c}{\frac{\pi^2 E}{(L/\rho)^2}} \quad \ldots\ldots (57)$$

Hence the ratios

$$\frac{R_b}{R_{bt}} = \frac{f_b}{f_{bt}} = \frac{M}{M_{bt}} \quad \ldots\ldots (58)$$

can be determined for any value of α, and vice versa.

Eqs. 56 are also plotted in Fig. 20(*a*). Thus, the problem of combined axial load and bending due to eccentricity or transverse loading is solved from one chart.

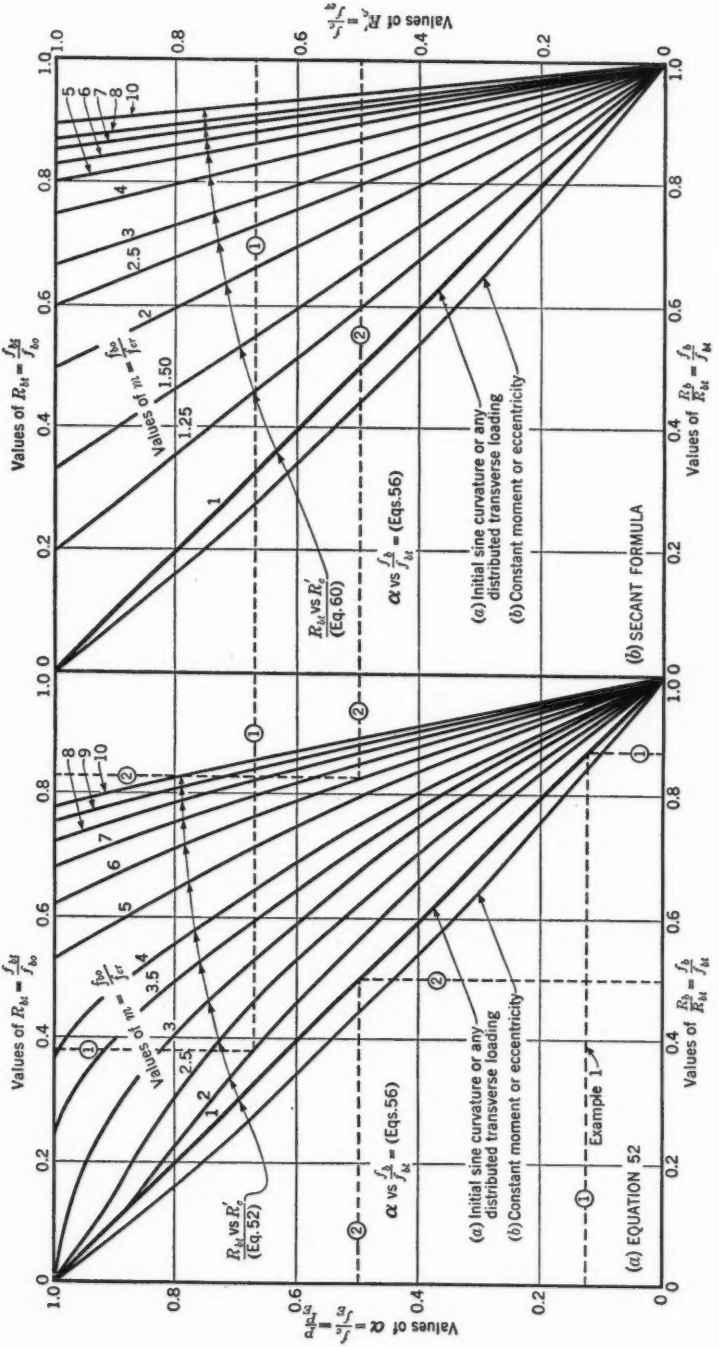
(a) EQUATION 52
(b) SECANT FORMULA
Example 1
Values of $R_M = \frac{f_M}{f_{bo}}$
Values of $\frac{R_b}{R_M} = \frac{f_b}{f_M}$
Values of $\alpha = \frac{f_b}{f_M} = \frac{f_b}{f_b + f_a}$
Values of $R'_e = \frac{f_a}{f_a + f_b}$
Values of $m = \frac{f_{bo}}{f_{cr}}$
R_M vs R'_e (Eq. 52)
R_M vs R'_e (Eq. 60)
α vs $\frac{f_b}{f_M}$ = (Eqs. 56)
(a) Initial sine curvature or any distributed transverse loading
(b) Constant moment or eccentricity

FIG. 20.—INTERACTION CURVES FOR COMBINED BENDING AND AXIAL LOADING

Two examples of the use of Fig. 20(*a*) applied to the data in Fig. 14 follow:

(1) Given: $L/\rho = 30$; and, in kips per square inch, $f_{bo} = 120$, $f_{cr} = 60$, $f_c = 40$, and $E = 29{,}200$. The problem is to compute f_b. From the assumed data, $m = 120/60 = 2$; $f_E = 320$ kips per sq in; $\alpha = 40/320 = 0.125$; and $R'_c = 40/60 = 0.667$. From Fig. 20(*a*), $R_{bt} = 0.38$; hence, $f_{bt} = 0.38 \times 120 = 45.6$ kips per sq in. From Fig. 20(*a*), $f_b/f_{bt} = 0.875$; hence, $f_b = 0.875 \times 45.6 = 39.9$ kips per sq in. From Fig. 14, test $f_b = 40$ kips per sq in.

(2) Given: $L/\rho = 120$; and, in kips per square inch—$f_{bo} = 120$, $f_{cr} = f_E = 20$, and $f_b = 50$. It is required to compute f_c. From the given data, $m = 120/20 = 6$; $f_b/f_{bo} = 50/120 = 0.417$. Guess $R'_c = 0.498 = \alpha$. From Fig. 20(*a*), $f_b/f_{bt} = 0.502$; hence, $R_{bt} = 0.83$. From Fig. 20(*a*), $R'_c = 0.498$, which checks the guess. Hence, $f_c = 20 \times 0.498 = 9.96$ kips per sq in. From Fig. 14, test $f_c = 10$ kips per sq in.

It is recognized that the addition of stresses in the inelastic range is a convenient fiction; but, in the foregoing treatment, Eq. 49 has the merit of being a close approximation to the experimental truth and of indicating the important variables in a problem not solved hitherto in the general case. Since Eq. 49 assumes a gradual change in the total stress as the loading changes from pure compression to pure bending, it seems logical enough to be generally valid. Furthermore, if f_{bo} is considered to represent not only the ultimate modulus of rupture, but also a limiting bending stress in general, the usefulness of Fig. 20(*a*) is extended. Thus, in aircraft design, it can be used for limit loads as well as for ultimate loads. The writer was able to check the test data by J. A. Van den Broek,[31] M. ASCE, on 1-in. mild steel round bars for both initial yielding and ultimate capacity by using the yield point as the limiting bending stress in the first case and 1.7 times the yield point as the modulus of rupture in the second case.

The column theory, from which the secant formula is derived, is also presented for comparison. The total stress is given by the expression:

$$f_c + f_{bt} = m\, f_{cr} \qquad (59)$$

Dividing through both sides of Eq. 59 by $m\, f_{cr}$,

$$\frac{f_c}{m\, f_{cr}} + \frac{f_{bt}}{m\, f_{cr}} = 1 \qquad (60)$$

Expressed as stress ratios, Eq. 60 becomes

$$\frac{R'_c}{m} + R_{bt} = 1 \qquad (61)$$

Eq. 61 is a family of straight lines, as represented in Fig. 20(*b*) for various values of m. It is obviously correct only for a value of $m = 1$. This is true in the short column range for structural steel, in which the limiting stress for both bending and compression is the yield point stress. For values of m greater than 1, it gives less conservative results than Eq. 52. The relation of primary to total bending stress is given by Eqs. 56, and use of the chart is similar to the method presented for Fig. 20(*a*).

[31] "Rational Column Analysis," by J. A. Van den Broek, *The Engineering Journal*, December, 1941.

AMERICAN SOCIETY OF CIVIL ENGINEERS

Founded November 5, 1852

DISCUSSIONS

PHOTOGRAMMETRY, POSTWAR

Discussion

BY COURTLANDT EATON

COURTLANDT EATON,[2] M. ASCE.—The long strides that have been made in aerial photography in recent years are brought out in this informative paper. Of particular interest to the writer are the applications of aerial photography to the production of contour maps. About 1930, the Fairchild Aerial Surveys under contract with the Los Angeles County (California) Flood Control District made two aerial surveys in particularly difficult terrain—one, a contour map of the main San Gabriel River Canyon from its mouth, including the east and west forks; and the other, a contour map of a quarry site in the lower canyon about 600 ft high with a practically vertical face.

From the San Gabriel Canyon survey some fourteen possible dam sites were located, from which, by field reconnaissance and office studies, the sites that finally resulted in San Gabriel rock-fill dams Nos. 1 and 2 were selected. Much of the territory was passable only on horseback and on foot. Time was important. The contour maps were prepared in a fraction of the time necessary for field party surveys. Cost data are not available, but the cost was less than was possible by ordinary field methods. The contract called for a high degree of accuracy and field survey spot check areas indicated that aerial contours were more accurate than field surveys. This accuracy was due to the facilities, under aerial methods, for following up small creeks and draws, which in the aggregate add up to substantial areas.

The quarry survey was equally satisfactory as developed by spot checks. Because the vertical face made a field survey extremely difficult, hazardous, and costly, it would have involved delays that were inadvisable.

Aside from costs and time savings, there are many advantages in aerial surveys well known to engineers who have used them. One advantage is that aerial surveys can decide questions of accuracy of original ground surveys arising between the contracting parties in the case of large excavations such as dams. Each party may claim the superiority of his survey. With a photographic record such claims either can be reconciled or will not be made.

NOTE.—This paper by Leon T. Eliel was published in May, 1949, *Proceedings*.

[2] Denver, Colo.

Another advantage is that aerial photographs bring out details not visible by ground inspections—for instance, rights of way where photographs give evidences of old watercourses through improved properties. The writer remembers an aerial survey of lands now occupied by the Santa Anita (Calif.) race track which showed evidences of an early race track said to be one built by Lucky Baldwin and later changed in direction for better sun conditions.

Since there are also many other advantages in aerial surveys, topographic surveys by present archaic and laborious methods probably will become obsolete for major areas.

The writer's only "criticism" of the paper is that it is too short. In his closure, it is hoped that Mr. Eliel will elaborate on this most interesting subject.

AMERICAN SOCIETY OF CIVIL ENGINEERS

Founded November 5, 1852

DISCUSSIONS

CONTROL OF THE HYDRAULIC JUMP BY SILLS

Discussion

BY CHARLES JAEGER, AND LOUIS M. LAUSHEY

CHARLES JAEGER.[12]—The research work reported in this paper is to be commended because of its general interest.[13] The equation of momentum is one of the most powerful devices for computing uniform and nonuniform flow, and any effort to check the theoretical results by laboratory experiment should be supported and encouraged. The principal results of the study are summarized in Figs. 3 and 7. Fig. 3 and Eq. 15 are in the form presented by the writer in 1936.[13] Assuming that Eq. 15 can be written directly for profiles (1) and (3), in Fig. 1(*c*) (assuming $\gamma = 1$),

$$\frac{d_1^2}{2} - \left(\frac{d_3 + h}{2}\right)^2 - \xi \frac{V_1^2}{2g} h = \alpha'_3 \frac{V_3^2 d_3}{g} - \alpha'_1 \frac{V_1^2 d_1}{g} \quad \ldots\ldots (27)$$

Substituting $\alpha'_3 = \alpha'_1 = 1$ and $\xi = 0$ in Eq. 27 the result gives a momentum equation similar to Eq. 15. The factor $\alpha'_1 \cong (\alpha'_1 > 1)$ takes account of the nonuniform velocity distribution and $\xi \frac{V_1^2}{2g} h$ accounts for a pressure distribution that may be different from the hydrostatic pressure on the sill or weir—ξ being a coefficient. Since $\eta_2 = \frac{d_3}{d_1}$; $\phi_1 = \frac{V_1^2}{2g d_1} = \frac{\mathbf{F}^2}{2}$; and $\frac{h}{d_1} = \delta$ Eq. 27 becomes

$$\phi_1 = \frac{\mathbf{F}^2}{2} = \frac{\eta_2 [(\eta_2 + \delta)^2 - 1]}{4(\eta_2 \alpha'_1 - \alpha'_3) - 2\xi \eta_2 \delta} \quad \ldots\ldots (28a)$$

If $\alpha'_1 = \alpha'_3 = 1$; and $\xi = 0$;

$$\phi_1 = \frac{\mathbf{F}^2}{2} = \frac{\eta_2 [(\eta_2 + \delta)^2 - 1]}{4(\eta_2 - 1)} \quad \ldots\ldots (28b)$$

NOTE.—This paper by John W. Forster and Raymond A. Skrinde was published in April, 1949, *Proceedings*. Discussion on this paper has appeared in *Proceedings*, as follows: September, 1949, by En-Yun Hsu, and Steponas Kolupaila.

[12] Special Lecturer on Technical Hydraulics and Hydr. Structures, Imperial College, London, England; Cons. Engr., English Electric Co., London, England.

[13] "Der Mischungsvorgang bei ploetzlichem Querschnittsuebergang," by Charles Jaeger, *Wasserkraft und Wasserwirtschaft*, Vol. 31, No. 24, 1936.

The curves $\phi_1 = \frac{\mathbf{F}^2}{2}$ in function η_2 are represented in Fig. 11 which is comparable to Fig. 3. A straight line in Fig. 3 becomes a parabola in Fig. 11; the curve $\frac{d_3}{d_1} = \mathbf{F}^{2/3}$ in Fig. 3 is curve $\phi_1 = \frac{\eta^3_2}{2}$ in Fig. 11; and curve $\frac{h}{d_1} = 0$ (hydraulic jump) in Fig. 3 is the curve $\delta = 0$ in Fig. 11. Fig. 12, for the case of a negative sill, should be interpreted in a similar manner, as can also the problem of river bed enlargement.[14] Figs. 11 and 12 represent all possible solutions of Eq. 27, for positive as well as for negative sills. Fig. 3 represents

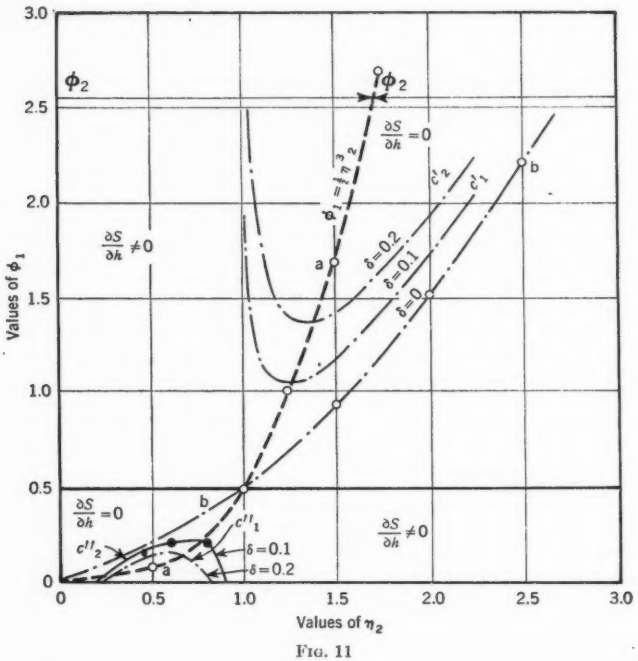

FIG. 11

only part of this range of solutions. It is a satisfaction to the writer thus to find his own studies confirmed by more recent laboratory experiments; and he is in agreement with the physical interpretations presented by the authors. The writer proposes to comment on three phases of the paper:

(*a*) In Fig. 7 the experimental curves are offset somewhat to the right of the theoretical curves. The authors attribute this offset effect to the non-uniform distribution of velocities. On the other hand, if $\alpha'_1 \cong \alpha'_3 > 1$ the quantities ϕ_1 and $\mathbf{F}$ actually decrease and the theoretical curve will then, in fact, move to the left. The writer has found that α'_1 and α'_3 are always very nearly equal to 1. (One does not need to know the value of α'_2 in profile (2), Fig. 1(*c*).) If $\xi > 0$ (as it probably is), the theoretical curve is moved to the right to meet the experimental curve. To the writer, this translation of the

[14] "Technische Hydraulik," by Charles Jaeger, Birkhäuser, Basel, 1949, pp. 150, 152, 158, and 159. Figs. 88, 89, 94, and 95, respectively.

curve means that the pressure distribution on the vertical sill is not hydrostatic—it cannot be hydrostatic because of the necessity of curving the stream tubes and because of the turbulence near the sill. In some experiments by students at the Imperial College, London, England, values of $\xi > 0$ were found in cases where the occurrence of bridge piers narrowed the section.

(*b*) There are other parts of Figs. 11 and 12 that are not represented in Fig. 3. These characteristics have been investigated, thus indicating that real hydraulic solutions are available for these problems as well. A. Koch and M. Carstanjen[15] have done some research on the problem of streaming flow over a positive sill and L. Escande[16] spent a long time investigating conditions at negative sills.

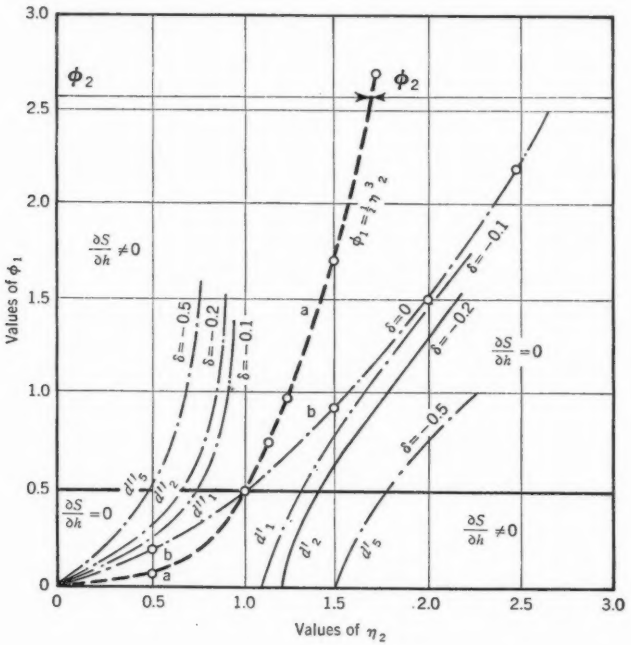

FIG. 12

When analyzing the energy of the flow that is represented by some of the other solutions of these diagrams, the investigator finds that some parts of the curves are not adaptable to real hydraulic solutions.

(*c*) There is need for further research work to explore the possibility of further solutions for the different curves in Figs. 11 and 12. To date, only parts of the entire areas have been investigated. For example, more accurate measurements of α'_1, α'_3, and ξ will probably show an even closer agreement with theory. On the whole, the results found by the momentum equation

[15] "Von der Bewegung des Wassers und den dabei auftretenden Kräften," by A. Koch and M. Carstanjen, Springer, Berlin, 1926.

[16] "Etude théorique et expérimentale de l'écoulement par vanne de fond," by L. Escande, *Revue Générale de l'Hydraulique*, Nos. 19 to 21, 1938, and Nos. 25 and 26, 1939.

have agreed remarkably well with the results of tests, but an extension of these tests is still indicated.

The momentum equation was introduced into hydraulics by J. B. Bélanger[17] in 1849 and J. A. Bresse[18] in 1860. They established a comprehensive theory, introducing the function—

$$S = \frac{h^2}{2} + \frac{Q\,v}{g} \quad \ldots\ldots\ldots\ldots\ldots\ldots\ldots\ldots\ldots\ldots (29)$$

—or "total momentum." Experimental research followed by H. Bazin, A. H. Gibson, Mr. Koch, J. Einwachter, J. Smetana, Mr. Escande, G. Nebbia, Boris A. Bakhmeteff, Hon. M. ASCE, and others.[19,20] K. Woycicki investigated the case of the drowned flow below a gate and H. Favre studied the lateral spillway and the lateral flow of water into a primary stream. The equation of momentum has also been used for the computation of nonuniform flow (translation waves). Model tests have demonstrated how the height of the wave crest depends not only on the variation of the discharge (as in the case of the wave body) but also on the variation of impulse. No systematic research work has been done on this interesting problem.

One important case that was solved on similar lines by Eq. 8 is the computation of partly working surge tanks, as proposed in 1930 for the power station in Wettingen, Switzerland.[21] In that particular case, the computations for translation waves had to be combined with surge tank computations. These are some of the problems whose solution by means of the momentum equation represents a considerable amount of successful research work.

Figs. 11 and 12 also indicate the particular domain where the equation of momentum offers no solution. Physically, this means that the hydraulic jump becomes unstable and moves upstream or downstream. Similarly, there are certain areas in which the Bernoulli equation does not apply. Are these two domains, with their imaginary solutions, the same? What is the connection between "total momentum" and energy? These theoretical problems have led to some further research as reported by the writer in 1931,[22] 1943,[23] 1947,[24] 1948,[25] and 1949.[26]

When the investigator is dealing experimentally with particular problems as outlined in this discussion under topic (*c*), the more general aspect of the equation of momentum described in the paragraphs following topic (*c*) should be kept in mind because it is there that the explanation of many of the difficulties encountered is to be found.

---

[17] "Notes sur le cours d'hydraulique," by J. B. Bélanger, *Mémoires*, École Nationale des Ponts et Chaussées, Paris, 1849–1850.

[18] "Cours de Mécanique Appliquée," Pt. 2, "Hydraulique," by J. A. Bresse, Mallet-Bachelier, Paris, 1860.

[19] "Technische Hydraulik," by Charles Jaeger, Birkhäuser, Basel, 1949, pp. 87 to 92.

[20] *Ibid.*, pp. 137 to 160.

[21] "Über die Eigenschaften von Schwällen und die Berechnung von Unterwasserstollen," by E. Meyer-Peter and H. Favre, *Schweizerische Bauzeitung*, Nos. 4 and 5, 1932.

[22] "Analogien zwischen Stützkraftminimum und Energieminimum in der Hydraulik," by Charles Jaeger, *ibid.*, April 18, 1931.

[23] "Contribution à l'étude des courants liquides à surface libre," by Charles Jaeger, *Revue Générale de l'Hydraulique*, Nos. 33 and 34, 1943.

[24] "De l'impulsion totale et de ses rapports avec l'énergie totale d'un courant liquide à surface libre," by Charles Jaeger, *ibid.*, Nos. 37–41, 1947.

[25] "Steady Flow in Open Channels: The Problem of Boussinesq," by Charles Jaeger, *Journal*, Inst. C. E., February, 1948, p. 338.

[26] "Technische Hydraulik," by Charles Jaeger, Birkhäuser, Basel, 1949.

LOUIS M. LAUSHEY,[27] JUN. ASCE.—The results of this paper present unusually good data on the hydraulic jump, and the authors are to be commended for the manner in which they conducted the tests. The curves presented lead the engineer closer to the rational design of stilling basins. The discrepancy between the theoretical and the experimental curves leads to a more complete analysis than that given in the paper.

Abrupt Rise.—The authors state that the experimental curves for the abrupt rise (Fig. 7) are parallel, straight lines. An equation to fit the experimental data was easily found by plotting d_3/d_1 against h/d_1, with the parameter being straight-line curves of values of **F** all having approximately the same slope. The resulting equation fits the experimental curves within $\pm$ 5%, and had no greater error than the spread of the plotted points: $d_3 = d_2 - 1.40\,h$; or $d_3/d_1 = d_2/d_1 - 1.40\,h/d_1 = \phi\,(\mathbf{F}) - \psi\,(h/d_1)$. To complete Eq. 14—

$$\frac{h}{d_1} = \phi_4\left(\mathbf{F}, \frac{d_3}{d_1}\right) = 0.71\left(\frac{d_2}{d_1} - \frac{d_3}{d_1}\right) \ldots\ldots\ldots\ldots\ldots\ldots (30)$$

—which includes the necessary variables **F**, d_1, and h. Fig. 13 shows the agreement between the authors' experimental curves and the empirical equation.

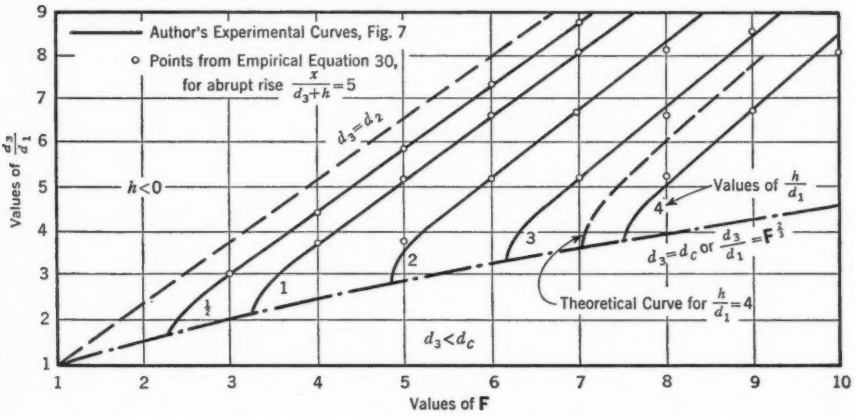

FIG. 13.—VERIFICATION OF EMPIRICAL EQUATION WITH EXPERIMENTAL DATA OF FIG. 7

An adjusted equation then follows:

$$d_2 - (d_3 + h) = 0.40\,h = \Delta d \ldots\ldots\ldots\ldots\ldots\ldots (31)$$

showing the resulting drop in the water surface below that required for a jump without an abrupt rise. Within the limits of the authors' studies, it follows that the ratio $h/\Delta d = 2.5$. It may prove to be a useful rule of thumb that the drop in the water surface below that level required theoretically for d_2 would be about 40% of the height of the abrupt rise.

[27] Asst. Prof. of Civ. Eng., Carnegie Inst. of Technology, Pittsburgh, Pa.

Fig. 14 is another plotting of the authors' data (based on the curves in Fig. 7) to show this drop. The care with which the experimental work must have been done is evident. Denoting K as the ratio $(d_3 + h)/d_2$, in which d_2 is the depth computed from Eq. 4, these observations follow:

(1) The ratio K is decreased by raising h/d_1 (**F** constant) or by decreasing **F** (h/d_1 constant);
(2) The jump and the drop in the water surface are little affected by the rise when **F** is high;
(3) The ratio K approaches 1.00 for all values of **F** and h/d_1 when **F** becomes very large;
(4) If h were increased (**F** and d_1 constant), d_3 must be lowered if the jump is not to move in the basin; and
(5) An empirical equation for K follows:

$$K = \frac{(d_3 + h)}{d_2} = \frac{d_3}{d_2} + \frac{h}{d_2} = 1 - \frac{1.40\,h}{d_2} + \frac{h}{d_2} \ldots\ldots\ldots (32a)$$

and

$$K = 1 \frac{- 0.40\,h}{d_2} = \phi\,(h, d_1, \mathbf{F}) \ldots\ldots\ldots\ldots\ldots (32b)$$

A designer might consider the ratio d_3/d_2 of importance when the tailwater is low and a depressed basin is considered. The ratio of the depth of tailwater which may be used compared to the depth d_2 is computed for the plain jump. It is not to be considered a new variable, but may be useful in design as shown in the form of Fig. 15. Calling on the empirical data,

$$d_3 = d_2 - 1.40\,h \text{ or } \frac{d_3}{d_2} = 1 - 1.40\,\frac{h}{d_2} = K' \ldots\ldots\ldots (33a)$$

Again,

$$K' = \frac{d_3}{d_2} = \phi'\,(\mathbf{F}, h, d_1) \ldots\ldots\ldots\ldots\ldots\ldots (33b)$$

Fig. 15 shows the agreement between the experimental data and the curves computed from Eq. 33*a*. This was facilitated by choosing $d_1 = 1$, values being taken directly from Fig. 7 or being computed as a function of **F**.

The difference between the theoretical and experimental curves was explained by the authors to be due to a nonuniform velocity distribution which existed at the ratio $X/(h + d_3) = 5$. They are correct in stating that, when $X/(h + d_3)$ approaches 10, the experimental data will check closer with the theoretical curves. However, nonuniform velocity distribution will not explain all the discrepancy.

The omission of a dynamic force on the face of the abrupt rise is not permissible. Although the force is small in some cases, it becomes exceedingly important when the jump is close to the rise.

As long as X is greater than the length of the jump, the assumption can be made that the jump is not changed by the rise that follows. Thus, the authors assumed that there is a drop in the water surface from a depth d_2 to

a lower level on the rise. This problem can also be analyzed easily by the energy equation. The following basic equation applies as long as $X > L_J$:

$$d_1 + \frac{V^2_1}{2g} - \frac{(d_2 - d_1)^3}{4 d_2 d_1} = d_2 + \frac{V^2_2}{2g} h + d_3 + \frac{\alpha V^2_3}{2g} + \frac{K V^2_3}{2g} \quad \ldots\ldots (34)$$

in which $\frac{(d_2 - d_1)^3}{4 d_2 d_1}$ is the head loss in jump; α is the correction coefficient for kinetic energy; and K is the coefficient for contraction loss at the rise. In fact, the exact theoretical curves can be duplicated by Eq. 34 if $\alpha = 1$ and $K = 0$. The writer computed a half dozen points which checked exactly.

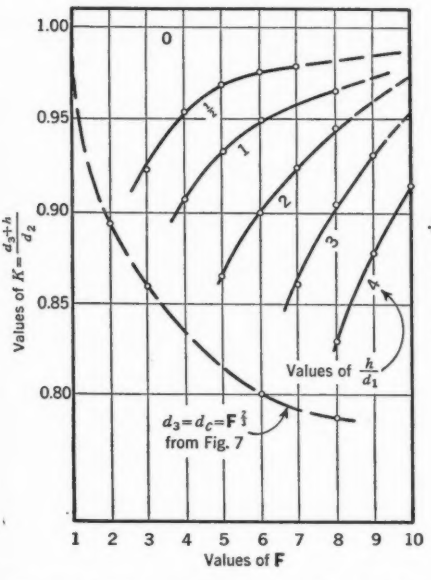

FIG. 14.—PERCENTAGE DROP IN THE WATER SURFACE OVER THE ABRUPT RISE AS A FUNCTION OF F AND H/d_1

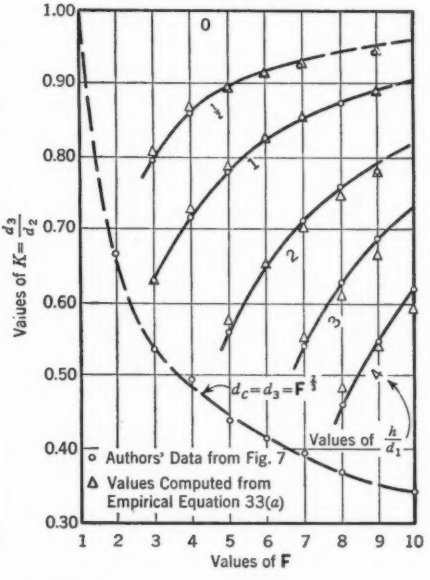

FIG. 15.—VERIFICATION OF EXPERIMENTAL DATA AND EMPIRICAL EQUATION FOR DEPTHS ON AND BEFORE THE ABRUPT RISE

It is a basic fact that the hydraulic jump can be analyzed by the energy or the momentum principles provided the head loss is known when the energy equation is applied. Thinking may be less confusing if both are applied to provide a better understanding of the problem. However, in both the energy equation and the momentum principles, it is imperative to know the velocity distribution to compute, correctly, the true momentum and energy at point 3, thus deriving an equation that checks experimental data.

The abrupt rise can easily be analyzed by the following equation as long as $X > L_J$:

$$d_2 + \frac{V^2_2}{2g} = h + d_3 + \frac{(\alpha + K) V^2_3}{2g} = h + d_3 + \frac{(\alpha + K) q^2}{2g d^2_3} \quad \ldots\ldots (35)$$

The writer computed fifteen values of $\alpha + K$ from the experimental data. This coefficient averaged 5/3 and varied very little from this value, which is a reasonable one. In Fig. 16 points are shown computed from Eq. 35, which show the close agreement, when $\alpha + K$ is taken equal to 5/3.

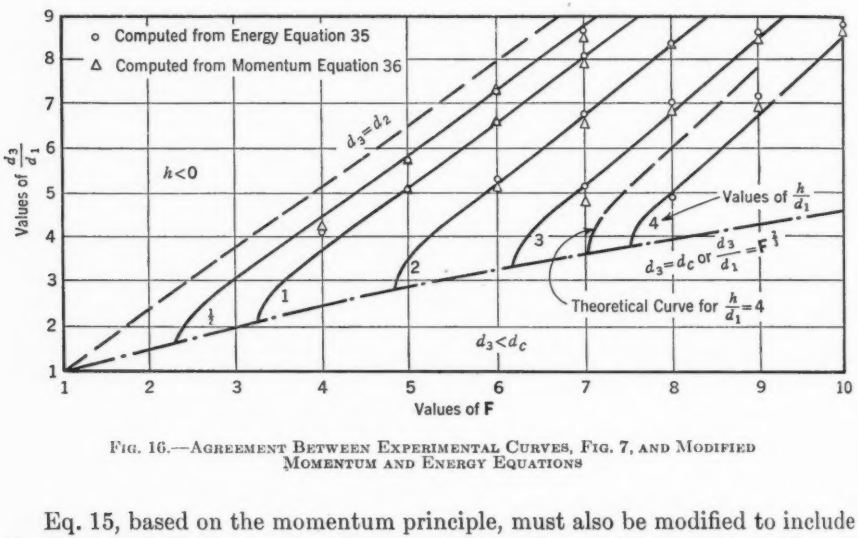
o Computed from Energy Equation 35
Δ Computed from Momentum Equation 36
$d_3 = d_2$
$h<0$
Values of $\frac{h}{d_1}$
$d_3 = d_c$ or $\frac{d_3}{d_1} = F^{\frac{2}{3}}$
Theoretical Curve for $\frac{h}{d_1} = 4$
$d_3 < d_c$
Values of $\frac{d_3}{d_1}$
Values of F

FIG. 16.—AGREEMENT BETWEEN EXPERIMENTAL CURVES, FIG. 7, AND MODIFIED MOMENTUM AND ENERGY EQUATIONS

Eq. 15, based on the momentum principle, must also be modified to include the correct coefficient for momentum at point 3 and, therefore, Eq. 15 must be modified as follows:

$$\frac{\gamma\, d_2^2}{2} - \frac{\gamma\, d_3^2}{2} - \left[\frac{\gamma\, h\, (2\, d_2 - h)}{2}\right] - \frac{2\, h\, \gamma\, q^2}{2\, g\, d_2^2} = \left[\frac{\gamma\, q^2}{g}\left(\frac{\alpha'}{d_3} - \frac{1}{d_2}\right)\right] \ldots (36)$$

in which α' is the correction coefficient for momentum; C_D is assumed to be 2.0, the value for a rectangular flat plate; and the dynamic force on the rise is

$$\mathbf{F}_d = \frac{C_D\, \gamma\, h\, V^2}{2\, g} = \frac{C_D\, \gamma\, h\, q^2}{2\, g\, d_2^2} \ldots (37)$$

Actually C_D varies, but the force is small within the experimental range, and the variation would produce a negligible difference. An average value of 1.25 was computed from the data for α'. However, it varied considerably more than $\alpha + K$, and it seemed to be a function of the Froude number. The variation of average values of α' with **F** is as follows:

α'	F
1.06	4
1.21	6
1.27	8
1.32	9
1.38	10

The use of the proper value of α' and of the dynamic force on the rise corrects Eq. 15. By using values of $\alpha' = 1.25$ and of the drag force with $C_D = 2.0$, points were computed and they are shown for comparison in Fig. 16. Of course, the correct coefficients would give exact agreement.

The fact that the momentum and energy at section 2 could be computed from the average value of the velocity also may be incorrect. However, the error would be smaller than at section 3—either the coefficients introduced could provide the lump correction, or further investigation of velocity distribution could provide more exact values.

The writer has emphasized the fact that, when the abrupt rise is placed after the jump, the problem is simple and need not be confused directly with the hydraulic jump. If **F** and d_1 are known, then d_2 and V_2 follow, and the correct drop down can be computed easily by either momentum or energy principles provided the velocity distribution and the contraction loss at the rise are known.

Weir.—It was stated that in the abrupt rise when $d_3 = d_c$ the rise and weir should be interchangeable. It is important to superimpose the experimental curves of Fig. 7 at $d_c = d_3$ onto Fig. 6 for the weir. The agreement between the two is shown in Fig. 17 where it is noted that the values for the ratio $X/d_2 = 4 +$ fall perfectly into line.

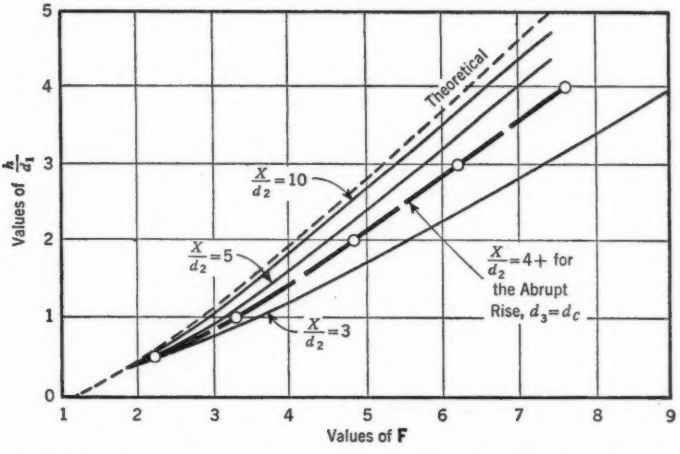

FIG. 17.—SIMILARITY OF THE ABRUPT RISE AT CRITICAL DEPTH WITH THE WEIR, FIG. 6

The two theoretical curves (at X/d_2 equals about 10), Fig. 2, also agree reasonably well. Why should not curves for the weir and abrupt rise at critical depth be the same for other ratios, as long as $X > L_J$? The same barrier height should cause approximately the same velocity distribution and force on the rise, irrespective of what happens immediately after the barrier. These observations on the close correlation between the limiting case of the abrupt rise, $d_3 = d_c$, and the weir suggest that one analysis (the abrupt rise) should suffice for both. The main criterion is whether the flow is above or at or below

critical depth at the rise. The trend in the analysis should be the same, although slight variations naturally may occur due to the difference between the length of the rise in the two cases. It would be most acceptable if the limiting case of the abrupt rise would eliminate the terrifying Eq. 13*a*, based on questionable coefficients, for the weir. Nothing should be that complicated.

The weir analysis is unnecessary, therefore, except to show the variation in h/d_1 in terms of x/d_2 for values of **F**. The authors state that, when the downstream slope is steep and the depth is less than critical, a weir or abrupt rise of the same height are interchangeable. Fig. 17 supports this statement.

An attempt to predict the change in the experimental curves of the abrupt rise (Fig. 7) when $x/(d_3 + h)$ is not equal to 5, is possible by combining the data for the weir with the abrupt rise. A first approximation for similar curves of other ratios of $x/(d_3 + h)$ in Fig. 7 can be obtained as follows: Project points from Fig. 6 to the line $d_3 = d_c$ of Fig. 7. Then rough curves can be sketched in parallel to the existing ones of Fig. 7.

Additional Variables.—The fact that an H3-backwater curve exists upstream from the jump may be the cause of some error if the depth d_1 is measured at a constant distance upstream from the rise, which may be upstream from the toe of the jump. As a matter of interest, if there were no backwater curves upstream and downstream from the jump, it could probably take place anywhere along the channel and would likely be unstable as to position. To move the jump upstream, the downstream depth must be increased. Some of this added depth is required simply to satisfy the new, higher Froude number (the discharge being constant). If d_1 is measured too far upstream, the depth at the toe of the jump will be higher than expected and the Froude number should really be lower. This condition, combined with a slightly lower h/d_1 than computed, would move the experimental points toward closer agreement with the theoretical curves. Hence, for precise work the depth should be measured at the toe of the jump, especially when the ratio X/d_2 varies considerably. At any rate, the backwater curve is a separate problem whose solution can be handled adequately for each situation that occurs in practice. It is not fundamentally important in the analysis of the hydraulic jump, and there is no need to duplicate model studies of the backwater curve in an already complicated problem.

The ratio d_2/d_1 must frequently be computed as a function of **F**. Ordinarily, $\mathbf{F}^2$ or $V^2_1/(g\,d_1)$ will be known by the engineer. A rapid method for approximating $d_2/d_1 = f(\mathbf{F}^2)$ mentally is as follows: Set down values of d_2/d_1 from 0 to n. Values of $\mathbf{F}^2$ are then tabulated quickly as n plus the previous $\mathbf{F}^2$-value—

$\frac{d_2}{d_1} =$	0	1	2	3	4	5	6	7	8	9	10
$\mathbf{F}^2 =$	0	1	3	6	10	15	21	28	36	45	55

The value of d_2/d_1 will be the difference between the preceding and the existing values of $\mathbf{F}^2$, or $\Delta(\mathbf{F}^2)$.

It would be of interest if the authors would state whether they measured d_2, which was assumed to exist before the rise, to see if it agreed with the computed value. In other words, is the jump preceding a barrier (as long as $X > L_J$) any different in dimensions or energy loss from a similar jump in a level channel?

The methods presented for the abrupt rise and weir cannot be used when the X-distance is less than the length of the jump. The theoretical depth d_2 would certainly not exist upstream from the rise, and possibly not at all. It would be a difficult problem. The momentum equation would be most applicable, but a study of the velocity distribution, dynamic force on the face of the rise, and assumption of hydrostatic pressure would be absolutely necessary. Research of this kind may have value in the design of even shorter satisfactory stilling basins in certain instances.

A complete study of velocity distribution is necessary in the problem presented by the authors. As long as $X > L_J$, it should be possible to express the coefficients α, α', K, and C_D as functions of X/d_1 which would complete the problem by also considering the placement of the jump with respect to the rise.

AMERICAN SOCIETY OF CIVIL ENGINEERS

Founded November 5, 1852

DISCUSSIONS

MISSISSIPPI RIVER BRIDGE AT DUBUQUE, IOWA

Discussion

BY R. N. BERGENDOFF AND JOSEF SORKIN

R. N. BERGENDOFF[29] AND JOSEF SORKIN,[30] MEMBERS, ASCE.—The primary purpose of presenting this paper, giving a detailed description of the design and construction of one of the major structures across the Mississippi River, was to establish a permanent record regarding this bridge in the belief that it may prove helpful to colleagues in the profession, in the planning of structures of comparable magnitude. In a sense the urge to present this paper was a reflection of the writers' own experiences and difficulties encountered in the usual exploratory work, in planning major bridge crossings and in pursuit of determining best suitable types and features for a given site. There is an abundance of theory on design analysis of every known type of structure and, although it is valuable in the final design of a structure, theory alone offers little help in preliminary studies of comparative types, particularly when the time element is limited as has been the usual case in the past several years.

The writers were particularly pleased, therefore, in the concurrence with this logic as indicated in the opening paragraphs of Mr. Jones' discussion. It is also noted that Mr. Jones concurs in the pleasing appearance of the bridge. In this instance the structure as located is in full view of the inhabitants of the cities served on both banks of the river as well as to railway traffic across the river and along the east and west banks. The designers felt particularly gratified when the structure received the 1943 Bridge Award of the American Institute of Steel Construction in Class I for the most beautiful bridge opened to traffic in that year.

Mr. Jones questions the inherent economic advantage in the erection of this type of bridge as compared to the conventional cantilever or continuous truss construction. He concedes, however, that "Unfortunately, no data can be assembled quickly to prove or disprove a contention of this type." The writers fully agree that mere comparative weights would not be necessarily con-

NOTE.—This paper by R. N. Bergendoff and Josef Sorkin was published in June, 1947, *Proceedings*. Discussion on this paper has appeared in *Proceedings*, as follows: September, 1947, by Jonathan Jones; October, 1947, by A. Floris, and T. H. Rust; May, 1948, by Charles W. Dohn; and May, 1949, by Louis Balog.

[29] Cons. Engr., Howard, Needles, Tammen & Bergendoff, Kansas City, Mo.

[30] Chf. Design Engr., Howard, Needles, Tammen & Bergendoff, Kansas City, Mo.

clusive criteria. Even bids received on alternative types, although they would serve to indicate the economic preference in one particular case, would not permit drawing general conclusions, as unfortunately too many elements significant at the moment may be totally irrelevant at some other time, or at a different geographical location. It is well recognized that, aside from such fundamental costs as those of material and labor, the contractors' bids also reflect in no small measure the lack or abundance of prospective work, the chance location of the major part of their equipment necessary to the job, and various other factors of similar nature.

In the design of the bridge a 50% increase in stresses was allowed for erection including wind. To the best knowledge of the writers, such an increase is conventional. Mr. Jones' statement that "This increase was the occasion for considerable worry * * *" is fully appreciated; but it is believed that the structure through various construction stages was not devoid of ample safety factors. The erection stresses, although higher than normal, were still well below the elastic limit of the metal, and the structure was sectioned for a 30-lb wind against a maximum recorded wind velocity equivalent to an 11-lb wind.

The writers cannot agree with Mr. Jones' deduction that in conventional cantilever and continuous truss construction by cantilever method "* * * members carry the moment from cantilevering only the half length of the suspended span; instead of half the length of the main span, as at Dubuque." In cantilever erection of a cantilever truss the temporary chord members, introduced at the hinge of the suspended span, necessarily produce a moment at this point, which carries along the anchor arm to the support; in essence then, the final result is the same as for that of the Dubuque bridge. For purposes of record it may be of interest to note that the total amount of metal added for erection of the Dubuque bridge is 150 tons (not 345 tons, as erroneously stated in Mr. Balog's discussion) which in the knowledge of the writers compares quite favorably with conventional cantilever or continuous bridges of similar magnitude. The Mississippi River Bridge at Greenville, Miss., opened to traffic in 1940 and designed also by the writers' firm has approximately the same length of channel span, but is of conventional cantilever type. The final weight of metal added for erection purposes is comparable with that in the Dubuque span.

Mr. Floris would apparently prefer to use deck truss construction for the end spans,

> "* * * by making the top chord of the end spans straight, while arching their bottom chord. This arrangement permits the lowering of the mid-piers, if the suspended floor of the center span is also raised to the level of the top chord of the end spans."

Mr. Floris states that such an arrangement would result in "Additional navigation clearance * * * without increase in cost * * *." It is not quite clear whether Mr. Floris implies additional horizontal clearance or additional vertical clearance. Additional horizontal clearance would necessarily mean an increase in the length of the center span. Additional vertical clearance would require either an appreciable steepening of the approach grades or an increase in the height of approach, span piers, or both; in any event there is reason to believe such construction would result in additional cost. Furthermore, vertical

clearance requirements under the west end span eliminated the possibility of such an alternative in this case. The writers appreciate Mr. Floris' reference to three publications in German as regards other applicable methods of stress analysis. Since, however, Mr. Floris explains "These methods * * * have found * * * little favor among authors and stress analysts in the United States," the writers are pleased to learn that they alone did not miss the opportunity of using these methods. Mr. Floris could make a real contribution to the profession if he would translate these publications into English. The customary procedure used in the design was found neither "cumbersome" nor "laborious." All basic data preliminary to the development of Eqs. 17*a*, 17*b*, and 17*c* were analyzed by slide rule without any significant loss of accuracy. The solution of the three simultaneous equations by any accurate method certainly cannot be classed as laborious. It is the writers' considered opinion that in most instances the difference between one method of analysis and numerous others which are generally available is not material. The best method for any individual analyst is the one that best appeals to his logic. The time element, if any, is usually of secondary importance and is generally compensated by elimination of errors, because of the analyst's clear understanding of the theory.

Mr. Rust emphasizes the particular importance of stable foundations for statically indeterminate structures. The foundations for the Dubuque bridge did not involve any extraordinary problems as regards possible settlement. Piles were used primarily to afford assurance against underscour. These considerations, rather than bearing capacity, dictated the specified penetration. The piles were driven into a thick sand stratum. The design loads were limited to usual current specifications. Redrive tests indicated a bearing capacity considerably greater than that required, averaging well over twice the required capacity. The writers fully agree that statically indeterminate structures may well be avoided in instances where considerable settlement may be anticipated. It should be recognized, however, that nominal settlements are of no material significance. As was pointed out in the paper, a settlement of 1 in. in one of the end piers would result in a change of the reaction at that pier on the order of 10 kips, which is small, "percentagewise" and its effect upon the stresses in the truss members would be equally insignificant. Similarly, the same settlement of the intermediate piers would be of no great importance. Actual observations, since completion of the structure, have disclosed no evidence of settlement of the foundations.

Mr. Dohn raises the question of secondary stresses in the truss members, particularly near the intermediate piers. Contrary to Mr. Dohn's presumption there are few if any unusual features in the framing which would cause secondary stresses of extraordinary magnitude. It is also difficult to follow Mr. Dohn's deduction that the use of silicon steel will necessarily result in greater secondary stresses. Geometric cambering to neutralize the secondary stresses was used for the Dubuque bridge. It is to be appreciated that in long continuous highway bridge spans stresses due to live load are relatively small as compared to the total static stress, particularly in the region of intermediate supports; and, therefore, the effect of live loading is relatively small. As

indicated in Table 4, none of the truss members is subjected to reversal because of primary loads and very few members are subject to reversal due to wind.

Mr. Balog's protracted discussion represents a great deal of effort and time. Such effort could be a distinct contribution to the original paper. Unfortunately, Mr. Balog's comments are so thoroughly misapplied as to merely confuse the factual data presented in the original paper. The discussion can be criticized on the following elemental points of recognized sound engineering practice.

1. Construction costs are not, and never have been, constant.
2. Minimum amount of material does not necessarily represent the most economical design. If so, wide flange rolled beams would have no place in bridge design.
3. Foundations on rock available at nominal depth can be designed cheaper than foundations necessarily supported on long friction piles.
4. The cost per linear foot of a span 845 ft long is more than the cost per linear foot of a span 740 ft long.
5. The ability to compute stresses and strains is not the sole qualification of a good designer. Knowledge backed by practical experience with problems dealing with properties of materials, fabrication of parts, function of details, limitations and adaptability of erection equipment, costs of material and labor, restrictions of War Department requirements, etc., is necessary to permit the designer to solve his problems properly.
6. In any design, due consideration must be taken of relative costs of labor and materials. European practice favors more labor and less material because labor is cheaper in Europe; the reverse is true in American practice.

Mr. Balog makes an extremely questionable comparison of the cost of the Dubuque bridge with that of the Bettendorf (Iowa) bridge. After arriving at a misleading difference in the cost per square foot of roadway by ignoring elemental facts, Mr. Balog accepts it as prima-facie evidence for his thesis. The Bettendorf bridge was constructed in 1935 when the *Engineering News-Record* Construction Cost Index was 196.44. The Dubuque bridge was constructed at 1941 costs when the *Engineering News-Record* Construction Cost Index was 257.84, a difference of 31.5%. The main span of the Dubuque bridge is 845.17 ft, whereas that of the Bettendorf bridge is 740 ft. An increase of the Bettendorf span to the length of the Dubuque span would result in approximately a 15% increase in the pull on the cables, height and load on the towers, and in the pull on the anchorages. Furthermore, the entire Bettendorf bridge, including approaches, is founded on shallow rock foundations. At Dubuque subsurface material for a depth of 400 ft is sand, silt, and clay. It is obvious that, transposed to the Dubuque site, the Bettendorf bridge would entail materially greater foundation costs. On the other hand, foundation costs for the Dubuque bridge would be correspondingly lower if that structure were transposed to the Bettendorf site. Taking proper account of these factors further confirms the writers' conclusions, as stated in the original paper, that the bridge, as finally constructed, compared favorably in cost to a suspension span. Mr. Balog overlooks these factors altogether and seemingly

bases his conclusions as regards similarity of the two bridges on the mere fact that the ratio of cost of substructure to superstructure is 0.52 in the case of either bridge. The identity of these ratios is purely accidental, and has nothing to do with comparative economy of the structures. Misuse of perfectly good data is no reflection on the Bettendorf bridge. This bridge was designed by eminently able engineers and built by competent contractors. The type and other features of this bridge were undoubtedly dictated by sound principles and logic.

Mr. Balog takes further issue with comparative economy studies of the Dubuque bridge, stating thus:

> "The cantilever, being a statically determinate system, cannot utilize the the tenacity and ductility of the steel; * * * and * * * must necessarily cost more than the continuous truss."

Although this argument is applicable to short span structures, in which the live load forms a significant part of the total load, it is totally irrelevant in spans of the magnitude under consideration. (For the Dubuque bridge, the live load is 15% of the total load.) In long spans, introduction of articulated joints at inflection points of the continuous truss span, thus converting it into a cantilever system, will not in the least detract from the economic aspects of "tenacity and ductility" which in Mr. Balog's opinion are inherent in continuous systems only.

Mr. Balog is concerned with the position of the mass centroid in the Dubuque bridge. However, since later in his discussion he takes issue with the spacing of the trusses and maintains that the trusses could just as well be spaced closer, he apparently is quite satisfied with the stability of the bridge. Thus one part of his discussion answers the other. His argument relative to the mass centroid of the structure, if carried to its logical conclusion, would condemn every through braced arch, including the Hellgate Bridge (New York, N. Y.), Sydney (Australia) Harbor Bridge, and many other equally prominent structures. It also leads to the implication that, since the Empire State Building in New York could not possibly have the stability of a single-story frame, skyscrapers are follies. To emphasize his point Mr. Balog even cites the dangers of earthquakes. Such logic has no substance. The question is not which type of structure is infinitely more stable, but rather, "Is the structure stable?"

By the way of further comparison, Mr. Balog proposes two other types of structures in addition to the suspension bridge as shown in Fig. 10. As regards the bridge indicated in Fig. 10(*a*), a structure quite similar was actually studied for the Dubuque bridge. Owing to the span length involved, no advantage was found in this type of construction and it was dismissed primarily due to anticipated erection difficulties. Because of the similarity of this system to the one finally adopted, the writers did not deem it pertinent to mention this study in their original paper. Subsequent to the Dubuque project, consideration was again given to the use of a girder type tied arch at another site where the span was materially shorter. Designs of a trussed arch similar to that at Dubuque and of a girder arch similar to that shown in Fig. 10(*a*) were sub-

mitted to competent fabricators and erectors for their views as regards relative economy of the two structures. Their conclusions, too, were in favor of the trussed arch, principally because of necessary maintenance of channel traffic, as was also the case at Dubuque. Erection matters apparently are of no concern to Mr. Balog. To state "Erection considerations, being subject also to many unforeseen circumstances, should not govern the design," is for the engineer to adopt the proverbial habit of the ostrich, hiding his head in the sand hoping that the contractor will complete the job at a cost which will not divulge the ignorance of the engineer. Evidently Mr. Balog envisages bridge engineering as simply a matter of wrangling with "tenacity and ductility," torsion, stresses, and strains and throwing the mathematical brain child into the omniscient hands of the contractor, and hoping for the best. The outcome of such procedure is obvious. The contractor may either build the structure at a cost fully reflecting all the follies of the design or he may redesign the structure where any similarity between the original design and the final structure is purely coincidental.

The continuous truss unit propounded by Mr. Balog in Fig. 10(*c*) is thoroughly contrary to all recognized concepts of economic proportioning of truss spans. The writers cannot agree with Mr. Balog that a truss with 85-ft panels, 85-ft chords, and diagonals in excess of 100 ft in length, with the truss members unbraced in the plane of the trusses, could possibly result in an economical type of structure. In this case again the mere weight of metal is only a part of the problem. The cost of handling and transporting the long, heavy members and the field costs of splicing and erecting them are clearly of significant importance.

As regards the design of the stringers, Mr Balog misinterpreted the admittedly ambiguous statement in the paper. Actually, although the crossbeams were designed as continuous beams over the stringers, the load distribution to the stringers was substantially in accordance with the 1935 specifications of the American Association of State Highway Officials (A.A.S.H.O.). The differences in weight arrived at by Mr. Balog as indicated in Table 8 are due to serious oversights of certain factors and effects by Mr. Balog. In the first place, the weight of the stringers and crossbeams is 530 lb per ft instead of 575 lb. Furthermore, half of the sidewalk including its live load is supported by the stringer adjacent thereto. The floor systems indicated by Mr. Balog as type (*a*), Table 8, ignore this load completely. Similarly, the type (*b*) floor, Table 8 (Mr. Balog's design), would obviously require a thicker slab. The additional cost of concrete, reinforcing steel, and the cost of additional metal in the floor beams and trusses to carry the extra dead load would more than offset the gain in stringer weight. The same applies in varying degree to type (*c*) and type (*d*) floors, from Table 8, where in addition to these factors, Mr. Balog fails to account for diaphragms required by specifications and for the additional weight of connection angles as well as for the cost of additional field riveting. Therefore, Mr. Balog's comparisons are irrelevant since they lack common basis with the writers' design, and ignore details considered essential by engineers, for design as well as for construction. Mr. Balog's conclusions stated thus,

> "* * * extensive comparative investigation of the type of floor system used by the authors and a five stringer arrangement. * * * and even then type (*a*), Table 8, cost more,"

do not correspond to the numerous studies made by the writers. In fact, the writers have found that designed on a common basis, with all pertinent elements properly appraised, all conventional floor systems result in the same cost for all practical purposes. As regards the use of silicon steel for stringers, Mr. Balog fails to account for the difference in cost as compared to carbon steel. Aside from the difference in direct costs, use of silicon steel for floor systems where the live load is the principal load carried, and where the system is therefore subjected to numerous stress cycles, is seriously questioned by many engineers. In this connection it is pertinent to note the specifications of the American Railway Engineering Association thus,

> "On account of the possibility of fatigue failure, the allowable unit stresses in Article 1801 shall not apply to members that will be subjected to a large number of stress cycles during the life of the bridge and having either reversal of stress or low dead load stress. For such members the allowable unit stresses shall be reduced, and in floor systems shall not exceed those specified in Article 301 (for carbon steel)."

In discussing the lateral and sway bracing Mr. Balog cites several European bridges where sway bracing and lateral bracing at the lower arch chord were omitted. Undoubtedly, however, this is only a part of the story. Cross frames can be eliminated if strut type portals are provided in lieu thereof. It is entirely possible that such portals require less metal. However, the thing of utmost importance is not the type but the ultimate cost thereof. It is well recognized that European practice conserves metal by taking advantage of the cheaper labor. This, in fact, demonstrates the universality of the engineer's ingenuity. However, it is not by mere accident that these practices neither were originated, nor have found application, in the United States where the relative costs of labor and materials differ radically from European costs. Indiscriminate comparison of these practices is absolutely improper.

As a simple observation as to the advantage of unobstructed view, the writers stated: "The three-span continuous truss structure * * * affords to traffic a view unobstructed by diagonal truss members across the 845-ft main channel span * * *." Of course, the writers presumed the pertinent line of sight of from 4.5 ft to 5 ft above roadway level. This observation is simple, factual, and clear. Mr. Balog complains of the obstruction caused by the bracing of the arch, which is from 25 ft to 100 ft above the floor.

Mr. Balog claims his alternate designs show 20% less metal. This is contrary to results obtained by the writers in preliminary studies made for the crossing and the writers believe such extreme claims are as erroneous as the basis of the other criticisms of Mr. Balog's discussion.

The writers wish to express their appreciation to the constructive contributions of the discussers, which helped in crystallizing some of the phases of the structure described in the paper.